IN VITRO AND *IN VIVO* ANTIMALARIAL, ANTIOXIDANT AND TOXICOLOGICAL EFFECTS OF METHYL GALLATE AND PALMATINE COMBINATION

BY

ADEGUNLOYE, ADEGBENRO PETER

BSc. (AGO IWOYE), MSc. (ILORIN)

11/68EZ001

A Thesis Submitted to the Department of Biochemistry, Faculty of Life Sciences, University of Ilorin, Ilorin, Nigeria, in Fulfilment of the Requirement for the Award of the Degree of Doctor of Philosophy (Ph.D.) Degree in Biochemistry

February, 2018

DECLARATION

I, Adegbenro Peter ADEGUNLOYE (Matric Number – 11/68EZ001) declare that this thesis entitled "*In vitro* and *in vivo* antimalarial, antioxidant and toxicological effects of methyl gallate and palmatine combination"is the result of a study carried out by me under the supervision of Dr. J.O. Adebayo in the Department of Biochemistry, University of Ilorin, Nigeria. I confirm that this thesis presents the results of my findings and that its contents are entirely my ideas unless otherwise stated with appropriate referencing. This thesis has neither been submitted to any University nor is it before any other University for consideration for the award of a Doctor of Philosophy (Ph.D.) degree in Biochemistry.

Adegunloye, A.P.

(February, 2018).

CERTIFICATION

I certify that this work was carried out by Mr. Adegunloye, Adegbenro Peter in the Department of Biochemistry, Faculty of Life Sciences, University of Ilorin, Ilorin, Nigeria, under my supervision.

---------- ----------

Dr. J.O. Adebayo **Date**

B.Sc., M.Sc., Ph.D. (Ilorin)

(Supervisor)

APPROVAL PAGE

This thesis has been read and approved as having met the requirement of the Department of Biochemistry, Faculty of Life Sciences and Postgraduate School, University of Ilorin, Ilorin, Nigeria, for the award of Doctor of Philosophy (Ph.D.) degree in Biochemistry.

---------- ----------

Dr. J.O. Adebayo **Date**

(Supervisor)

---------- ----------

Prof. E. A. Balogun **Date**

(Head of Department)

---------- ----------

External Examiner **Date**

DEDICATION

This thesis is dedicated to the Almighty God, whose word of light and life teaches in Ecclesiastes chapter four verse twelve that “though one may be overpowered by another, two can withstand him, but a threefold cord is not quickly broken”

Also, this thesis is dedicated to everyone who progressively seeks the uncovering of their own ignorance.

ACKNOWLEDGEMENT

I am deeply grateful to my supervisor, a distinguished scholar, Dr. Joseph Oluwatope Adebayo, for his caring heart, listening ears, attention to details, encouragement, and intellectual, moral and godly leadership. He is indeed a light to the world, a blessing to me, and to generations.

Sincere appreciation to the Head of Department, Prof. M.T. Yakubu for being accessible and creating a conducive atmosphere for intellectual discourse. Also, my appreciation goes to other lecturers in the department like Prof. M.A. Akanji, Prof. H.O.B. Oloyede, Prof. C.O. Bewaji, Prof. (Mrs) E.A. Balogun, Prof. (Mrs) S.O. Malomo, and Prof. (Mrs) A.T. Oladiji for their valuable contributions. I am also grateful to Dr. R.O. Arise, Dr. (Mrs) F.A. Suleiman, Dr. A. Igunnu, Dr. M.O. Nafiu, Dr. M.O. Salawu, Dr. A.L. Quadri, Dr. (Mrs) R.A. Oyegoke Mrs H.F. Murtala, Mrs F.A. Abubakar, Mr. O. Modupe, Mrs O. Soji-Omoniwa, Mr. K. Bello and Mrs. S.A. Omar for their various advice and support. Technical assistances were also provided by departmental laboratory staff members, especially Messrs Joseph Akosewa, Ibrahim Akolade, and Dele Aiyepeku, to whom I am grateful.

I am grateful to my ever-supportive and ever-loving parents, Mr. Adebisi Adegunloye and Mrs Eunice Adegunloye, for being my first teachers who laid the solid foundation of the way that I should go. I am so grateful for their sacrificial lifestyle of denying themselves pleasure that I may be in abundance. Special thanks to my sisters, Aderonke, Adenike, Adebimpe and Aderinsola, for their unwavering supports. And what a joy to also have Rev. Gabriel Esrom, Deacon Collins Akintemi, Mr. Gbenga Omoniyi, Life, Light, Love, Olamide, and Olaoluwa as family.

Special thanks to Architect Victor Adegunloye, and Mr. & Mrs. Rufus Adegunloye, for their moral and financial supports.

Sincere appreciation to my spiritual fathers, Pastors Sanya Kolajo and Dare Akintunde, for feeding me spiritually and declaring words of grace over my life.

I am also grateful to my students during my time at Wesley University of Science and Technology, Ondo, especially Dami Olayele, God'sPromise Adeuga, Amen Ishola, and Ini-Obong Ekpenyong who challenged me to reach higher mental levels through thought provoking questions.

Special thanks to friends like Kayode Adewole, Habibu Tijjani, Gideon Gyebi, Ishola Ahmed Adebayo, David Nwikwe, and Faith Ogbodo, for their voluntary supports at crucial times of the research.

Finally, I remain eternally grateful to the Almighty God, for the gift of life and wisdom, and for His Goodness and Mercy unto me. To Him alone be all the glory.

Adegunloye, Adegbenro Peter

TABLE OF CONTENTS

LIST OF ABBREVIATIONS

AAPH	2,2'-Azobis(2-amidinopropane) dihydrochloride
ACT	Artemisinin-based combination therapy
ALP	Alkaline phosphatase
ALT	Alanine aminotransferase
Asp	Aspartate
AST	Aspartate aminotransferase
ATP	Adenosine triphosphate
BHT	Butylated hydroxytoluene
BSA	Bovine serum albumin
CAT	Catalase
CQ	Chloroquine
CVD	Cardiovascular diseases
DHFR	Dihydrofolate reductase
DHPS	Dihydropteroate synthase
DMSO	Dimethyl Sulphoxide
DNA	Deoxyribonucleic acid
DPPH	2,2-Diphenyl-1-picrylhydrazyl

FPP	Ferriprotoporphyrine IX
G6PD	Glucose-6-phosphate dehydrogenase
GGT	Gamma-glutamyl transferase
GPx	Glutathione peroxidase
GR	Glutathione reductase
GSH	Reduced glutathione
GSSG	Oxidised glutathione
GST	Glutathione-S-transferase
H_2O_2	Hydrogen peroxide
HAP	Histo-aspartic protease
IC_{50}	Median inhibitory concentration
LDL	Low-density lipoprotein
MDA	Malondialdehyde
NO	Nitric oxide
P.	*Plasmodium*
*Pf*LDH	*Plasmodium falciparum* lactate dehydrogenase
*pf*mdr1	*P. falciparum* multi drug resistance 1
pLDH	Parasite lactate dehydrogenase

Plm	Plasmepsin
RNS	Reactive nitrogen species
ROS	Reactive oxygen species
SOD	Superoxide dismutase
TBA	Thiobarbituric acid
TBARS	Thiobarbiturate reactive substances
WHO	World Health Organization

LIST OF FIGURES

LIST OF TABLES

ABSTRACT

Resistance of malaria parasite to conventional drugs and the high cost of potent ones have necessitated the search for new drugs. Methyl gallate and palmatine are compounds with known *in vitro* activities against multidrug-resistant strains of *Plasmodium falciparum*, but without *in vivo* activities, which are associated with plants from which they have been isolated. This, therefore, necessitates the evaluation of antimalarial activities of combination of isolated compounds. Thus, the objectives of this study were to evaluate: (i) *in vitro* antimalarial activity of methyl gallate and palmatine combination (MGPAL); (ii) interaction of methyl gallate and palmatine with selected *P. falciparum* proteins *in silico*; (iii) antimalarial activity of MGPAL in *P. berghei*-infected mice; (iv) antimalarial activity of MGPAL when co-administered with a bio-enhancer in *P. berghei*-infected mice; (v) antioxidant activities of MGPAL *in vitro* and in *P. berghei*-infected mice when co-administered with a bio-enhancer; and (vi) *in vivo* toxicity of MGPAL when co-administered with a bio-enhancer using selected organ function indices.

In vitro antimalarial activity of methyl gallate and palmatine combination was determined using inhibition of β-hematin formation assay. Suppressive and curative antimalarial activities of the individual drugs and their combination, with or without piperine (bio-enhancer), were evaluated using *P. berghei* NK65-infected mice. Antioxidant activities of MGPAL *in vitro* and in *P. berghei*-infected mice when co-administered with piperine were evaluated. Toxicological effects of MGPAL when co-administered with piperine were also evaluated in rats. Data were analyzed using Analysis of Variance at $P<0.05$.

The findings of this study were that:

i. MGPAL inhibited β-hematin formation *in vitro* (IC_{50} - 0.73 µg/mL, indicating antimalarial activity), with the compounds exhibiting synergistic interaction when combined in ratio 3:2;
ii. Methyl gallate and palmatine exhibited higher affinity for plasmepsins I, II and III than for other proteins studied *in silico*;
iii. MGPAL in ratio 3:2 (MGPAL3:2), in the absence of piperine, exhibited no *in vivo* antimalarial activity, causing less than 30% reduction in parasitemia;
iv. MGPAL3:2, in the presence of piperine, caused more than 30% reduction in parasitemia (especially at 12.5 and 25 mg/kg body weight in the suppressive and curative antimalarial tests) in *P. berghei* NK65-infected mice mainly on days 6 and 8 post-inoculation;
v. MGPAL3:2 demonstrated DPPH, nitric oxide, hydroxyl radical scavenging activities and induced antioxidant defense system in murine malaria model in the presence of piperine; and
vi. MGPAL3:2, in the presence of piperine, significantly increased ($p<0.05$) plasma conjugated bilirubin concentration (at the highest dose), HDL-cholesterol concentration (at doses higher than 12.5 mg/kg body weight) and liver aspartate aminotransferase activity (at doses higher than 25 mg/kg body weight) but significantly reduced ($p<0.05$) atherogenic index and Low density lipoprotein-cholesterol concentration (at doses higher than 6.25 mg/kg body weight) and plasma Ca^{2+} concentration (at the highest dose) compared to controls.

The study concluded that, in the presence of piperine, MGPAL3:2 exhibited antimalarial activity, ameliorated ROS-mediated secondary complications of

malaria and adversely affected some liver and kidney functions, especially at higher doses. Further studies on the mechanisms of action of the compound combination should be carried out.

CHAPTER ONE

1.0 INTRODUCTION

1.1 Background of Study

Malaria is an infectious parasitic disease that causes mortality and morbidityin Africaand other parts of the world.Transmitted by female anopheles mosquitos and caused by *Plasmodium* species, malaria has serious socio-economic and health impact on lives especially in tropical regions.Worldwide, malaria is estimated to be about 212 millioncases resulting in about 429,000 deaths annually with 90% of the cases and 92% of deaths occurring in the WHO African Regionwith Nigeria bearing the highest burden (WHO, 2016).Severe complications of malaria include severe anaemia, jaundice, renal impairment, pulmonary oedema, cerebral oedema, decreased consciousness leading to coma and death (Cohee and Laufer, 2017) and severity of malaria is suggested to be mediated by oxidative stress, which results in intravascular haemolysis (Plewes *et al*., 2017), hence depriving vital organs of oxygen and nutrients.

While different medications are available and approved for the treatment of malaria, emergence of parasite resistance to these lines of drugs has limited the therapeutic usage of several of them. Hence, the recommendation of combination therapy for the treatment of malaria with artemisinin-based combination therapies (ACTs) recommended as first line treatment for malaria caused by *Plasmodium falciparum*,but emergence of resistance against ACTs has also threatened their effectiveness (WHO, 2016). Therefore, there is the need for alternative treatment options.

Despite the availability of conventional drugs, due to cheaper cost, cultural and historic reasons, herbal medicine remains popular in Africa for the treatment of

malaria(Hirt *et al.*,2008; Adebayo and Krettli, 2011) and the decoction, infusion or tincture of bark, fruits, leaves and/or roots of different medicinal plants are usually formulated (Odugbemi *et al*., 2007).The combinations of different species of plants or plant parts are favoured because of the understanding that each of these plant species/parts are made of arrays of chemical components that serve as defence agents against pathogens (Rasoanaivo *et al.*, 2011). Hence, various phytochemicals are available to work together in overcoming the parasite, its resistance and the clinical manifestations of malaria.Some of these herbal plants are*Alstonia boonei, Annickia kummeriae, Azadirachta indica, Curcuma longa, Dacryodes edulis, Enantia chlorantia, Khaya grandifoliola, Piper nigrum, Zanthoxylum zanthoxyloides* (Odugbemi *et al*., 2007; Jantarat, 2013; Malebo *et al.*, 2013; Zofou *et al.*, 2013) and they possess active or supportive components such as methyl gallate, palmatine, and piperine.

Using scientific approaches, many active chemical constituents of herbal plants have been isolated with reported *in vitro* antiplasmodial activity. These isolated, pure, active agents when administered *in vivo*, singly, were mostly without tangible antimalarial activity, despite the substantial activity associated with the crude extract of the plants (Wagner and Ulrich-Merzenich, 2009; Rasoanaivo *et al*., 2011).Since the focus has been on the usage of a single isolated chemical agent to treat malaria, several of these chemical compounds that were active *in vitro* but inactive *in vivo* were consequently left out of consideration for malaria treatment.Methyl gallate and palmatine are some of the pure active agents from antimalarial plants with reported *in vitro* antiplasmodial activities (Malebo *et al.*, 2013; Zofou *et al.*, 2013), but without *in vivo*antimalarial activity. Also, piperine is a compound from herbal antimalarial

remedy plant reported as a natural bio-enhancer but without antimalarial activity (Lambert *et al.*, 2004; Martinelli *et al*., 2008; Jantarat, 2013).

Mimicking the traditional combination of plant species and/or parts in the treatment of malaria, pure chemical agents which are usually discarded due to poor *in vivo* antimalarial activities, could be refocused through appropriate combinations especially those with additional benefits such as antioxidant properties.

CHAPTER TWO

2.0 LITERATURE REVIEW

2.1 Malaria Burden and Prevalence

Malaria is a life-threatening infectious disease that majorly affects people in tropical areas of the world, with children and pregnant women being the most vulnerable (Arama and Troye-Blomberg, 2014).

Malaria was said to be endemic in 91 countriesand territories at the start of 2016 and estimated cases of malaria was recorded as 212 million worldwide in 2015 with 90% of the cases occurring in WHO African Region (WHO, 2016). From this number of cases in 2015, an estimated 429,000 deaths were recorded with about 92% of these deaths occurring in the WHO African Region(WHO, 2016). Children suffer the most blows as 70% ofglobal deaths from malaria occur in children aged less than 5 years and a child's life is estimated to be taken every 2 minutes (WHO, 2016).

Countries in sub-Saharan Africa dominated global burden of malaria in 2015, with both Nigeria (26%) and Democratic Republic of the Congo (10%) accounting for more than 36% of malaria deaths worldwide (WHO, 2016). In Nigeria, transmission of malaria occurs all year round and almost all malaria cases in the country are caused by *Plasmodium falciparum*(Adebayo *et al.*, 2012).

Over the years there has been notable progress in the fight against malaria, yet the effects of malaria on health and livelihoods of humans continue to be overwhelming. Worldwide there has been about 60% reduction in death rate over the last 15 years and this can be attributed to increase accessibility and availability of preventive measures such as insecticide treated bed nets, indoor residual spraying and new but more effective diagnostic tools and treatment approaches (Cohee and Laufer,

2017). Of these interventions aimed at eliminating malaria cases and/or mortality, widespread deployment of insecticide treated bed nets has been declared as most important (Bhatt *et al.,* 2015). Five countries (Armenia, Morocco, Sri Lanka, Turkmenistan and United Arab Emirates), as at 2016, have been declared free from malaria and twenty-six more are prepared to attain such status by 2020 (Newby *et al.*, 2016). Further progress in malaria control is majorly challenged by increase in drug and insecticide resistance.

2.2 Susceptibility to Malaria

All individuals in nonendemic and low transmission areas are at risk of malaria whereas multiple malaria infections in highly endemic areas may lead to development of partial immunity to a strain of malaria parasite but not complete immunity against the infection. Also, this partial immunity is not life-long because if such individuals are no longer exposed to the infection for about a year they become highly susceptible upon repeated exposure (Cohee and Laufer, 2017).

Susceptibilities to malaria infection is altered by haemoglobinopathies, as sickle cell trait (HbAS) provides about 90% defence from severe malaria, 75% safety from hospitalization due to malaria but no defence from asymptomatic infection (Williams *et al.*, 2005). Also, haemoglobin C, alpha-thalassemia and beta-thalassemia provide protection from malaria. However, despite these protections, individuals with any of these haemoglobinopathies can still have severe malaria (Cohee and Laufer, 2017).

People with partial immunity or those who took incomplete or ineffective prophylactic drugs may have delayed clinical manifestation of malaria. *P. malariae*may persist at low levels for up to a year while *P. vivax* and *P. ovale,* due to

their dormant stages, may persist after initial infections for months to years (Cohee and Laufer, 2017).

2.3 Malaria Parasite

Malaria is caused by *Plasmodium* and six species of *Plasmodium*, that is, *Plasmodium falciparum, Plasmodium vivax, Plasmodium ovale, Plasmodium malariae, Plasmodium knowlesi, Plasmodium cynomolgi*(the last twountil recently were considered as a nonhuman primate parasite) are known to cause human malaria and are transmitted by over 30 species of female *Anopheles* mosquitoes (Philippe *et al.*, 2012).

Malaria in humans is primarily caused by *P. falciparum*and *P. vivax,* though with distinct geographical distribution. *P. falciparum*was responsible for about 99% of malariadeaths worldwide whereas *P. vivax* was responsible for majority of malaria deaths (about 86%) occurring outside Africa (WHO, 2016). *P. malariae* has similar geographical distribution as *P. falciparum*while *P. ovale* is mainly found in West Africa. Though *P. knowlesi*and *P. cynomolgi*mainly infect nonhuman primate, there are few human cases in Southeast Asia.

2.3.1 The Life Cycle of *Plasmodium* species

Malaria parasite requires both female anopheles mosquitoes (the definitive host or vector) and human (an intermediate host) for a complete life cycle and the parasite goes through 10 morphological changes in five different tissues of hosts (Mackinnon and Marsh, 2010). The parasite cycle (Figure 1) can be summarized thus: Sporozoites from an infected mosquito pass to the human host during a blood meal. These infect hepatocytes and then erythrocytes for their asexual cycle. The sexual forms of the parasite that develop during the erythrocytic stage are ingested by a feeding mosquito.

The sexual cycle takes place in the mosquito to generate new sporozoites, hence completing the cycle.

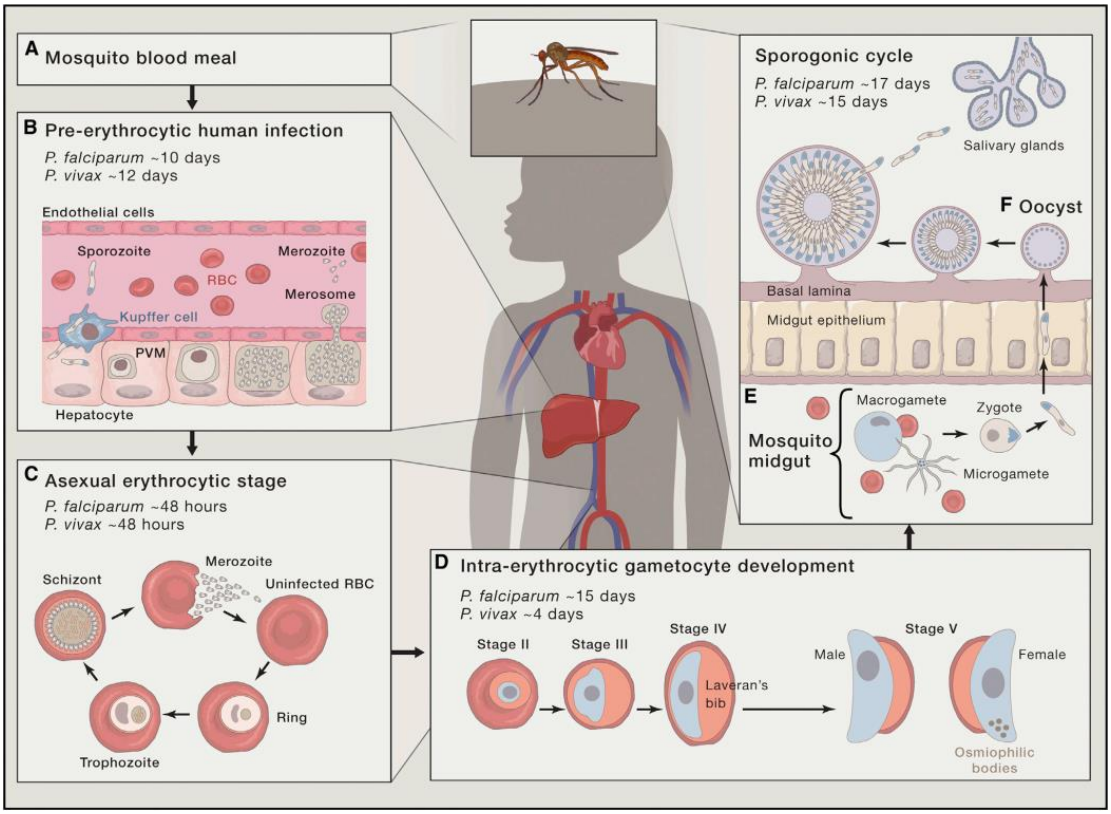

Figure 1: Life cycle of *Plasmodium*species in human host and Anopheles mosquito vector

Source: Cowman *et al.* (2016).

The parasite cycle in human and mosquito hosts includes;

i. the skin stage;
ii. the pre-erythrocytic or hepatic stage, which involves inoculation of sporozoites to infect the hepatocytes;
iii. the erythrocytic stage, which involves asexual reproduction of the parasite in theblood and consequently producing the clinical symptoms of the disease;
iv. the gametocyte stage, which makes possible the male and female gametocytes; and
v. the sexual or sporogonic stage, which involves the sexual fusion of gametocytes that subsequently form sporozoites.

During a blood meal by an infected female Anopheles mosquito, parasites in the form of sporozoites are injected into the skin and/or blood stream of human. The skin-infecting sporozoites stage, which last for about 5-8 minutes, initiate rapid suppression of immunity and establishes early tolerance to subsequent life cycle stages of the parasite (Guilbride *et al.*, 2012). The sporozoites in the blood stream moves about in search of suitable hepatocytes for invasion (Arama and Troye-Blomberg, 2014). Meanwhile, at the site of injection, sporozoites can linger for some time (Yamauchi *et al.*, 2007) and a third portion of sporozoites leaving the site could end up entering the draining lymph nodes through the lymphatic vessels (Amino *et al.*, 2006). Hence, for there to be 100% assurance of an individual becoming infected, such must have been bitten at least five times by *P. falciparum*-infected mosquitoes because of the low capacity of sporozoites to generate asexual erythrocytic-stage infection (Verhage *et al.*, 2005).

These sporozoites then infect susceptible hepatocytes where they may either remain dormant (as in *P. vivax and P. ovale* infections) or undergo asexual reproduction to produce merozoites. This is the hepatic or exoerythrocytic phase. Increase in number of merozoites causes the rupture of hepatocytes thereby releasing thousands of infectious merozoites into circulation and consequently they invade erythrocytes. Within 48 h, this initiate the intraerythrocytic cycle of asexual reproduction, which is responsible for the clinical symptoms associated with malaria. Young parasites feed on erythrocyte's haemoglobin and after 24–32 h, mature from rings stage, through trophozoites and schizonts stages to form 16-32 infective daughter merozoites that are released as the erythrocytes rupture (Boddey and Cowman, 2013; Cowman *et al.*, 2016; Cowman *et al.*, 2017). These then invade uninfected erythrocytes for the cycle to be repeated.

Some of the merozoites, within a 15-day period, differentiate into male and female gametocytes. Upon ingestion by a feeding female mosquito, the male and female gametocytes undergo sexual reproduction, by fusion, in midgut of the mosquito to form a zygote and developing within 24 h into a motile ookinete. The ookinetes penetrate the midgut epithelial cells and stay between the midgut epithelium and the basal lamina to form oocysts. The oocysts undergo complex asexual development to become infective sporozoites (Boddey and Cowman, 2013; Arama and Troye-Blomberg, 2014; Cowman *et al.*, 2016). These can reach the mosquito's salivary gland and are ready to be inoculated into another host through the mosquito saliva during its blood meal, thereby ensuring the continuation of the *Plasmodium* life cycle.

2.3.2 Cellular Impact of *Plasmodium* species

The cellular impact of *Plasmodium*species on human can be classified into; inflammation, anaemia and organ impairment.

Inflammation: Inflammation results from parasite metabolism and rupture of erythrocyte, but also from parasite sequestration as observed in *P. falciparum*infection. Huge amounts of proinflammatory cytokines are released by splenic macrophages and monocytes in response to phagocytosis of hemozoin and other erythrocyte remnants (Cohee and Laufer, 2017). The proinflammatory cytokines then give rise to;

(i) the systemic inflammatory response syndrome,

(ii) oedema and inflammation in perivascular tissues in organs, and

(iii) increased expression of cytoadhesion molecules and more sequestration of infected erythrocyte.

Anaemia: Anaemia resulting from *Plasmodium* species infection is multi-level linked. Haemolysis results, directly, from asexual reproduction in infected erythrocytes. Also, intraerythrocytic parasites bring about reduction in erythrocyte deformability, thereby leading to further haemolysis and splenic clearance. This is made worse by splenic sequestration in *Plasmodium falciparum*infections. Furthermore, during infection, haemolysis is not compensated for because tumour necrosis factor-alpha is released, and this suppresses haematopoiesis (Cohee and Laufer, 2017).

Organ impairment: Organ impairment is facilitated by cytoadherence (sequestration) of infected erythrocyte. Of the species capable of infecting humans, only*Plasmodium falciparum* causes adherence of infected erythrocyte to the endothelial cells of the host. This cytoadhesion is made possible by a family of antigens called *P. falciparum* erythrocyte membrane protein 1 (PfEMP1) which are encoded by the *var* gene (Cohee

and Laufer, 2017). They are produced by the intraerythrocytic parasite and exported to the membrane of infected erythrocyte to facilitate the adhesion of infected red blood cells to specific receptors (intercellular adhesion molecule-1[ICAM-1], CD36, E-selectin, neural cell adhesion molecule, endothelial protein C receptor [EPCR] which are expressed on the endothelial cells and leucocytes, chondroitin sulfate A for placental syncytiotrophoblasts, and CD31 [PECAM-1] for on endothelial cells of organs such as brain, heart, kidney, lung, placenta and subcutaneous tissues (Turner*et al.,* 2013; Storm and Craig, 2014; Gallego-Delgado and Rodriguez, 2017; Wassmer and Grau, 2017).

Endothelium breakdown (endothelial activation), obstruction of blood flow (pro-coagulant response) and inflammation (pro-inflammatory response) are the outcomes of infected erythrocyte binding with uninfected erythrocyte, platelets and inflammatory cells thereby causing organ impairment. Moreover, splenic clearance is evaded because cytoadherence removes parasites from circulation thereby ensuring that the infection continues (Cohee and Laufer, 2017). Cytoadherence in the brain brings about cerebral malaria and results in adverse birth consequences, during pregnancy, when the placenta is involved.

2.4 Clinical Manifestation and Severity of Malaria

Malaria can be classified, clinically, as uncomplicated or severe. It is classified as uncomplicated when there are symptoms and/or signs of malaria and a positive parasitological test but no evidence of organ impairment. Symptoms that may be associated with uncomplicated malaria are; fever (greater than 40^{o}C with severe rigours and chills), malaise, fatigue, headache, cough, abdominal pain, nausea, vomiting, anorexia, myalgias, and back pain (Cohee and Laufer, 2017). Mild jaundice due to haemolysis and splenic enlargement are some signs associated with

uncomplicated malaria while laboratory abnormalities may include mild anaemia, thrombocytopenia, mild coagulopathy, increased blood urea nitrogen, and elevated creatinine level that do not meet criteria for acute kidney injury (Cohee and Laufer, 2017).

Severe malaria is mainly caused by cytoadherence of *P. falciparum*–infected erythrocytes to the endothelial cells of organs. Malaria is classified as severe when a test for the malaria parasite is positive and one or more of the following features is/are present; impaired consciousness, prostration, multiple convulsions, acidosis, hypoglycaemia, severe anaemia, renal impairment, jaundice, pulmonary oedema, significant bleeding, shock, and hyperparasitaemia (Cohee and Laufer, 2017). Severe anaemia can lead to metabolic acidosis, renal impairment, and noncardiogenic pulmonary oedema. Cerebral malaria can present with seizures and/or decreased consciousness, including coma, and can lead to cerebral oedema, increased intracranial pressure, herniation and death (Cohee and Laufer, 2017).

2.5 Diagnosis of Malaria

Diagnostic test is carried out to ascertain the presence of malaria parasite in patient. Malaria diagnostic tests are only reliable to detect blood-stage disease but not reliable for dormant malaria in an asymptomatic patient. The diagnosis could be done by microscopy, rapid diagnostic tests, polymerase chain reaction, and antibody detection by serology.

Blood smear and detection by microscopy: For laboratory confirmation of malaria, thick and thin smears are the gold standard wherein smears are stained with either Wright's or Giemsa stain. The thick smear is considered as the most sensitive approach to detect low-density infection while the thin smear, which gives room for greater

resolution of the parasite and the erythrocyte morphology, is used to ascertain the *Plasmodium* density and the species (Cohee and Laufer, 2017).

Antigen-detecting rapid diagnostic tests (RDTs): These are generally cassette- or card-based lateral flow immunochromatographic assays. Labelled antibodies detect 1 of 3 *Plasmodium* antigens that may or may not be species specific, depending on the test. They could be based on the detection of histidine-rich protein II (HRP-II) antigen or *Plasmodium falciparum*-specific lactate dehydrogenase (PfLDH). Histidine-rich protein II is a water-soluble protein produced by trophozoites and young but not mature gametocytes of *P. falciparum,* while PfLDH is produced by asexual and sexual stages (gametocytes) of *Plasmodium*. RDTs are considered useful tools for initial diagnosis since they tend to significantly reduce the time spent on preliminary diagnosis (Ota-Sullivan and Blecker-Shelly, 2013).

Polymerase chain reaction (PCR): Polymerase chain reaction is highly specific and sensitive for detecting *Plasmodium*-specific nucleic acid sequences. Genotyping by PCR serves as useful way to differentiate between recrudescence and reinfection (WHO, 2010). However, the use of this method is limited by cost, speed and availability of technology, and is not presently used for routine clinical practice (Walker *et al.*, 2014).

Antibody detection by serology: Immunofluorescence antibody testing (IFA) has no place in the clinical diagnosis of acute malaria. It only measures prior exposure and not specifically current infection. IFA is based on the knowledge that within 2 weeks of initial infection by any *Plasmodium* species, specific antibodies are produced and continues for about 3 to 6 months after clearance of the *Plasmodium*. Hence, specific antigen prepared on a slide is used to quantify both IgG and IgM antibodies in the

sample. IFA is sensitive, simple, and useful for assessing recent infection in non-immunes, and likely blood donors. However, it wastes time, cannot be automated, requires fluorescence microscopy, and result is subjective (Tangpukdee *et al.*, 2009).

Quantitative buffy coat (QBC) technique: This approach enhances detection of *Plasmodium* by microscopy. It utilises fluorescent dyes such as acridine orange to stain the parasite deoxyribonucleic acid in micro-haematocrit, and then use epi-fluorescent microscopy for detection (Tangpukdee *et al.*, 2009). This method is sensitive for detection of *P. falciparum* but not sensitive for other species. The specificity is also reduced because it stains leukocyte DNA (Moody, 2002). Despite being a simple and reliable technique, it is more expensive than conventional light microscopy;it requires special equipment and supplies such as centrifuge, centrifuge tubes, filters and special light sources and not good for determining numbers of parasites (Tangpukdee *et al.*, 2009).

2.6 Prevention and Treatment of Malaria

Early diagnosis and treatment is crucial to ensuring reduction of malaria cases, *Plasmodium* transmission and prevention of death from malaria. Different malaria prevention approaches are personal protection against mosquito bite, use of insecticide-treated mosquito nets and indoor spraying of residual insecticides while control of mosquito breeding site represents community-level intervention at reducing malaria (WHO, 2016).

2.6.1 Vaccine

Unlike *P. falciparum*, *P. vivax* has wider geographical distribution but largely absent in Africa due to the widespread Duffy-negative phenotype that renders erythrocytes resistant to *P. vivax* attack (Birkett, 2016). Thus, developing vaccines that

target all *Plasmodium*species might prove challenging because of the lack of homology in antigens as observed in *P. falciparum*and *P. vivax*. With pitfall of partial protection against malaria projected, vaccine is likely to serve as potential complement to the current set of antimalarial measures, rather than replace them (WHO, 2016), and there is currently no approved malaria vaccine.

The development of malaria vaccine can be categorized into three approaches with each targeting different stages of the *Plasmodium* life cycle. The types of vaccines are: (i) pre-erythrocytic vaccines, whose target is to induce antibodies that prevent hepatic attack by sporozoites and/or generate cell-mediated immune responses that target infected hepatic cells; (ii) blood stage vaccines, which aim to protect against clinical manifestation by inhibiting parasite multiplication; and (iii) sexual, sporogonic, and/or mosquito stage vaccines, which aim to interrupt human-to-mosquito transmission (Birkett, 2016).

Presently, the most advanced malaria vaccine candidate is RTS,S/AS01 and took 30 years to get it ready to obtain approval from a major regulatory authority (Greenwood, 2017). The phase III trial of this candidate vaccine was conducted in 2014 with some successes and challenges. The final results established that vaccination with the three-dose primary series reduced clinical malaria cases by 28% in young children and 18% in infants over a median follow-up of 48 months and 38 months respectively, after first dose across trial sites. A booster dose of RTS,S, administered 18 months after completion of the primary series, reduced the number of cases of clinical malaria, over the study period, by 36% in young children and 26% in infants, aged 5–17 months and 6–12 weeks respectively at first vaccination (Theander and Lusingu, 2015). These results were achieved in conjunction with existing malaria interventions, such as insecticide-treated mosquito nets, which were used by

approximately 80% of the trial participants and efficacy of the vaccine diminished over time in both age categories (Theander and Lusingu, 2015).

The adverse effects which were observed often after RTS,S administration include fever and local reactions such as pain or swelling but very few of the adverse effects were severe (Agnandji *et al.*, 2012). The effectiveness of the vaccine, in infants at ages 6–12 weeks, was reduced when administered with routine expanded programme of immunization (EPI) vaccine, and older children (but not in younger children) had an increase in cases of unexplained meningitis (Theander and Lusingu, 2015).

2.6.2 Antimalarial Drugs

Antimalarial agents target different points of the *Plasmodium* life cycle, and thus can be classified as: (i) tissue schizonticides such as pyrimethamine and primaquine, which act against hepatic schizonts, thereby functioning as prophylactic agents and preventing invasion of erythrocytes; (ii) hypnozoiticides such as primaquine, which act against intrahepatic stages of *P. vivax* and *P. ovale*, thereby preventing relapses from the dormant phases; (iii) blood schizonticides such as chloroquine, mefloquine, quinine, pyrimethamine, halofantrine, sulfadoxine, and tetracyclines, which act against the asexual intraerythrocytic stages of *Plasmodium*species, thereby terminating the clinical manifestation of malaria; and (iv) gametocytocides such as primaquine and chloroquine, which act against the intraerythrocytic sexual forms of *Plasmodium*, thereby preventing transmission from human to mosquito (Schlitzer, 2007).

2.6.2.1 Classification of Antimalarial Drugs Based on Chemical Family

Based on chemical class, antimalarial drugs can be grouped as 4-aminoquinolines, arylamino alcohols, 8-aminoquinolines, antibiotics, antifolates, naphthoquinone, and sesquiterpene lactones (WHO, 2010).

2.6.2.1.1 4-Aminoquinolines

The 4-aminoquinolines complexes with ferriprotoporphyrin IX (FPP) in the digestive vacuole, thus preventing its polymerization. This action of 4-aminoquinolines ensures that the product of haemoglobin degradation remains toxic to the parasite (O'Neill *et al.,* 2006). Mutation of the transport protein on the parasite digestive vacuole facilitates the efflux of antimalarial drugs, thus leading to emergence of resistance (Wellems, 2004; Bray *et al.,* 2005). Amodiaquine and chloroquine are examples of 4-aminoquinolines.

2.6.2.1.1.1 Chloroquine

Chloroquine (CQ) has been the most used single drug for the treatment of malaria (Stocks *et al.,* 2001) and was effective until resistant strains started to emerge in the 1960s (Schlitzer, 2008). It is relatively tolerated by the body and has its therapeutic effect at the dosage of 10 $mgkg^{-1}$ b.wt, but with small selective index (Taylor and White, 2004). Adverse effects associated with chloroquine usage at therapeutic dosage include; dizziness, headache, nausea, malaise, dysphagia, pruritus, visual hallucinations, and confusion (Costedoat-Chalumeau *et al*., 2015; Bogaczewicz and Sobów, 2017). Long-term usage can cause rare but serious side effects such as retinopathy, neuromyopathy and bone-marrow toxicity (Schlitzer, 2007). While most strains of *P. vivax, P. malariae,* and *P. ovale* remain sensitive to chloroquine, more

than 80% of field isolates of *P. falciparum* have been reported to be resistant to chloroquine (Ginsburg, 2005).

Though the mechanism of action of chloroquine remains debateable, a common consensus is that it acts by inhibiting the polymerization of haem in the digestive vacuole of the parasite during its erythrocytic stage (Schlitzer, 2007). The digestion of the protein component of haemoglobin by various proteases yields peptides and haem, and the oxidation of the central iron in haem produces ferriprotoporphyrin IX also called haematin (Banerjee and Goldberg, 2001) which can cause membrane disruption, hence its toxicity to the parasite. Chloroquine interacts and forms complex with this ferriprotoporphyrin IX, thus preventing its polymerization by the parasite into a non-toxic insoluble molecule called hemozoin. The accumulation of ferriprotoporphyrin IX, and its chloroquine complex, therefore kills the parasite (Schlitzer, 2007).

2.6.2.1.2 Arylamino alcohols

Arylamino alcohols seem to interfere with the digestion of haem but its mechanism of action appears to be different from that of 4-aminoquinolines (Hoppe *et al.*, 2004). Resistance to arylamino alcohols appears to be mainly caused by polymorphisms of the *pf*mdr1 (*P. falciparum* multidrug resistance 1) gene which codes for the transport protein located on the membrane of digestive vacuole (Woodrow and Krishna, 2006). Changes in *pf*mdr1 sequence or copy number alters sensitivity to many antimalarial drugs.

The arylamino alcohols are quinine, mefloquine, halofantrine and lumefantrine. Some adverse effects associated with quinine include nausea, headache, tinnitus, hearing impairment, dysphoria, blurred vision, and arrhythmogenic potential (Schlitzer, 2007), while neuropsychiatric side effects, such as insomnia, depression,

and panic attacks are associated with mefloquine. High risk of cardiac arrhythmias is associated with halofantrine and its usage has been stopped in several countries, but lumefantrine is not associated with this risk, though it has lower antimalarial activity compared to halofantrine (Schlitzer, 2008).

2.6.2.1.3 8-Aminoquinolines

The only member of 8-aminoquinoline presently in use is primaquine. It is distinguished from other antimalarial agents as it acts against both the hepatic stage and sexual erythrocytic forms of all human *Plasmodium* species, and remains the only antimalarial drug approved for radical (anti-relapse) treatment of *P. vivax* (Schlitzer, 2008). Primaquine has the adverse effect of being potentially life-threatening causing haemolysis in people with glucose-6-phosphate dehydrogenase (G6PD) deficiency, a common genetic polymorphism in Africa (Taylor and White, 2004).

2.6.2.1.4 Antibiotics

Numerous antibiotics act against protein biosynthesis process of the mitochondrion and/or the apicoplast. Their action is usually directed towards parasite that invade a new (secondary) cell but not initial intracellular phase, hence they have delayed activity which is described as “delayed death phenotype” or “delayed kill effect” (Dahl *et al.*, 2006). They are therefore usually used in combination with faster acting antimalarial agents such as artesunate or fosmidomycin (Schlitzer, 2008). Examples of antibiotics used in malaria treatment are azythromycin, clindamycin, and doxycycline.

2.6.2.1.5 Antifolates

Antifolates act against dihydropteroate synthase (DHPS) and dihydrofolate reductase (DHFR), which are enzymes of tetrahydrofolate biosynthesis (Plowe, 2001).

Inhibitors of DHPS act as false substrates of DHPS or as competitive inhibitors of 4-aminobenzoic acid, and have weak antimalarial activity but act synergistically with inhibitors of DHFR. Sulphonamides such as sulphadoxine and dapsone inhibit DHPS while pyrimethamine and cycloguanil inhibit DHFR. Mutation over the years has caused substantial resistance against DHPS inhibitors (Schlitzer, 2008), likewise DHFR. The mutational status of DHFR is the key factor that determines the success of antifolate combination (Krudsood *et al.,* 2005).

2.6.2.1.6 Naphthoquinone

Naphthoquinone causes quick fall of the mitochondrial membrane potential by inhibiting the mitochondrial electron transport chain. It accomplishes this by attaching to the ubiquinone binding site of cytochrome bc_1 complex, thereby preventing the mobility of an iron-sulphur cluster protein that is essential for electron transport (Vaidya and Mather, 2005). Example of a naphthoquinone is atovaquone. The usage of atovaquone as a single agent has resulted in treatment failure with emergence of resistant strains. The sensitivity of cytochrome bc1 complex to atovaquone is reduced by over 1000-fold, due to alteration in a single amino acid composition of the ubiquinone binding site (Looareesuwan *et al.,* 1999; Srivastava *et al.,* 1999).

2.6.2.1.7 Sesquiterpene Lactones

This refers to artemisinin, its derivatives and analogues. Artemisinin is the active antimalarial ingredient of *Artemisia annua* (sweet wormwood). The sesquiterpene lactones act mainly against the ring stages of thelife cycle of *Plasmodium*species. They act early and are capable of reducing the parasite biomass in a single asexual cycle by about 10,000-fold (Woodrow *et al.,* 2005), hence are the most active and rapid acting antimalarial agents so far. The endoperoxide bridge is the

main structural feature of the artemisinins, and is thought to be cleaved by intraparasital iron-II sources to produce carbon-centred radicals (Schlitzer, 2008).

The sesquiterpene lactones include artemisinin, arteether, artemether, artesunate, and dihydroartemisinin, of which artemether and artesunate are the most widely used derivatives of artemisinin (Schlitzer, 2008). Artemether is better resorbed from the gastrointestinal tract and more lipophilic than artemisinin, hence tolerating oral administration (Kokwaro *et al.*, 2007), while artesunate is an unstable drug and the cleavage of its succinic ester releases dihydroartemisinin as the active agent. Artesunate has the advantage of being water soluble and can be administered for the treatment of severe malaria via intravenous route (Schlitzer, 2008). Animal experiments suggest neurotoxicity to be a concern regarding the use of artemisinin derivatives due to their biotransformation into dihydroartemisinin (Schmuck *et al.*, 2002).

2.6.2.1.7.1 Artemisinin-based Combination Therapies

Artemisinin-based combination therapy (ACT) is currently the best available treatment option approved for *P. falciparum* (WHO, 2016), and are formulated as combinations of artemisinins, mostly artesunate, with drugs such as amodiaquine, mefloquine, and sulfadoxine/pyrimethamine that were losing their efficacy as monotherapy (Schlitzer, 2008).

Artemisinins have the advantage of greatly reducing parasite loads by about 60% within 48 hours of commencement of administration but the disadvantage of having short plasma half-life of about 1 hour; hence, it is usually partnered with another drug that has far higher plasma half-life (Dondorp *et al.*, 2017). Therefore, the partner drug has a mandatory function of clearing the remaining parasite load.

The partner drug in an ACT should be sufficiently effective against the parasite otherwise, failure rate of ACT will be high even without artemisinin resistance (Gadalla *et al.,* 2013; Mishra *et al.*, 2014). And in areas with artemisinin resistance, the partner drug in ACT should be highly efficacious against the parasite without having to depend on the artemisinin component (Dondorp *et al.*, 2017), otherwise, high failure rate will arise. Examples of ACTs are artesunate-amodiaquine, artesunate-mefloquine, artesunate-sulfadoxine/pyrimethamine, artesunate-chlorproguanil/dapsone, artemether-lumefantrine, and dihydroartemisinin-piperaquine.

2.7 Resistance and Limitations of Therapeutic Options

The misuse or indiscriminate use of antimalarial drugs results in selective pressure, hence resistant strains, arising through mutations in sites of drug targets and/or biochemical alterations in the drug receptors (Foley and Tilley, 1998; Vennerstrom *et al.*, 1999). The spread of resistant strains has rendered antimalarial agents, that were once the hallmark of treatment, ineffective in most malaria-threatened areas (Schlitzer, 2008). Resistance of malaria parasite to artemisinin was first described in the year 2008, and artemisinin-based combination therapies (ACTs) which are presently used as the first-line treatment for uncomplicated malaria caused by *P. falciparum* are also increasingly losing their effectiveness as resistance continue to emerge (Dondorp *et al.*, 2011).

Artemisinin is best known for its ability to quickly clear ring-stage parasite hence artemisinin resistance is easily described by lower rate of blood parasite clearance, expressed as increase in parasitaemia half-life or as higher number of patient remaining parasitaemic at 72 hours after commencement of treatment (Flegg *et al.*, 2011; White, 2011).

Of note is that emergence of artemisinin resistance also facilitates the emergence of resistance towards the partner drug in an ACT and this is so because the partner drug alone is now exposed to high residual parasite biomass even after the 3-day ACT regimen, hence giving room for selection of partner drug resistance and consequently high treatment failure of artemisinin combination therapies (Dondorp *et al.*, 2017). High failure rates are now being recorded with usage of ACTs containing mefloquine and piperaquine in malaria treatment (Spring *et al.*, 2015; Phyo *et al.*, 2016).

Increase in treatment failure will ultimately lead to increase in the transmission of resistant strain of the parasite and this is made worse by the fact that both recrudescent infections, and infections with artemisinin-resistant parasites have higher gametocyte densities (Bousema and Drakeley, 2011; Ashley *et al.*, 2014). Continuous emergence of resistant strains of *Plasmodium*species poses a serious threat to malaria treatment and elimination efforts globally.

2.8 Approaches to Drug Development

There are diverse approaches to developing antimalarial drugs, and several significant current efforts include, but are not limited to, the following:

i. Optimization of therapy with available drugs, including the use of combined therapy;
ii. Development of analogues of existing agents;
iii. Discovery of natural antimalarial products;
iv. Investigation of compounds that were originally developed to treat other diseases;
v. Evaluation of drug resistance reversers; and
vi. Chemotherapeutic exploitation of novel molecular targets (Rosenthal, 2003).

2.8.1 Drug Combination

Combination of chemotherapeutic agents appears to be essential for malaria control, given the increase in resistance of *Plasmodium* speciesto monotherapy and advantages associated with combination therapy over monotherapy (Boni *et al.,* 2008).

Combination therapies offer the advantage of improved efficacy. Though the combinations should be carefully chosen such that it offers additive or synergistic potency rather than antagonistic potency (Fidock *et al.,* 2004). Also, drug combinations increase the chance of retaining clinical activity against parasite in case of emergence of resistance, more so that drug combinations are expected to reduce cases of resistance given their ability to attack the parasite from multiple points (Plowe, 2007). Also, if the combination of drugs is active against different cellular targets on the parasite, it may offer the advantage of decrease in dosage of individual drug, consequently reducing toxicity and/or cost (Fidock *et al.,* 2004).

It is important that the chemotherapeutic agents to be combined are both new drugs in the treatment of malaria. This is to ensure that resistant parasites to either agent are not already in circulation. Also, the agents should be efficacious and preferably have similar pharmacokinetics to ensure that a single agent is not exposed to resistance pressure (Fidock *et al.,* 2004). Unfortunately, it is challenging to have combination of agents that fulfil all these requirements.

2.9 Molecular Targets for Antimalarial Activity

Improved understanding of the biochemistry of *Plasmodium* species has led to identification of some sites on malaria parasite which are viable targets for antimalarial drugs (Figure 2). Some targets such as dihydrofolate reductase are shared by both human host and the parasite, although with some structural differences which are

exploited. On the other hand, some of these pathways or targets, such as haemozoin, are only present and/or important to the parasite but not to the human host (Fidock *et al.,* 2004). Inhibition of these targets suggest antimalarial capability of a compound, and could help unravel the mechanism of action of antimalarial agents. The different sites on the parasite that can be targeted for antimalarial action are; cytosol, food vacuole, mitochondrion, membrane, and apicoplast.

2.9.1 Cytosol of *Plasmodium* species

Some of the pathways in the parasite cytosol and molecules that can be targeted by antimalarial agents are folate metabolism (dihydrofolate reductase, dihydropteroate synthase), glycolysis (thymidylate synthase, lactate dehydrogenase, peptide deformylase), protein synthesis (heat-shock protein 90), glutathione metabolism (glutathione reductase), and signal transduction (protein kinases) (Fidock *et al.*, 2004).

2.9.1.1 Inhibition of Parasite Lactate Dehydrogenase

Unlike eukaryotes, *P. falciparum* appears to have incomplete tricarboxylic acid cycle (TCA) enzymes and a mitochondrial electron transport chain that is not coupled with ATP synthesis. Hence the parasite relies on anaerobic glycolysis for its source of ATP (Schlitzer, 2007).

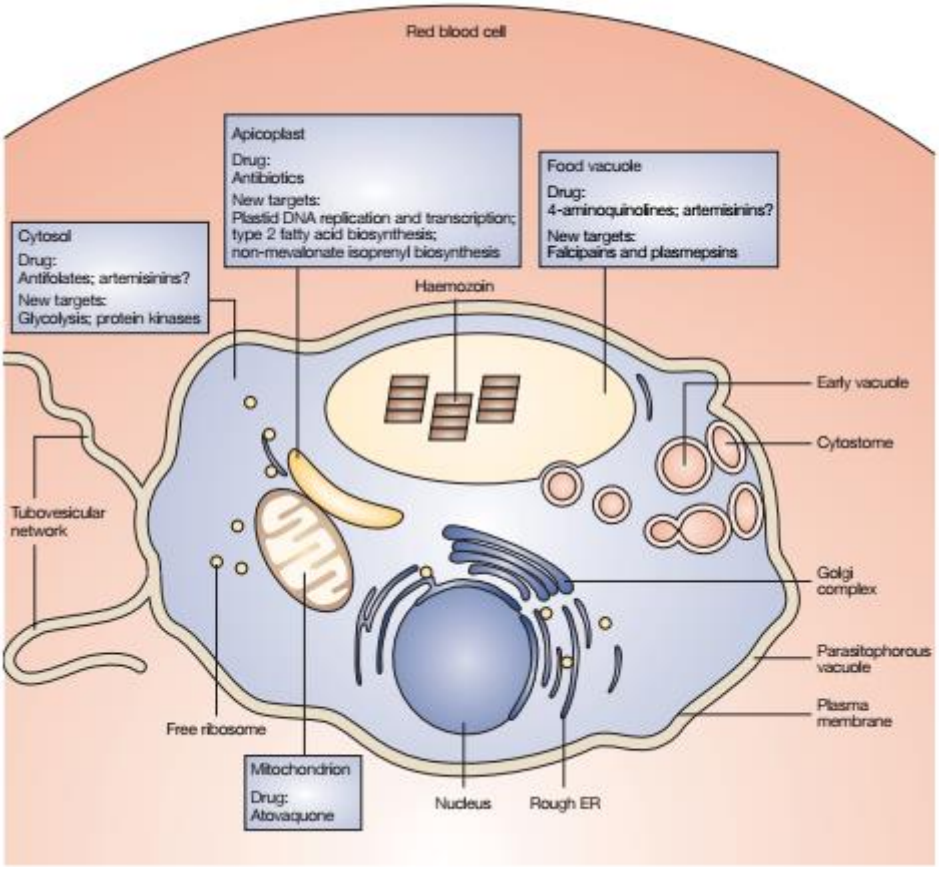

Figure 2: Representation of intracellular sites in *Plasmodium*species as targets for antimalarial drugs

Source: Fidock *et al.* (2004).

The parasite lactate dehydrogenase (pLDH) is a cytosolic enzyme that catalyses the final step in the glycolytic pathway. The enzyme is a 2-hydroxy acid oxidoreductase that catalyses the interconversion of pyruvate and lactate, with the concurrent interconversion of NADH and NAD^+ (Penna-Coutinho *et al.*, 2011). In *Plasmodium* species, LDH functions as the main source of NADH regeneration from NAD^+, and since the supply of NADH is a requirement for glycolysis, inhibition of the enzyme could starve the parasite of energy, impair its development, and cause its subsequent death (Cameron *et al.*, 2004).

The LDH of *P. vivax, P. malariae,* and *P. ovale* are closely related to those of *P. falciparum* lactate dehydrogenase (*Pf*LDH) having about 90% similarity (Penna-Coutinho *et al.*, 2011). But *Pf*LDH varies from the human isozymes of LDH, having a five-residue addition in the substrate-specificity site, change in sequence, and shows other structural and kinetic differences (Cameron *et al.*, 2004). Hence, any compound that inhibit the activity of PfLDH could disrupt the glycolytic pathway of the parasite, and has potent antimalarial potential (Read *et al.*, 1999).

2.9.2 Food Vacuole of *Plasmodium* species

The parasite digestive vacuole is an acidic (pH 5.0–5.4) organelle where, among other processes, haemoglobin degradation and haem polymerization (Figure 3) take place. Essential to these processes are proteins such as aspartic proteases (plasmepsins), cysteine protease (falcipain), metalloprotease (falcilysin), and haem polymerase (Banerjee and Goldberg, 2001).

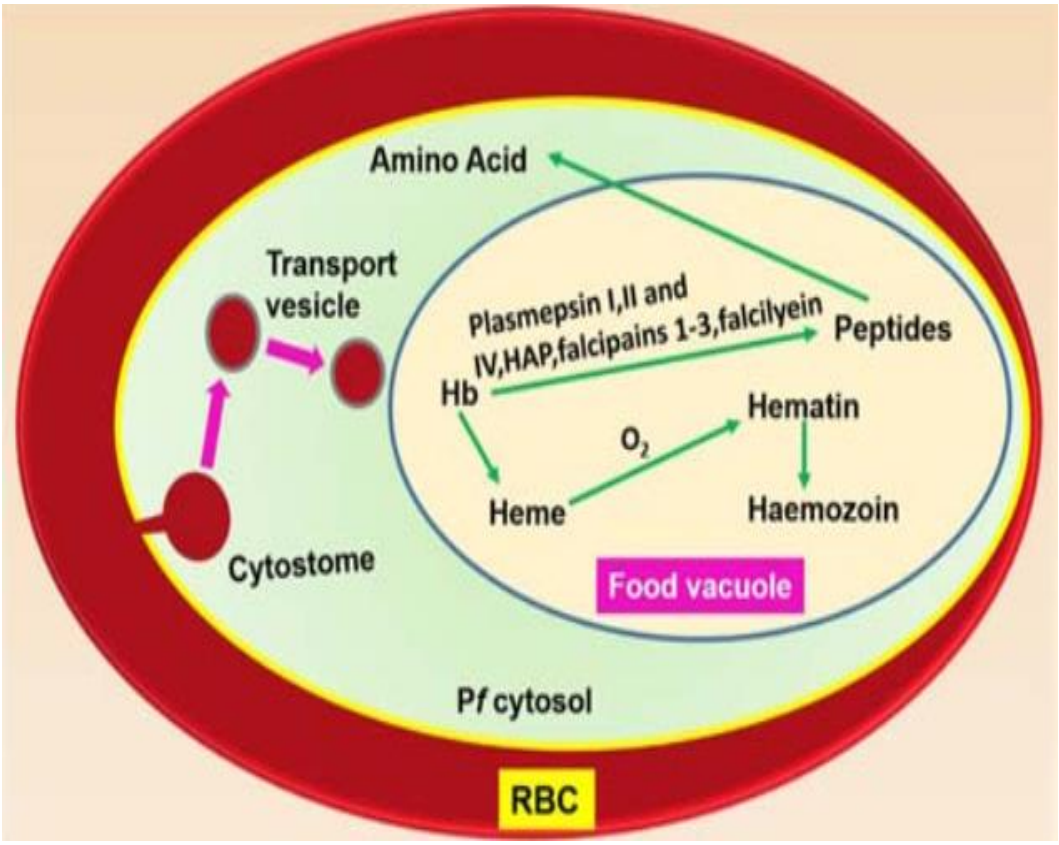

Figure 3: Illustration of haemoglobin ingestion and degradation by *Plasmodium* species

Source: Deshmukh and Trivedi (2014).

2.9.2.1 Haemoglobin Degradation

The *de novo* synthesis of amino acids during intraerythrocytic stages of *Plasmodium*species is very limited, hence the parasite relies on the amino acids from extracellular environment and degradation of haemoglobin for its protein synthesis (Banerjee and Goldberg, 2001). The parasite also degradeshaemoglobin at a rate that exceeds its need for amino acids, and the excess is diffused out. This is essentially to create space within the erythrocyte (host cell) because more space is needed for the parasite development as it multiplies during this intraerythrocytic phase (Ginsburg, 1990). The parasite also degrades haemoglobin to preserve its osmotic stability (Lew *et al.*, 2003).

During very early ring stages of development, the parasite may obtain nutrients micro-pinocytotically from the host erythrocyte cytosol (Banerjee and Goldberg, 2001). While during advance stages of development such as trophozoite stage, haemoglobin in the cytosol of host erythrocyte is taken up by the cytostome which is formed by the parasite plasma membrane and the parasitophorous vacuole membrane. Transport vesicles shoot off from the cytostome, move towards the digestive vacuole and fuse with it (Slomianny, 1990; Goldberg, 1993). The transport vesicle is hypothesized to be lysed by a phospholipase, therefore discharging its contents (Krugliak *et al.*, 1987).

The catabolism of haemoglobin seems to be the primary interest of the digestive vacuole rather than general protein catabolism (Banerjee and Goldberg, 2001). The haemoglobin tetramer is made up of polypeptide chains called globin, and prosthetic group of haem. The globin component is catabolised by different proteases in semi ordered steps. The action of plasmepsins I–IV (aspartate proteases) is followed

by the action of cysteine protease called falcipain, and further by the action of zinc protease called falcilysin (Ersmark *et al.,* 2006). These result in the generation of small peptides which are transported out of the parasite digestive vacuole into its cytosol, and are hydrolysed into amino acids by the action of aminopeptidases (Gavigan *et al.*, 2001).

Inhibition of these proteases results in the accumulation of haemoglobin thereby starving the parasite of nutrients, and denying it the space needed for its development, which ultimately leads to the death of the parasite (Banerjee *et al.*, 2002). Hence, inhibiting these proteases is of therapeutic importance in the treatment of malaria.

2.9.2.1.1 Plasmepsins

The plasmepsins are aspartic proteases formerly referred to as aspartic haemoglobinases. In *P. falciparum,* plasmepsinsI to X (Plm I to X) have been identified, with plasmepsin III aptly called histo-aspartic protease (HAP) (Coombs *et al.*, 2001). The transcription of Plm I takes place during the early ring stage of the life cycle of*Plasmodium* species while Plm II is optimally transcribed during the trophozoite stage (Francis *et al.,* 1997a). HAP and Plm IV become detectable from trophozoite stage and all Plm I, II, IV and HAP are expressed to schizont stage (Banerjee *et al.,* 2002). The proplasmepsins (proenzyme forms) are processed into mature forms by proplasmepsin convertase, which itself has been proposed as promising target (Banerjee *et al.*, 2003).

Plasmepsin I, II, and IV and HAP are expressed during the erythrocytic stage of *Plasmodium* species development;they are present in the digestive vacuole and are involved in degradation of haemoglobin, while Plm V, IX, and X are expressed during

this stage but appear not to function in the digestive vacuole. On the contrary, the expression of Plm VI, VII, and VIII is during the exo-erythrocytic stage of *Plasmodium* development (Banerjee *et al.*, 2002).

Both Plm I and II have amino acid sequence similarity of about 73%, while Plm IV and HAP have about 60% identity with Plm I and II (Dame *et al.*, 1994; Muraleedharan and Avery, 2007). The active site region of Plm I, II, and IV contains two aspartic acid residues, Asp32 and Asp215, while HAP has histidine in place of Asp32 (Berry *et al.*, 1999).

In the degradation of haemoglobin, Plm I and II appear to act first, cleaving native haemoglobin in the hinge region of the alpha chain at peptide bond Phe33-Leu34 (Gluzman *et al.*, 1994), while HAP and Plm IV seem to act later, preferring to break down globin rather than native haemoglobin (Banerjee *et al.*, 2002). The combination of these proteases acts synergistically, leaving haemoglobin faster than isolated action of each enzyme (Liu *et al.*, 2005). Activities of Plasmepsins remain high after complete degradation of haemoglobin at schizont stage, therefore suggesting additional functions (Banerjee and Goldberg, 2001).

Inhibitors of Plm has been shown to cause the death of *Plasmodium*, both *in vitro*and *in vivo* (Bailly *et al.*, 1992; Boss *et al.*, 2003; Ersmark *et al.*, 2006), hence proving Plm to be a viable drug target. Despite the similarity in sequence, the response of each Plm to inhibitors differs (McGillewie and Soliman, 2015), and chemical agents that can inhibit several Plm would be more efficient at killing the parasite and may delay emergence of resistance (Ersmark *et al.*, 2006). Mammalian aspartic protease such as lysosomal enzyme cathepsin D, which is the closest human equivalent to Plm differ from it by about 65% (Dame *et al.*, 1994; Muraleedharan and Avery, 2007).

Hence, cathepsin D could serve as marker for inhibitor selectivity of the host cell or the parasite (McKay *et al.*, 2011).

2.9.2.1.2 Falcipain

Falcipains are cysteine proteases localized in the digestive vacuole of the parasite, and falcipains 1, 2, 2′, and 3 have been identified. They contain cysteine in their catalytic site with which they hydrolyse susceptible peptide bonds through nucleophilic attack on the carbonyl carbon (Rosenthal, 2004). Falcipain-1 is encoded on chromosome 14, while others are encoded on chromosome 11. Falcipain-1 differs from others, having 40% sequence similarity to falcipain-2 and falcipain-3 (Sijwali *et al.,* 2004). Falcipain-2 and falcipain-2′ share 99% homology in the catalytic domain, while falcipain-2 and falcipain-3 have 68% similarity in sequence identity, and have catalytic domain amino-terminal extension that is absent in falcipain-1 (Rosenthal, 2004).

Falcipain-2 is expressed earlier than other falcipains and it is vital for haemoglobin degradation (Rosenthal, 2013). Falcipain-2 and falcipain-3 can partially cleave native haemoglobin but cleaves denatured globin faster, causing hydrolysis at multiple sites, and require reducing environment in the parasite digestive vacuole, which appears to be sufficiently provided by reductants such as cysteine and glutathione (Rosenthal, 2004). Falcipain-2 is the most prominent of the cysteine proteases performing about 90% of cysteine protease activity during trophozoite stage at which majority of haemoglobin degradation takes place (Shenai *et al.*, 2000). Falcipain-1 seems to be essential for oocysts production during parasite development in mosquito (Rosenthal., 2013).

The development of the parasite is hindered by inhibitors of falcipain (Rosenthal., 2013). Inhibition of cysteine proteases has been reported to cause swelling of the parasite digestive vacuole suggesting that the parasite transports cytosol contents of erythrocyte into its digestive vacuole unhindered, but its degradation of haemoglobin is inhibited as proven by the accumulation of large quantities of uncut native haemoglobin (Rosenthal, 1995; de Dominguez and Rosenthal, 1996; Rosenthal, 2004). Hence, the role of initial cleavage of native haemoglobin is not limited to plasmepsin.

Inhibition of cysteine proteases appears to also block the rupture of infected erythrocyte thereby preventing the release of infective merozoites which are needed to reinitiate the parasite asexual cycle in other erythrocytes (Salmon *et al.,* 2001; Wickham *et al.,* 2003; Rosenthal, 2004).

2.9.2.2 Haem Polymerization

The digestion of the protein part of haemoglobin leaves behind the potentially toxic heme part, and the oxidation of the central iron in haem produces ferriprotoporphyrin IX (FPP), also called haematin (Banerjee and Goldberg, 2001). Free haem and haematin cause toxicity through peroxidation of membranes, enzyme inhibition, productionof reactive species and impaired leukocyte function (Orjih *et al.*, 1981; Schwarzer *et al.,* 1992). Ferriprotoporphyrin IX can also compete with NADH for the active site of *Plasmodium* LDH resulting in parasite death (Egan and Ncokazi, 2005). To circumvent the toxicity threat of FPP, the parasite polymerizes the soluble FPP to insoluble, crystalline, non-toxic substance called haemozoin, also referred to as malaria pigment (Egan, 2003). It has been suggested that in the digestive vacuole,

histidine-rich protein (HRP) II and III promote polymerization of haematin (Sullivan *et al.*, 1996).

Compounds that inhibit polymerization of FPP can cause the death of *Plasmodium*species, hence their antimalarial activity (Krettli *et al.*, 2009). The quinoline derivatives are suggested to prevent formation of haemozoin by complexing with haematin (Ncokazi and Egan, 2005). Chloroquine is a known inhibitor of haem polymerisation.Notwithstanding the emergence of chloroquine-resistant strains, inhibition of haem polymerisation remains a viable target since the process of polymerization inhibition appears not to depend on any enzyme (Sanchez and Lanzer, 2000). Also, mutation could only result in production of altered proteins essential for drug action either to transport drugs, or bind drugs. Therefore, resistance strain cannot emerge against this target by a simple mutation (Wiesner *et al.*, 2003).

The synthetic equivalent of haemozoin is β-haematin, and the *in vitro* inhibition of β-haematin formation allows for the study of antimalarial capacity of compounds (Ncokazi and Egan, 2005).

2.10 *In silico* Drug Evaluation

Docking is an important approach in drug design and discovery process (Kitchen *et al.*, 2004). Molecular docking also called *in silico* study refers to computer-aided method for predicting the orientation of ligand within the receptor (protein) binding site, and the stability of the complex formed (Meng *et al.*, 2011). Molecular docking is performed to forestall the binding orientation of chemical compounds to target proteins. This enable the determination of the intermolecular interactions that stabilize the ligand-receptor complex, and the prediction of binding affinity and activity of such compounds (Huang and Zou, 2010; Chaudhary and Mishra, 2016).

Both the ligand and receptor can be modelled with software or obtained from appropriate database. The docking type could be rigid or flexible. In rigid docking (lock and key docking), both the ligand and receptor are kept fixed during the docking process, while in flexible docking (induced fit docking), the ligand, and receptor are conformationally flexible with the best pose selected from calculated free energy and surface orientation (Trosset and Scheraga, 1999).

Molecular docking software searches a large conformational space of possible binding modes, and predict the binding energy associated with each conformation (Kapetanovic, 2008). Hence, *in silico* study aims to determine the optimized conformation in which the free energy of the system is minimized (Chaudhary and Mishra, 2016), therefore enabling the prediction of the biological activity associated with the ligand.

In silico methods can be used to: identify drug targets, analyse active sites on the target molecule, study drug-likeness of ligand, dock ligand to receptor, rank the binding affinities and optimize ligands to improve binding features (Maithri *et al.*, 2016).

At variance with what is obtainable in biological system, the solvent molecules are removed from consideration in molecular docking, leaving behind the ligand and receptor. This is to reduce the enormous degree of freedom number connected to solvent molecules, therefore allowing effective sampling of the search space (Sousa *et al.*, 2006).

2.11 Combination of Compounds from Medicinal Plants

Over the years, there has been a shift from monotherapy to multidrug therapy, and this is especially so because of loss of effectiveness of drugs due to rapid upsurge

in resistance associated with monotherapy. Also, since multidrug promotes targeting multiple site of action to achieve optimum therapeutic effect, hence the preference and advocacy for combination approaches (Kerbel *et al.*, 2001; Degenhardt *et al.*, 2010).

In traditional practice, the formulation of antimalarial as mixture of several plants or plant parts is an age long approach. This allows interactions of chemical components of plants such as alkaloids, polyphenols, and terpenoids which have diverse biological activities to produce combined therapeutic efficacy (Rasoanaivo *et al.*, 2011) such as antimalarial and antioxidant activities. Such synergy is observed, for instance, in combination of polyphenols and terpenoids in which the polyphenols bind different molecular targets like proteins or glycoproteins, while the terpenoids have affinities for cell membranes, thereby working synergistically to permeate through cell membrane of invading organism to exert therapeutic effect (Wagner and Ulrich-Merzenich, 2009). In other situations, a component of the combination of secondary metabolites may not directly contribute to the therapeutic effect, but may function to enhance the overall efficacy of the other active components of the combination (Yang *et al.*, 2014), like is observed in reported cases of piperine combination with curcumin, ampicillin, or metronidazole (Shoba *et al.*, 1998; Amar *et al.*, 2010; Janakiraman and Manavalan, 2011).

2.11.1 Alkaloids

Alkaloids are cyclic, organic, nitrogen-containing bases present in diverse plants. They represent a group of secondary metabolites with various structures and functions (Roberts and Wink, 1998; Grycova´ *et al.*, 2007). While majority of alkaloids have only one nitrogen atom in their chemical structure, some possess up to five. The nitrogen atom(s) may occur as primary amine (RNH_2), secondary amine

(R_2NH) or a tertiary amine (R_3N) (Robbers *et al.*, 1996). Most alkaloids are colourless with a bitter taste, and are isolated in crystalline, amorphous, and non-volatile forms except low molecular weight alkaloids and those without oxygen atom in their structure, which occur in liquid form (Kukula-Koch and Widelski, 2017).

Rather than as free bases, alkaloids exist in tissues of plant as water-soluble salts of organic acids, esters, or combined with tannins or sugars (Kukula-Koch and Widelski, 2017). With few exceptions, alkaloids in the free base form are sparingly soluble in water but soluble in nonpolar organic solvents, whereas their salts are soluble in water but sparingly soluble in organic solvents (Kukula-Koch and Widelski, 2017).

Alkaloids have been reported to possess pharmacological properties such as antifungal, anti-inflammatory, antimicrobial, antiplasmodial, antioxidant, antiviral and vasodilatative activities and they also act as enzyme inhibitor (Wansi *et al.*, 2013).

The classification of alkaloids can be done according to chemical structure, biochemical origin and/or natural origin (Evans, 2009). Based on chemical structure, those that contain nitrogen in the side chain are called non-heterocyclic alkaloids (also referred to as biological amines or proto-alkaloids), while those that contain nitrogen in the heterocyclic ring are called heterocyclic alkaloids (also referred to as typical alkaloids), which can further be sub-classified, based on the ring type as indole, isoquinoline, norlupinane, piperidine, pyridine, pyrrole, pyrrolidizine, and quinoline alkaloids (Wansi *et al.*, 2013).

2.11.1.1 Palmatine

Palmatine is a yellow quaternary protoberberine alkaloid found in many plants (Pustovidko *et al.*, 2013; Dhingra and Bhankher, 2014). The structure of palmatine

(Figure 4) consists of 5,6-dihydrodibenzo(α,g)quinolizinium, a tetracyclic skeleton, with four methoxy groups at positions 2, 3, 9, and 10 (Vrba *et al.*, 2015).

Palmatine has been isolated from several medicinal plants such as *Berberis vulgaris* (Fatehi *et al.*, 2005), *Tinospora cordifolia* (Giri *et al.*, 2006), *Fibraurea tinctoria* (Su *et al.*, 2007), *Coptidis rhizome* (Jung *et al.*, 2009), *Mahonia oiwakensis* (Chao *et al.*, 2013), *Coptis chinensis* and *Berberis aristata* (Lo *et al.*, 2013).

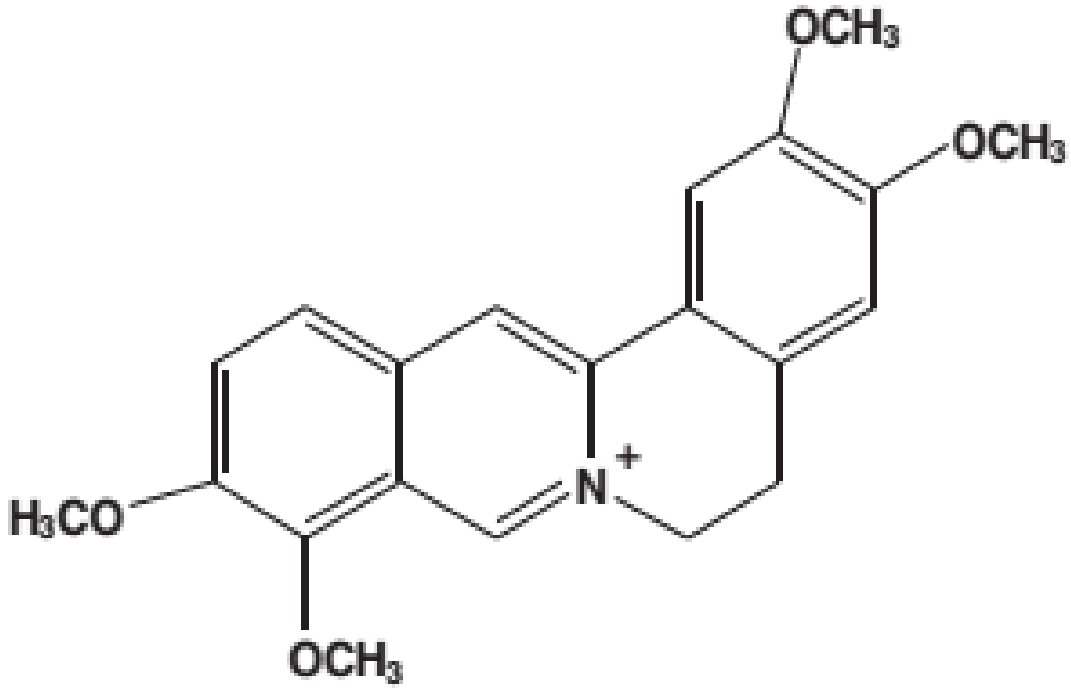

Figure 4: Structure of palmatine

Source: Liu *et al.* (2013).

Palmatine has been identified as the major antiplasmodial agent in *Enantia chlorantha* (Vennerstrom and Klayman, 1988) and leaf of *Annickia kummeriae* (Malebo *et al.*, 2013), and as the pharmacologically active constituent of some other plants, demonstrating significant anti-inflammatory effect, hepatoprotective activities, memory enhancing effect, antidepressant activity, antimicrobial and antimalarial activities (Smith, 1994; Dhingra and Kumar, 2012; Zhang *et al.*, 2012; Dhingra and Bhankher, 2014).

The bioavailability of palmatine has been reported to be apparently low in rats after oral administration (Ma and Ma, 2013), and this has been attributed to metabolism by intestinal microflora and liver microsomes (Yang *et al.*, 2009b).

The *in vitro* antiplasmodial activity of palmatine against multi-drug resistant K1 strain of *P. falciparum*has been reported, having anIC_{50} of 0.08 µg/mL and selectivity index (SI) of 1,154 (Malebo *et al.*, 2013).

2.11.1.2 Piperine

Piperine (1-piperoyl piperidine) is an amide alkaloid (Figure 5) found in *Piper nigrum* L. (black pepper) or *Piper longum* L (long pepper). Black pepper is a commonly used component of herbal antimalarial preparation (Jantarat, 2013), and piperine isolated from it has been reported to act as bioenhancer of other compounds (Lambert *et al.*, 2004).

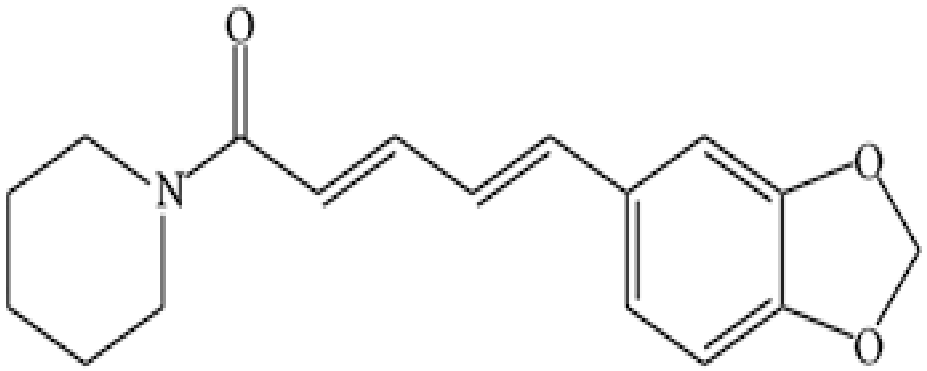

Figure 5: Structure of Piperine

Source: Cho and Yoon (2015).

The bioavailability and metabolism of chemical agents can be greatly altered by other plant constituents. This can be achieved through several mechanisms such as increase in permeability of the membraneof *Plasmodium*species to antimalarial agents, inhibition of pump mechanisms for drug efflux, modification of absorption, distribution, metabolism and excretion of active constituents (Williamson, 2001; Spinella, 2002; Gilbert and Alves, 2003).

Piperine has been reported to enhance the bioavailability of curcumin by about 2000%. This was suggested to be due to the inhibition of glucuronidation by piperine, and reduction of gastrointestinal transit rate (Shoba *et al.*, 1998). It has also been reported to enhance bioavailability by inhibiting efflux transporter (P-glycoprotein), and hepatic and non-hepatic drug metabolising enzymes (Bhardwaj *et al.*, 2002). Both P-glycoprotein and cytochrome P450 3A4 (CYP3A4) which piperine inhibits play major role in first-pass elimination of many drugs (Kesarwani and Gupta, 2013). It was also reported that 20mg/kg body weight of piperine enhanced the serum concentration, absorption and bioavailability of curcumin in both rats and humans with no adverse effects (Shoba *et al.*, 1998).

And piperine has also been reported to possess no antimalarial activity (Martinelli *et al.*, 2008). Thus, piperine may serve as a bio-enhancer for other natural products/synthetic compounds. However, piperine may not enhance bioavailability of all drugs, and may be inconsistence with some drugs (Kesarwani and Gupta, 2013). Therefore, for best result, its usage may follow traditional recommendation.

Piperine may be essential in chemotherapeutic formulation against malaria because bioenhancer may help delay/prevent emergence of drug resistance by increasing the absorption of drugs, altering activities of drug metabolising enzymes,

altering efflux transporter, delaying drug excretion, and enhancing drug affinity for targets (Kumar *et al.*, 2018).

2.11.2 Polyphenols

Polyphenols, also called phenolics, refer to a group of compounds that have one or more aromatic rings as well as one or more hydroxyl groups (Dai and Mumper, 2010). The phenolics function generally as defence chemicals against ultraviolet radiation, pathogens, parasites and predators (Dai and Mumper, 2010). The presence of hydroxyl groups and their relative position to the carboxylic group appears to be essential in determining the biological activity of polyphenols (Lu *et al.* 2006).

In animal and human, polyphenols have been shown to; have protective effects against oxidative stress, improve cardiovascular health, modulate signaling pathways, and have antimalarial effects (Hamilton *et al.*, 2004; Jayeola *et al.*, 2011; Giovannini and Masella, 2012; Khurana *et al.*, 2013). The antioxidant capacity of polyphenols is suggested to be enhanced when combined with other antioxidants (Dai and Mumper, 2010). Phenolics are water-soluble and have the major problem of bioavailability, but this can be improved by using bioenhancers (Kesarwani and Gupta, 2013).

Polyphenols can be categorized as phenolic acids, flavonoids, tannins and the less common stilbenes and lignans (Dai and Mumper, 2010). The phenolic acids category can be sub-classified as derivatives of benzoic acid such as methyl gallate, and derivatives of cinnamic acid such as coumaric, caffeic and ferulic acids (Dai and Mumper, 2010).

2.11.2.1 Methyl gallate

Methyl gallate (methyl 3,4,5-trihydroxybenzoate), a methyl ester of gallic acid, is a phenolic compound that is present in many plants (Fan *et al.*, 2014). This derivative of gallic acid has some hydroxyl groups (Figure 6) through which it can form bonds with many targetbiomolecules such as enzymes, carriers, ion channels, and receptors, causing their alteration, thereby exhibiting its therapeutic activities (Wang, 2007).

Methyl gallate has been isolated from diverse plants and plant parts. Among other plants and parts, it was reportedly isolated from leaf of *Sapium sebiferum* (Kane *et al.*, 1988), leaf of *Toona sureni* (Ekaprasada *et al.*, 2009), seed kernel of *Mangifera indica* (Nithitanakool *et al.*, 2009), stem bark of *Entada abyssinica* (Teke *et al.*, 2011), leaf of *Alchornia cordifolia* (Okomor *et al.*, 2012), fruit and stem bark of *Dacryodes edulis* (Atawodi *et al.* 2009; Zofou *et al.*, 2013) and the seed coat of *Givotia rottleriformis* (Kamatham *et al.*, 2015).

Methyl gallate has been reported to be capable of diverse biological activities such as antioxidative, anti-asthmatic, anti-inflammatory, anti-tumour, antiviral, vasodilative and immune modulatory activities, with attenuation of oxidative stress, and protection against DNA damage (Chaubal *et al.*, 2005; Acharyya *et al.*, 2012; Asnaashari *et al.*, 2014; Choi *et al.*, 2014; Khurana *et al.*, 2014). Also reported, is the strong bactericidal effect of methyl gallate, which it exhibits through inhibition of bacterial respiratory functions, thereby interfering with their energy metabolism (Fan *et al.*, 2014).

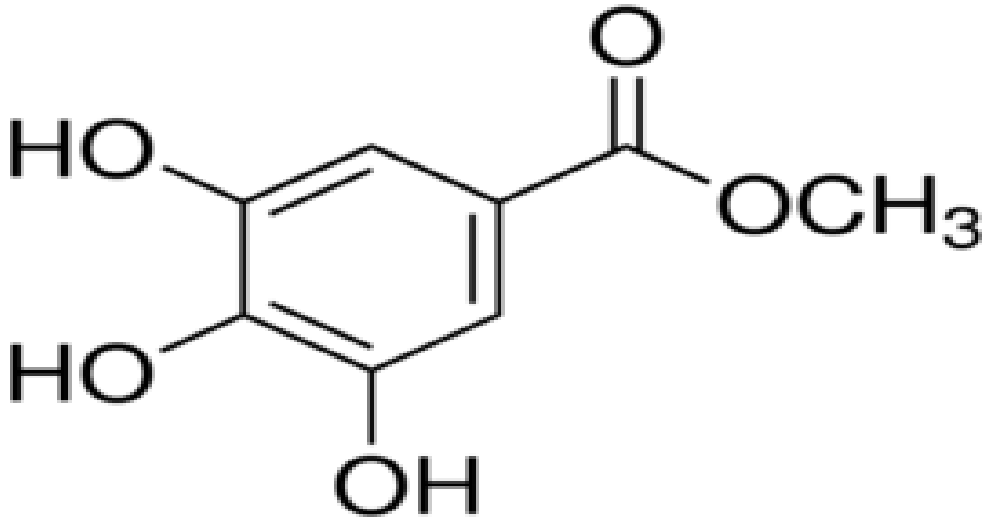

Figure 6: Structure of methyl gallate

Source: Lee (2013).

While methyl gallate and other low molecular weight phenolic compounds can act as antioxidants, they also possess the ability to act as pro-oxidants, interacting with target molecules to elicit therapeutic effects (Hagerman *et al.*, 1998; Galati and O'Brien, 2004; Tachibana *et al.*, 2004; Yang *et al.*, 2009a), and this depends on their level of assimilation into cells.

Methyl gallate has been reported to be subjected to *in vivo* sulphate and glucuronide conjugation after oral administration (Feng, 2006; Jiamboonsri *et al.*, 2015, 2016). Due to first pass effect, some phenolic compounds are eliminated fast before reaching systemic circulation, thereby leading to poor bioavailability and reduced efficacies (Wu *et al.*, 2011).

Methyl gallate reportedly has good *in vitro* antiplasmodial activity against 3D7 and the multidrug-resistant Dd2 strain of *Plasmodium falciparum* with IC_{50} of 0.37 µg/ml and 0.55 µg/ml respectively (Zofou *et al.*, 2013).

2.12 Reactive Species, Oxidative Stress, and Antioxidants in Malaria

The generation of reactive species has been reported to be increased during malaria infection. After a while, the production of reactive species (oxidants) becomes excessive, and this overwhelms the counter-acting antioxidant system, hence oxidative stress emerges which promotes systemic complications associated with malaria (Becker *et al.*, 2004; Sonnen *et al.*, 2010; Percário *et al.*, 2012).

2.12.1 Free Radicals and other Reactive Species

Free radicals refer to molecular species that contain unpaired electron(s). They are unstable, very reactive, and can remove electrons from biomolecules thereby causing their oxidation (Cheeseman and Slater, 1993).

Reactive species refer to both free radicals and non-radicals, that can directly initiate oxidation or be converted to radicals. These reactive species could be those that have unpaired electron(s) in its oxygen, referred to as reactive oxygen species (ROS) or others that have unpaired electron(s) in association with nitrogen, referred to as reactive nitrogen species (RNS). Examples of these reactive species are; superoxide anion radical ($O_2^{\bullet -}$), hydroxyl radical ($HO^{\bullet}$), alkoxyl radical ($RO^{\bullet}$), peroxyl radical ($ROO^{\bullet}$), and nitric oxide radical ($NO^{\bullet}$) (Nimse and Pal, 2015) while hydrogen peroxide (H_2O_2) and singlet oxygen ($^1_2O_2$) are reactive species that are non-radicals. Peroxynitrite ($ONOO^-$) is a very potent and versatile oxidant and it is produced by the reaction of superoxide anion radical and nitric oxide radical (Zhu *et al.*, 1992) as shown by the following equation;

$$NO^{\bullet} + O_2^{\bullet -} \rightarrow ONOO^-$$

These reactive species are generated through normal biochemical reactions of metabolism, and immune response to foreign materials. They can also be induced by dietary xenobiotics, and environmental factors such as smoke, radiation, and herbicides (Bagchi and Puri, 1998). Their generation in normal cells is continuous but regulated, and occur during such processes that involve respiratory chain, phagocytosis, cytochrome P-450 system, and prostaglandin synthesis (Liu *et al.*, 1999).

Reactive species are essential for cellular roles such as signal transduction, gene expression, immunity, and destruction of precancerous cells and infective agents (Salganik, 2001). However, excess radical must be neutralised by antioxidants to ensure that cells function optimally (Dasgupta and Klein, 2014). While reactive species could be produced as a defence mechanism in response to disease conditions, they could also be generated as a consequence of damages from these disease conditions

(Kehrer *et al.,* 2010). Several pathophysiological conditions are associated with reactive species as excessive radicals results in release of toxic derivatives, and/or damage to macromolecules (Sonnen *et al.,* 2010) which causes further cellular dysfunction. Reactive species attack on cellular membranes bring about increase in cell membrane permeability and the release of cytosolic constituents into extracellular fluid (Gupta *et al.,* 2005).

Reactive species can cause cellular damage through four major ways and occur through: damage to lipids of cell membranes and organelles, leading to their impairment; damage to proteins and amino acids; damage to genetic materials (RNA and DNA) thereby altering the function, growth and cellular repair; damage to lysosomes thereby causing the release of digestive enzymes which could result in self-digestion of cells (Aldred *et al.,* 2009). Malondialdehyde and 4-hydroxynonenal are indicators of lipids oxidation, 8-hydroxydeoxyguanosine is an indicator of DNA damage, while protein oxidation brings about loss of activity through thiol oxidation, carbonylation, unfolding and misfolding, and fragmentation (Pisoschi and Pop, 2015).

2.12.2 Oxidative Stress

Oxidative stress refers to state of imbalance in the rate of reactive species generation and the response of antioxidant defence system (Rizvi *et al.,* 2012). Oxidative stress occurs when the rate of reactive species generation far exceeds the ability of antioxidant system to detoxify these reactive species. This could result from either of the following or their combinations: (i) elevated levels of endogenous and exogenous reactive specie-producing compounds; (ii) reduction of reserves of non-enzymatic antioxidants; (iii) inactivation of enzymatic antioxidants; and, (iv) reduced production of enzymatic and non-enzymatic antioxidants (Lushchak, 2014).

While oxidative stress may arise from injury to tissues caused by trauma, toxins, drugs, and infections (Lobo *et al.*, 2010), it may also cause damages to tissues. The production of ROS and RNS is greatly increased during *Plasmodium* infection, and the reactive species cause degradation of cells especially red blood cells (both parasitized and non-parasitized) and consequently, oxidative stress (Isamah and Asagba, 2003; Bozdech and Ginsburg, 2004). In addition to the damages caused by *Plasmodium* to thebiological host, oxidative stress triggered by the infection also contributes to the pathogenesis of malaria and can lead to development of severe secondary complications (Becker *et al.*, 2004) such as endothelial dysfunction, microvascular obstruction, pulmonary oedema, anaemia, thrombocytopenia, ischaemia-reperfusion injury, liver and kidney dysfunctions (Autino *et al.*, 2012; Hanson *et al.*, 2015).

Plasmodium infection has been reported to cause peroxidation of membrane lipids, and alterations of cellular and extracellular constituents (Nimse and Pal, 2015) such as enzymes activities, electrolytes concentrations, and haematological make up.

2.12.3 Lipid Peroxidation

Lipid peroxidation is the oxidative degradation of lipids and involves removal of electrons from the lipids in cell membranes by free radicals thereby causing cell damage (Fuchs *et al.*, 2014). High level of reactive species can cause direct damage to lipids. These reactive species are produced, endogenously, primarily from mitochondria, endoplasmic reticulum, and plasma membrane (Moldovan and Moldovan, 2004), and can be stirred by stimuli such as pathogen infections, tobacco smoke, environmental toxins, herbicide/insecticides, ionizing radiation, and drugs (Ayala *et al.*, 2014). Polyunsaturated fatty acids of membranes are mostly affected

because of the presence of methylene (CH_2) bridge in between multiple double bonds (Fuchs *et al.,* 2014).

Lipid peroxidation can be segmented into three major processes of initiation, propagation, and termination. Production of fatty acid radical takes place during the initiation stage, and this radical reacts readily with molecular oxygen to yield peroxyl-fatty acid radical at the phase described as propagation stage. The termination stage is said to be achieved when radicals react to produce a non-radical specie (Muller *et al.*, 2007). Lipid hydroperoxides (LOOH) are the primary products of lipid peroxidation while aldehydes such as 4-hydroxylnonenal (4-HNE) and malondialdehyde are the main secondary products (Demir *et al.,* 2011; Ayala *et al.,* 2014).

2.12.3.1 Malondialdehyde

Malondialdehyde (MDA) is an end-product of enzymatic or non-enzymatic decomposition of arachidonic acid and polyunsaturated fatty acids (Ayala *et al.*, 2014).MDA, a marker of lipid peroxidation, is a highly unstable aldehyde that induces oxidative stress by forming covalent protein adducts (Goel *et al.,* 2005). The high reactivity of MDA is primarily based on its electrophilicity, hence very reactive towards nucleophiles likes basic amino acids such as arginine, histidine, and lysine (Ayala *et al.,* 2014).

Membrane fluidity is impaired by extensive lipid peroxidation of membranes. It also brings about inactivation of membrane-bound enzymes, and cell death (Goel *et al.,* 2005). And excessive MDA is associated with different pathological conditions such as liver disease, diabetes, cardiovascular diseases, and cancer (Li *et al.,* 2012; Garcia *et al.,* 2013).

2.12.4 Cellular Antioxidants

Antioxidants refer to molecules that are able to prevent, slow down or stop the oxidation of biomolecules, thereby delaying or inhibiting cellular damage, and usually perform this functions at low concentrations (Halliwell and Gutteridge, 1995; Young and Woodside, 2001). They perform their functions by scavenging radicals, donating electrons or hydrogen, decomposing peroxides, and/or by chelating metal ions (Lobo *et al.*, 2010). Enhanced activities of cellular antioxidants ensure that free radicals are effectively neutralized (Pal and Nimse, 2006), therefore preventing their damaging effects to cells.

The antioxidant defence mechanism of organism comprises of biomolecules and enzymes. Based on their reaction types in the intracellular and extracellular environments, antioxidants can be categorized as enzymatic and non-enzymatic. While the enzymatic antioxidants utilise cofactors such as copper, iron, manganese, and zinc to decompose and remove free radicals, non-enzymatic antioxidants function by disrupting free radical chain reactions (Nimse and Palb, 2015). Examples of enzymatic antioxidants are; superoxide dismutase, catalase, and glutathione systems (glutathione peroxidases, glutathione reductase, and glutathione-S-transferase). The non-enzymatic antioxidants include glutathione, uric acid, bilirubin, and albumin.

2.12.4.1 Enzymatic Antioxidants

2.12.4.1.1 Superoxide Dismutase (EC 1.15.1.1)

Superoxide dismutase (SOD) refers to family of metalloenzymes that catalyse the dismutation of superoxide anions to molecular oxygen and hydrogen peroxide, thereby rendering the superoxide anion less harmful and protecting cells from the deleterious effects of reactive species which could arise from the superoxide (Miller,

2012). The superoxide is a radical generated by one electron reduction of molecular oxygen, and the reaction catalysed by SOD can be represented generally as follows;

$$2O_2^{\bullet -} + 2H^+ \xrightarrow{SOD} H_2O_2 + O_2$$

The catalytic mechanism can be described by the following reaction sequence, whereby M represents the metal cofactor;

$$M^{3+} + O_2^{\bullet -} + H^+ \xrightarrow{SOD} M^{2+}(H^+) + O_2$$

$$M^{2+}(H^+) + O_2^{\bullet -} + H^+ \xrightarrow{SOD} M^{3+} + H_2O_2$$

Generation of superoxide anion occurs in normal oxidative processes such as aerobic metabolism, and oxidative phosphorylation. But the cellular level of this reactive specie is elevated during respiratory burst that takes place through stimulation of neutrophils and macrophages as immune response (Perry *et al.*, 2010) to pathological conditions such as malaria. Excessive generation of reactive oxygen species such as superoxide radical can cause inflammation, and cell injury, and Fenton chemistry-mediated DNA damage (Imlay *et al.*, 1988). Since the superoxide anion is membrane-impermeable, it must be dismutated where formed. Hence, SOD are found in mitochondria, cytosol and other compartments such as peroxisomes, microsomes, and extracellular matrix where oxygen is utilised and superoxide is formed (Bafana *et al.*, 2011).

SOD can be classified into three, based on their unique genes, peculiar protein folds, the metal ions required as cofactor, and distinct subcellular localizations. These are; Cu,Zn-SOD also called SOD1 (a cytosolic enzyme which uses copper and zinc as cofactor), Mn-SOD also called SOD2 (a mitochondrial enzyme which uses manganese

as cofactor), and EC-SOD also called SOD3 (an extracellular SOD) which is a structural homologous of SOD1 (Zelko *et al.*, 2002).

Dysfunctional or overwhelmed SOD results in oxidative damage to cells whereas elevated activities of the enzyme could protect against reactive oxygen species (Wheeler *et al.*, 2001; Elchuri *et al.*, 2005).

2.12.4.1.2 Catalase (EC 1.11.1.6)

Catalase (CAT) is a homo-tetramer antioxidant enzyme present in tissues that make use of oxygen. It is a constitutive enzyme with a "housekeeping" role of catalysing the reduction of hydrogen peroxide to water and molecular oxygen, utilising iron or manganese as cofactor. Hence, the action of CAT prevents the formation of hydroxyl radical from hydrogen peroxide and brings the detoxification process initiated by SOD to a safer end (Chelikani *et al.*, 2004). The reaction catalysed by CAT is represented as follows;

$$2H_2O_2 \xrightarrow{CAT} 2H_2O + O_2$$

While hydrogen peroxide is not a radical and its reaction with many biomolecules is modest, it can penetrate membranes and react with transition metals, such as Cu^{2+} and Fe^{2+} to produce very reactive specie such as hydroxyl radical (Kehrer *et al.*, 2010). Low cellular level of hydrogen peroxide is beneficial, regulating physiological processes such as platelet activation, signalling in cell proliferation, mitochondrial function, and redox status of cell (Dröge, 2002). But high cellular level of it could bring about damaging effects to organelles and normal cells (Ercal *et al.*, 2001). Therefore, it is important that the concentration of hydrogen peroxide within the cells be kept low through the activities of antioxidant enzymes such as CAT.

The K_m of catalase for hydrogen peroxide is high. Therefore, it functions slowly in the presence of low concentration of hydrogen peroxide, but effectively at high concentration of hydrogen peroxide. Implying that catalase is particularly important for its protective role against high concentration of cellular hydrogen peroxide observed during oxidative stress (Turrens, 2010).

The intracellular localization of catalase varies in organs. It is found primarily in the peroxisomes of most tissue, but localized in the cytosol of erythrocytes, and absent in most mammalian mitochondria (Radi *et al.,* 1991; Turrens, 2010), hence, the essential presence of glutathione peroxidase in mammalian mitochondria.

Malaria has been reported to significantly reduce the activity of catalase (Becker *et al.,* 2004), and dysfunctional catalase is often associated with several disease conditions (Kodydková *et al.,* 2014).

2.12.4.1.3 Glutathione Peroxidase (EC. 1. 11. 1. 9)

Glutathione peroxidase (GPx) is a metalloenzyme that uses the selenium at its active site to catalyses the reduction of hydrogen peroxide, through the transfer of reducing equivalents from glutathione (GSH) to hydrogen peroxide, to generate oxidized glutathione (GSSG) and water (Kehrer *et al.,* 2010). GPx also catalyses the reduction of lipid hydroperoxides to their corresponding alcohols, and detoxification of phase 1 electrophiles (Farrell, 2002). The catalysis of hydrogen peroxide and other peroxides such as organic hydroperoxides by GPx can be represented as follows;

$$H_2O_2 + 2GSH \xrightarrow{GPx} GSSG + 2H_2O$$

$$ROOH + 2GSH \xrightarrow{GPx} ROH + GSSG + H_2O$$

Unlike catalase, GPx has low $K_{m,}$ thus very effective at low levels of hydrogen peroxide (Kehrer *et al.,* 2010), and more effective compared to catalase at low peroxide concentration. There are about eight isozymes of GPx encoded by different genes. The enzyme is found in almost all cells and localized in the mitochondria and cytoplasm (Messner *et al.,* 2012).

GPx plays vital role in protecting cells from oxidative stress by inhibiting lipid peroxidation process (Gill and Tuteja, 2010). GPx deficiency could predispose individual to impaired antioxidant protection and consequently oxidative damage to proteins and membrane lipids (Rayman, 2005; Chabory *et al.*, 2009), which could result in cellular dysfunction and disease conditions.

2.12.4.1.4 Glutathione Reductase (EC 1.6.4.2)

Glutathione reductase (GR) is a homodimeric flavoprotein that catalyses the NADPH-dependent reduction of GSSG (oxidised glutathione) to GSH (glutathione in the reduced state) (Kehrer *et al.*,2010). GR therefore serves to regenerate reduced glutathione. The reaction catalysed by GR is represented as follows;

$$2\text{NADPH} + \text{GSSG} \xrightarrow{\text{GR}} 2\text{GSH} + 2\text{NADP}^{+}$$

Unlike SOD, CAT, and GPx, GR does not eliminate reactive species directly, rather makes available antioxidant enzyme (GSH) that can perform such role, and used by other antioxidant enzymes such as GPx for detoxification. Therefore, it can be categorised as a secondary antioxidant enzyme (Noori, 2012).

GR is highly conserved across organisms and this points out its essential role in aerobic life (Kehrer *et al.*,2010). It is found in all tissues that utilises glutathione, and localized in cytoplasm, mitochondria, and nuclei (Kehrer *et al.*,2010). GR is activated

by reduction in cellular levels of GSH (Messner *et al.*, 2012), and has been shown to increase during malaria infection (Gallo *et al.*, 2009; Fabbri *et al.*, 2013).

2.12.4.1.5 Glutathione-S-Transferase (EC 2.5.1.18)

Glutathione-S-transferases (GST) is a family of enzymes that play significant part in metabolism and detoxification of several endogenous compounds and xenobiotics (Oakley, 2011).

GST has two active sites referred to as the G site (GSH-binding site) and H site (substrate-binding site). While the G site is highly conserved and has a primary role of binding glutathione, the H site which is located adjacent to the G site, has highly variable regions and binds the hydrophobic substrate (Wu and Dong, 2012). GST is of different isoforms which are made up of two similar subunits and show a common fold. They are classified into three families of cytosolic, microsomal, and mitochondrial GST (Wu and Dong, 2012; Mazzetti *et al.*, 2015).

GST catalyses the conjugation of glutathione (GSH) to electrophiles. This forms glutathione-S-conjugate, which is more water soluble and easily excreted, thereby forbidding the interaction of electrophilic metabolites with cellular macromolecules (Kehrer *et al.*,2010), and preventing cellular damage or formation of radicals. This therefore ensures detoxification. Also, GST functions as transport proteins, binding to unconjugated bilirubin and ensures its transport to endoplasmic reticulum where they are conjugated with glucuronic acid (Gourley, 2004; Smith *et al.*, 2013). The reaction catalysed by GST, utilising GSH as co-substrate, can be represented as follows;

$$\mathrm{GSH} + \mathrm{R-X} \xrightarrow{\mathrm{GST}} \mathrm{GSR} + \mathrm{H-X}$$

Furthermore, GST functions as antioxidant enzyme displaying glutathione peroxidase activity which is independent of selenium. Hence, metabolising reactive species and offering protection against oxidative stress (Osman *et al.,* 2016).

2.12.4.2 Non-Enzymatic Antioxidant

2.12.4.2.1 Reduced Glutathione

Reduced glutathione (GSH) is a low molecular weight, non-enzymatic antioxidant defence molecule. It is a tripeptide synthesized from glutamate, cysteine, and glycine in an energy-demanding reaction catalysed consecutively by cytosolic enzymes called γ-glutamylcysteine synthetase and GSH synthetase (Wu *et al.,* 2004). The cysteine residue of GSH is its key functional element containing a reactive thiol group with which GSH performs its roles, and GSH is a major source of reduced thiols (–SH) in cells. Low levels of these reduced thiols are associated with disorders that result from elevated production of free radicals (Muttigi *et al.,* 2009).

GSH is mostly found in cytosol, but also present in mitochondria, peroxisomes, nuclear matrix, endoplasmic reticulum, and in lower concentration in extracellular fluid (Lu, 2001; Jones, 2002).

Non-enzymatically, GSH readily reduce electrophilic substances, while itself is oxidized to glutathione disulphide (GSSG), and efflux of GSSG from cells will result in lower intracellular concentration of GSH (Wu *et al.,* 2004). Under normal physiological conditions, the ratio of GSH to GSSG is greater than 10, and its commonly used as a measure of the cellular redox state (Griffith, 1999) and anti-oxidative capacity of cells, though this ratio could be altered by other redox couples such as NADPH/$NADP^+$ (Jones, 2002). Cellular GSH concentration is easily maintained through replenishment from its oxidized (disulphide) form by the action of

glutathione reductase. But homeostasis of GSH is mainly achieved by *de novo* synthesis whenever GSH is used up via detoxification processes or by GSSG excretion (Mazzetti *et al.*, 2015).

GSH can perform its roles directly (non-enzymatically), or indirectly via enzymatic reactions (Fang *et al.*, 2002). Antioxidant defence role of GSH include; scavenging free radicals, removing hydrogen and lipid peroxides, and preventing oxidation of biomolecules (Wu *et al.*, 2004). Also, GSH has metabolic and regulatory roles which include; storage and transport of cysteine biomolecules, synthesis of leukotrienes and prostaglandins, DNA and protein synthesis, cytokine production and immune response, signal transduction and gene expression (Wu *et al.*, 2004).

Lower intracellular concentration of GSH is observed in cases of oxidative stress, protein malnutrition, and several pathological conditions (Lu, 2001).

2.13 Studied Organs

The organs considered in this study include liver, kidney, heart, and brain.

2.13.1 The Liver

The liver is the largest internal organ. The liver (Figure 7) is made up of two lobes, the bigger right lobe and the smaller left lobe, and occupies the centre and upper right abdominal chamber, below the diaphragm (Lefkowitch, 2011). The structural unit is called liver lobule, and each has network of capillaries called sinusoids which receive oxygenated blood from hepatic artery. The sinusoids also receive blood with nutrients and xenobiotics from the digestive organs and spleen via the portal vein. The liver performs its functions with this double blood supply, and then move blood out of the liver to the inferior vena cava through hepatic veins which is formed from unification of central veins present in each lobule (Scanlon and Sanders, 2007).

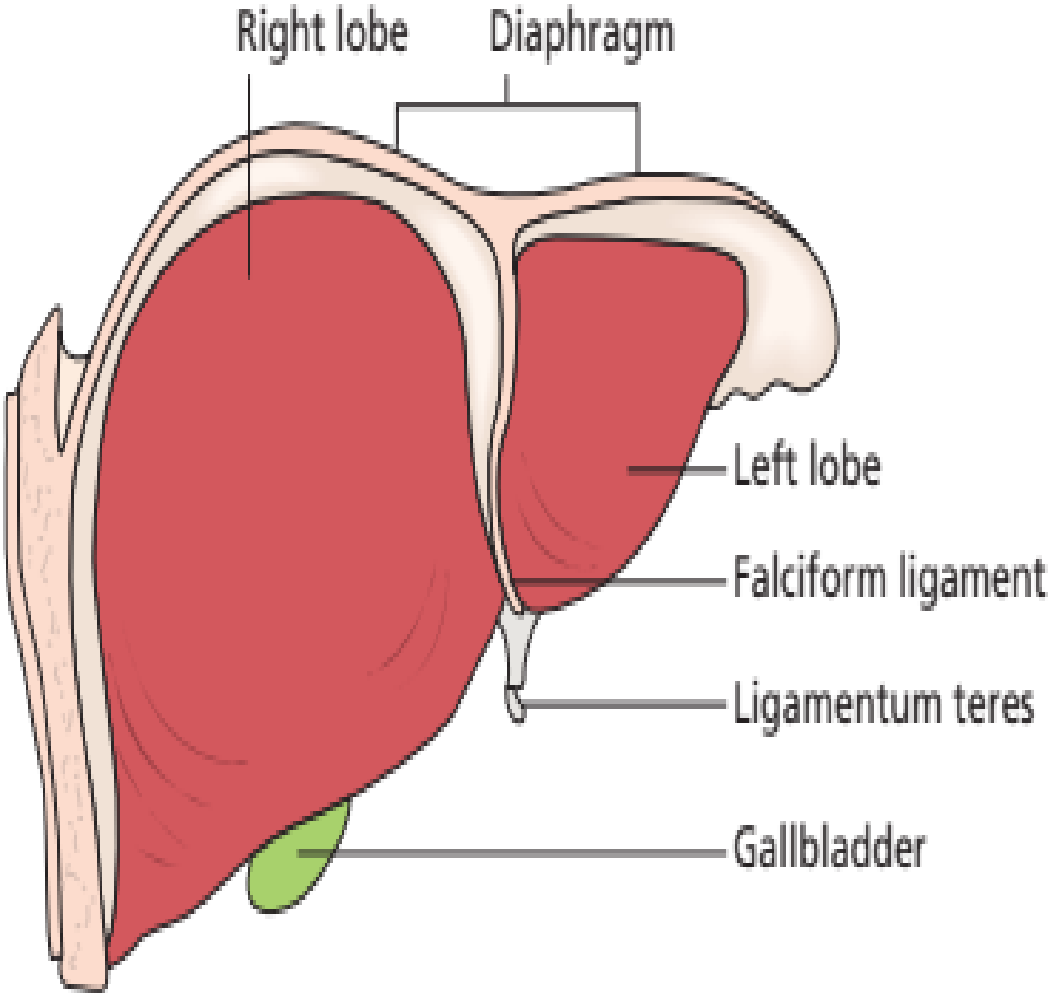

Figure 7: The anterior view of the liver

Source: Lefkowitch (2011).

2.13.1.1 The Cells and Functions of the Liver

The liver structure is functionally made up of at least seven types of cells which can be classified as parenchymal cells (hepatocytes), and non-parenchymal cells (stellate cells, sinusoidal endothelial cells, Kupffer cells, cholangiocytes, pit cells, and lymphocytes of different phenotypes) (Tsutsumi *et al.*, 2017), and these cells perform series of biochemical and metabolic functions. The liver is the site for synthesis of albumin and most plasma proteins with major exceptions such as immunoglobulins and von Willebrand factor, a clotting factor (McPherson and Pincus, 2011). The liver is also responsible for the metabolism of carbohydrates, proteins, and lipids, production of bile, storage of vitamins and minerals, and detoxification of xenobiotics (Lefkowitch, 2011).

The hepatocytes are the most abundant type of cell in the liver (about 70% of the liver mass), and perform majority of its synthetic, storage, and metabolic functions. This they accomplish through the presence of several mitochondria, lysosomes, peroxisomes, rough and smooth endoplasmic reticulum, Golgi apparatus, and many transport vesicles (Tsutsumi *et al.*, 2017). The stellate cells, along with hepatocytes, contribute to the metabolism of vitamin A and store them in lipid enclosures. They also function in growth factors production, and synthetize, secrete, and degrade components of the perisinusoidal extracellular matrix (Tsutsumi *et al.*, 2017).

The Kupffer cells are the liver specialised macrophages performing their phagocytic action of clearing bacteria, weakened erythrocytes, and damaged hepatocytes. They contain abundant lysosomes, and along with sinusoidal endothelial cells, they form the main system for the removal of weak cells and proteins (Tsutsumi *et al.*, 2017). The pit cells are the structurally and functionally modified form of blood

natural killer cells, and participate in first–line, innate defence against bound tumour cells and viral infection (Cerwenka and Lanier, 2001; Waldhauer and Steinle, 2008). The lymphocytes of different phenotypes form part of the liver-based immune system, essential for presentation of antigen, removal, or neutralization of several foreign materials that get to the liver from the gut, and play regulatory role in liver repair (Ferrari and Mondelli, 2009).

2.13.1.2 Pathological Conditions of the Liver

Xenobiotics are majorly metabolised in the liver, and this takes place primarily in hepatocyte microsomes, and liver damage that affects microsomes results in compromised metabolism of xenobiotics (McPherson and Pincus, 2011). The detoxification process is also associated with production of reactive species that interact with hepatic macromolecules, and consequently causing hepatic damage (Fausto, 2000). Examples of pathological conditions of the liver include; hepatitis, cirrhosis, cholestasis, jaundice, and steatosis.

2.13.1.3 Liver Function Indices

Liver function indices refer to parameters used for evaluating abnormalities in liver functions. They are used to screen for liver damage, assess severity, and response to treatment (Mukherjee and Gollan, 2011). Also, hepatic cells, being highly metabolically active cells, contains several enzymes that are leaked into the plasma in cases of hepatic injury, hence are useful for diagnosis (McPherson and Pincus, 2011). Some of the liver function indices are; total protein, albumin, globulin, and bilirubin concentrations.

2.13.1.3.1 Plasma Total Protein Concentration

Total plasma protein concentration reveals the amount of different proteins in plasma. This include molecules responsible for clot formation such as clotting factor and fibrinogen which are not captured in total serum protein concentration (Smith *et al.*, 2013). Hence, plasma protein concentration is about 0.3–0.5 g/L more than serum protein (Smith *et al.*, 2013). The main fractions of plasma proteins are albumin, globulins, and fibrinogen (Ochei and Kolhatkar, 2000), but the major plasma proteins measured are albumin and globulin.

Plasma proteins are synthesized and secreted from hepatocytes with the exception of immunoglobulins which are produced by B-lymphocytes (Eckersall, 2008). The characteristic function of each plasma protein is determined by the number, the types, and the sequence of amino acids it has (Ochei and Kolhatkar, 2000).

The ratio of plasma albumin to globulin may be altered by liver diseases (Ochei and Kolhatkar, 2000). Also, the level of total protein in plasma/serum can be altered by hydration status of the system. The level of total protein is falsely elevated during dehydration, likewise that of albumin and globulins. Hence, hypoproteinaemia which is associated with anaemia and other conditions may be masked during dehydration (Smith *et al.*, 2013). Also, hyperproteinaemia may arise from dehydration whereby there is water loss without change in the level of protein fractions (Eckersall, 2008).

2.13.1.3.2 Plasma Albumin Concentration

The total serum protein concentration is made up of about 50% albumin and albumin account for approximately 75% of plasma colloidal activity (Smith *et al.*, 2013). Function of albumin include maintenance of osmotic pressure and blood volume, transportation of endogenous and exogenous substances such as drugs,

metabolites and molecules that are lipophilic like bilirubin, fatty acids, and cholesterol (Evans, 2002; Eckersall, 2008).

The synthesis of albumin takes place in hepatocyte and its rate of synthesis is controlled by colloid osmotic pressure, and hormones such as cortisol, thyroxine and insulin (Evans, 2002). Reduction in osmotic pressure, and pathophysiological alterations during infectious or inflammatory disease stimulate secretion of albumin as a way of restoring it back to normal level (Evans, 2002; Eckersall, 2008). The catabolism of albumin takes place in tissues such as kidney, liver, and muscle and is degraded by action of protease (Evans, 2002; Prinsen, 2004).

Albumin has half-life of about 20 days and as such, may be a late indicator of pathological condition (McPherson and Pincus, 2011; Goldstein-Fuchs and LaPierre, 2014). Reduction in plasma level of albumin may indicate inflammatory conditions (Smith *et al.*, 2002), and in chronic situation, may suggest renal loss of albumin, or compromised hepatic synthesis of albumin (Grauer, 2005; Eckersall, 2008). Hypoalbuminemia is a feature of chronic liver disease but may indicate terminal liver cirrhosis when accompanied by significant reduction in total protein (Sevelius and Andersson, 1995). Since albumin is osmotically active, hypoalbuminaemia often lead to oedema (McPherson and Pincus, 2011).

2.13.1.3.3 Plasma Globulin Concentration

A number of heterogeneous proteins make up globulins, and these include transport proteins, coagulation factors, mediators of inflammation and immunoglobulins. With the exception of immunoglobulins which are produced by B lymphocytes in bone marrow, spleen, and lymph nodes, majority of globulins are synthesized by the liver (Eckersall, 2008; Smith *et al.*, 2013).

Globulins can be categorised, based on size and charge, as alpha, beta, and gamma globulins. While alpha globulin (such as ceruloplasmin) and beta globulin (such as transferrin and plasmin) act as enzymes and transport proteins, gamma globulin (immunoglobulins) function as antibody (Cunningham-Rundles, 1998; Guerra and Porbén, 2015; Shenton *et al.*, 2015).

Hyperglobulinaemia may occur in response to inflammation, presence of pathogen or falsely by dehydration (Smith *et al.*, 2002; Eckersall, 2008).

2.13.1.3.4 Plasma Bilirubin Concentration

Bilirubin is a yellowish pigment that occurs as conjugated (direct) and unconjugated (indirect) forms. It is mostly transported in a bound form with albumin with only a small fraction of existence as free bilirubin. This is so because bilirubin is highly insoluble in water in its common isomeric trans-form, though the cis-form, made possible by photoisomerization, is more water soluble and can be excreted in urine (McPherson and Pincus, 2011). Likewise, conjugated bilirubin is water soluble, therefore, it can be filtered by glomerulus and excreted in urine.

Bilirubin is derived largely from the degradation of haem from haemoglobin but can also be derived from unsuccessful erythropoiesis and from different haem proteins such as myoglobin and cytochromes. The daily formation of bilirubin in healthy adult is about 250–350 mg (Dancygier, 2010). Methaemoglobin from erythrocyte is split to free globin chain and haem mainly by macrophages of spleen. The haem is oxidized to biliverdin by microsomal haem oxygenase with corresponding release of iron. Tis biliverdin is then reduced to bilirubin by biliverdin reductase, a NADPH-dependent enzyme. The bilirubin is then transported, in a bound form with albumin, to the liver and enters hepatocyte by either passive diffusion or receptor-

mediated endocytosis (via the membrane surface in contact with sinusoids) (McPherson and Pincus, 2011). Within the hepatocyte, bilirubin is transferred through series of protein complexes to smooth endoplasmic reticulum (SER) where it becomes a substrate of glucuronyl transferase for conjugation with glucuronic acid (present as uridine diphosphoglucuronic acid). Conjugated bilirubin is thereafter secreted into the canaliculi by energy-dependent mechanism (McPherson and Pincus, 2011).

The plasma concentration of bilirubin is determined by extrahepatic bilirubin formation, its transport in plasma (bounded to albumin), its uptake, conjugation and transport across hepatocyte, and its canalicular biliary excretion (Dancygier, 2010).

The plasma level of bilirubin could serve as a measure of metabolic capacity of the liver. Impairment of bilirubin metabolism can result in elevated plasma levels of unconjugated, or conjugated bilirubin. Elevated plasma level of Unconjugated bilirubin can arise from haemolysis whereby the rate of bilirubin production exceeds that of its clearance, or from ineffective erythropoiesis. Rise in plasma level could also be due to low activity of glucuronyl transferase essential for conjugation process, that is, normal production of bilirubin but decreased hepatic conjugation (Dancygier, 2010). In addition, fasting in healthy individual can also result in elevated level of unconjugated bilirubin. On the other hand, elevated plasma level of conjugated bilirubin could arise from biliary obstruction caused by stone made up of bilirubin or cholesterol. Obstruction can also arise from inflammation of the biliary tract. Some drugs such as androgens can also result in elevated levels of conjugated bilirubin. In cases of toxic destruction of hepatocyte by chemicals, viral infection or traumatic conditions, cellular injury results in blockage of both bilirubin conjugation and excretion of conjugated bilirubin, consequently leading to elevated plasma levels of both conjugated and unconjugated bilirubin (McPherson and Pincus, 2011).

Bilirubin can function as an antioxidant, at low concentrations, by scavenging reactive species and preventing peroxidation of membrane lipids (Pisoschi and Pop, 2015). But it can also act as prooxidant, at high concentrations, by causing oxidative stress through generation of intracellular reactive species which could serve to inhibit multiplication of parasite, or cause damages to cells and induce apoptosis (Kumar *et al.*, 2008). Therefore, bilirubin may either be in response to oxidative stress or an inducer of oxidative stress.

2.13.2 The Kidney

The kidneys are two bean-shaped structures positioned in the upper abdominal cavity, behind the peritoneum, on each side of the vertebral column (Hall, 2011). Three areas of the kidney (Figure 8) can be distinguished. The first is the outer tissue layer which is made of renal corpuscles and convoluted tubules and is called renal cortex. The second is the inner tissue layer which is made of loops of Henle and collecting tubules, and is called the renal medulla, while the third area is called the renal pelvis and it is cavity within the kidney formed by the expansion of the ureter (Scanlon and Sanders, 2007).

The functional and structural unit of the kidney is called nephron (Figure 9). While each unit of the kidney has about 1 million nephrons, each of these has two main parts, referred to as the renal corpuscle, and the renal tubule (Barrett *et al.*, 2010). The renal corpuscle consists of a glomerulus which is a network of capillaries surrounded by a Bowman's capsule, and renal filtration occurs at this part of the nephron. Blood pressure within the glomeruli forces plasma, and dissolved substances into the Bowman's capsules, to form renal filtrate. Glomerular filtration is selective only in terms of size, but not in usefulness of materials (Scanlon and Sanders, 2007).

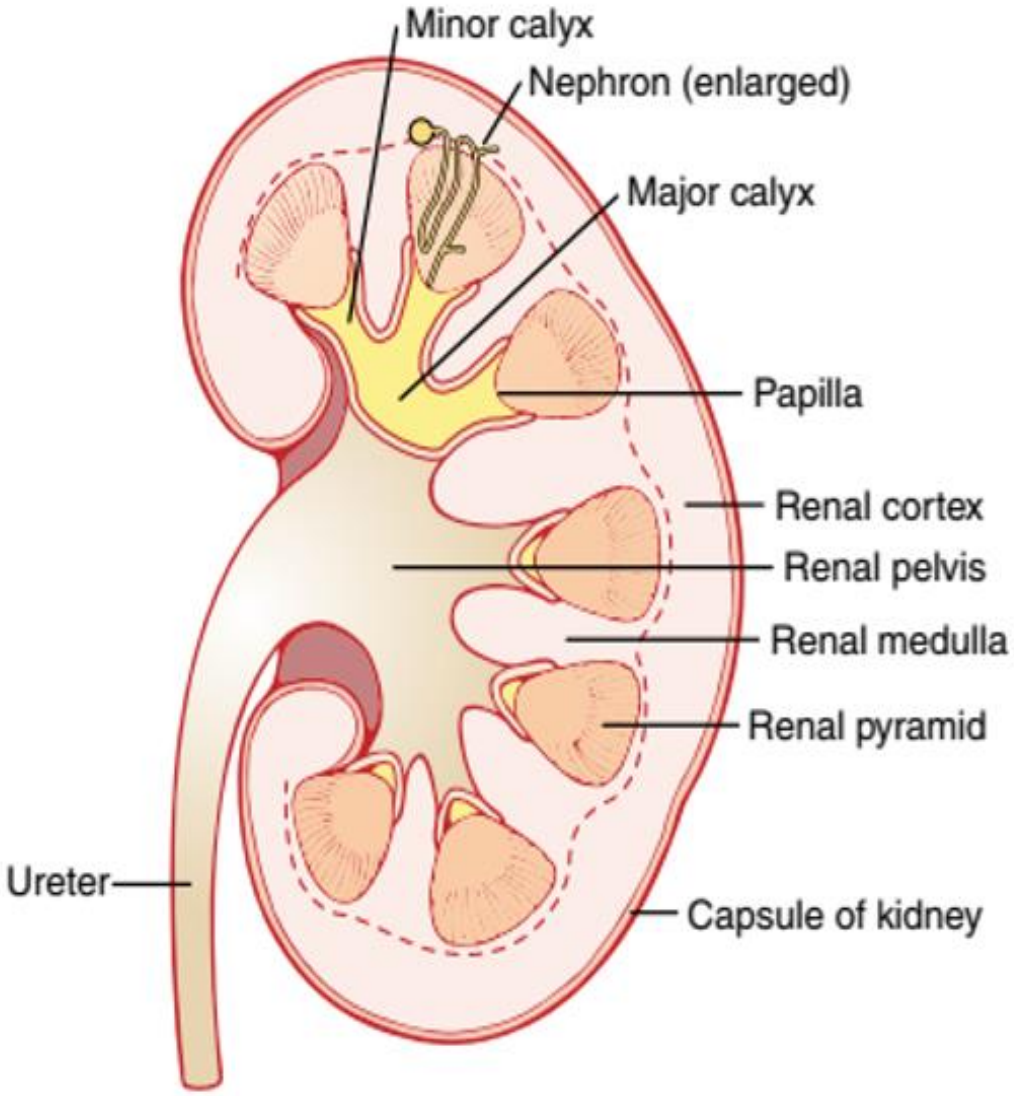

Figure 8: Structure of the left kidney showing internal parts

Source: Hall (2011).

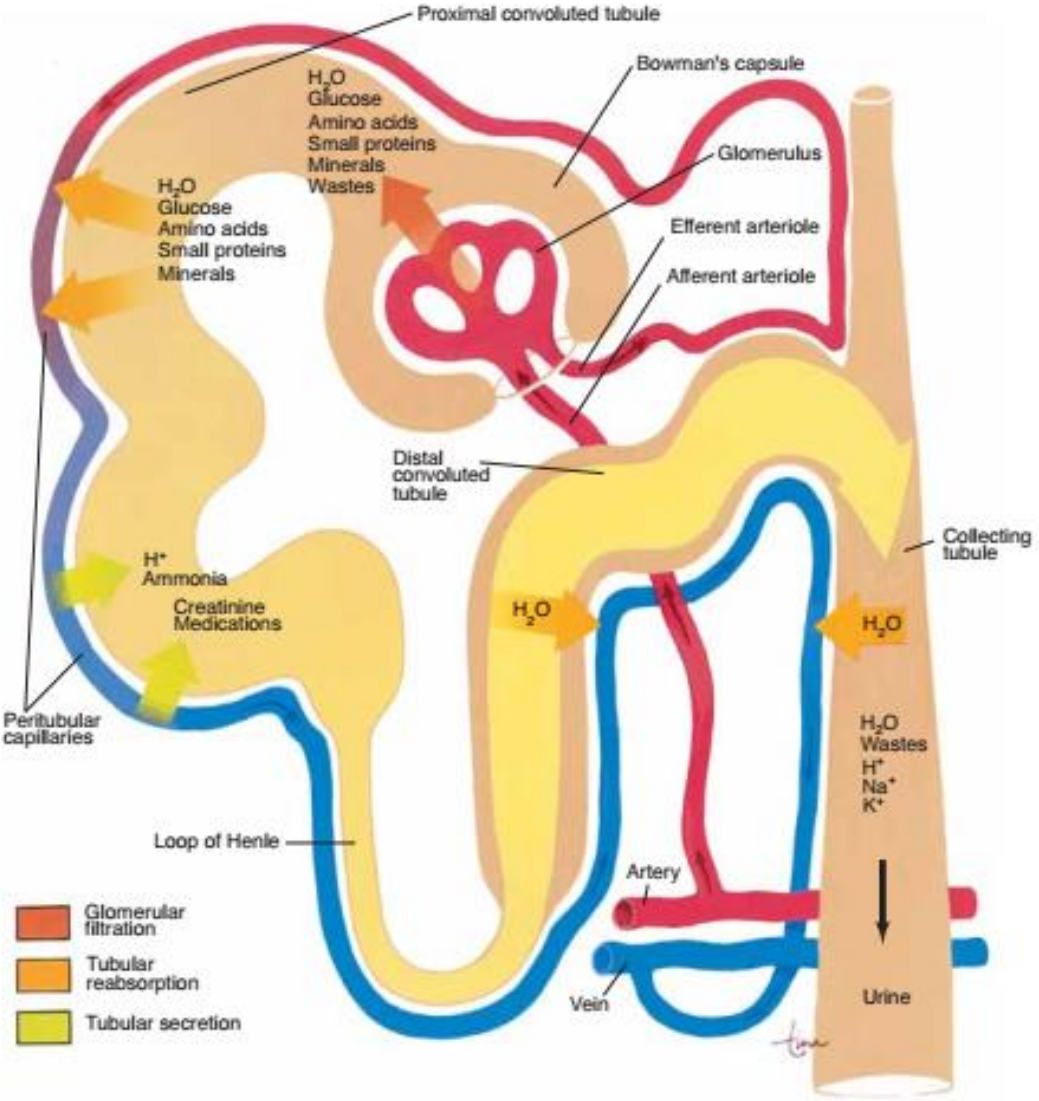

Figure 9: Schematic illustration of the nephron

Source: Scanlon and Sanders (2007).

The filtrate flows into the renal tubule which consist of proximal convoluted tubule, loop of Henle, and distal convoluted tubule. The distal convoluted tubules aggregate into collecting duct and discharge its contents into a calyx of the renal pelvis (Barrett *et al.,* 2010). Active tubular reabsorption of substances from filtrate, and tubular secretion of substances into filtrate occur at the renal tubules. While tubular reabsorption is based on usefulness of the substance to the blood, tubular secretion is selectively performed based on the excessive quantity of the substance in blood. About 65% of this reabsorption and secretion occur at the proximal convoluted tubules (Scanlon and Sanders, 2007).

Some of the main functions of the kidneys are excretion of waste, regulations of water and salt levels (blood volume and pressure), regulations of pH, and electrolytes, production of vitamin D and other hormones such as erythropoietin (DeFronzo *et al.* 2012).

Damage to kidney caused by disease conditions, and/or xenobiotics results in dysfunctions. Consequences of renal dysfunction include presence of protein, leukocytes, and erythrocytes in urine, acidosis, impaired urine dilution or concentration capacity, uraemia, and abnormal retention of sodium ion (Barrett *et al.*, 2010).

2.13.2.1 Kidney Function Indices

Biomarkers are indicators for assessment of normal or pathologic state of an organ or tissue (Adler, 2010). Renal injury or dysfunction which could arise from disease conditions, environmental toxins and/or experimental drugs are revealed by kidney biomarkers. While some kidney biomarkers reveal renal oxidative stress, immune responses within the kidney, or kidney structural and cellular impairment,

others reveal renal function (Tesch, 2010). Some of the indices by which the functional capacity of the kidney is measured are; creatinine, urea, and uric acid concentrations.

2.13.2.1.1 Plasma Creatinine Concentration

Creatinine is formed as the final product of creatine or phosphocreatine decomposition and it is excreted in urine. The amount of creatinine present in plasma of a healthy biological system per day is fairly constant and controlled mainly by glomerular filtration (Lamb and Price, 2008). The amount of creatinine in plasma is proportional to their generation, glomerular filtration and tubular secretion (Nisha *et al.,* 2017). Therefore, plasma concentration of creatinine and its clearance are used as markers of renal function. Creatinine filtration is reduced in renal dysfunction thereby causing increased plasma creatinine, and chemical agents that inhibit the tubular secretion of creatinine also bring about increased level of plasma creatinine that is independent of glomerular filtration rate (Dalton, 2010).

2.13.2.1.2 Plasma Urea Concentration

Urea is a nitrogenous product of protein and amino acids catabolism and it is majorly removed from the body by the kidney while minor losses maybe through gastrointestinal tract and skin (Lamb and Price, 2008). Urea is synthesised in the liver from amino acid-derived ammonia and requires availability of bicarbonate, aspartate, energy input in the form of adenosine triphosphate and series of urea cycle enzymes (Auron and Brophy, 2012).

Reduced plasma urea level may be caused by low-protein diet but pathologically by liver dysfunction as synthesis of urea is dependent on functional liver (Kalhan, 2000) and compromised urea synthesis reduces the ability of a biological system to remove potentially toxic levels of nitrogenous substances

(Glavind *et al.*, 2016) whereas stressful situations such as pain, surgery extrahepatic inflammation could increase urea synthesis (Greisen *et al.*, 1999; Thomsen *et al.*, 2013). Urea is freely filtered by the glomeruli and elevated plasma urea level is associated with kidney dysfunction (Lamb and Price, 2008). Apart from renal insufficiency, many other factors such as high-protein diet, elevated catabolism of protein, dehydration, among others influence the level of urea present in plasma. These therefore limits full reliability on plasma urea concentration as a test of kidney function (Lamb and Price, 2008).

2.13.2.1.3 Plasma Uric Acid Concentration

Uric acid is a nitrogenous product of purine metabolism (Hediger, 2005) distributed in extracellular fluid as sodium urate. At physiological level, it may act as antioxidant by scavenging carbon-centred radicals and peroxyl radicals (Nimse and Pal, 2015), and may prevent degradation of extracellular antioxidants which are essential for preserving endothelial and vascular function (Simic and Jovanovic, 1989; Becker, 1993; Hink *et al.*, 2002). In association with ascorbic acid and thiols, uric acid is an excellent scavenger of peroxynitrite ($ONOO^-$) in hydrophilic environment (Squadrito *et al.*, 2000), and protects the membrane of erythrocytes from lipid peroxidation (Pisoschi and Pop, 2015).

The plasma level of uric acid is controlled by glomerular filtration, reabsorption, secretion, and post-secretory reabsorption (Mount *et al.*, 2006; Kutzing and Firestein, 2008). Hyperuricemia may be caused by increased production of uric acid resulting from excessive dietary purine intake, altered ATP metabolism, tissue hypoxia, and elevated nucleic acid turnover as occasioned by leukemia, myeloma or trauma (Lamb and Price, 2008). Hyperuricemia may also be caused by decreased excretion of uric acid resulting from acute or chronic kidney dysfunction (Lamb and

Price, 2008; Nashar and Fried, 2012). Hyperuricemia is linked to diseases and conditions such as gout, myocardial infarction, renal disease, and cardiovascular disease (Bos *et al.,* 2006; Corrado *et al.,* 2006; Chonchol *et al.,* 2007) but remains vague whether some of these are the cause or consequence of elevated uric acid (Kutzing and Firestein, 2008). Hypouricemia, though less common, may be caused by reduced purine synthesis resulting from severe hepatocellular disease, or caused by impaired renal reabsorption of uric acid (Lamb and Price, 2008).

2.13.3 The Heart

The heart is positioned between the lungs in the thoracic cavity, and functions primarily to pump blood to all the tissues of the body and back to the heart through the arteries, capillaries, and veins (Scanlon and Sanders, 2007). The heart is made up of three types of muscles called atrial muscle, ventricular muscle, and excitatory and conductive muscle fibres. The atrial and ventricular muscles are contractile in nature, while the excitatory and conductive muscle fibres contract weakly but provide excitatory system that controls cardiac contraction and the rhythmical beating of the heart (Hall, 2011) through action potential which consists of depolarization and repolarization phases, and the action potential are conducted from cell to cell unlike in skeletal muscle (VanPutte *et al.,* 2016).

The heart has four chambers (Figure 10) which are called right atrium, left atrium, right ventricle, and left ventricle. These chambers have valves which allow the flow of blood in one direction, and their opening is determined by the pressure changes in the heart (Scanlon and Sanders, 2007). The left ventricle, through the aorta, pumps oxygenated blood to systemic circulation. And from the systemic circulation, deoxygenated blood then returns via the inferior and superior vena cava to the right

atrium, and passes to the right ventricle via the tricuspid valve. Then, the right ventricle

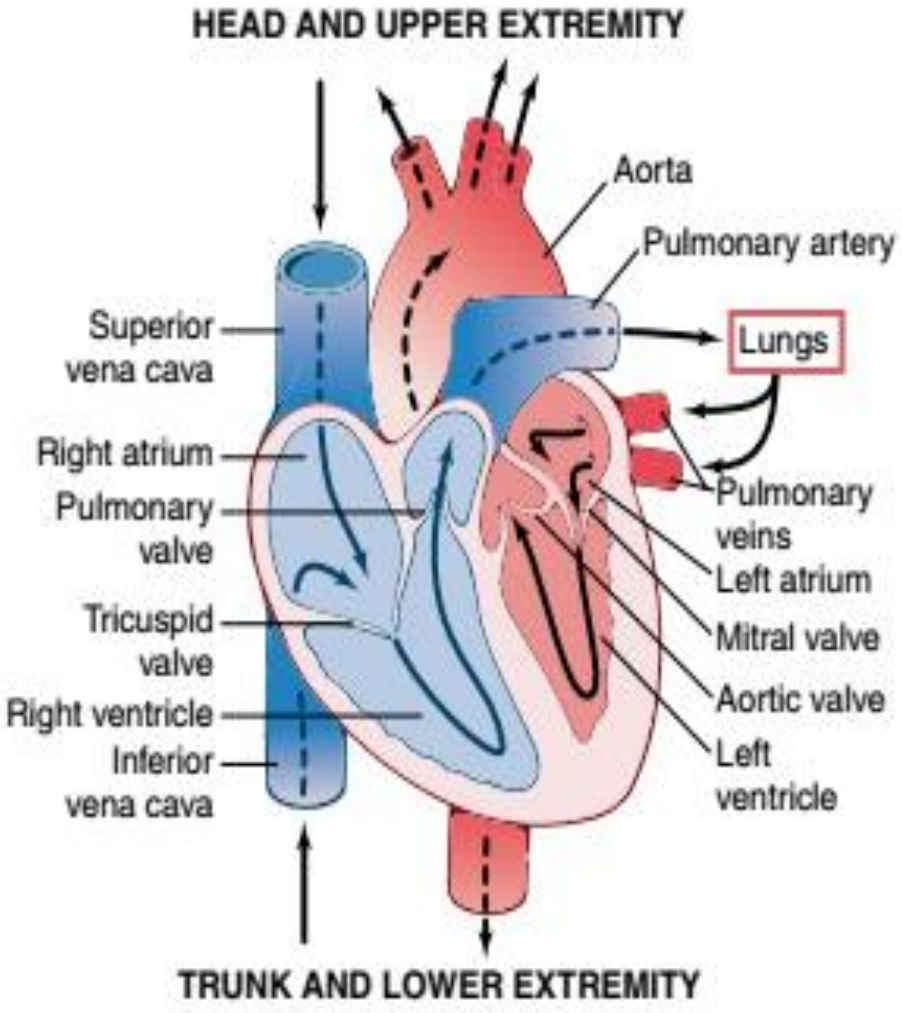

Figure 10: Structure of the heart, and course of blood flow

Source: Hall (2011).

then pumps blood via the pulmonary valve, and the pulmonary artery to pulmonary circulation for oxygenation, and returns from the lungs as oxygenated blood via the pulmonary vein into the left atrium. The oxygenated blood then passes through the mitral valve (bicuspid valve) into the left ventricle (Scanlon and Sanders, 2007).

The hepatic portal circulation is a segment of systemic circulation and represents circulation of blood from digestive organs (stomach, small intestine, colon, pancreas) and spleen through the liver before returning to the heart. The hepatic portal circulation ensures modification of blood constituents by the liver. it allows storage or modification of nutrients, excretion of bilirubin from spleen into bile, and detoxification of poisons before the return of blood to the heart and subsequently to other parts of the body (Scanlon and Sanders, 2007).

The cardiac muscle depends on Ca^{2+} and ATP for contraction. In response to action potentials, Ca^{2+} moves into cardiac cells and activate contraction process. Since the energy demand of cardiac cells are enormous, they are rich in mitochondria and their ATP production relies on O_2 availability which is enhanced by extensive network of capillaries. Cardiac muscle cannot afford significant oxygen deficit, otherwise muscular fatigue and stoppage of cardiac muscle contraction could arise (VanPutte *et al.*, 2016).

2.13.3.1 Cardiovascular Diseases and Indices

Cardiovascular diseases (CVD) refer to different conditions such as cardiomyopathy, coronary heart disease, strokes, and rheumatic heart disease, that affects the functions of the heart and blood vessels. Majority of CVD are due to atherosclerosis (coronary heart disease and ischemic strokes) while others caused by infections (cerebrovascular complications of malaria, rheumatic heart disease,

cardiomyopathy from human immunodeficiency virus infection) are common in developing nations of the world (Celermajer *et al.*, 2012).

The risk factors for CVD could be genetic, environmental, or lifestyle related. These factors include inheritance, high blood pressure, diabetes, alcohol, tobacco, physical inactivity, poor diet (especially those containing high saturated fats and trans fats), and overweight/obesity (O'Donnell and Elosua, 2008).

Also linked to cardiovascular alteration is malaria. Many pathogenic events in severe malaria is due to cytoadherence of parasitized erythrocytes to the endothelium, which brings about microvascular sequestration and obstruction, consequently causing ischemia, tissue hypoxia and injury (Pongponratn *et al.*, 2003; Beare *et al.*, 2006).

Biomarkers such as alkaline phosphatase, aspartate aminotransferase, ATPases, B-type natriuretic peptide (BNP) cardiac troponin, creatine kinase, C-reactive protein (CRP), lactate dehydrogenase, and myoglobin (Jaffe *et al.*, 2006) could reveal cardiac functional, structural and cellular impairment with different precisions. Indices such as plasma levels of total cholesterol, triacylglycerol, high-density lipoprotein cholesterol, and low-density lipoprotein cholesterol are commonly used to assess risk of cardiovascular diseases.

2.13.3.1.1 Total Cholesterol Concentration

Cholesterol is a structural constituent of cellular membrane vital for its fluidity, and a precursor of bile acids, vitamin D, and steroid hormones such as cortisol, progesterone and testosterone (Berg *et al.*, 2002). The cholesterol needs of cells are derived from dietary uptake of lipoprotein as well as from *de novo* synthesis, but the blood brain barrier prevents uptake from circulation, hence, the brain relies on *de novo* synthesis (Orth and Bellosta, 2012). The liver controls the plasma levels of cholesterol,

and its metabolism which yields bile acids (Lütjohann *et al.*, 1996; Wadhera *et al.*, 2016). Elevated level of cholesterol is associated with atherosclerosis, myocardial infarction, and other cardiovascular diseases (Bhatnagar *et al.*, 2008;Nelson, 2013).

Because cholesterol is basically insoluble in water, it is transported bound to lipid transporters (apolipoproteins) to form lipoproteins in aqueous extracellular environment (Zhornitsky *et al.*, 2016). These lipoproteins are chylomicrons, very low-density lipoprotein, intermediate-density lipoprotein, low-density lipoprotein, and high-density lipoprotein (Wadhera *et al.*, 2016).

2.13.3.1.2 Triacylglycerol Concentration

Triacylglycerol (TAG) is an ester of glycerol and three fatty acids. Triacylglycerol can be synthesised by the liver from carbohydrates, fatty acids, and cholesterol (Larson, 2015). Synthesis of TAG actively takes place in the liver, adipose tissues, and intestine (Quiroga and Lehner, 2012).

Triacylglycerol is the main form of storing energy in cells, and vital for absorption of dietary lipids in enterocytes, essential for synthesis of very low-density lipoprotein in liver, storage of essential and non-essential fatty acids, and functions as insulator and mechanical cushion for organs (Coleman and Mashek, 2011).

Fatty acids are assembled as TAG in chylomicrons and very low-density lipoproteins, and transported to peripheral tissues for instant use or storage (Coleman and Lee, 2004). The storage of fatty acids as TAG ensures that cellular membranes are protected from the potential damaging effects of fatty acids or derivatives of their acyl-CoA (Coleman and Mashek, 2011). Excess intracellular TAG are stored once the cellular needs of TAG such as energy generation via β-oxidation, membrane synthesis, and VLDL secretion, are met (Quiroga and Lehner, 2012).

The plasma level of TAG is controlled by the synthesis, and degradation of chylomicron and very low-density lipoprotein particles (Chatterjee and Sparks, 2011). Increased plasma level of TAG is associated with hypercholesterolaemia, and atherosclerosis and is an additional risk for cardiovascular disease (Parks, 2002; Sarwar *et al.,* 2007).

2.13.3.1.3 High-Density Lipoprotein Cholesterol

High-density lipoprotein cholesterol (HDL) is the smallest and densest lipoprotein particle. Also, it has the highest amount of phospholipids and protein compared to other lipoproteins (Larson, 2015). HDL obtains cholesterol and phospholipids that are removed from cells and transfers them to the liver by directly interacting with hepatic cells, or by indirect method of transporting the cholesterol to VLDL or LDL. This transport of lipids by HDL to the liver and intestine from peripheral tissues is referred to as reverse cholesterol transport (Lund-Katz and Phillips, 2010). Cholesterols which are accumulated by peripheral cells through synthesis and uptake from lipoproteins are delivered to the liver mainly by HDL as most cells cannot catabolise cholesterol (Guyton, 2008).

HDL is anti-atherogenic and it removes cholesterol from macrophages. The reverse cholesterol transport is therefore essential for most cells to reduce their cholesterol content and this may help in preventing the development of atherosclerosis (Eren *et al.,* 2012). Once in the liver, the cholesterol can be removed by being changed to bile acids or secreted directly into bile. While hepatic lipase hydrolyses the phospholipids and triacylglycerol in HDL, the endothelial cell lipase acts as phospholipase hydrolysing phospholipids present in HDL (Cilingiroglu and Ballantyne, 2004; Chatterjee and Sparks, 2011). Hence, HDL is cholesterol-rich and functions to transfer the cholesterol to hepatocytes for removal or recycling.

HDL particles possess anti-inflammatory, and antioxidant properties which are associated with protection from cardiovascular diseases (Eren *et al.*, 2012).

2.13.3.1.4 Low-Density Lipoprotein Cholesterol

Low-density lipoprotein (LDL) is formed from cholesterol which is absorbed from the gut, or those derived from *de novo* synthesis (Cohen, 2008). This is packaged with triacylglycerol, phospholipids, and proteins to form very low-density lipoprotein (VLDL). This is then converted, in circulation, by lipoprotein lipase and cholesteryl ester transfer protein into intermediary density lipoprotein, and then low-density lipoprotein which are more enriched with cholesterol (Wadhera *et al.,* 2016). LDL transports cholesterol from the liver to other tissues and majority of the cholesterol in circulation is carried by LDL, hence its major function (Guyton, 2008; Larson, 2015). LDL is easily prone to oxidation, thereby promoting their uptake by macrophages, and like VLDL, it is pro-atherogenic (De Man *et al.*, 2000; Lopez *et al.*, 2016).

The regulation of lipoprotein concentration is mainly done by the liver. The rate of LDL generation, and clearance determine its plasma level, and these are controlled by the amount of LDL receptors (transmembrane glycoprotein) on hepatic surface (Zhang *et al.,* 2016). And the number of LDL receptors on hepatic surface are controlled by the level of cholesterol in cells. A decrease in cellular cholesterol level results in stimulation of LDL receptor transcription (Zhang *et al.*, 2016). The activity of LDL receptor and LDL production are inversely related while LDL receptor activity and LDL clearance are directly related (Twisk *et al.*, 2000).

2.13.4 The Brain

The brain consists of many interconnected parts that function as a unified set. These major regions (Figure 11) are the brainstem (the medulla oblongata, the pons,

and the midbrain), the cerebellum, the diencephalon (the hypothalamus, and the thalamus), and the cerebrum (VanPutte *et al.*, 2016). The brain performs several functions such as regulation of heart rate, control of blood vessels' diameter, moderation of breathing, coordination of reflexes, maintenance of posture and equilibrium, production of hormones (antidiuretic hormone, oxytocin), regulations of body temperature, and interpretation of sensory impulses (Scanlon and Sanders, 2007).

Impulses are received by the brain and sent to appropriate parts of the body via neurons (nerve cells). The neurons receive stimuli, conduct action potentials, and transmit signals to other neurons, or effectors only in one direction (VanPutte *et al.*, 2016). A neuron is said to be polarized when not carrying an impulse, and has more of Na^+ outside the cell, but more of K^+ and negative ions within the cell. Hence, positively and negatively charged on the outside and inside respectively. This is reversed by the action of stimulus such as neurotransmitters, and the neuron is said to be depolarized. Afterwards, Na^+ and K^+ are pumped outside and inside respectively by Na^+,K^+ ATPase, hence the neuron is repolarized and ready for another signal transmission (Scanlon and Sanders, 2007).

The junction of interaction between one neuron and another, or cells of an effector is called the synapse. At this synapse, the transmission of signal changes from electrical to chemical and relies on neurotransmitters which are stored in synaptic vesicles (VanPutte *et al.*, 2016). The best known neurotransmitters are acetylcholine and norepinephrine. Other are serotonin, dopamine, γ-aminobutyric acid (GABA), glycine, and endorphins (VanPutte *et al.*, 2016). Drugs can alter the action of neurotransmitters at the synapse, thereby causing excitatory or inhibitory effects.

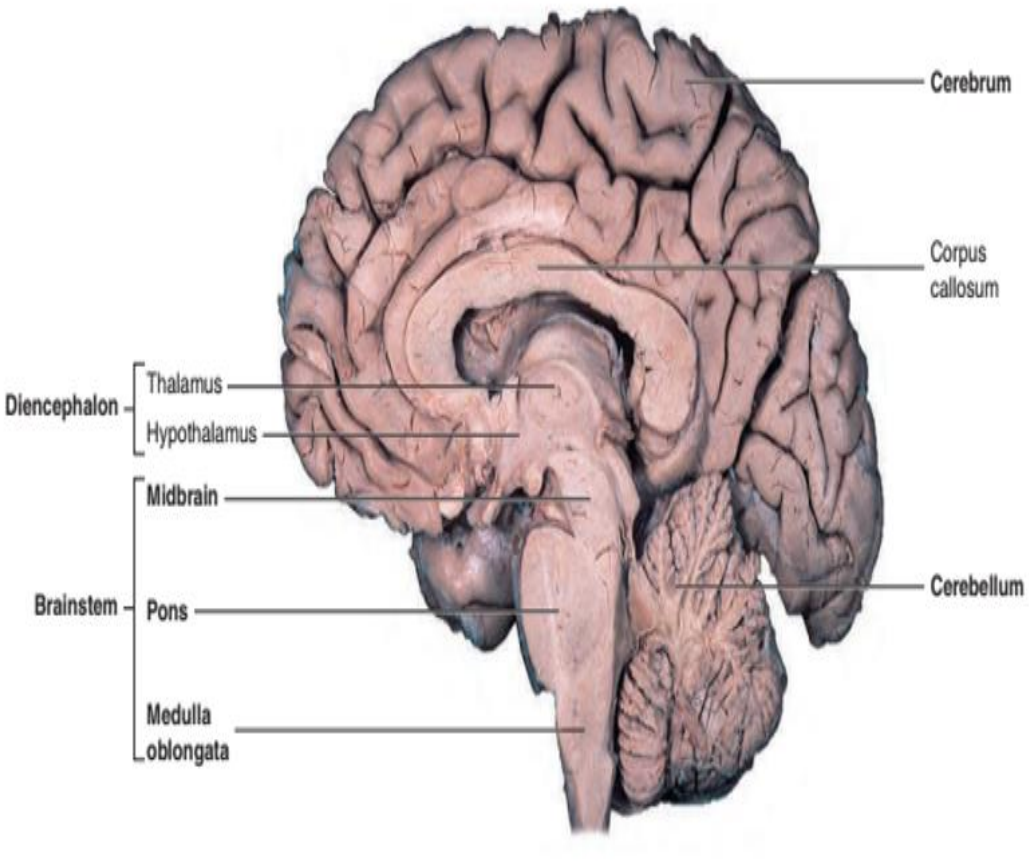

Figure 11: Structure of the brain, showing major regions

Source: VanPutte *et al.* (2016).

Several factors such as aging, nutrition, exposure to some toxicants and drugs could cause brain damage. Also, infection and disease such as malaria (cerebral malaria) could result in brain damage through cerebral oedema and increased intracranial pressure (Cohee and Laufer, 2017).

2.14 Cellular Enzymes

The measurement of cellular enzymatic activities permits the detection of acute and chronic tissue injuries before the emergence of symptoms (Woreta and Alqahtani, 2014). These tests consist of biomarkers of synthetic functions, cellular injuries, and metabolic functions.

2.14.1 Aminotransferases

The aminotransferases catalyse the reversible transfer of amino group of alanine or aspartate to α-ketoglutarate to form glutamate and the corresponding ketoacid of the initial amino acid i.e. pyruvate or oxaloacetate (McPherson and Pincus, 2011). They catalyse the intermediary reactions of amino acid and glucose metabolisms. Both alanine and aspartate aminotransferases require pyridoxal phosphate as cofactor and any condition that increases or decreases the level of pyridoxal phosphate (metabolically active form of vitamin B6) affects the activities of aminotransferases (McPherson and Pincus, 2011).

2.14.1.1 Aspartate Aminotransferase (EC 2.6.1.1)

Aspartate aminotransferase (AST) exists as two isoenzyme forms present in the cytoplasm and mitochondria, with the cytoplasmic isoenzyme being the predominant form in plasma (Johnson-Davis and McMillin, 2010), and has a half-life of 17 hours (York, 2017). The enzyme is broadly distributed in tissue with highest concentrations

in liver, cardiac tissue, and skeletal muscle, but present in smaller amounts in kidney, erythrocytes, and pancreas (Johnson-Davis and McMillin, 2010).

AST is a pyridoxal 5′-phosphate (PLP)-dependent enzyme that catalyses reversible transamination reaction. In its presence, aspartate and pyridoxal phosphate reacts to form oxaloacetate and pyridoxamine phosphate. Pyridoxal phosphate is then regenerated from the reaction of pyridoxamine phosphate with α-ketoglutarate and concomitant formation of glutamate (York, 2017). AST plays important role in amino acid metabolism and vital physiological function of maintaining cellular NAD^+/NADH ratio, through the malate-aspartate shuttle whereby cytosolic NADH is oxidised and mitochondrial NAD^+ is reduced thereby facilitating glycolysis and electron transport (ATP generation), respectively (McGill, 2016).

Elevated plasma levels of AST are usually due to increased expression, or release of enzyme from tissues resulting from membrane blebbing and cell death (McGill, 2016). But in some instances, increase activity of plasma AST could result from complexing of the enzyme with immunoglobulins or other proteins to form a "macroenzyme" thereby protecting the enzyme from degradation, and prolonging their half-lives (Moriyama *et al.*, 1990; Briani *et al.*, 2003), hence, the accumulation of enzyme despite their normal release. Asymptomatic increase in plasma AST without increase in ALT or other biomarkers may therefore suggest "macroAST" formation (Moriyama *et al.*, 1990). A significant increase in mitochondrial form of AST in plasma may suggest cellular necrosis (Johnson-Davis and McMillin, 2010). Since AST is found in many tissues unlike ALT, a ratio of plasma AST to ALT greater than 5 may suggest extrahepatic injury, especially when ALT activity is normal or slightly raised (Woreta and Alqahtani, 2014).

2.14.1.2 Alanine aminotransferase (EC 2.6.1.2)

Alanine aminotransferase (ALT) is made up of 496 amino acids which are coded by the ALT gene, located on the long arm of chromosome 8 (Sohocki *et al.*, 1997). It has a half-life of about 10 hours in rat and 50 hours in humans (York, 2017). It is majorly found in the cytosol of hepatocytes and catalysis transamination reaction. In the presence of ALT, the reaction between alanine and pyridoxal phosphate yields pyruvate and pyridoxamine phosphate. The pyridoxamine phosphate then reacts with α-ketoglutarate to form glutamate and the regeneration of pyridoxal phosphate (McPherson and Pincus, 2011). ALT has primary role in gluconeogenesis and amino acid metabolism (York, 2017). It is important for energy homeostasis via the alanine-glucose cycle whereby in the muscle, it converts pyruvate to alanine using an amino group from glutamate, and ALT of hepatocyte converts the alanine back to pyruvate, which can be used to make glucose. Thus, ensuring glucose regulation which is important to biological system especially during stressful periods such as fasting or vigorous exercise (McGill, 2016).

While ALT is found in other tissues in smaller concentrations, its presence is highest in liver, hence, its usefulness as a biomarker of hepatocellular damage or its function. Acute hepatotoxicity usually leads to rise in plasma ALT activity within 6-12 hours and this peak within 2 days and then decline (York, 2017). While enzymatic induction may result in elevated activity of ALT (York, 2017), cell death, plasma membrane damage and enzyme leakage represent common reason for elevated plasma activity of the enzyme (McGill, 2016). Mild increase in plasma ALT activity may suggest membrane blebbing and reversible hepatic injury, but pronounced increase in activity may indicate irreversible cellular damage and necrosis (York, 2017). Deficiency or inhibition of pyridoxal phosphate by xenobiotics such as isoniazid or

lead could prevent elevation of ALT activity despite the presence of hepatic injury (Aulbach and Amuzie, 2017).

2.14.2 Alkaline Phosphatase (EC 3.1.3.1)

Alkaline phosphatase (ALP) is a homo-dimeric enzyme that has five cysteine residues, two Zn^{2+} and one Mg^{2+} in each of its catalytic sites. The metals are essential for the catalytic activity of the enzyme. ALP catalyses the hydrolysis of monophosphate esters, and in the presence of abundant concentrations of phosphate acceptors, catalyses transphosphorylation reaction (Millan, 2006). ALP influences transportation of metabolite and lipid, and calcification of bone (Gowda *et al.*, 2009). The enzyme is membrane-bound, has optimum activity at alkaline pH, and can be inhibited via uncompetitive mechanism by L-amino acids and peptides (Millan, 2006). ALP is activated by some divalent ions such as Co^{2+}, Mg^{2+}, and Mn^{2+} but can be inhibited by Ca^{2+}, Hg^{2+}, borate, cyanide, oxalate and phosphate (Varley *et al.* 1988)

ALP is found in the bone, kidney, liver, placenta, small intestine, and white blood cells (Lee *et al.*, 2012). ALP isoforms in humans are encoded by four genes; placental ALP, intestinal ALP, germ cell ALP, and tissue nonspecific ALP which is expressed in bone, kidney, and liver. The tissue nonspecific ALP gene is located on chromosome 1, while the genes for other isoforms of ALP are found on chromosome 2 (Harris, 1990; Millan, 2006).

In assessing liver injury, with both plasma activities of ALT and ALP above upper limit of normal range, the ratio of ALT to ALP of less than two could indicate cholestasis, between two to five could indicate mixed cholestatic-hepatocellular injury, while ratio greater that five may suggest hepatocellular injury (Woreta and Alqahtani, 2014).

Inborn defects in ALP gene results in hypophosphatasia. This is characterised by deficiency in ALP activity, inadequate skeletal and dental mineralization, and accumulation of the substrates of ALP, namely, pyridoxal-5′ phosphate, phosphoethanolamine, and inorganic pyrophosphate (Wendling *et al.*, 2001; Mornet, 2008).

2.14.3 Gamma-Glutamyltransferase (EC 2.3.2.2)

Gamma-glutamyltransferase (GGT) is a membrane-bound transferase present in tissues such as liver, proximal renal tubule, pancreas, spleen, and intestine. It catalyses the transfer of gamma-glutamyl group of peptides such as glutathione to amino acids or other peptides (Mukherjee and Gollan, 2011). Though found in higher concentration in kidney, plasma GGT activity is primarily credited to hepatobiliary system (Panteghini and Bais, 2008) with apical membrane of hepatocytes and biliary epithelial cells as the main sources (Sotil and Jensen, 2004).

Plasma activities of GGT is an indicator of bile ducts or liver injury. Elevated activities of GGT in the plasma may suggest membrane damage or death of biliary epithelial cells (Sotil and Jensen, 2004). However, other non-hepatic disorders such as renal failure, and diabetes could bring about increase in the plasma activities of the enzyme (Woreta and Alqahtani, 2014).

The activities of GGT in plasma is also clinically useful for determining source of elevated alkaline phosphatase. A concomitant increase in GGT and alkaline phosphatase activities suggest hepatobiliary source while increased activity of alkaline phosphatase without significant alteration in activity of GGT suggest skeletal (bone) source (Lee *et al.*, 2012).

2.14.4 Glutamate Dehydrogenase (EC 1.4.1.3)

Glutamate dehydrogenase (GDH) is a mitochondrial enzyme present in the liver, kidney, heart muscle, and in small quantity in tissues like brain, skeletal muscle, and leucocytes. GDH catalyses the formation of α-ketoglutarate through the removal of ammonia from L-glutamate utilizing NAD^+ or $NADP^+$ as cofactor (Panteghini and Bais, 2008). The reaction catalysed by GDH is reversible and the reverse of this oxidative deamination is called reductive amination. GDH is essential for interconnecting amino acids, carbohydrate metabolism, cellular homeostasis of ammonia, and energy production (Plaitakis *et al.*, 2011).

The cellular activity of GDH is positively modulated by adenosine diphosphate (ADP) and inhibited by guanosine triphosphate (GTP), thereby suggesting that the enzyme is controlled by cellular energy need (Spanaki *et al.*, 2010). Mitochondrial enzyme such as GDH has elevated activity in plasma in cases of mitochondrial damage and dysfunction (McGill *et al.*, 2014; Weemhoff *et al.*, 2017). The activity of GDH in plasma is also elevated during necrosis (Panteghini and Bais, 2008).

2.14.5 Lactate Dehydrogenase (EC.1.1.1.27)

Lactate dehydrogenase (LDH) is cytoplasmic enzyme that catalyses interconversion of lactate and pyruvate. It utilises nicotinamide adenine dinucleotide (NAD) as hydrogen acceptor in catalysing the oxidation of lactate to pyruvate (Johnson-Davis and McMillin, 2010).

The enzyme plays essential role in anaerobic glycolysis, during which pyruvate generated from glucose is reduced to lactate by LDH, utilising NADH as cofactor and generating NAD^+. Hence, upregulation of cellular LDH activity during hypoxia

replenishes NAD^+ which is crucial for maintaining cellular energy production through glycolysis in anaerobic circumstances (Valvona *et al.*, 2016).

LDH can be categorised as five major isoenzymes with each made up of four polypeptide chains. These polypeptide chains are of two types, designated as H (heart) and M (muscle) and their different arrangements is what yield the major isoenzyme forms of LDH (Johnson-Davis and McMillin, 2010). LDH is found in heart, kidney, liver, skeletal muscle, and erythrocyte but in smaller amount in brain (Crook, 2013).

Due to the presence of the enzyme in many tissues, elevated levels of the enzyme in plasma may result from conditions affecting different tissues. The plasma activity of LDH is elevated in cardiac, hepatic, renal and skeletal muscle injuries or diseases, but highest level of its elevation is seen in pernicious anaemia, haemolytic disorders (Johnson-Davis and McMillin, 2010) and myocardial infarction (Crook, 2013).

2.14.6 Creatine kinase (EC 2.7.3.2)

Creatine is synthesized in the kidney, liver and pancreas in two enzymatic reactions. Transamidation of arginine and glycine forms guanidinoacetic acid, and its methylation by S-adenosylmethionine yields creatine. Creatine is then transported in blood to tissues such as brain and muscle where it is phosphorylated by creatine kinase to yield phosphocreatine, a high-energy compound (Lamb and Price, 2008). Creatine and phosphocreatine are interconverted during metabolic processes of muscle contraction (Lamb and Price, 2008).

Creatine kinase (CK) is found in abundance in brain, cardiac and skeletal muscles. CK exist as three isoenzymes and each is made up of two polypeptide subunits designated as M and B (Crook, 2013). In most vertebrate tissues, the

isoenzymes are expressed as a dimeric cytosolic CK and more commonly as octameric mitochondrial CK which is localized in cristae and intermembrane space (Schlattner *et al.,* 1998).

CK is commonly linked with regeneration of ATP in contractile or transport systems (Johnson-Davis and McMillin, 2010). In muscle cells, CK catalyses the formation of phosphocreatine, which is stored in muscle cells until needed. And during contraction, this phosphocreatine is broken down to creatine and regenerate ATP via N-phosphoryl group transfer to ADP (Andres *et al.,* 2008). The cellular activity of CK ensures that immediate high and fluctuating energy needs of cells are met. It serves to guarantee steady, locally buffered ATP/ADP ratios and preserve cellular energy homeostasis (Saks *et al.,* 1996; Ventura-Clapier *et al.,* 1998).

Pathological conditions often alter activity of CK either by directly compromising CK via oxidative and radical damage, or by up-regulating CK expression to compensate impaired energy state (Schlattner *et al.,* 2006). The plasma activity of CK is commonly increased in disorders of cardiac and skeletal muscle because of the presence of CK in high quantity in these tissues (Johnson-Davis and McMillin, 2010). Elevated plasma activities of CK may suggest myocardial infarction, thyrotoxic myopathy, or muscular dystrophy (Crook, 2013), and are sometimes increased in central nervous system disorders such as central nervous system shock, seizures, cerebrovascular accident, and nerve degeneration (Johnson-Davis and McMillin, 2010) involving blood-brain barrier damage.

2.14.7 Malate Dehydrogenase (EC 1.1.1.37)

Malate dehydrogenase (MDH) reversibly catalyses the oxidation of L-malate to oxaloacetate, utilising NAD as cofactor. In eukaryotic cells, MDH exist as two

isoenzymes called cytoplasmic MDH and mitochondrial MDH. The two isoenzymes exist as dimers in physiological state with similar subunits (homodimers) and two equivalent binding sites (Dasika *et al.,* 2015).

The isoenzymes are vital for tricarboxylic acid cycle and malate-aspartate shuttle. MDH plays vital roles in energy generation, metabolic pathways such as tricarboxylic acid cycle within the mitochondrial matrix, and formation of metabolites for biosynthesis (Rozova *et al.,* 2015). In malate-aspartate shuttle across the mitochondrial membrane, regeneration of NAD is made possible by the mitochondrial MDH involved in the reduction of oxaloacetate to malate in the presence of NADH, hence providing NAD needed for energy generation (Abtahi *et al.,* 2017).

MDH is allosterically regulated by citrate but inhibited by ATP, and high oxaloacetate concentrations (Dasika *et al.,* 2015). Elevated activity of MDH in plasma is associated with hepatic and cardiac injuries (Smith *et al.,* 2013).

2.14.8 Acetylcholinesterase (EC 3.1.1.7)

Acetylcholinesterase (AChE) has a key physiological function of terminating impulse transmission at nicotinic cholinergic synapses by hydrolysing acetylcholine (Aldunate *et al.,* 2004). Impulse stimulation of nerves results in migration of acetylcholine vesicles to nerve surface where they rupture and release acetylcholine into synaptic gap between nerve and muscle. Acetylcholine then diffuses across synaptic junction to interact with its receptor at post-synaptic gap. This causes opening of transmembrane channels, inflow of sodium and calcium, and outflow of potassium (Martyn *et al.,* 2000), hence depolarisation of the post-synaptic cells. This creates voltage and consequently propagate action potential and muscle contraction (Prior and

Marshall, 2006). This transmission of impulse and action is halted appropriately through hydrolyses of acetylcholine by acetylcholinesterase.

AChE hydrolyses acetylcholine at synapses and terminates its activity (Fujii *et al.*, 2017). The rapid and effective hydrolyses of acetylcholine prevents its accumulation, hence the quick return of the system to its resting state before the commencement of another motor nerve impulse (Caldwell, 2009) whereas, inhibition of AChE allows longer presence and higher concentration of acetylcholine at the neuromuscular, hence persistent stimulation and contraction of the muscle (Caldwell, 2009).

AChE has one anionic and one esteratic site of action. The anionic site is negatively charged and interacts with the positive quaternary nitrogen group of acetylcholine, while the esteratic site complexes with the carbamate group on the acetylcholine (Caldwell, 2009).AChE is present in neuromuscular junctions, nerve endings, gray matter of brain, erythrocyte, spleen and lungs (Panteghini and Bais, 2008).

Altered cellular activity of AChE suggest cholinergic dysfunction. In the absence of genetic cause or enzyme inhibition, a decrease in plasma AChE activity could suggest impaired synthetic function of the liver (Panteghini and Bais, 2008).

2.14.9 Adenosine Triphosphatases (ATPases)

ATPases are enzymes that catalyse the hydrolysis of adenosine triphosphate (ATP) into adenosine diphosphate (ADP) and a free phosphate ion, releasing energy for other cellular processes. Transport ATPases can be classified as; F-type ATPases, V-type ATPases, or P-type ATPases (Suhail, 2010).

The F-type ATPases (F_0F_1 ATPase) are active transporters and are key to energy-conserving reactions in mitochondria and chloroplasts. The F-type ATPases catalyse transmembrane movement of protons against concentration gradient and this is driven by ATP hydrolysis. Since this reaction is reversible, the F-type ATPases can utilise energy from the proton gradient in the reverse for ATP synthesis, and as a result are also called ATP synthases. The integral portion of F-type ATPases, (F_0) provides a transmembrane channel for protons while the peripheral domain (F_1) serves as the molecular machine, utilising energy of ATP hydrolysis to drive protons uphill, or synthesize ATP as protons flow down their electrochemical gradient. During oxidative phosphorylation and photophosphorylation in mitochondria and chloroplasts respectively, ATP synthases are key to the production of ATP (Nelson and Cox, 2013).

The V-type ATPases are proton-transporting ATPases, acidifying intracellular compartments such as lysosomes, secretory vesicles, and the Golgi complex in organisms. Since their function is associated with vacuole, hence the "V" in the class name. They have integral (transmembrane) domain (V_0) that functions as a proton pore and a peripheral domain (V_1) that has the ATP-binding site and the ATPase activity (Nelson and Cox, 2013). In *Plasmodium spp*. the V-type ATPase occurs both in its membranes of organelles and its plasma membrane where it functions to energise the secondary transport of various solutes (Moriyama *et al.,* 2003). The *Plasmodium* V-type ATPase is also exported to the cytoplasm of the host erythrocyte and is attached to the plasma membrane where it regulates the intracellular pH of infected erythrocyte (Marchesini *et al.,* 2005).

The P-type ATPases are ATP-driven cation transporters that are reversibly phosphorylated by ATP. Phosphorylation of P-type ATPases at a specific aspartate residue brings about conformational change which is essential to transporting the

cation across membrane (Nelson and Cox, 2013). The P-type ATPases are so called because they form a vital phosphorylated intermediate during transmembrane transport of molecules. Mg^{2+}-ATPase, Ca^{2+}, Mg^{2+}-ATPase and Na^{+}, K^{+}-ATPase are examples of P-type ATPases.

2.14.9.1 Mg2+-Adenosine Triphosphatase (E.C. 3.6.3.2)

The Mg^{2+}-ATPase functions to maintain high intracellular Mg^{2+} concentration. Alteration in levels of Mg^{2+} can control rates of protein synthesis and cell growth (Sanui and Rubin, 1982). Mg^{2+}-ATPase is said to be activated by millimolar concentrations of Mg^{2+} and is resistant to ouabain, or vanadate inhibition (Ravindran *et al.*, 2012). It has been reported that the enzyme in different brain region has varying affinity for ATP (Nedeljkovic *et al.*,1998), and unlike both Ca^{2+}-ATPase and Na^{+}, K^{+}-ATPase, moderate hypoxia is reported to increase the activity of synaptosomal Mg^{2+}-ATPase (Grochowalska and Bernat, 1997).

2.14.9.2 Ca2+,Mg2+-Adenosine Triphosphatase (E.C. 3.6.3.8)

The Ca^{2+},Mg^{2+} ATPase is classified as a P-type transport ATPase, because during catalytic cycle it forms covalent intermediate state by phosphorylation of its highly conserved aspartate residue (Pedersen and Carafoli, 1987).

Ca^{2+} ATPase function to maintain low cytosolic concentration of calcium ion. To achieve this, three calcium-pumping ATPase systems are involved. They are; (i) ATPases localized in Golgi and related vesicular compartments; (ii) sarco/endoplasmic reticulum ATPases (SERCAs) that sequester Ca^{2+} from cytosol into internal release compartments; and (iii) plasma membrane Ca^{2+}-ATPases (PMCAs) located in the surface membrane of cells that eject Ca^{2+} from cytosol against concentration gradient into extracellular environment, thereby ensuring Ca^{2+} homeostasis (Talarico Jr *et al.*,

2005). These pumps have high affinity for intracellular Ca^{2+} and upon binding the ion, they undergo conformational changes thereby allowing the transport of the ion across membrane where the pumps have lower affinity for Ca^{2+}, hence its dissociation (Mangialavori *et al.,* 2010; Brini and Carafoli, 2011). PMCA has a lower capacity for Ca^{2+} removal compared to SERCA as it removes one Ca^{2+} per ATP molecule hydrolysed unlike two Ca^{2+} removed per ATP by SERCA (Guerini *et al.,* 2000). PMCA is principally the Ca^{2+} removal system in cells where the resting intracellular Ca^{2+} levels is low (Zylin´ska and Soszyn´ski, 2000), whereas excitable cells such as neurons and myocytes which has more needs for removal of cytosolic Ca^{2+} requires the activities of PMCA (for removal into extracellular environment), SERCA (for reuptake into the sarco/endo-plasmic reticulum), and the sodium-calcium exchanger (Lytton *et al.,* 1989; Brini and Carafoli, 2011).

In humans, PMCA proteins (PMCA1-PMCA4) are encoded by four genes (ATP2B1-ATP2B4) and mutations in the genes encoding each PMCA are said to be associated with diseased cells and pathological conditions such as diabetes, hereditary deafness, cardiovascular diseases, autism, and adenoma (Stafford *et al.,* 2017). Ca^{2+}-ATPase of erythrocytes membrane is said to consist mainly of PMCA4 (coded by ATP2B4) and single nucleotide polymorphisms within the ATP2B4 has been reported to conferred resistance to a severe form of malaria among children, and protect against anaemia in pregnant women in a West African population (Timmann *et al.,* 2012; Bedu-Addo *et al.,* 2013). Therefore, PMCA4 may be an interesting target for anti-malarial drugs (Mohamed *et al.,* 2013).

Calmodulin is the major regulator of Ca^{2+} pump activity. Calmodulin binds to its domain thereby increasing the ATPase affinity for Ca^{2+}, making it active at cellular concentration of Ca^{2+} and elevating the ATPase activity to about six-fold (Enyedi,

1987; Elwess *et al.,* 1997). On the contrary, the pump can be inhibited by thapsigargin (Lytton *et al.,* 1991).

2.14.9.3 Na+,K+-Adenosine Triphosphatase (EC 3.6.3.9)

The Na^+,K^+-ATPase was discovered by Jens Christian Skou in 1957 (Cheng *et al.,* 2013). This ubiquitous transmembrane enzyme is made up of α, β, and γ subunits and requires one α and one β subunit in heterodimer as the minimal functional unit (Jorgensen *et al.,* 2003). The α subunit is a catalytic site and offers the binding sites for sodium, potassium, ATP and cardiac glycosides (inhibitors of the pump) while the β subunit is a sugar-rich auxiliary segment vital for maturation and stability of the α subunit (Pestov *et al.,* 2011). The γ subunit is a hydrophobic and single-membrane crossing protein with little known about its function, but appears to be obligatorily associated with the αβ complex (Therien *et al.,* 1997). There are four α and four β isoforms expressed in different fiber-type, and subcellular distribution.

Na^+,K^+-ATPase is primarily responsible for maintaining high extracellular sodium concentration relative to intracellular concentration, and high intracellular potassium ion concentration relative to extracellular concentration. To achieve this, Na^+,K^+-ATPase utilises energy from the hydrolyses ATP to pump, against concentration gradient, three molecules of sodium ions out of cells for every two molecules of potassium ions pumped into cell via a ping-pong like mechanism called Albers-Post cycle (Jorgensen *et al.,* 2003). Phosphorylation of the protein by ATP results in conformational change of the pump and increases its affinity for intracellular sodium whereas dephosphorylation of the ATPase brings about conformational change and increases its affinity for extracellular potassium. The action of Na^+,K^+-ATPase ensures generation and maintenance of transmembrane gradients of sodium and

potassium which is vital for the normal resting membrane potential (Cheng *et al.*, 2013). The electrochemical gradient created by this enzyme provides energy for transport of metabolites, nutrients, and ions across membrane. This electrochemical gradient is also important for regulation of intracellular pH and cell volume, and for the action potential of muscle and nerve (Therien *et al.*, 1997).

The activity of Na^+,K^+ pump can be regulated, likewise its abundance. While acute regulation affects the activity, chronic regulation tends to affect the abundance of the protein (Clausen, 1998). Change in substrate levels, that is, increase intracellular sodium and extracellular potassium levels stimulate the activity of Na^+,K^+-ATPase (Cheng *et al.*, 2013). Insulin is also an activator, stimulating Na^+, K^+-ATPase by increasing its affinity for intracellular sodium (decreasing concentration for half-maximal activation, Km) without changing its maximal pump activity (Vmax) and this is independent of glucose uptake (Kitasato *et al.*, 1980; Choi *et al.*, 2002). Compounds such as β-blockers (e.g. propranolol) that prevent phosphorylation of the pump can inhibit its activity. Chronic regulation of Na^+,K^+-ATPase is achieved at transcriptional and post-transcriptional levels resulting in altered protein synthesis of α and β subunits (Cheng *et al.*, 2013). Also, low dietary potassium intake and muscle inactivity could decrease the abundance of the enzyme in skeletal muscle (Clausen, 2003). Inhibition of skeletal muscle Na^+,K^+ pump by drugs such as cardiac glycosides digoxin or β-blockers may result in hyperkalemia while stimulation of the pump by drugs such as β2-agonists or cAMP enhancers theophylline and caffeine may result in hypokalemia (Perazella, 2000). Na^+,K^+-ATPase can be inhibited by digitoxigenin, ouabain, or vanadate.

2.15 Blood Parameters

The blood is made up of plasma, red blood cells, white blood cells, and platelets. The plasma is the liquid component of blood, consisting of mostly water, with dissolved proteins, electrolytes, nutrients, and metabolites while the red blood cells, white blood cells and platelets are the cellular components of blood (Scanlon and Sanders, 2007). The blood, among other things, functions to deliver oxygen and nutrients to tissue, remove carbon (IV) oxide and metabolic waste from tissues, fight infections and cause coagulation at site of broken vessel (Scanlon and Sanders, 2007).

The biochemical, physiological and pathological status of a biological system can be analysed through haematology parameters. Haematology parameters that are considered for safety and toxicity studies include; red blood cell (RBC) count, haemoglobin (Hb) concentration, packed cell volume (PCV), mean corpuscular volume (MCV), mean corpuscular haemoglobin (MCH), mean corpuscular haemoglobin concentration (MCHC), white blood cells (WBCs) count, lymphocytes (LYM), neutrophils (NEU), and platelet (PLT) counts. Pathological conditions bring about alterations in these parameters.

2.15.1 Red Blood Cell Parameters

Red blood cells (erythrocytes) develop from pluripotent haematopoietic stem cells in bone marrow. They become nucleated cells under the influence of various growth factors, but the nucleus is removed as the erythrocytes mature (Everds, 2007) and lack mitochondria at maturity. They are biconcave disc-shaped cells and transport oxygen to tissues and carbon (IV) oxide away from such. The biconcave shape enhances their flexibility and passage through vessels for delivery of gases and nutrients, and reduces the distance between haemoglobin and erythrocyte surface thereby enhancing efficiency (Washington and Van Hoosier, 2012). Chemical

compounds that alter the morphology, quantity and/or quality of erythrocytes affect their functionality.

Red blood cell indices refer to measurements that depict the size and oxygen-carrying haemoglobin content of erythrocytes. The parameters used for assessment of red blood cells are; RBC count, Hb concentration, PCV, MCV, MCH, and MCHC.

2.15.1.1 Red Blood Cell Count

The red blood cell (RBC) count refers to the estimation of the number of red blood cells per unit volume of blood (Everds, 2007). Since *Plasmodium* reproduces in RBCs and destroys them, the RBC count is reduced in malaria cases (Scanlon and Sanders, 2007).

2.15.1.2 Haemoglobin Concentration

Haemoglobin is made up of four haem prosthetic group and four globin chains. Each of the haem prosthetic group contains an atom of iron in combination with protoporphyrin IX, while the globin chains could be a combination of polypeptide chains which are designated alpha, beta, gamma, and delta chains (Hall, 2011). The iron in each of the four haemoglobin subunits can loosely and reversibly bind, through its coordination bonds, to one molecule of oxygen, hence each haemoglobin molecule can transport eight atoms of oxygen (Thomas and Lumb, 2012). The binding affinity of haemoglobin molecule for oxygen is determined by the types of haemoglobin chains that it comprised, and presence of abnormalities in the chains (Hall, 2011). In human, haemoglobin A is the most common form of haemoglobin and it is made up of two alpha chains and two beta chains. Amino acid alteration in the two beta chains results in sickle cell in which glutamate is replaced by valine (Cummings, 2008).

Haemoglobin concentration in healthy human is approximately one-third of the packed cell volume (Campbell and Ellis, 2013). Deficiency of haemoglobin in the blood is called anaemia. Anaemia could also arise from too few red blood cells in the blood (Hall, 2011). Malaria infection is associated with reduction in haemoglobin concentration, resulting in haemolytic anaemia (Siqueira *et al*, 2014). But, haemoglobin concentration is elevated during dehydration and polycythemia (Hall, 2011).

2.15.1.3 Packed Cell Volume

The packed cell volume (PCV) is also called haematocrit. It is a measure of the percentage of blood occupied by red blood cells (Everds, 2007). PCV is relatively constant among mammals, but red blood cell count and mean cell size differ among species (Campbell and Ellis, 2013).

2.15.1.4 Mean Corpuscular Volume

Mean corpuscular volume (MCV) is a measure of the average size of red blood cells (Washington and Van Hoosier, 2012).

2.15.1.5 Mean Corpuscular Haemoglobin

Mean corpuscular haemoglobin (MCH) is calculated from the haemoglobin concentration and red blood cell concentration (Washington and Van Hoosier, 2012).

2.15.1.6 Mean Corpuscular Haemoglobin Concentration

Mean corpuscular haemoglobin concentration (MCHC) is calculated from the haemoglobin concentration and packed cell volume, and provides the index of

haemoglobin volume in grams relative to PCV in g per dl or percent (Washington and Van Hoosier, 2012).

The MCHC value is reduced in severe iron-deficiency anaemia or microcytic anaemia as a result of reduced haemoglobin concentration. But the MCHC value is falsely elevated in haemolysed sample (Washington and Van Hoosier, 2012).

2.15.2 White Blood Cell Parameters

The white blood cells, also called leukocytes, are the mobile protective system of the body. They are formed partially in the bone marrow and partially in the lymph tissue (Hall, 2011). They are mostly specifically transported to locations of infection and inflammation to provide protection (Hall, 2011).

The white blood cells are nucleated and of different type, namely; lymphocytes, polymorphonuclear neutrophils, polymorphonuclear eosinophils, polymorphonuclear basophils, and monocytes (Hall, 2011). The polymorphonuclear cells (neutrophils, eosinophils, and basophils) have a granular appearance and are therefore referred to as granulocytes, or "polys," because of the multiple nuclei (Hall, 2011). The concentration of individual white blood cell types is a central indicator of disease (Washington and Van Hoosier, 2012).

2.15.2.1 White Blood Cell Count

The white blood cell (WBC) count is a measure of the total amount of white blood cells in a given blood sample. Increase in the WBC count is an indication of acute infection, leukaemia while decreased WBC count could indicate aplastic anaemia (Scanlon and Sanders, 2007).

2.15.2.2 Lymphocyte Count

The lymphocytes are associated with immunologic response, that is, perform their protective functions primarily in connection with the immune system (Washington and Van Hoosier, 2012). Lymphocytes are produced primarily in the lymphogenous tissues especially in the spleen, lymph glands, tonsils, and thymus, but partially produced in the bone marrow (Hall, 2011).

The lymphocytes can be classified as T-lymphocyte which is responsible for cell-mediated immunity, and the B-lymphocyte which is responsible for antibodies formation to promote humoral immunity. The T-lymphocytes originate from the bone marrow, then move to the thymus gland where they develop specificity for antigens. Thousands of these pre-processed antigen-specific T-lymphocytes move away from the thymus to be stored in lymphoid tissues (Hall, 2011). The B-lymphocytes are pre-processed in the liver, and later in the bone marrow, after which they migrate to lymphoid tissue, close to the T-lymphocyte areas, for storage. The B-lymphocytes form several millions of different B-lymphocyte antibodies, each with specific reactivities (Hall, 2011). Hence the B-lymphocytes have far more diversity compared to the T-lymphocytes.

The lymphocytes are majorly stored in the lymphoid tissues, with only small quantity transported temporarily in blood. The lymphocytes move in the circulatory system continually, moving forth and back between the lymph and the blood. Hence, circulating through the body continually having a lifespan of weeks or months depending on the body's need for them (Hall, 2011). They demonstrate specific immunity against individual invading agents, hence said to show acquired or adaptive immunity (Hall, 2011).

2.15.2.3 Neutrophil Count

The polymorphonuclear neutrophils protects against invading organism by phagocytosis, that is cellular ingestion of the invading organism (Hall, 2011). The neutrophils are formed in the bone marrow and are stored there until needed in the circulatory system. Once released, they circulate for few hours in the blood, move to tissues where their phagocytic action is needed and remains there for about five days (Hall, 2011).

The neutrophils provide the second line of defence against infection, within hours of inflammation, in support of the first line of action provided by macrophages (Hall, 2011). Bacteria, viruses, and other injurious agents are majorly attacked by the neutrophils and tissue macrophages. The neutrophils can destroy bacteria in the circulating blood through its bactericidal action even when its digestive lysosomal enzymes are prevented (Hall, 2011).

Infections and inflammation bring about acute increase in neutrophil count (Washington and Van Hoosier, 2012).

2.15.2.4 Other Myeloid Cells

The other white blood cells are polymorphonuclear eosinophils (also called eosinophils), polymorphonuclear basophils (also called basophils), and monocytes. They are formed in the bone marrow, are released into circulatory system when needed, and protect against invading organism by phagocytosis (Hall, 2011).

Eosinophils are weak phagocytes (less effective than neutrophils) which are usually released in large numbers in parasitic-infected humans and move in large numbers into parasitized tissues (Washington and Van Hoosier, 2012). The eosinophils

circulate for few hours in the blood, move to tissues where needed and remains there for about five days. In response to allergens and some chronic diseases, eosinophils are involved in the inactivation of histamine. While most parasites are too big for phagocytosis, eosinophils act primarily by attaching to the parasites and releasing hydrolytic enzymes and/or highly reactive oxygen that are lethal to the parasites (Hall, 2011).

The basophils are similar to large tissue mast cells and both liberate heparin (an anticoagulant) into the blood. Also, the basophils in association with the mast cells release histamine, small amount of serotonin, and play an important role in some types of allergic reactions. After circulating for few hours in the blood, the basophils move to tissues where needed and remains there for about five days. They are commonly found at spots of ecto-parasite infection (Washington and Van Hoosier, 2012).

The monocytes move in the blood for few hours after their release and then move through capillary membrane to tissues where they swell greatly to become tissue macrophages and can live for months in this form to provide effective long-term phagocytic defence against infection in the tissues (Hall, 2011). The tissue macrophages are better phagocytes than neutrophils. Within minutes of inflammation, the first line of defence against infection is carried out by tissue macrophages (Hall, 2011).

2.15.3 Platelet Count

Platelets, also known as thrombocytes, are fragments of a type of cell called megakaryocytes which is similar to white blood cells. They are produced in the bone marrow, do not have nuclei, hence cannot reproduce but possesses mitochondria and have lifespan of about ten days (Hall, 2011). The platelets function to activate the

blood clotting mechanism. After a cut in the blood vessel, platelets form the initial haemostatic plug (the platelet plug) to seal the cut and prevent haemorrhage (Washington and Van Hoosier, 2012). Platelets have several functional features (cytoplasmic organelles) of whole cells, and their membranes have coat of glycoproteins which help to repel attachment to normal endothelium but causes their adherence to injured areas of the vessel wall. Their membrane also has enormous quantity of phospholipids which activate various phases in the blood-clotting process (Hall, 2011).

2.15.4 The Plasma

The plasma is the liquid component of blood which is made up of mostly water. Nutrients, electrolytes, metabolic waste products, and proteins are carried in the plasma (Scanlon and Sanders, 2007).

2.15.4.1 Plasma Electrolytes

Electrolytes are categorised as either anions (negatively charged) or as cations (positively charged). Physiological electrolytes include; Na^+, K^+, Ca^{2+}, Mg^{2+}, Cl^-, HCO_3^-, $H_2PO_4^-$, $H_2PO_4^{2-}$, SO_4^{2-} and some anions like lactate. Of these, Na^+, K^+, Cl^-, and HCO_3^- are referred to as the major electrolytes and occur in plasma primarily as free ions whereas ions such as Ca^{2+} and Mg^{2+} exist in plasma in the bound state. Abnormal levels of electrolytes may either result in, or be the consequence of disorders or disease conditions (Scott *et al.,* 2008). The plasma composition of these electrolytes is controlled by various mechanisms but primarily by the kidney.

2.15.4.1.1 Plasma Sodium Ions

Sodium ion is the major extracellular cation and it is present in high concentration in extracellular fluid compared to intracellular environment, as such,

helps in maintaining osmotic pressure and normal distribution of water (Scott *et al.*, 2008) and this extracellular-intracellular gradient is maintained by the Na^+-K^+ ATPase. Sodium ions help to maintain acid-base balance, transmit nerve impulses, and in muscle contraction.

In healthy adult humans, the concentration of plasma sodium ion ranges from 135 to 145 mmol/L and the amount of sodium in the body is regulated by renal reabsorption. Sodium is filtered by the glomeruli and majority of it is actively reabsorbed in the proximal tubules with further reabsorption taking place in the loop of Henle and by influence of the hormone aldosterone on the distal convoluted tubules (Scott *et al.*, 2008).

Dehydration from severe diarrhoea, extensive burns, or excessive sweating without proper fluid replacement, renal loss of water and/or renal dysfunction can lead to high sodium ion concentration (hypernatremia). Severe osmotic pressure changes results when there is either extremely low (hyponatremia) or high (hypernatremia) concentration of sodium ion in plasma and this can lead to damages of organs (Kovesdy, 2012). Malaria is reportedly associated with hyponatremia (English *et al.*, 1996; Hanson *et al.*, 2009).

2.15.4.1.2 Plasma Potassium Ion

Potassium ion is the major intracellular cation. Because of its higher intracellular concentration, transmembrane electrical gradients cause its diffusion out of cell, but this is effectively reversed by Na^+-K^+ ATPase, hence controlling potassium ion intracellular-extracellular gradient (McPherson and Pincus, 2011). Potassium alongside other ions, contributes to the electrolyte balance of organism. It is also crucial for electrical signalling in cells, assist in conduction of nerve impulses and

transport of essential nutrients (Deshpande *et al.,* 2013). Potassium ion helps in the maintenance of cardiac rhythm and facilitate neuromuscular conduction. Therefore, high level (hyperkalaemia) or low level (hypokalaemia) of potassium ion leads to cardiac arrhythmias and neuromuscular weakness (Parham *et al.,* 2006; Viera *et al.,* 2015). Hypokalaemia and hyperkalaemia can be caused by alteration in potassium intake, altered excretion, or transcellular shifts. While hypokalaemia usually results from gastrointestinal losses and renal loss from diuretic use, hyperkalaemia is commonly caused by impaired renal function, hyperglycaemia, and medication use (Viera *et al.,* 2015).

The resting membrane potential of cells is highly determined by the concentration of potassium ion in extracellular environment and kept within a narrow range of 3 and 5 mmol/L in plasma of healthy humans (Cheng *et al.,* 2013). Only about 2% of the total body potassium is in the extracellular space, with interstitial space and plasma containing 75% and 25% respectively of this extracellular potassium. About 98% of the total body potassium is stored in the intracellular space, with muscle containing 80% of the intracellular potassium while the bone, liver, and erythrocytes contains the remaining 20% (Sjøgaard *et al.,* 1985; Youn and McDonough, 2009).

2.15.4.1.3 Plasma Calcium Ion

Calcium ion plays important roles in biological systems acting extracellularly as a key factor in adhesion, blood coagulation, bone mineralization and movement, and as intracellular second messenger essential for muscle contraction, hormone secretion, cell division, and glycogen metabolism (Talarico Jr *et al.,* 2005; Endres and Rude, 2008).

In plasma, calcium exists in three physiochemical states as free calcium ion, plasma protein-bound calcium, and anion-complexed calcium. Of these three states of existence, the biologically active form is the free calcium ion fraction and its concentration is regulated by calcium-regulating hormones, parathyroid hormone and 1,25-dihydroxyvitamin D (Endres and Rude, 2008).

Maintenance of calcium homeostasis is essential for proper functioning of biological system. In cases of hypercalcaemia over time, calcium may deposit in soft tissues such as pancreas and heart causing pathological conditions. Also, hypocalcaemia can lead to muscle paralysis, convulsion, and death. Chronic hypocalcaemia result in rickets and osteomalacia in children and adults respectively (Rosenthal and Glew, 2011). Calcium is also reportedly depleted in cases of malaria infection (Davis *et al.*, 1991; Sitprija, 2008). Decreased concentration of free calcium ion in plasma causes elevated neuromuscular excitability while increased concentration of free calcium ion result in reduced neuromuscular excitability (Endres and Rude, 2008).

2.15.4.1.4 Plasma Chloride Ion

Chloride ion is the major extracellular anion and helps in maintaining electrical neutrality with sodium. The plasma concentration of chloride ion in human is between 80 and 120 mmol/L. The intracellular concentration of this anion is very low. The chloride concentration in the body is regulated by renal reabsorption. Chloride is filtered from plasma at the glomeruli and it is passively reabsorbed in the proximal tubules while active reabsorption by chloride pump takes place in the thick ascending limb of the loop of Henle (Scott *et al.*, 2008). Inhibition of the chloride pump by chemical agents results in loss of chloride in urine. Increased levels of chloride (hyperchloremia) are related to acidosis while decreased levels (hypochloremia) may

lead to metabolic alkalosis (Clark and Kruse, 1990). Chloride is important in biological system in maintenance of water distribution, osmotic pressure and anion-cation balance in extracellular fluid (Yunos *et al.*, 2010).

2.15.4.1.5 Plasma Bicarbonate

Bicarbonate ion is produced from the reaction between carbon dioxide and water, and most of CO_2 in plasma exists in the form of bicarbonate ion with a fraction bound to carrier proteins. Bicarbonate ion concentration in plasma is between 10 and 40 mmol/L, in healthy adult. It serves as the main component of extracellular buffer system, and is regulated by renal tubular cells and erythrocytes (Arneson and Brickell, 2007b). Some bicarbonate is found intracellularly, where it serves to maintain electrical neutrality with potassium. Bicarbonate buffers H^+ in extracellular environment forming H_2CO_3. The carbonic acid is a weak acid which acts as a buffer and do not contribute to the pH of the body fluids (Arneson and Brickell, 2007b).

2.15.4.1.6 Plasma Phosphate Ion

Phosphate exist as both monovalent ($H_2PO_4^-$) and divalent ($H_2PO_4^{2-}$) forms in plasma. Phosphate is vital for the activities of several enzymes. In cells, most of the phosphate exist as organic form which is incorporated into nucleic acids, phospholipids, cyclic adenosine monophosphate, nicotinamide adenine dinucleotide phosphate, and adenosine triphosphate (Endres and Rude, 2008).

Hypophosphatemia can cause skeletal muscles weakness, reduced cardiac output and metabolic acidosis. Adenosine triphosphate (ATP) production from adenosine diphosphate (ADP) can be impaired by low level of intracellular phosphate and this could have a ripple effect as reduced cellular ATP stimulates phosphofructokinase activity, thereby enhancing glycolysis and lactate production,

hence acidosis (Palmer and Clegg, 2017). In erythrocytes, phosphate depletion causes reduction in 2,3-bisphosphoglycerate thereby leading to tissue hypoxia because of elevated affinity of haemoglobin for oxygen. Severe phosphate reduction may cause haemolysis (Endres and Rude, 2008) and hypophosphatemia is associated with malaria and can be severe (Davis *et al.,* 1991; Sitprija, 2008).

Hyperphosphatemia may result from decreased renal phosphate excretion, renal failure, and cell lysis. Rapid elevated plasma phosphate level may be associated with hypocalcaemia (Endres and Rude, 2008). Hyperphosphatemia can cause increased bone turnover and lead to osteomalacia. It can also encourage apoptosis of vascular smooth muscle cells, and the accumulation and mineralization of vessel wall collagen matrix (Reynolds *et al.,* 2004; Chen and Moe, 2015).

2.15.4.2 Plasma Biomolecules

The plasma biomolecules refer to the molecules which are carried in the plasma and can serve as indicators of organ functions or dysfunction resulting from disease conditions or action of chemical agents. Some of the plasma biomolecules usually considered for assessment of organ functions are total Protein, albumin, globulin, bilirubin, creatinine, urea, uric acid, total cholesterol, triacylglycerol, high-density lipoprotein cholesterol, and low-density lipoprotein cholesterol (Ozer *et al.*, 2008; Gowda *et al.*, 2010)

2.16 Justification for the Study

Despite the availability of different antimalarial drugs, malaria remains a global health threat, with millions at risk of the infection and thousands of deaths recorded yearly. This burden of malaria is borne majorly by sub-Sahara African region with Nigeria taking the lead (WHO, 2016).

Given the continuous emergence of resistance to commonly used antimalarial agents, including artemisinin derivatives (Phyo *et al.*, 2016, WHO, 2016; Dondorp *et al.*, 2017), combination of chemical agents that can possibly act against different targetmetabolic pathwaysof *Plasmodium* species and with no prior report of resistance, are urgently needed. Since many of the available chemotherapeutic agents have substantial toxic effects (Schmuck *et al.*, 2002; Schlitzer, 2007), a new combination therapy with lesser toxicity are needed. Also, malaria is associated with secondary complications such as oxidative stress and organ dysfunctions (Becker *et al.*, 2004; Percário *et al.*, 2012), therefore combination of chemical agents that can ameliorate these complications in addition to its antimalarial activity will be of interest.

Some of the scientific approaches to drug development involve optimisation and repurposing of available drugs and their use in combination (Rosenthal, 2003; Jourdan *et al.*, 2017). This combination approach is similarly used in traditional treatment of malaria whereby multiple plants are combined with effective therapeutic results. However, isolated principles from these plants tend to be inactive *in vivo*, in some cases, unlike their unrefined extracts (Wagner and Ulrich-Merzenich, 2009), and this could be attributed to isolated action of these active principles rather than synergistic actions of molecules which combination of active principles afford (Rasoanaivo *et al.*, 2011). Methyl gallate and palmatine are such compounds found in efficacious antimalarial plants that are used in combination in traditional practice. While methyl gallate and palmatine exhibited *in vitro* activities against multidrug-resistant strains of *Plasmodium falciparum*, such activity was lost *in vivo* (Vennerstrom and Klayman, 1988; Malebo *et al.*, 2013; Zofou *et al.*, 2013). Hence, mimicking the traditional use of plants in combination which affords interaction of molecules, the *in vivo* antimalarial activity of methyl gallate and palmatine may be

regained if administered in the combination. Thus, this study was set out toevaluate the antimalarial activity and toxicological effects of the combination of methyl gallate and palmatine with or without a bio-enhancer.

2.17 Objective of The Study

2.17.1 Overall Objective

The overall objective of the study was to evaluate the antimalarial, antioxidant and toxicological effects of methyl gallate and palmatine combination in *in vitro* and *in vivo* models.

2.17.2 Specific Objectives

The specific objectives of the study were to:

1. Evaluate the *in vitro* antimalarial activity of methyl gallate and palmatine combination;
2. Determine the nature of the interaction of methyl gallate and palmatine combination;
3. Evaluate the interaction of methyl gallate and palmatine with selected *falciparum* proteins*in silico*;
4. Evaluate the *in vivo* antimalarial activity of methyl gallate and palmatine combination in *P. berghei* NK65-infected mice;
5. Evaluate the *in vivo* antimalarial activity of methyl gallate and palmatine combination in *P. berghei* NK65-infected mice in the presence of a bio-enhancer;

6. Evaluate the *in vitro* antioxidant activities of methyl gallate and palmatine combination;
7. Evaluate the effects of methyl gallate and palmatine combination on the antioxidant defense system of selected tissues in *P. berghei* NK65-infected mice in the presence of a bio-enhancer; and
8. Evaluate the toxicity of methyl gallate and palmatine combination in the presence of a bio-enhancer using selected function indices of the brain, heart, kidney and liver in animal model.

CHAPTER THREE

3.0 MATERIALS AND METHODS

3.1 Materials

3.1.1 Chemicals and Reagents

Acetic acid, Acetonitrile, trifluoroacetic acid, ammonium bicarbonate, glacial acetic acid, n-butanol, ethanol, methanol, Pyridine, dimethyl Sulfoxide, bovine serum albumin, HEPES buffer, Giemsa stain, bovine hemin, 2, 2-diphenyl-1-picrylhydrazyl, reduced glutathione, glutathione, sodium acetate, sodium carbonate, dimethyl sulphoxide, thiobarbituric acid, trichloroacetic acid, epinephrine, and Tris buffer were products of Sigma-Aldrich Chemical Company, St. Louis, Mo, USA. Assay Kits were purchased from Randox Laboratories Ltd, Co-Antrim, UK. All other reagents used were of analytical grade.

3.1.1.1 Drugs

Chloroquine diphosphate, methyl gallate, and piperine were purchased from Sigma-Aldrich Chemical Company, St. Louis, Mo., USA, while palmatine was a product of Nanjing Spring & Autumn Biological Engineering Co Ltd China. The compounds were of analytical grades.

3.1.2 Parasite

Chloroquine-sensitive strain of *Plasmodium berghei* (NK65) was obtained from Institute for Advanced Medical Research and Training, University College Hospital Ibadan, Oyo State, Nigeria. The parasites were maintained in mice by serial passages of blood from infected donor mouse to naive recipient.

3.1.3 Animals

Swiss albino mice and rats (*Rattus norvegicus*) of average weights of 21 ± 2 g and 160 ± 20 g respectively were obtained from the Animal Holding Unit of the Department of Biochemistry, Faculty of Life Sciences, University of Ilorin, Ilorin, Nigeria. They were housed in well-ventilated cages at room temperature under natural lighting condition. The animals were allowed access to standard rodent chow (Vital Feed®, Grand Cereals Ltd, Jos, Nigeria) and water *ad libitum*.

3.2 Methods

3.2.1 *In vitro* Studies

3.2.1.1 Inhibition of β-Haematin Formation

The inhibition of β-haematin formation assay was carried out as described by Ncokazi and Egan, (2005).

Principle: The assay is based on the ability of compounds toinhibit the formation of β-haematin. Aqueous pyridine (5%v/v, pH 7.5) forms a low-spin complex with haematin but not with β-haematin. Theabsorbance of the complex obeys Beer's law, therefore making it useful for quantifying haematinconcentration present in a mixture of haematin and β-haematin.

Procedure: The compounds were prepared in methanol and acidified with HCl (1 M) to form concentrationsthat varied from 0-10 equivalents relative to haematin in total reaction volume, each containing 33.76 μL in the final mixture. An aliquot (20 μL) of hematin stock solution (1.68 mM in 0.1 M NaOH) was added to each test tube, then followed by addition of 2.02 μL of test compounds and 11.74 μL of acetate solution (12.9 M, pH 5.0, 60ºC). This was mixed and incubated at 60ºC for 60 min. The

reaction was stopped with 900 µL of pyridine solution (5% v/v) in 200 mM HEPES (pH 7.5). This was followed by the addition of 1100 µL pyridine solution (5% v/v) in 20 mM HEPES (pH 7.5). The mixture was shaken to ensure complete dissolution of hematin and allowed to settle at room temperature for 15 min. The supernatant was transferred to a cuvette without disturbing the precipitate and absorbance was read at 405 nm. The IC_{50} values for β-hematin inhibition were determined by fitting the percentage inhibitions calculated from absorbance data to a sigmoidal dose response curve by non-linear least squares fitting using Origin 8.0 software.

Calculation:

$$\% \text{ Inhibition} = \frac{A - B}{C - B} \times 100$$

Where;

A = Absorbance of test

B = Absorbance of control (without drug)

C = Absorbance of Hematin solution

3.2.1.2 Determinationof Nature of Interaction

The methodof fixed ratios of drug interaction described by Fivelman *et al.* (2004) was used.

Procedure: All compounds were initially dissolved in methanol and then diluted to the desired starting concentration. The starting concentration, for serial dilutions, was assigned so that the 50% inhibitory concentration (IC_{50}) of each drug would be the median test tube. Each compound was tested alone and at fixed ratios of its

IC_{50}(methyl gallate and palmatine at ratios 5:0, 4:1, 3:2, 2:3, 1:4 and 0:5 volume:volume). The IC_{50} obtained were used to calculate 50% fractional inhibitory concentrations (FIC_{50}). FIC_{50}s of drug A (methyl gallate) and drug B (palmatine) at different concentration ratios were used to calculate the nature of interaction. To obtain numeric values for the interactions, results were expressed as the sum FICs (ΣFICs) of the FIC(A) and FIC(B). Summation of FIC_{50} lesser than 1, equal to 1 and greater than 1 were taken to be synergistic, additive and antagonistic respectively (Ohrt *et al.*, 2002; He *et al.*, 2010).

Calculation:

(i) $FIC_{50}(A) = \frac{IC_{50}\ (A+B)}{IC_{50}(A)} \times Ai$

(ii) $FIC_{50}(B) = \frac{IC_{50}\ (A+B)}{IC_{50}(B)} \times Bi$

(iii) $\Sigma FIC_{50} = FIC_{50}(A) + FIC_{50}(B)$

Where

IC= inhibitory concentration

FIC = fractional inhibitory concentration

Ai = fraction of methyl gallate in each combination ratio

Bi = fraction of palmatine in each combination ratio

IC_{50} (A+B) = IC_{50} of combinations of two drugs; methyl gallate and palmatine

IC_{50} (A) = IC_{50} of methyl gallate alone

IC_{50} (B) = IC_{50} of palmatine alone

3.2.1.3 *In vitro* antioxidant studies

3.2.1.3.1 Determination of DPPH Radical Scavenging Activity

The DPPH radical scavenging activity of methyl gallate and palmatine, separately and in combination, was determined by procedure described by Sunand Wang (2010), with slight modification.

Principle: The DPPH assay is mainly based on electron transfer reaction, and hydrogen-atom abstraction is a marginal reaction pathway (Huang *et al.,* 2005). 2,2-diphenyl-1-picrylhydrazyl (DPPH) is a stable organic nitrogen radical. On accepting electron from a corresponding donor, its solutions lose the characteristic deep purple colour (λmax 515–517 nm). Hence, the reducing effect of sample on DPPH is measured.

Procedure: Briefly, 1.8 mL of 0.11 mM DPPH (in 80% ethanol) was added to 0.2 mL of varying concentrations of compound solution. The mixture was mixed and incubated at room temperature in the dark for 30 min and absorbance (A_{sample}) was read at 517 nm. Butylated hydroxyl toluene (BHT) was used as reference and solution of 0.11 mM DPPH in ethanol served as control ($A_{control}$). Lower absorbance of the reaction mixture indicated higher free radical-scavenging activity.

Calculation: The following equation was used to calculate the DPPH radical scavenging activity and expressed in percentage.

$$\% \text{ Inhibition of DPPH radical} = \frac{\text{Absorbance of control - Absorbance of sample}}{\text{Absorbance of control}} \times 100$$

3.2.1.3.2 Determination of Ferric ion Reducing Power

The reducing powers of methyl gallate and palmatine, separately and in combination, were determined according to the method described by Oyaizu (1986) with some modifications (Nam *et al.*, 2017).

Principle: This method is based on the principle of increase in the absorbance of the reaction mixtures. Increase in the absorbance indicates an increase in the antioxidant activity. In this method, antioxidant compound forms a coloured complex with potassium ferricyanide, trichloroacetic acid and ferric chloride, which is measured at 700 nm. Increase in absorbance of the reaction mixture indicates the reducing power of the samples (Jayaprakash *et al*., 2001).

Procedure: Briefly, 0.7 mL of each compound solution at different concentrations was added to 0.7 mL of 50 mM phosphate buffer (pH 7.0). Afterwards, 0.5 mL of potassium ferricyanide (1% w/v $K_3Fe(CN)_6$) was added and the resulting mixture was incubated at 50^oC for 20 min. Then, 0.5 mL of trichloroacetic acid (10% w/v) was added and the mixture was centrifuged at 3000 rpm for 10 min. Aliquot (0.5 mL) from the upper layer of the solution was then mixed with 0.5 mL of distilled water and 0.1 mL of $FeCl_3$(0.1% w/v). The absorbance was then measured at 700 nm against blank.

3.2.1.3.3 Determination of Hydroxyl Radical Scavenging Activity

The hydroxyl radical-scavenging activities of methyl gallate and palmatine, separately and in combination,were carried out by the method described by Smirnoff and Cumbes (1989).

Principle: Hydroxyl radical ($OH^{\cdot}$) were generated by the Fenton reaction in the system from $FeSO_4$ and H_2O_2, and detected by their ability to hydroxylate salicylate.

Procedure: The reaction mixture (3.0 mL) consisted of 1.0 mL $FeSO_4$ (1.5 mM), 0.7 ml hydrogen peroxide (6 mM), 0.3 ml sodium salicylate (20 mM) and 1.0 mL of each compound solution at various concentrations. The mixture was incubated at 37°C for 60 min and the absorbance of the hydroxylated salicylate complex formed was measured at 562 nm. BHT was used as the standard.

Calculation: The percentage hydroxyl radical scavenging activity was calculated as:

$$\% \text{ Hydroxyl radical scavenging activity} = \left[1 - \frac{(A_1 - A_2)}{A_0}\right] \times 100$$

Where: A_0 = absorbance of the control (without test compounds)

A_1 = the absorbance in the presence of the test compounds

A_2 = the absorbance without sodium salicylate

3.2.1.3.4 Nitric Oxide Scavenging Activity

The nitric oxide-scavenging activities of methyl gallate and palmatine, separately and in combination, were determined according to the method described by Marcocci *et al.* (1994).

Principle: The compound, sodium nitroprusside, is known to decompose in aqueous solution at physiological pH (7.2) producing nitric oxide(NO). Under aerobic conditions, nitric oxide reacts with oxygen to produce stable products (nitrate and nitrite), which form a pink-coloured diazonium salt with Griess reagent, the quantities of which can be determined spectrophotometrically at 530 nm (Marcocci *et al*., 1994; Chanda and Dave, 2009).

Procedure: Briefly, 2 mL of 10 mM sodium nitroprusside (dissolved in 0.1 M phosphate buffer saline, pH 7.4) was mixed with 0.5 mL of sample at various

concentrations and incubated at 25^{o}C for 150 min. Thereafter, 0.5 mL of the incubated solution was withdrawn and mixed with 0.5 mL of Griess reagent [1 mL of 0.33% sulfanilic acid reagent (in 20% glacial acetic acid at room temperature for 5 min) and 1 mL of naphthylethylenediamine dichloride (0.1% w/v)]. The mixture was incubated at room temperature for 30 min andabsorbance of the chromophore formed during diazotization ofnitrite with sulfanilamide and later *N*-naphthylethylenediaminedihydrochloride was read at 546 nm.The control was similarly prepared containing all reagents except test compounds and BHT was used as standard.

Calculation: The nitric oxide radical scavenging activity was calculated as:

NO radical scavenging activity (%)=

$$\frac{\text{Absorbance of control - Absorbance of sample}}{\text{Absorbance of control}} \times 100$$

3.2.1.4 Inhibition of Conjugated Diene Formation Assay

The plasma oxidation assay was carried out by the method described by Schnitzer *et al.* (1995).

Principle: Cupric ions initiate oxidation of lipoproteins in plasma to yield conjugated diene hydroperoxides. The conjugated dienes formed can be progressively monitored by spectrophotometric means at absorbance of 245 nm (Kleinveld *et al*., 1992; Jialal and Devaraj, 1996).

Procedure: Heparinized blood from healthy rat was centrifuged at 1500 g for 10 min to obtain plasma. This was diluted 40-fold with phosphate buffered saline (0.1 M, pH 7.4) and 0.5 mL of the diluted plasma was mixed with 0.5 mL of standard (Vitamin C) or test compound at different concentrations and incubated at 37°C for 20 min.

Subsequently, 1.0 mL of $CuCl_2$ (200 µM) was added as oxidant (for lipid oxidation) and incubated at 37°C for 2 h. Levels of copper-induced oxidation were determined every 30 min by measuring conjugated dienes formed at absorbance of 245 nm. Two controls were used with the first control consisting of only diluted plasma while the second control consisted of diluted plasma and $CuCl_2$.

Calculation:

Inhibition of conjugated diene formation (%) =

$$\frac{\text{Absorbance}_{CuCl_2} - \text{Absorbance}_{Sample}}{\text{Absorbance}_{CuCl_2}} \times 100$$

3.2.1.5 Oxidative Haemolysis Inhibition Assay

The oxidative haemolysis inhibition assay was carried out as described by Cheung *et al.* (2003).

Procedure: Blood was collected from rats into heparinized bottle and centrifuged at 1500 g for 10 min. The erythrocyte was washed three times with phosphate buffered saline (0.1 M, pH 7.4) at 1,500 g for 10 min and re-suspended in same buffer to give 20% hematocrit level. An aliquot (0.1 mL) of this erythrocyte suspension was mixed with 0.1 mL of standard (vitamin C) or test compounds at various concentrations and incubated at 37°C for 20 min with gentle shaking. Afterwards, 0.2 mL of 200 mM 2,2'-Azobis(2-amidinopropane) dihydrochloride (AAPH) was added and incubated at 37°C temperature for 2 h. The mixture was diluted with 4 mL phosphate buffered saline and centrifuged at 1500 g for 10 min. The absorbance of the supernatant was read at 540 nm. To achieve complete hemolysis for the control, 4 mL of distilled water was added to the mixture in place of phosphate buffered saline.

Calculation:

$$\% \text{ Haemolysis inhibition} = \left(1 - \frac{\text{Absorbance for complete hemolysis}}{\text{Absorbance of test compound}}\right) \times 100$$

3.2.2 In silico Studies

Proteins/receptors for the ducking studies were downloaded from the Protein Databank (http://www.rcsb.org) with their various PDB identification codes [Plasmepsin I (3QS1), Plasmepsin II (1SME), Plasmepsin III (3FNU), Plasmepsin IV (2ANL), Plasmepsin V (4ZL4), *Plasmodium falciparum*Lactate Dehydrogenase *Pf*LDH (1T2C) and Falcipain-2 (1YVB)]. The native ligand and water molecules were deleted from the proteins and saved as pdb file format. Ligands (methyl gallate and palmatine) in sdf format were downloaded from PubChem (https://pubchem.ncbi.nlm.gov/) and were converted to pdb format using OpenBabel software. The receptor and the ligands (in pdb format) were then prepared by adding polar hydrogen, appropriate number of torsion and grid box size using AutoDockTools v1.5.6 and were saved in pdbqt file format. The ligands were then docked into the active site of the receptor using AutoDock vina 4.2. (Trott and Olson, 2010) and revalidated with the native ligand of the receptor. Affinity energy of different ligand pose, best conformation fits and root mean square deviation (RMSD) values, 2D protein-ligand interactions (Discovery Studio Visualizer version 16) were studied and used in comparison for each docking study. The mode with lowest binding energy (kcal/mol) were taken as the best pose.

3.2.3 *In vivo* studies

3.2.3.1 *In vivo* Antimalarial Studies

Blood from donor mouse was diluted with citrate-glucose solution (3.8% citrate and 0.5% glucose) to prepare an inoculum size of 1×10^5 of parasitized erythrocytes in0.2 mLwith which each mouse was intra-peritoneally injected.

Calculations

The percentage parasitaemia and the percentage reduction in parasitaemia were calculated thus;

$$\% \text{ Parasitaemia} = \frac{\text{Number of parasitized erythrocyte}}{\text{Total number of erythrocyte}} \times 100$$

Parasitaemia Reduction (%) =

$$\frac{\%\text{Parasitaemia of control - }\%\text{Parasitaemia of Test}}{\%\text{Parasitaemia of control}} \times 100$$

$$\text{Mean survival time (MST)} = \frac{\text{Sum of survival of animal in each group (days)}}{\text{No of animals in each group}}$$

Compounds causing percentage reduction in parasitaemia of less than 30% were considered inactive. Those causing chemo-suppression of 30% to 40% were considered partially active while those causing percentage reduction in parasitaemia above 40% were considered active (Souza *et al*., 2014).

3.2.3.1.1 Suppressive Antimalarial Study

The 4-day suppressive test against chloroquine sensitive *Plasmodium berghei* (NK65) infection in mice, as described by Peters (1965), was used to test the efficacy of the

compounds. Mice (115) were randomly grouped into twenty-three, of five mice each. On day zero (D_0), mice were inoculated with 1×10^5 of parasitized erythrocytes (inoculum size). Treatment with compounds and reference drug started 24 hours post-inoculation and was given orally, once daily, for three consecutive days as follows:

Group A: 5% DMSO

Group B: 10 mg/Kg bwt Chloroquine

Group C: 20 mg/Kg bwt Piperine

Group D: 6.25 mg/Kg bwt Methyl gallate

Group E: 12.5 mg/Kg bwt Methyl gallate

Group F: 25 mg/Kg bwt Methyl gallate

Group G: 50 mg/Kg bwt Methyl gallate

Group H: 100 mg/Kg bwt Methyl gallate

Group I: 6.25 mg/Kg bwt Palmatine

Group J: 12.5 mg/Kg bwt Palmatine

Group K: 25 mg/Kg bwt Palmatine

Group L: 50 mg/Kg bwt Palmatine

Group M: 100 mg/Kg bwt Palmatine

Group N: 6.25 mg/Kg bwt M*P*

Group O: 12.5 mg/Kg bwt M*P*

Group P: 25 mg/Kg bwt M*P*

Group Q: 50 mg/Kg bwt M*P*

Group R: 100 mg/Kg bwt M*P*

Group S: 6.25 mg/Kg bwt M*P* + 20 Pip

Group T: 12.5 mg/Kg bwt M*P* + 20 Pip

Group U: 25 mg/Kg bwt M*P* + 20 Pip

Group V: 50 mg/Kg bwt M*P* + 20 Pip

Group W: 100 mg/Kg bwt M*P* + 20 Pip

Where: **bwt** = body weight; **20 Pip** = 20 mg/Kg bwt Piperine

M*P* = 3:2 of Methyl gallate and Palmatine (most active ratio from *in vitro*antimalarial study)

Thin blood smears were made from the mouse tail blood on days 4, 6 and 8 post-inoculation. The blood smears were fixed with methanol, stained with Giemsa stain, and microscopically examined (x1000 magnification). The percentage parasitaemia was recorded and the survival time of the mice in each treatment group was monitored for 30 days and the mean survival time was calculated.

3.2.3.1.2 Curative Antimalarial Study

Evaluation of the curative potential of the combination was carried out as described by Ryley and Peters (1970). On day zero (D_0), mice were inoculated with 1×10^5 of parasitized erythrocytes (inoculum size). Mice (75) were randomly grouped into fifteen groups of five mice each. Treatment commenced 72 hours (day 3) post-inoculation.

Daily administration of compounds and reference drug was for three consecutive days (D_3 to D_5) as follows:

Group A: 5% DMSO

Group B: 10 mg/Kg bwt Chloroquine

Group C: 20 mg/Kg bwt Piperine

Group D: 100 mg/Kg bwt Methyl gallate

Group E: 100 mg/Kg bwt Palmatine

Group F: 6.25 mg/Kg bwt M*P*

Group G: 12.5 mg/Kg bwt M*P*

Group H: 25 mg/Kg bwt M*P*

Group I: 50 mg/Kg bwt M*P*

Group J: 100 mg/Kg bwt M*P*

Group K: 6.25 mg/Kg bwt M*P* + 20 Pip

Group L: 12.5 mg/Kg bwt M*P* + 20 Pip

Group M: 25 mg/Kg bwt M*P* + 20 Pip

Group N: 50 mg/Kg bwt M*P* + 20 Pip

Group O: 100 mg/Kg bwt M*P* + 20 Pip

Where: **bwt =** body weight; **20 Pip**= 20 mg/Kg bwt Piperine;

M*P* **=** 3:2 of Methyl gallate and Palmatine (most active ratio from *in vitro* antimalarial study)

Thin blood smears were made from the mouse tail blood on days 6, 8 and 10 post-inoculation. The blood smears were fixed with methanol, stained with Giemsa stain, and microscopically examined (x1000 magnification). The percentage parasitaemia were recorded and the survival time of the mice, in each treatment group, was monitored for 30 days and the meansurvival time calculated.

3.2.3.1.3 Prophylactic Antimalarial Study

Evaluation of the chemo-prophylactic potential of methyl gallate and palmatine combination was carried out as described by Fidock *et al*. (2004). Mice (35) were randomly grouped into seven, of five mice each. Daily single dose administration of compounds and reference drug was for four consecutive days ($-D_3$ to $-D_0$) as follows:

Group A: 5% DMSO

Group B: 10 mg/Kg bwt Chloroquine

Group C: 20 mg/Kg bwt Piperine

Group D: 100 mg/Kg bwt Methyl gallate

Group E: 100 mg/Kg bwt Palmatine

Group F: 100 mg/Kg bwt M*P*

Group G: 100 mg/Kg bwt M*P* + 20 Pip

Where: **bwt =** body weight; **20 Pip**= 20 mg/Kg bwt Piperine; **M*P*** **=** 3:2 of Methyl gallate and Palmatine (most active ratio from *in vitro* antimalarial study)

Three hours after the last administration, mice were inoculated intraperitoneally with$1\times10^5$of parasitized erythrocytes per mice. Thin blood smears were made from mouse tail blood on days 3, 5 and 7 post-inoculation. The blood smears were fixed with methanol, stained with Giemsa stain, and microscopically examined (x1000 magnification). The percentage parasitaemia was recorded and the survival time of the mice in each treatment group was monitored for 30 days and the mean survival time calculated.

3.2.3.2 *In vivo* Antioxidant Studies

3.2.3.2.1 Induction of Oxidative Stress

The 4-day suppressive method described by Peters (1965) was used to induce oxidative stress and evaluate the effect of compounds on antioxidant defense system of the mice. On day zero (D_0), sixty of the seventy mice used were inoculated intraperitoneally with 1×10^5 of parasitized erythrocytes (inoculum size) per mouse. The remaining ten mice were not inoculated.Treatment with compounds and reference drug started 24 h post-inoculation and were given orally, once daily, for three consecutive days as follows:

Group A: Uninfected and received 5% DMSO (control)

Group B: Infected and received 5% DMSO (negative control)

Group C: Infected and received 10 mg/Kg bwt Chloroquine

Group D: Infected and received 6.25 mg/Kg bwt M*P* + 20 Pip

Group E: Infected and received 12.5 mg/Kg bwt M*P* + 20 Pip

Group F: Infected and received 25 mg/Kg bwt M*P* + 20 Pip

Group G: Infected and received 50 mg/Kg bwt M*P* + 20 Pip

Where: **bwt** = body weight; **20 Pip** = 20 mg/Kg bwt Piperine

M*P* = 3:2 of Methyl gallate and Palmatine (most active ratio from *in vitro*antimalarial study)

3.2.3.2.2 Preparation of Erythrocytes and Organs

Twenty-four hours after the last administration (day 4), half of the mice in each group were sacrificed under slight diethyl ether anaesthesia. Jugular venous blood was collected into heparinized bottles (sodium heparin of 0.1–0.2 mg/ml in bottles) and centrifuged at 3000 rpm for 5 min to remove the plasma. The erythrocytes were washed three times with ice-cold phosphate-buffered saline (PBS: 145 mM NaCl, 1.9 mM NaH_2PO_4 and 8.1 mM Na_2HPO_4, pH 7.4) and centrifuged at 3000 rpm for 5 min. The erythrocyte pellets obtained were thereafter resuspended in PBS at 1:9 dilution. The cells were lysed by repeated freeze-thaw method and the lysates were used for erythrocyte antioxidant assays. The organs (liver, kidney, heart and brain) of each mouse were excised, cleansed of superficial connective tissues/blood and were then homogenized in ice-cold 0.25 M sucrose solution (1:5 w/v). The homogenates were centrifuged at 10,000 rpm for 4 min in a refrigerated centrifuge and the supernatants were stored overnight at -20^{o}C to ensure maximum release of the enzymes. These were then used for organ antioxidant assays. On day 8 post-inoculation, the remaining mice were also sacrificed and treated similarly.

3.2.3.2.3 Markers of Oxidative Stress and Antioxidant Assays

3.2.3.2.3.1 Determination of Lipid Peroxidation

The extent of lipid peroxidation in tissues was determined by measuring the malondialdehyde concentration as described by Buege and Aust (1978).

Principle: Oxidation of polyunsaturated fatty acids forms malondialdehyde (MDA) which serves as an index for the determination of the extent of lipid peroxidation. Two molecules of chromogenic reagent, 2-thiobarbituric acid (TBA) react with one molecule of malondialdehyde in the sample to yield a chromophore (pink-coloured product) which absorbs maximally at 532 nm.

Procedure: Aliquot (0.4 mL) of sample was mixed with 1.6 mL of Tris KCl buffer, followed by addition of 0.5 mL 30% trichloroacetic acid (TCA) and 0.5 mL 0.75% thiobarbituric acid (TBA). This was incubated at 80 ^{o}C for 45 min and thereafter cooled on ice. The mixture was centrifuged at 3000 g for 15 min and the absorbance of the supernatant was read at 532 nm against blank.

Calculation:

MDA (units/mg protein) =

$$\frac{\text{Absorbance} \times \text{volume of mixture}}{1.56 \times 10^{5} \times \text{volume of sample} \times \text{mg protein}} \times \text{dilution factor}$$

Where: 1.56×10^{5} M^{-1} cm^{-1} = Molar extinction coefficient

3.2.3.2.3.2 Determination of Superoxide Dismutase Activity

The superoxide dismutase (SOD) activity was determined by the method described by Misra and Fridovich (1972).

Principle: Xanthine oxidase reaction generates superoxide radical ($O^{\cdot -2}$) which oxidizes epinephrine to adenochrome. The adenochrome produced is proportional to the superoxide radical generated, increasing pH and increasing concentration of epinephrine. The auto oxidation of epinephrine at pH 10.2 is inhibited by superoxide dismutase.

Procedure: Aliquot (100 µL) of appropriately diluted sample was added to 1000 µL of 0.05 M carbonate buffer (pH 10.2) to equilibrate in the spectrophotometer. The reaction was initiated by addition of 150 µL freshly prepared 0.3 mM epinephrine to the mixture. The blank contained 1000 µL buffer, 150 µL of epinephrine and 100 µL of distilled water. The increase in absorbance at 480 nm was monitored every 0.5 min for 2.5 min.

Calculations:

$$\text{Increase in absorbance per minutes} = \frac{A_5 - A_0}{2.5}$$

Where; **A0** = absorbance after 0.5 min; **A5** = absorbance after 2.5 min

$$\% \text{ Inhibition} = \frac{\text{Increase in absorbance of substrate}}{\text{Increase in absorbance of blank}} \times 100$$

1 unit of SOD activity was given as the amount of SOD necessary to cause 50% inhibition of the oxidation of adrenaline to adenochrome in 1 minute.

3.2.3.2.3.3 Determination of Catalase Activity

The activity of catalase was determined by the method described by Sinha (1972).

Principle: When heated in the presence of hydrogen peroxide, dichromate in acetic acid is reduced to chromic acetate which can be quantified colorimetrically between 570 – 610 nm. The catalase in the tissue of interest splits hydrogen peroxide over specific minutes after which the reaction is terminated by the addition of dichromate/acetic acid mixture. The hydrogen peroxide left unsplit is quantified by measuring chromic acetate colorimetrically after heating the reaction mixture.

Procedure: An aliquot (1 mL) H_2O_2 solution (800 µM), 1.25 mL of phosphate buffer (0.1 M, pH 7.4) and 1 mL of appropriately diluted tissue supernatant were rapidly mixed by gentle swirling. An aliquot (1 mL) of this reaction mixture was pipetted and added to 2 mL dichromate/acetic acid (5% solution of $K_2Cr_2O_7$ with glacial acetic acid ratio 1:3 by volume) reagent and the absorbance was read at 570 nm for 3 min at 60 sec intervals.

Calculation: The activity of catalase was expressed as Units/mg protein

$$\text{Catalase activity} = \frac{\Delta \text{ Abs/min} \times \text{Conc. of standard} \times \text{Volume of assay}}{\text{Abs of standard} \times \text{Volume of enzyme} \times \text{Protein conc.}} \times \text{d.f}$$

Where: **Abs** = Absorbance at 570 nm; **Δ Abs** = Change in Absorbance; **d.f** = dilution factor

3.2.3.2.3.4 Determination of Glutathione Peroxidase Activity

The glutathione peroxidase activity was determined by the method described by Rotruck *et al.* (1973).

Principle: Glutathione peroxidase utilizes two molecules of reduced glutathione (GSH) to catalyse the splitting of one molecule of H_2O_2 and other peroxides (^{-}OOH)**.** The reaction proceeds for a specified period (in minutes) and then terminated by the addition of trichloroacetic acid. The residual GSH in the reaction mixture is then quantified by the addition of Ellman's Reagent [(5',5'-dithiobis- (2-nitrobenzoic acid), DTNB)].

Procedure: A reaction mixture containing 800 µL Tris-HCl buffer (0.1 M, pH 7.4), 400 µL GSH (2 mM), 200 µL sodium azide (10 mM), 50 µL of appropriately diluted

tissue sample was made up to 2 mL with distilled water and the reaction was initiated by the addition of 200 µL of H_2O_2 (10 mM). This mixture was incubated at 37 ^{0}C for 5 min and the reaction was terminated by the addition of 500 µL of TCA (10 %). This was centrifuged at 4000 x g for 10 min. Aliquot (250 µL) of the supernatant was pipetted to 1000 µL of DTNB (0.004%) and 250 µL of disodium hydrogen phosphate (0.3 M) solution. The colour developed was read at 420 nm and a reaction mixture without enzyme was used as the blank. The glutathione peroxidase activity was expressed as Units per milligram protein (Units/mg protein).

Calculation:

$$\text{GPx activity} = \frac{\Delta\text{Abs/min} \times \text{conc. of GSH standard} \times \text{total reaction volume} \times \text{d.f}}{\text{Abs of standard} \times 307.32 \times \text{volume of enzyme source} \times \text{protein conc.}}$$

Where: **307.32** = molecular weight of GSH; **Abs** = Absorbance at 420 nm;

Δ Abs = Change in Absorbance; **d.f** = dilution factor

3.2.3.2.3.5 Determination of Glutathione Reductase Activity

Glutathione reductase (GR) activity was determined according to the method described by Goldberg and Spooner (1983).

Principle: Glutathione reductase is responsible for the conversion of oxidized glutathione (GSSG) or glutathione disulphide to reduced glutathione (GSH) oxidizing reduced nicotinamide adenine dinucleotide phosphate (NADPH) or reduced nicotinamide adenine dinucleotide (NADH) in the process, although its main activity is with NADPH as co-factor. The oxidation of NADPH results in decrease in absorbance at 340 nm which is directly proportional to the activity of GR in the tissue sample.

Procedure: The reaction mixture was made up of 1 mL of 0.1 M phosphate buffer (pH 7.4), 0.5 mL of 15 mM EDTA, 0.1 mL of appropriately diluted tissue sample and 0.2 mL of 0.66 mM GSSG. This was incubated at room temperature for 10 min and 0.1 mL of 0.1 mM NADPH was then added to initiate the reaction. Decrease in absorbance was read at 340 nm every min for 3 consecutive minutes against a blank which was devoid of GSSG. The enzyme activity was expressed as unit/mg protein.

Calculation:

$$\text{GR activity} = \frac{\Delta\text{Abs/min} \times \text{volume of assay} \times 1000}{6.22 \times \text{volume of enzyme source} \times \text{protein conc.}} \times \text{dilution factor}$$

Where: **6.22** = molar extinction coefficient of NADPH

3.2.3.2.3.6 Determination of Glutathione-S-Transferase Activity

The activity of glutathione-S-transferase (GST) was determined using the method described by Habig *et al*. (1974).

Principle: The principle relies on the ability of glutathione-S-transferase to use 1-chloro- 2, 4,-dinitrobenzene (CDNB) as second substrate. Conjugation of CDNB with GSH leads to a shift in maximum absorption to a longer wavelength. The increase in absorption at the new wavelength of 340 nm provides a direct measurement of GST activity.

Procedure: The reaction mixture was made up of 30 µL of GSH, 150 µL of CDNB, 2.79 mL of 0.1 M phosphate buffer (pH 6.5) and 30 µL of post mitochondria fraction (PMF). The reaction was left for 1 min after which the absorbance was read against blank at 340 nm. The temperature was maintained at 31 ^{o}C. The activity of GST was expressed in µmole/min/mg protein.

Calculation:

GST activity (µmole/min/mg protein)=

$$\frac{\text{Absorbance} \times \text{reaction volume} \times \text{dilution factor}}{9.6 \times \text{volume of enzyme source} \times \text{protein concentration}}$$

Where; **9.6** = extinction coefficient of CDNB (9.6 $mmol^{-1}cm^{-1}$)

3.2.3.2.3.7 Determination of Reduced Glutathione Concentration

The levels of reduced glutathione in the tissues were determined by the method described by Beutler *et al*. (1963).

Principle: A relatively stable yellow colour develops when 5', 5'-dithiobis- (2-nitrobenzoic acid) (DTNB), reacts with sulphydryl compounds such as GSH. This coloured product (2-nitro-5-benzoic acid) absorbs maximally at 412 nm and the amount of GSH in the sample is proportional to the absorbance. Since majority of cellular non-protein sulphydryl groups are in the reduced form of glutathione, thus, deproteinization of samples with sulphosalicylic acid is necessary to ensure no protein cysteine thiol groups can react with the colour reagent.

Procedure: Briefly, 1.5 mL of 4% sulphosalicylic acid (precipitating reagent) was added to 1 mL of appropriately diluted sample and then left at room temperature for 10 min. The mixture was centrifuged at 3000 x *g* for 4 min and 0.25 mL of the supernatant was added to 2 mL of phosphate buffer (0.1 M, pH 7.4). Thereafter, 0.25 mL of DTNB was added and the absorbance was read at 412 nm. The absorbance obtained was proportional to GSH concentration in the tissue samples, which was estimated using the GSH standard plot.

3.2.3.3 Toxicological Studies

Sixty albino rats (*Rattus norvegicus*) of average weight of 160 ± 20 g were randomly grouped into six, of ten rats each. They were acclimatized for seven days and

administered treatment for 28 days. Each group of rats received 0.5 mL of appropriate drug solution orally as follows;

Group A: 5% DMSO

Group B: 6.25 mg/Kg bwt M*P* + 20 Pip

Group C: 12.5 mg/Kg bwt M*P* + 20 Pip

Group D: 25 mg/Kg bwt M*P* + 20 Pip

Group E: 50 mg/Kg bwt M*P* + 20 Pip

Group F: 100 mg/Kg bwt M*P* + 20 Pip

Where: **bwt** = body weight; **20 Pip** = 20 mg/Kg bwt Piperine

M*P* = 3:2 of Methyl gallate and Palmatine (most active ratio from *in vitro* antimalarial study)

3.2.3.3.1 Sample Collection and Preparation

Twenty-four hours after the last set of doses were administered, rats were sacrificed under slight diethyl ether anaesthesia. Jugular venous blood was collected into EDTA and heparin sample bottles for haematological and biochemical analyses respectively. The heparinized blood samples were centrifuged at 1,500 rpm for 10 mins and the plasma was carefully pipetted into properly labelled tubes. These were stored frozen until needed for analysis. The organs (liver, kidney, heart and brain) of each rat were excised, cleansed of superficial connective tissues/blood, weighed and were then homogenized in ice-cold 0.25 M sucrose solution (1:5 w/v). The homogenates were stored overnight at -20 ^{o}C to ensure maximum release of enzymes. They were thawed thereafter and centrifuged at 10,000 rpm for 5 mins in a refrigerated

centrifuge and the supernatants were pipetted into new sample tubes. These were stored at -20 ^{o}C for biochemical analyses. Organs of two rats from each group were not homogenized. They were collected and transferred into sample bottles containing 10% formalin for histological studies.

3.2.3.3.2 Determination of Organ-Body Weight Ratio

The relative weight of an organ to the body weight of corresponding rat, expressed as percentage, was calculated using the formula:

$$\% \text{ Organ-body weight ratio} = \frac{\text{Weight of the organ}}{\text{Weight of the animal}} \times 100$$

3.2.3.3.3 Haematological Analysis

Whole blood collected in EDTA sample bottle was used to determine red blood cell count (RBC), haemoglobin concentration (Hb), packed cell volume (PCV), mean corpuscular volume (MCV), mean corpuscular haemoglobin (MCH), mean corpuscular haemoglobin concentration (MCHC), white blood cell count (WBC), neutrophils (NEU), lymphocytes (LYM) and platelets count (PLT) using automated haematology analyser (SYSMEX XS-1000i model, SYSMEX Corporation, Japan).

Principle: The machine uses cell packs which functions as a detergent and self-rinses the system to avoid introduction of errors and a stromatolyzer which works on the cells. The stromatolyzer counts the red cells and lyses them thereby releasing the haemoglobin and estimates its concentration photometrically. The machine assumes that all nucleated cells are white and therefore counts them into their different forms of lymphocytes and neutrophils. It lyses the white blood cells based on the size of the nucleus and counts the number of white cells.

3.2.3.3.4 Determination of Plasma Electrolytes Concentrations

3.2.3.3.4.1 Plasma Sodium and Potassium Ions Concentration

Flame Emission Photometry was used to determine plasma sodium and potassium ion concentrations.

Principle: Sodium and potassium ions emit spectra, when excited thermally, with sharp bright lines at 589 and 768 nm respectively. On returning to the ground state, the internal standard signal is taken as a reference against which the analytical signal (sodium and potassium) is compared. The system is standardized with reference to low and high concentration of each analyte and the relation of signal to concentration is computed by an associated microprocessor upon aspiration of controls and samples into the standardized instrument.

Procedure: Aliquot (0.1 mL) of plasma was diluted with 19.9 mL of distilled of water and shaken. The samples were then aspirated into the flame photometer and the results read (in mmol/L on a digital read-out device) after setting instrument to zero with glass distilled water and calibrated with respective standards (140 mEq/L for Na^+ and 5 mEq/L for K^+).

Calculation: Unit conversion formula is given as:

$$\text{mmol/L} = \frac{\text{mEq/L}}{\text{valency of ion}}$$

3.2.3.3.4.2 Plasma Calcium Ion Concentration

Calcium ion concentration in plasma was determined by the method described by Biggs and Moorehead (1974).

Principle: At alkaline pH, calcium ion reacts with O-cresolphthalein complexone to form a deep violet coloured complex which absorbs maximally at 578 nm. Increase in absorbance is directly proportional to the concentration of calcium ion present in the sample. Interference by magnesium and iron is eliminated by the addition of 8-hydroxyquinoline.

Procedure: Briefly, 1000 µL of the working reagent (360 mmol/L diethylamine, 0.15 mmol/L O-cresolphalein complex, 17.2 mmol/L 8-Hydroxyquinoline) was added to separate test tubes containing aliquot (10 µL) of sample, standard calcium solution (10 mg/dL) and distilled water which served as test, standard and blank respectively.These were mixed and incubated at room temperature for 5 min. The absorbances of the test (sample) and standard were read against the reagent blank at a wavelength of 578 nm.

Calculation: The concentration of calcium ions in plasma was calculated using the expression:

$$\text{Calcium ion concentration (mg/dL)} = \frac{\text{Absorbance of sample}}{\text{Absorbance of standard}} \times 10$$

Where: **10** = concentration of standard in mg/dL

Unit conversion formula is given as:

$$\text{Concentration (mmol/L)} = \frac{\text{Concentration (mg/dL)}}{\text{Molar mass (g/mol)}} \times 10$$

3.2.3.3.4.3 Plasma Chloride Ion Concentration

The concentration of chloride ion was determined by the method described by Yoshinaga and Ohta (1990).

Principle: Chloride ion reacts with mercury-II-thiocynate, in an acidic medium, to form thiocynate ion which when reacted with HNO_3 and iron-III-ions produce a red colouration. The intensity of the colour is directly proportional to the concentration of chloride ion present.

Procedure: Aliquot (1000 µL) of the working reagent (2 mmol/L mercuric (II) thiocyanate, 29 mmol/L nitric acid, 20 mmol/L ferric nitrate) was added to separate test tubes containing aliquot (10 µL) of sample, standard solution and distilled water which served as test, standard and blank respectively. These were mixed and incubated at 37 ºC for 1 min. The absorbance of the sample and standard were read against the reagent blank at 492 nm.

Calculation: The concentration of chloride ion in the plasma was calculated using the formula:

$$\text{Chloride ion concentration (mg/dL)} = \frac{\text{Absorbance of sample}}{\text{Absorbance of standard}} \times 5$$

Where: **5** = concentration of standard in mg/dL

Unit conversion formula is given as:

$$\text{Concentration (mmol/L)} = \frac{\text{Concentration (mg/dL)}}{\text{Molar mass (g/mol)}} \times 10$$

3.2.3.3.4.4 Plasma Bicarbonate Ion Concentration

The plasma concentration of bicarbonate ion was determined by the enzymatic method described by Forrester (1976).

Principle: The reaction between phosphoenolpyruvate and bicarbonate is catalysed by phosphoenolpyruvate carboxylase (PEPC) to form oxaloacetate and phosphate ion.

The oxaloacetate is catalysed by malate dehydrogenase (MDH) in the presence of NADH to form malate and NAD^+ respectively. This lead to a decrease in absorbance that is directly proportional to bicarbonate concentration in the sample.

$$\text{Phosphoenolpyruvate} + HC0_3^- \xrightarrow{\text{PEPC}} \text{Oxalate} + H_2PO_4$$

$$\text{Oxalate} + \text{NADH} + H^+ \xrightarrow{\text{MDH}} \text{Malate} + NAD^+$$

Procedure: Aliquot (1000 µL) of carbon dioxide reagent (1.8 mM PEP, 2.5 mM sodium oxalate, 10 mM magnesium sulphate, 0.40 mM NADH, 1250 U/L MDH (porcine), 200 µ/L PEPC) was pipetted into test tubes for blank, standard and sample respectively and incubated at 37ºC for 3 min. Aliquot (50 µL) of distilled water, standard solution (30 mmol/L), and sample was pipetted into their respective test tubes, mixed and incubated at 37ºC for 5 mins. The absorbances of standard and tests were read against reagent blank at 340 nm.

Calculation: Bicarbonate concentration in sample was calculated using the expression:

$$\text{Bicarbonate Conc. (mmol/L)} = \frac{\text{Absorbance of blank - absorbance of sample}}{\text{Absorbance of blank - absorbance of standard}} \times 30$$

Where; **30** = Concentration of standard in mmol/L

3.2.3.3.4.5 Plasma Phosphate Ion Concentration

Phosphate ion concentration was determined using the method described by Tietz (1995).

Principle: Ammonium molybdate and sulphuric acid react with potassium ions in the sample to form a coloured phosphomolybdic complex. The intensity of this complex is proportional to the concentration of phosphate ions in the sample.

$$\text{Ammonium molybdate} + \text{Sulphuric acid} \xrightarrow{\text{phosphorus}} \text{Phosphomolybdic complex}$$

Procedure: Aliquot (1000 µL) of working reagent (210 mmol/L sulphuric acid, 650 mmol/L ammonium molybdate) was pipetted into test tubes for blank, standard and sample respectively. Then, 20 µL of distilled water, standard solution (5 mg/dL), and sample was pipetted into their respective test tubes, mixed and incubated at 37ºC for 1 min. The absorbances of standard and tests were read against reagent blank at 340 nm.

Calculation: Phosphate ions concentration in sample was calculated using the formula:

$$\text{Phosphorus conc. (mg/dL)} = \frac{\text{Absorbance of sample}}{\text{Absorbance of standard}} \times 5$$

Where: **5** = concentration of standard in mg/dL

Unit conversion formula is given as:

$$\text{Concentration (mmol/L)} = \frac{\text{Concentration (mg/dL)}}{\text{Molar mass (g/mol)}} \times 10$$

3.2.3.3.5 Determination of Plasma Biomolecules Concentrations

3.2.3.3.5.1 Plasma Urea Concentration

The concentration of Urea in the plasma was determined using the Urease-Berthelot method as described by Weatherburn (1967).

Principle: The catalytic hydrolysis of urea by the enzyme urease produces ammonia which can be measured photometrically by Berthelot's reaction.

$$\text{Urea} + H_2O \xrightarrow{\text{Urease}} 2NH_3 + CO_2$$

$$2NH_3 + \text{hypochlorite} + \text{phenol} \rightarrow \text{Indophenols (blue compound)}$$

Procedure: Aliquot (100 µL) of working reagent (6 mmol/L sodium nitroprusside and 1 g/L urease, 37:1 v/v) was pipetted into test tubes for blank, standard and sample respectively. Then 10 µL of distilled water, standard solution (13.20 mmol/L Urea), and sample was pipetted into their respective test tubes, mixed and incubated at 37^{o}C for 10 mins. Thereafter, 2,500 µL each of phenol (120 mmol/L) and sodium hypochlorite (27 mmol/L) were added to the mixture and incubated at 37^{o}C for 15 mins. The absorbances of standard and sample were read against reagent blank at 546 nm.

Calculation: Concentration of plasma urea was calculated using the following formula:

$$\text{Urea conc. (mmol/L)} = \frac{\text{Absorbance of sample}}{\text{Absorbance of standard}} \times 13.20 \times \text{d.f}$$

Where; **13.20** = concentration of standard urea; **d.f.** = dilution factor

3.2.3.3.5.2 Plasma Creatinine Concentration

The concentration of Creatinine was calculated by the described method of Bartels and Bohmer (1972).

Principle: In alkaline medium, creatinine reacts with picric acid to form a coloured complex whose amount is directly proportional to creatinine concentration.

Procedure: Aliquot (1,000 µL) of working reagent (35 mmol/L picric acid and 0.32 mmol/L NaOH, 1:1 v/v) was pipetted into test tubes for standard and sample respectively. Then 100 µL of standard solution (181 µmol/L creatinine)and sample was pipetted into their respective test tubes, mixed and incubated at room temperature for 30 sec. At 492 nm, absorbance A_1 and A_2 were read at 2 mins interval.

Calculation: Concentration of plasma creatinine was calculated thus:

$$\text{Creatinine conc. (µmol/L)} = \frac{\Delta\text{Absorbance of sample}}{\Delta\text{Absorbance of standard}} \times 181 \times \text{d.f}$$

Where; **ΔAbsorbance of sample** = $A_2 - A_1$; **ΔAbsorbance of standard** = $A_2 - A_1$

181 = concentration of standard creatinine (µmol/L); **d.f.** = dilution factor

3.2.3.3.5.3 Plasma Uric Acid Concentration

The concentration of uric acid was determined using the procedure described by Fossati and Prencipe (1980).

Principle: Uric acid is converted to allantoin and hydrogen peroxide by uricase. The hydrogen peroxide is utilised by peroxidase to oxidize 3,5-dichloro-2-hydroxybenzensulfonic acid and 4-aminophenazone to form a red-violet quinoneimine compound which absorbs maximally at 520 nm.

$$\text{Uric acid} + O_2 + 2H_2O \xrightarrow{\text{Uricase}} \text{Allantoin} + CO_2 + H_2O_2$$

Procedure: Aliquot (20 µL) of standard solution (0.595 mmol/L uric acid) and sample were pipetted into their respective test tubes and mixed with 1000 µL of pre-mixed working reagent 1a (50 mmol/L Hepes buffer, pH 7.0 and 4 mmol/L 3,5-Dichloro-2-hydroxybenzensulfonic) and working reagent 1b (0.25 mmol/L 4-aminophenazone, ≥1000 U/I peroxidase and ≥ 200 U/I Uricase). The mixture was incubated at 25ºC for 15 mins after which the absorbances of standard and samples were read at 520 nm against reagent blank.

Calculation: Concentration of plasma uric acid was calculated thus:

$$\text{Uric acid conc. (mmol/L)} = \frac{\text{Absorbance of sample}}{\text{Absorbance of standard}} \times 0.595 \times \text{d.f}$$

Where: **0.595** = concentration of standard uric acid; **d.f.**= dilution factor

3.2.3.3.5.4 Sample Total Protein Concentration

The total protein concentration of sample was determined using the biuret method described by Gornall *et al*. (1949).

Principle: In alkaline medium, Cu^{2+} forms purple-coloured complex with peptide bonds of protein and this can be quantified at 540 nm independently of the solution's blue colouration.

Procedure: Biuret reagent (1,000 µL) was added to respective test tubes containing 250 µL of standard (5mg/mL bovine serum albumin) or diluted sample. This was mixed and incubated at room temperature for 30 mins after which the absorbance was read at 540 nm against reagent blank.

Calculation: The protein concentration of sample was calculated using the following expression:

$$\text{Total protein conc. (g/L)} = \frac{\text{Absorbance of sample}}{\text{Absorbance of standard}} \times 5 \times \text{d.f}$$

Where: **5** = concentration of BSA standard (mg/mL); **d.f.** = dilution factor

3.2.3.3.5.5 Plasma Albumin Concentration

The method described by Doumas *et al.* (1971) was used to determine albumin concentration in samples.

Principle: Albumin reacts with bromocresol-green (BCG) to produce a complex that absorbs maximally at 630 nm. The absorbance of the albumin-BCG complex is proportional to the concentration of albumin in the sample.

Procedure: Aliquot (1000 µL) of working reagent (75 mmol/L succinate buffer pH 4.20, 1.7mmol/L bromocresol green) was pipetted into test tubes for blank, standard and sample respectively. Then 10 µL of distilled water, standard solution (30 g/L albumin), and sample was pipetted into their respective test tubes, mixed and incubated at room temperature for 5 mins. Absorbance was then read at 630 nm against reagent blank.

Calculation: The concentration of albumin was calculated using the formula:

$$\text{Albumin Concentration (g/L)} = \frac{\text{Absorbance of sample}}{\text{Absorbance of standard}} \times 30 \times \text{d.f}$$

Where: **30** = concentration of standard albumin (g/L); **d.f** = dilution factor

3.2.3.3.5.6 Plasma Globulin Concentration

The concentration of globulin was determined using the method described by Tietz (1995). The plasma albumin concentration was subtracted from the plasma total protein concentration.

Globulin concentration (g/L) = Plasma Total Protein (g/L) - Plasma Albumin (g/L)

3.2.3.3.5.7 Plasma Total Bilirubin Concentration

Bilirubin concentration was determined according to the method described by Jendrassik and Grof (1938).

Principle: Total bilirubin is determined in the presence of caffeine; releasing albumin bound bilirubin, by the reaction with diazotized sulphanilic acid.

Procedure: Briefly, 200 µL of solution 1 (29 mmol/L sulphanilic acid and 0.17 N hydrochloric acid), 50 µL of solution 2 (38.5 mmol/L sodium nitrite), 1000 µL of solution 3 (0.26 mol/L caffeine and 0.52 mol/L sodium benzoate) and 200 µL of

sample were mixed and left at 25^{o}C for 10 mins, then 1000 µL of solution 4 (0.93 mol/L tartrate, 1.9 N sodium hydroxide) was added and the mixture incubated at 25^{o}C for 20 mins. The absorbance of the sample was read at 578 nm against sample blank. Sample blank was prepared without solution 2.

Calculation: Concentration of plasma total bilirubin was calculated thus:

$$\text{Total bilirubin (µmol/L)} = 185 \times \text{absorbance}$$

3.2.3.3.5.8 Plasma Conjugated Bilirubin Concentration

Conjugated bilirubin concentration was determined according to the method described by Jendrassik and Grof (1938).

Principle: Conjugated (direct) bilirubin reacts with diazotized sulphanilic acid in alkaline medium to form a blue-coloured complex.

Procedure: Aliquot (200 µL) of solution 1 (29 mmol/L sulphanilic acid and 0.17 N hydrochloric acid), 50 µL of solution 2 (38.5 mmol/L sodium nitrite), 2000 µL of 0.9% NaCl and 200 µL of sample were mixed and incubated at 25^{o}C for 10 mins. The absorbance of the sample was read against sample blank at 546 nm. Sample blank was prepared without solution 2.

Calculation: Concentration of plasma conjugated bilirubin was calculated thus:

$$\text{Conjugated bilirubin (µmol/L)} = 246 \times \text{absorbance}$$

3.2.3.3.5.9 Cardiovascular Indices

3.2.3.3.5.9.1 Plasma Total Cholesterol Concentration

Total cholesterol concentration was determined according to the method described by Tietz (1995).

Principle: The enzymatic hydrolysis and oxidation of cholesterol ester yields hydrogen peroxide which is utilized by peroxidase in the presence of phenol and 4-aminoantipyrene to yield quinoneimine compound which absorbs maximally at 500 nm.

$$\text{Cholesterol ester} + H_2O \xrightarrow{\text{Cholesterol esterase}} \text{Cholesterol} + \text{Fatty Acids}$$

$$\text{Cholesterol} + O_2 \xrightarrow{\text{Cholesterol oxidase}} \text{Cholestene-3-one} + H_2O_2$$

$$2H_2O_2 + \text{Phenol} + \text{4-Aminoantipyrene} \xrightarrow{\text{peroxidase}} \text{Quinoneimine} + 4H_2O$$

Procedure: Briefly, 1000 µL of cholesterol reagent (0.30 mmol/L 4-aminoantipyrine, 6 mmol/L phenols, peroxidase ≥0.5 U/mL, cholesterol oxidase ≥0.1 U/mL, cholesterol estarases ≥0.1 U/mL, 80 mmol/L Pipes buffer, pH 6.8) was pipetted into test tubes for blank, standard and sample respectively. Aliquots (10 µL) of distilled water, standard solution, and sample were pipetted into their respective test tubes, mixed and incubated at 37ºC for 5 min. The absorbances of standard and tests were read against reagent blank at 500 nm.

Calculation: Cholesterol concentration was calculated using the formula:

$$\text{Cholesterol concentration} = \frac{\text{Absorbance of sample}}{\text{Absorbance of standard}} \times \text{Concentration of standard} \times \text{d.f}$$

3.2.3.3.5.9.2 Plasma Triacylglycerol Concentration

Triacylglycerol concentration was determined according to the method described by Tietz (1995).

Principle: The enzymatic hydrolysis of triacylglycerol by lipases yields products which when coupled with other enzymatic processes produce hydrogen peroxide. The

catalytic influence of peroxidase on hydrogen peroxide, 4-aminophenazone and 4-chlorophenol then produce quinoneimine compound which can be measured spectrophometrically.

$$\text{Triacylglycerols} + H_2O \xrightarrow{\text{lipases}} \text{Glycerol} + \text{Fatty Acids}$$

$$\text{Glycerol} + \text{ATP} \xrightarrow{\text{GK}} \text{Glycerol-3-Phosphate} + \text{ADP}$$

$$\text{Glycerol-3-Phosphate} + O_2 \xrightarrow{\text{GPO}} \text{Dihydroxyacetone phosphate} + H_2O_2$$

$$2H_2O_2 + \text{4-Aminophenazone} + 4\ \text{Chlorophenol} \xrightarrow{\text{POD}} \text{Quinoneimine} + HCl + 4H_2O$$

Procedure: Briefly, 1000 µL of working reagent (50 mmol/L Pipes-buffer pH 7, 5.3 mmol/L p-chlorophenol, 10 mmol/L potassium ferrocynate, 17 mmol/L magnesium salt, 0.9 mmol/L 4-aminoantipyrine, 3.15 mmol/L ATP, 1800 U/L lipoprotein lipase, 450 U/L glycerol kinase, 3500 U/L glycerol - 3- phosphate oxidase, 450 U/ L peroxidase) was pipetted into test tubes for blank, standard and sample respectively. Aliquots (10 µL) of distilled water, standard solution (200 mg/dL), and sample were pipetted into their respective test tubes, mixed and incubated at 37ºC for 5 min. The absorbances of standard and tests were read against reagent blank at 500 nm.

Calculation: Triacylglycerol concentration was calculated using the formula:

$$\text{Triacylglycerol conc. (mg/dL)} = \frac{\text{Absorbance of sample}}{\text{Absorbance of standard}} \times 200 \times \text{d.f}$$

Where: **200** = concentration of standard (mg/dL); **d.f** = dilution factor

Unit conversion formula is given as:

$$\text{Concentration (mmol/L)} = \frac{\text{Concentration (mg/dL)}}{\text{Molar mass (g/mol)}} \times 10$$

3.2.3.3.5.9.3 Plasma High Density Lipoprotein Cholesterol Concentration

The concentration of plasma high density lipoprotein cholesterol (HDL-C) was determined according to the method described by Friedwald *et al.* (1972).

Principle: In the presence of magnesium ions, the addition of phosphotungstic acid to sample precipitate low density lipoprotein (LDL and VLDL) and chylomicron fractions. Centrifugation yields supernatant, the HDL-C concentration of which is determined.

Procedure: Briefly, 500 µL of working reagent (0.55 mmol/L phosphotungstic acid, 25 mmol/L magnesium chloride) was pipetted into test tubes for standard and sample respectively. Aliquots (200 µL) of standard solution and sample were pipetted into their respective test tubes, mixed and incubated at room temperature for 10 min. This was then centrifuged at 4000 rpm for 10 min and the supernatant was pipetted out for determination of cholesterol concentration.

Calculation: The HDL-C concentration was calculated using the formula:

$$\text{HDL-C (mmol/L)} = \frac{\text{Absorbance of sample}}{\text{Absorbance of standard}} \times \text{Concentration of Standard}$$

3.2.3.3.5.9.4 Plasma Low Density Lipoprotein Cholesterol Concentration

The LDL-Cholesterol concentration was calculated using the formula described by Friedwald *et al*. (1972).

$$\text{LDL-Cholesterol (µmol/L)} = \text{Total Cholesterol} - \frac{\text{Triacylglycerol}}{5} - \text{HDL Cholesterol}$$

3.2.3.3.5.9.5 Atherogenic Index

The atherogenic index (AI) was calculated using the method described by Lamarche *et al*. (1996).

$$\text{Atherogenic index} = \frac{\text{Total Cholesterol}}{\text{HDL-cholesterol}}$$

3.2.3.3.6 Cellular Enzymes

3.2.3.3.6.1 Alkaline Phosphatase Activity

The method described by Wright *et al.* (1972) was used to determine the alkaline phosphatase (ALP) activities of tissue homogenates and plasma.

Principle: The hydrolysis of p-nitrophenylphosphate by alkaline phosphatase yields p-nitrophenol and inorganic phosphate. The p-nitrophenol formed has a yellowish colouration and its rate of formation can be monitored spectrophotometrically at 405 nm.

$$\text{p-nitrophenyl phosphate} + H_2O \xrightarrow{\text{alkaline phosphatase}} \text{p-nitrophenol} + \text{Pi}$$

Procedure: Briefly, 20 µL of appropriately diluted sample was mixed with 1000 µL of reagent (1 mmol/L diethanolamine buffer pH 9.8, 0.5 mmol/L $MgCl_2$ and 10 mmol/L p-nitrophenylphosphate). The initial absorbance and absorbances at 1, 2, 3 min were read at 405 nm against air.

Calculation: Specific activity of Alkaline phosphatase (Units/mg protein) was calculated using the expression:

$$\Delta\text{Abs/ min} = \frac{(Abs_1 - Abs_0) + (Abs_3 - Abs_2)}{2}$$

$$\text{Specific activity of Alkaline phosphatase} = \frac{\Delta\text{Abs/min} \times 2760 \times \text{dilution factor}}{\text{Protein concentration (mg/L)}}$$

Where; Abs_0, Abs_1, Abs_2, Abs_3 are absorbances at 0, 1, 2 and 3 min respectively.

One unit of alkaline phosphatase activity is the enzyme activity which hydrolyses 1 µmole of 4-nitrophenyl phosphate in 1 minute at 37°C under assay conditions.

3.2.3.3.6.2 Gamma Glutamyltransferase Activity

The method described by Szasz *et al*. (1969) was used to determine the gamma glutamyltransferase (GGT) activity in sample.

Principle: In the presence of glycylglycine, L-γ-glutamyl-3-carboxy-4-nitroanilide is converted to L-γ-glutamylglycylglycine and 5-amino-2-nitrobenzoate by gamma-glutamyl transferase. The concentration of 5-amino-2-nitrobenzoate formed can be spectrophotometrically measured at 405 nm.

Procedure: Briefly, 100 µL of appropriately diluted sample was mixed with 1000 µL of reagent (100 mmol/L tris buffer pH 8.25, 100 mmol/L Glycylglycine and 2.9 mmol/L L-γ-glutamyl-3-carboxy-4-nitroanilide). The initial absorbance and absorbances at 1, 2, 3 min were read at 405 nm against air.

Calculation: Gamma-Glutamyl transferase activity was calculated using the formula:

$$\Delta\text{Abs/ min} = \frac{(Abs_1 - Abs_0) + (Abs_3 - Abs_2)}{2}$$

$$\text{Specific activity of GGT (Units/mg protein)} = \frac{\Delta\text{Abs/min} \times 1158 \times \text{dilution factor}}{\text{Protein concentration (mg/L)}}$$

Where; Abs_0, Abs_1, Abs_2, Abs_3 are absorbances at 0, 1, 2 and 3 min respectively

3.2.3.3.6.3 Aspartate Aminotransferase Activity

Aspartate aminotransferase (AST) activity was determined according to the method described by Reitman and Frankel (1957).

Principle: The reaction between α-ketoglutarate and L-aspartate is catalysed by AST to form L-glutamate and oxaloacetate. The oxaloacetate reacts with 2,4-dinitrophenylhydrazine to yield oxaloacetate-2,4-dinitrophenylhydrazone which absorbs maximally at 546 nm.

$$\text{α-ketoglutarate} + \text{L-aspartate} \xrightarrow{\text{aspartate aminotransferase}} \text{L-glutamate} + \text{Oxaloacetate}$$

Procedure: Briefly, 50 µL of appropriately diluted sample was mixed with 250 µL of reagent (100 mmol/L pH 7.4 Phosphate buffer**,** 100 mmol/L L-aspartate, and 2 mmol/L α-ketoglutarate) and incubated at 37ºC for 30 min. Thereafter, 250 µL of 2,4-dinitrophenylhydrazine (2 mmol/L) was added and incubated at 25ºC for 20 min. The reaction was stopped by the addition of 2500 µL sodium hydroxide (0.4 N) and after 5 min, absorbance was read against reagent blank at 546 nm.

Calculation: The activity of AST (Units/L) was determined from calibration curve (Appendix V) and specific activity (Units/mg protein) was determined using the formula:

$$\text{Specific activity of AST} = \frac{\text{AST activity from calibration curve}}{\text{Protein concentration (mg/L)}} \times \text{dilution factor}$$

One unit of enzyme activity is defined as the quantity of enzyme that catalyses the reaction of 1 µmole of substrate per minute at 37°C.

3.2.3.3.6.4 Alanine Aminotransferase Activity

The method described by Reitman and Frankel (1957) was used to determine alanine aminotransferase (ALT) activity.

Principle: The reaction between α-ketoglutarate and L-alanine is catalysed by ALT to form L-glutamate and pyruvate. The pyruvate reacts with 2,4-dinitrophenylhydrazine to yield pyruvate-2,4-dinitrophenylhydrazone which absorbs maximally at 546 nm.

$$\text{α-ketoglutarate + L-alanine} \xrightarrow{\text{alanine aminotransferase}} \text{L-glutamate + Pyruvate}$$

Procedure: Briefly, 50 µL of appropriately diluted sample was mixed with 250 µL of reagent (100 mmol/L pH 7.4 Phosphate buffer**,** 100 mmol/L L-alanine, and 2 mmol/L α-ketoglutarate) and incubated at 37ºC for 30 mins. Thereafter, 250 µL of 2,4-dinitrophenylhydrazine (2 mmol/L) was added and incubated at 25ºC for 20 min. The reaction was stopped by the addition of 2500 µL sodium hydroxide (0.4 N) and after 5 min, absorbance was read against reagent blank at 546 nm.

Calculation: The activity of ALT (Units/L) was determined from calibration curve (Appendix VI) and the specific activity (Units/mg protein) was obtained using the formula:

$$\text{Specific activity of ALT} = \frac{\text{ALT activity from calibration curve}}{\text{Protein concentration (mg/L)}} \times \text{dilution factor}$$

One unit of enzyme activity is defined as the quantity of enzyme that catalyses the reaction of 1 µmole of substrate per minute at 37°C.

3.2.3.3.6.5 Lactate Dehydrogenase Activity

The procedure described by Wróblewski and Ladue (1955) was used for determination of lactate dehydrogenase (LDH) activity.

Principle: In the presence of reduced nicotinamide adenine dinucleotide, lactate dehydrogenase converts pyruvate to L-lactate with concomitant production of nicotinamide adenine dinucleotide.

$$\text{Pyruvate} + \text{NADH} \xrightarrow{\text{LDH}} \text{L-lactate} + \text{NAD}^+$$

Procedure: Briefly, 20 µL of appropriately diluted sample was mixed with 3000 µL of reagent (50 mmol/L Phosphate buffer pH 8.25, 0.6 mmol/L Pyruvate, 1.8 mmol/L NADH). The initial absorbance and absorbances at 1, 2 and 3 min were read at 340 nm against air.

Calculation: Specific activity of lactate dehydrogenase (Units/mg protein) was calculated using the formula:

$$\text{Specific activity of LDH (Units/mg protein)} = \frac{\text{Change in absorbance/min}}{\text{Protein concentration (mg/L)}} \times 4127$$

Where: **4127** = Standard conversion value according to manufacturer's instruction

3.2.3.3.6.6 Glutamate Dehydrogenase Activity

Glutamate dehydrogenase (GDH) activity was determined using the method described by Shimizu *et al.* (1979).

Principle: This approach is centred on the reductive amination of α-ketoglutarate. Using reduced nicotinamide adenine dinucleotide (NADH) or reduced nicotinamide adenine dinucleotide phosphate (NADPH) as cofactor, glutamate dehydrogenase converts α-ketoglutarate, in the presence of ammonium ion, to glutamate with corresponding formation of NAD^+ or $NADP^+$. The decrease in absorbance at 340 nm corresponds to the rate of reaction which is proportional to the enzyme activity.

$$\text{Glutamate} + NADP^{+} \xleftrightarrow{\text{Glutamate dehydrogenase}} \alpha\text{-ketoglutarate} + NH_4^{+} + NADPH$$

Procedure: The reaction mixture was made up of 2000 µL Tris-HCl Buffer (85 mM, pH 7.2), 200 µL α-Ketoglutarate (7.6 mM), 200 µL NH_4Cl (0.22 mM), 100 µL NADH (0.25 mM) and 100 µL EDTA (0.85 mM). Aliquot (50 µL) of appropriately diluted sample was then added to initiate the reaction at room temperature for 5 min. The decrease in absorbance per minute at 340 nm was read against reagent blank.

Calculation: The specific activity of glutamate dehydrogenase (Units/mg protein) was calculated thus:

$$\text{Specific activity of GDH} = \frac{\Delta Abs/\text{min} \times \text{Total reaction volume} \times \text{Dilution factor}}{6.22 \times \text{Volume of sample} \times \text{Protein concentration (mg/L)}}$$

Where: **6.22** = Millimolar Extinction Coefficient of NADPH

3.2.3.3.6.7 Malate Dehydrogenase Activity

The activity of malate dehydrogenase was assayed by the method described by Ochoa (1955).

Principle: The rate of reaction is determined by measuring the decrease in absorbance at 340 nm resulting from the oxidation of NADH.

Procedure: The reaction mixture was made up of 2600 µL phosphate buffer (0.1 M pH 7.4), 200 µL of NADH (3.75 mM freshly prepared in phosphate buffer), and 100 µL of oxaloacetate (6 mM freshly prepared in phosphate buffer, pH 7.4). This was incubated at 25ºC for 4 min and 100 µL of appropriately diluted sample was added. The blank was setup similarly without NADH. Decrease in absorbance, at 340 nm, was measured at 1 min intervals for 3 min.

Calculation:

$$\text{MDH activity (Units/mg protein)} = \frac{\Delta\text{Abs/min}}{6.22 \times \text{mg enzyme/mL reaction mixture}}$$

3.2.3.3.6.8 Creatine kinase Activity

The activity of creatine kinase (CK) was assayed using the method described by Di Witt and Trendelenburg (1982).

Principle: Creatine kinase catalyses the reversible phosphorylation of ADP in the presence of creatine phosphate to yield ATP and creatine. The ATP formed is utilised by hexokinase for the phosphorylation of glucose to produce ADP and glucose-6-phosphate. This glucose-6-phosphate is then oxidized by glucose-6-phosphate dehydrogenase to form 6-phosphogluconate with the concomitant production of NADPH. The rate of NADPH formation, measured at 340 nm is directly proportional to creatine kinase activity.

$$\text{Creatine phosphate} + \text{ADP} \xrightarrow{\text{Creatine kinase}} \text{Creatine} + \text{ATP}$$

$$\text{ATP} + \text{D-glucose} \xrightarrow{\text{Hexokinase}} \text{G-6-P} + \text{ADP}$$

$$\text{G-6-P} + \text{NADP}^{+} \xrightarrow{\text{G-6-P dehydrogenase}} \text{6-phosphogluconate} + \text{NADPH} + \text{H}^{+}$$

Procedure: Briefly, 200 µL of reagent 1 (125 mmol/L imidazole pH 6.7, 25 mmol/L D-glucose, 25 mmol/L N-acetyl-L-cysteine, 12.5 mmol/L magnesium acetate, 2.4 mmol/L NADP, 2.0 mmol/L EDTA, hexokinase 6800 U/L) was mixed with 50 µL of reagent 2 (250 mmol/L creatine phosphate, 15.2 mmol/L ADP, 25 mmol/L AMP, 103 µmol/L diadenosine pentaphosphate, glucose-6-phosphate dehydrogenase 8800 U/L). Aliquot (10 µL) of appropriately diluted sample was then added, mixed and incubated

at 37ºC for 2 min. The initial absorbance and absorbances at 1, 2, 3 min were read at 340 nm against distilled water.

Calculation: The specific activity of creatine kinase (Units/mg protein) was calculated thus:

$$\text{Specific activity of CK} = \frac{\text{Change in absorbance/min x 4127}}{\text{Protein concentration (mg/L)}} \times \text{dilution factor}$$

3.2.3.3.6.9 Acetylcholinesterase Activity

The activity of acetylcholinesterase (AChE) was assayed using the method described by Magnotti *et al*. (1987).

Principle: Thiocholine, produced by acetylcholinesterase, reacts with 5,5'-dithiobis(2-nitrobenzoic acid) to form colorimetric product which absorbs maximally at 412 nm. The intensity of the colour is proportional to the enzyme activity present in the sample.

Procedure: To separate test tubes labelled blank and standard were 1000 µL of distilled water and 1000 µL of calibrator (200 U/L) added respectively. Aliquot (50 µL) of appropriately diluted sample was mixed and incubated at room temperature in a final reaction mixture of 1 mL, containing 100 mM phosphate buffer (pH 7.5), 1 mM 5,5′-dithiobisnitrobenzoic acid (DTNB), and 0.8 mM acetylthiocholine iodide. After 2 and 10 min, initial and final absorbances of sample, at 412 nm, were read respectively.

Calculation: The enzyme activity was calculated thus:

$$\text{AChE activity (Units/L)} = \frac{\text{Abs}_{10} - \text{Abs}_{2}}{\text{Abs}_{\text{Cal}} - \text{Abs}_{\text{water}}} \times n \times 200$$

$$\text{Specific activity of AChE (Units/mg Protein)} = \frac{\text{AChE activity (Units/L)}}{\text{Protein Conc. (mg/L)}}$$

Where: **Abs_2** = Absorbance at 2 min; **Abs_{10}** = Absorbance at 10 min;

Abs_{Cal} = Absorbance of Calibrator at 10 mins; **Abs_{water}**= Absorbance of water at 10 mins; **200 =** Equivalent activity (Units/L) of the calibrator; **n** = Dilution factor

One unit of acetylcholinesterase is the amount of enzyme that catalyses the production of 1.0 mmole of thiocholine per minute at room temperature at pH 7.5.

3.2.3.3.6.10 ATPase Activities Assay

Principle: The hydrolysis of adenosine triphosphate (ATP), in the presence of appropriate cations, yields inorganic phosphate which can be measured by ammonium molybdate-ascorbic acid system. Ammonium molybdate is oxidised by concentrated sulphuric acid to give molybdic acid which reacts with inorganic phosphate to produce yellow colouration. The molybdic acid is then reduced by ascorbic acid to form a blue colouration whose intensity is proportional to the concentration of inorganic phosphate released into the reaction medium. A calibration curve of inorganic phosphate is prepared and used for the estimation of phosphate in samples.

3.2.3.3.6.10.1 Preparation of Phosphate Calibration Curve

Different volumes (20-120 µL) of 1 mM $NaH_2PO_4.2H_2O$ were pipetted into testtubes and made up to 1000 µL by addition of distilled water. Then, 2000 µL of reagent C (H_2SO_4-Ammonium molybdate-Ascorbate solution) was added and incubated at room temperature for 30 min. Absorbance was read at 820 nm against reagent blank which was made without $NaH_2PO_4.2H_2O$. The absorbances obtained were then used to plot the calibration curve for inorganic phosphate(Appendix VII).

3.2.3.3.6.10.2 Mg^{2+}-ATPase Activity

The Mg^{2+}-ATPase activity was assayed using the method described by Ronner *et al.* (1977) with modifications by Fleschner and Kraus-Friedmann (1986).

Procedure: Briefly, 400 µL of working buffer (240 mM KCl/60 mM Tris pH 7.4), 20 µL of $MgCl_2.6H_2O$ (80 mM), 20 µL of EGTA (20 mM), 220 µL of distilled water, 20 µL of sample and 20 µL of ouabain (1 mM) were mixed and incubated at 37ºC for 5 mins. Aliquot, (100 µL) of 8 mM ATP was added and the mixture was incubated at 37ºC for 30 mins. Thereafter, 200 µL of SDS (5%) and 2,000 µL of reagent C were added. This was incubated at room temperature for 30 mins to allow development of colour. The blank was similarly prepared with 20 µL of distilled water instead of sample. The absorbance of the test was read against blank at 820 nm.

Calculation: Concentration of inorganic phosphate in sample was estimated by extrapolation from the calibration curve. (Appendix VII). The specific activity of ATPase (µmole P_i/mg Prot./hr) was calculated using the formula:

$$Na^+ K^+ \text{ATPase activity} = \frac{[P_i] \times 2 \times \text{Dilution factor}}{1000 \times \text{Protein Concentration (mg/L)}}$$

Where:

$[P_i]$ = Concentration of inorganic phosphate in µmoles (obtain from calibration Curve)

2 = Factor introduced to obtain the amount of P_i released per hour

1000 = Factor introduced to convert the P_i released to µmoles

3.2.3.3.6.10.3 Na^+,K^+-ATPase Activity

The activity of Na^+, K^+-ATPase was assayed according to the method described by Ronner *et al.* (1977) and modified by Bewaji *et al.* (1985).

Procedure: Briefly, 400 µL of working buffer (200 mM NaCl/40 mM KCl/60 mM Tris, pH 7.4), 20 µL of $MgCl_2.6H_2O$ (80 mM), 20 µL of EGTA (20 mM), 240 µL of distilled water and 20 µL of appropriately diluted sample were mixed and incubated at

37°C for 5 min. Aliquot (100 µL) of 8 mM ATP was added and the mixture was incubated at 37°C for 30 min. Thereafter, 200 µL of SDS (5%) and 2,000 µL of reagent C were added. This was incubated at room temperature for 30 min to allow development of colour. The blank was similarly prepared with 20 µL of distilled water used instead of sample. The absorbance of the test was read against blank at 820 nm.

Calculation: Concentration of inorganic phosphate in sample was estimated by extrapolation from the calibration curve. (Appendix VII). The specific activity of ATPase (µmole P_i/mg Prot./hr) was calculated using the formula:

$$Na^{+}\ K^{+}\text{ ATPase activity} = \frac{[P_i] \times 2 \times \text{Dilution factor}}{1000 \times \text{Protein Concentration (mg/L)}}$$

Where:

[P_i] = Concentration of inorganic phosphate in µmoles (obtain from calibration Curve)

2 = Factor introduced to obtain the amount of P_i released per hour

1000 = Factor introduced to convert the P_i released to µmoles

The actual specific activity of Na^+,K^+-ATPase was obtained by the subtraction of the specific activity of Mg^{2+}-ATPase from that of Na^+,K^+-ATPase.

3.2.3.3.6.10.4 Ca^{2+},Mg^{2+}-ATPase Activity

The Ca^{2+}, Mg^{2+}-ATPase activity was assayed according to the method described by Ronner *et al*. (1977) with modifications by Bewaji *et al*. (1985).

Procedure: Briefly, 400 µL of working buffer (240 mM KCl/60mM Tris, pH 7.4), 40 µL of $CaCl_2$ (4 mM), 20 µL of $MgCl_2$.6H2O (80 mM), 220 µL of distilled water and 20 µL of appropriately diluted sample were mixed and incubated at 37°C for 5 min.

Aliquot, (100 µL) of 8 mM ATP was added and the mixture was incubated at 37°C for 30 min. Thereafter, 200 µL of SDS (5%) and 2,000 µL of reagent C were added. This was incubated at room temperature for 30 min to allow development of colour. The blank was similarly prepared by using 20 µL of distilled water instead of sample. The absorbance of the test was read against blank at 820 nm.

Calculation: Concentration of inorganic phosphate in sample was estimated by extrapolation from the calibration curve (Appendix VII). The specific activity of ATPase (µmole P_i/mg Prot./hr) was calculated using the formula:

$$Ca^{2+}, Mg^{2+}\text{ATPase activity} = \frac{[\text{Pi}] \times 2 \times \text{Dilution factor}}{1000 \times \text{Protein Concentration (mg/L)}}$$

Where:

[P_i] = Concentration of inorganic phosphate in µmoles (obtained from calibration Curve)

2 = Factor introduced to obtain the amount of P_i released per hour

1000 = Factor introduced to convert the P_i released to µmoles

3.2.4 Statistical Analysis of Data

Data were analyzed for statistical significance by one-way analysis of variance followed by Duncan's post hoc multiple comparisons, using IBM SPSS Statistics for Windows, version 23.0 (IBM Corp., Armonk, N.Y., USA). Difference at $p < 0.05$ was considered significant. Graphs were created using GraphPad Prism 6 software for Windows (GraphPad Software, California, USA).

CHAPTER FOUR

4.0 RESULTS

4.1 *In vitro* Studies

4.1.1 *In vitro* Antimalarial Study

4.1.1.1 Inhibition of β-Haematin Formation and Nature of Interaction

Methyl gallate and palmatine inhibited β-haematin formation with IC_{50} of 2.56 µg/mL and 0.82 µg/mL respectively while chloroquine had IC_{50} of 0.74 µg/mL (Appendix VIII and X). The combination of methyl gallate and palmatine in the ratios 1:4, 2:3, 3:2 and 4:1 inhibited β-haematin formation with an IC_{50} of 2.14 µg/mL, 1.02 µg/mL, 0.73 µg/mL and 3.85 µg/mL respectively (Appendix XI to XIV).

The combination of methyl gallate and palmatine were antagonistic at ratios 1:4 and 4:1 with ΣFIC_{50} of 2.25 and 2.14 respectively while their combination at ratios 2:3 and 3:2 resulted in synergistic interaction with ΣFIC_{50} of 0.91 and 0.53 respectively (Tables 1 and 2).

Table 1: Inhibition of β-hematin formation as a measure of *in vitro* antimalarial activities of methyl gallate and Palmitine

Compound	**IC_{50} (µg/mL)**
Chloroquine	0.74
Methyl gallate	2.56
Palmatine	0.82

Table 2: Nature of interaction of methyl gallate and palmatine combinations

Ratio (M.G:PAL)	IC_{50} (µg/mL)	FIC_{50} (M.G)	FIC_{50} (PAL)	ΣFIC_{50}	Nature of interaction
0:5	0.82	---	---	---	---
1:4	2.14	0.17	2.09	2.25	Antagonistic
2:3	1.02	0.16	0.75	0.91	Synergistic
3:2	0.73	0.17	0.36	0.53	Synergistic
4:1	3.85	1.20	0.94	2.14	Antagonistic
5:0	2.56	---	---	---	---

$\Sigma FIC_{50} < 1$ is synergistic, $\Sigma FIC_{50} = 1$ is additive, $\Sigma FIC_{50} > 1$ is antagonistic (Ohrt *et al.*, 2002; He *et al.*, 2010). **M.G** = Methyl gallate; **Pal** = Palmatine; **IC_{50}**= Median inhibitory concentration; **FIC_{50}** = Median fractional inhibitory concentration; **$\sum FIC_{50}$** = Summation of median fractional inhibitory concentrations

4.1.2 *In vitro* Antioxidant Studies

4.1.2.1 DPPH Radical Scavenging Activity

Palmatine exhibited higher DPPH radical scavenging activity at lower concentrations compared to butylated hydroxytoluene while methyl gallate alone and its combination with palmatine in the ratio 3:2 had higher DPPH radical scavenging activity at all concentrations compared to butylated hydroxytoluene and palmatine (Figure 12).

4.1.2.2 Ferric Ion Reducing Power

Palmatine had lower ferric ion reducing power compared to butylated hydroxytoluene while methyl gallate (at all concentrations) and its combination with palmatine in the ratio 3:2 (at higher concentrations) had higher reducing power compared to butylated hydroxytoluene (Figure 13).

4.1.2.3 Hydroxyl Radical Scavenging Activity

The hydroxyl radical scavenging activities of methyl gallate, palmatine and their combination in the ratio 3:2 were lower compared to that of butylated hydroxytoluene (Figure 14).

4.1.2.4 Nitric Oxide Scavenging Activity

The nitric oxide scavenging activities of methyl gallate, palmatine and their combination (in ratio 3:2) were lower compared to butylated hydroxytoluene at the concentrations considered (Figure 15).

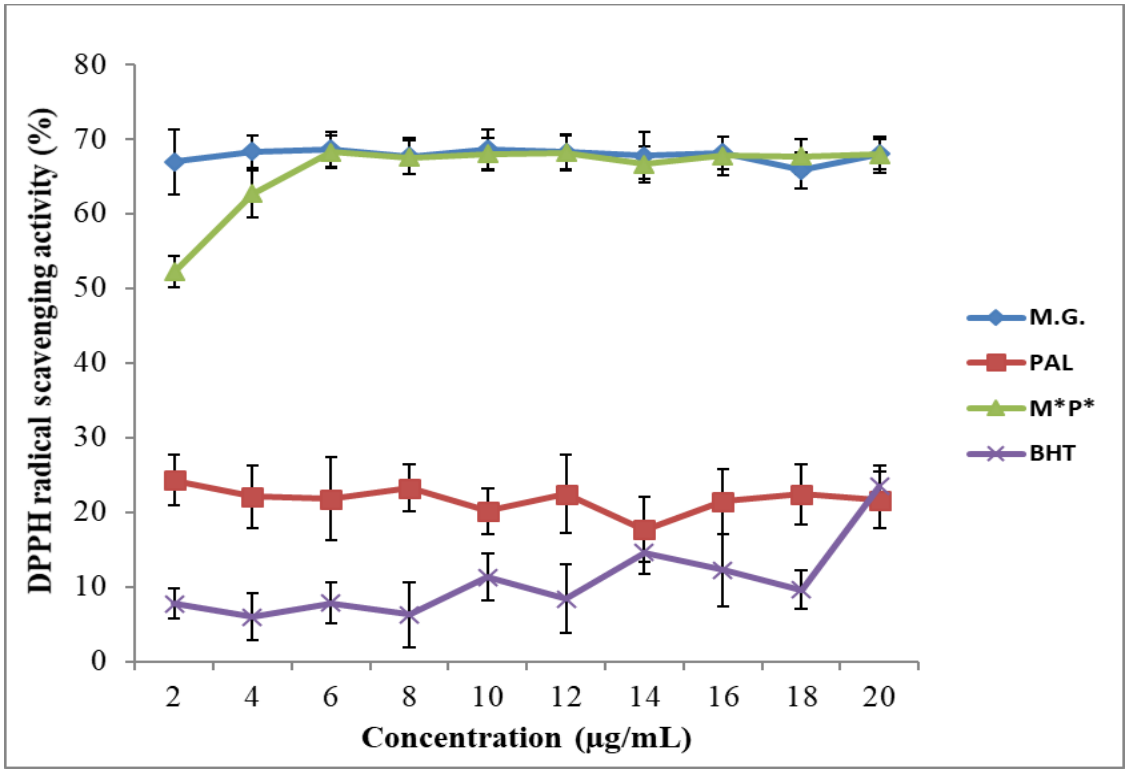

Figure 12: DPPH (2, 2-diphenyl-1-picrylhydrazyl) radical scavenging activities of palmatine, methyl gallate and methyl gallate-palmatine combination (3:2)
Values are means ± SD of three replicates. **M.G.** = Methyl gallate; **PAL**= Palmatine; **BHT** = Butylated hydroxytoluene; **M*P*** = 3:2 of methyl gallate and Palmatine (most active ratio from *in vitro*antimalarial study)

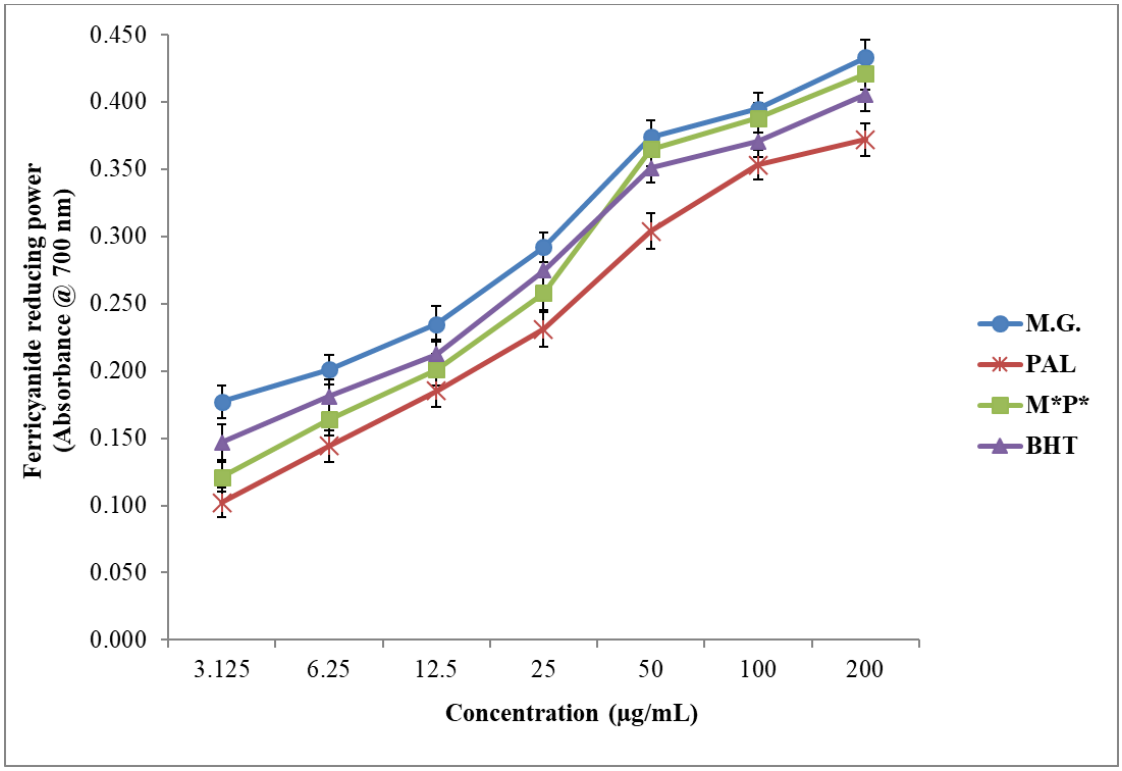

Figure 13: Ferric ion reducing power of palmatine, methyl gallate and methyl gallate-palmatine combination (3:2)

Values are means ± SD of three replicates. **M.G.** = Methyl gallate; PAL= Palmatine; **BHT** = Butylated hydroxytoluene; **M*P*** = 3:2 of methyl gallate and Palmatine (most active ratio from *in vitro*antimalarial study).

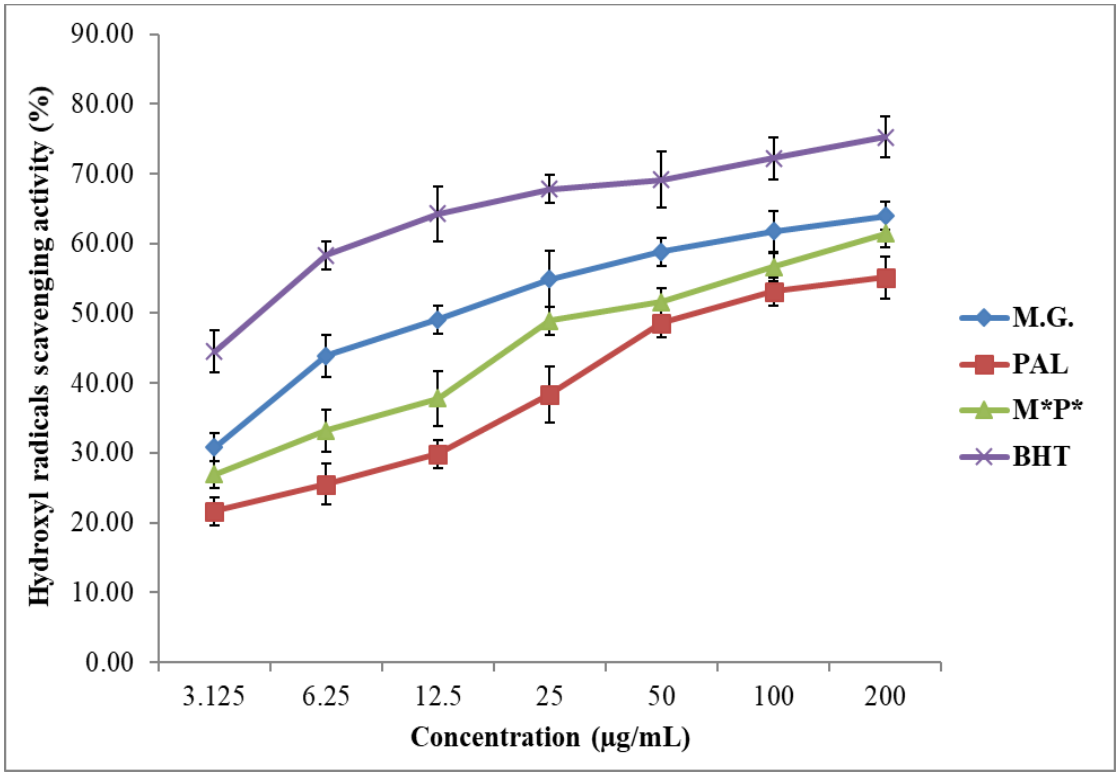

Figure 14: Hydroxyl radical-scavenging ability of palmatine, methyl gallate and methyl gallate-palmatine combination (3:2)

Values are means ± SD of three replicates. **M.G.** = Methyl gallate; **PAL**= Palmatine; **BHT** = Butylated hydroxytoluene; **M*P*** = 3:2 of methyl gallate and Palmatine (most active ratio from *in vitro*antimalarial study)

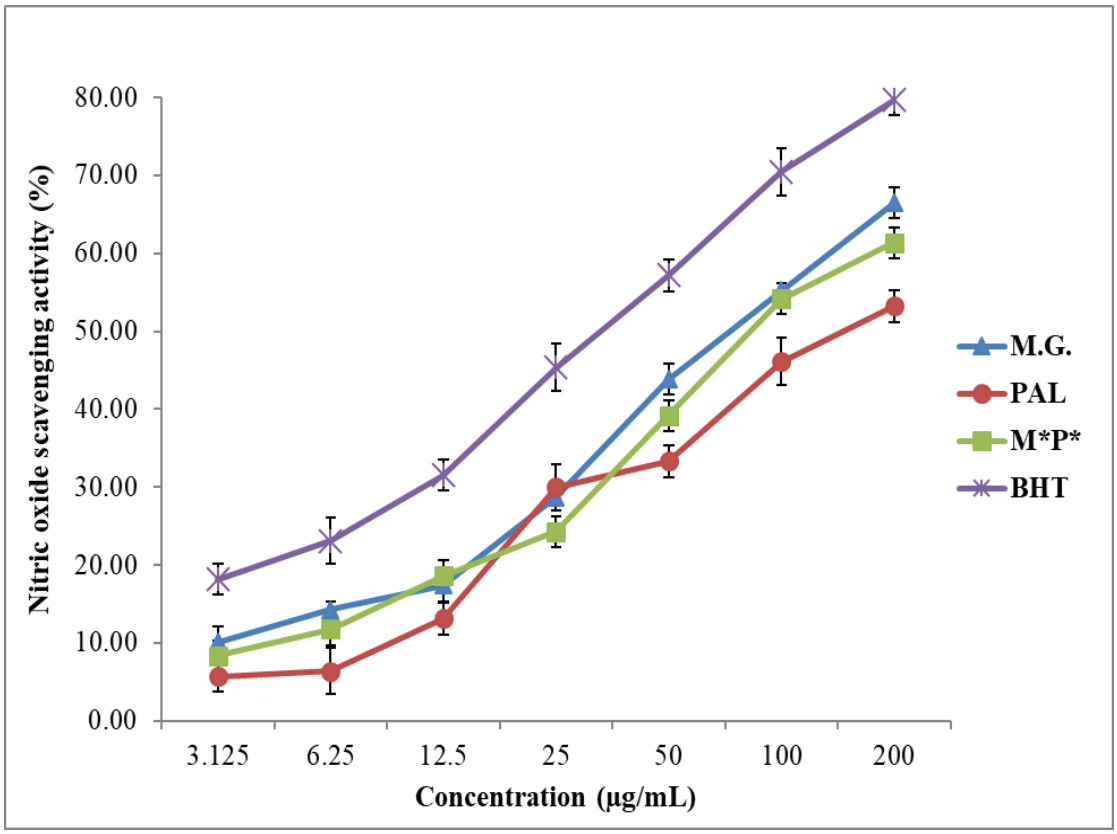

Figure 15: Nitric oxide-scavenging activity of palmatine, methyl gallate and methyl gallate- palmatine combination (3:2)
Values are mean ± SD of three replicates. **M.G.** = Methyl gallate; **PAL**= Palmatine; **BHT** = Butylated hydroxytoluene. **M*P*** = 3:2 of methyl gallate and Palmatine (most active ratio from *in vitro* antimalarial study)

4.1.2.5 Inhibition of Conjugated Diene Formation

The formation of conjugated diene induced by copper was inhibited by methyl gallate and palmatine, though their inhibitory effects were lower than that of vitamin C but the combination of methyl gallate and palmatine (3:2), in addition to inhibiting the formation of conjugated diene, demonstrated better stability in resisting oxidation over the course of two hours (Figure 16).

4.1.2.6 Oxidative Haemolysis Inhibition

Methyl gallate, palmatine and their combination inhibited oxidative haemolysis induced by AAPH, comparing favourably well with vitamin C (Figure 17).

4.2 In silico Studies

The binding of methyl gallate with plasmepsin I (PDB ID: 3QS1) occurred at amino acids Asn11D, Gln276D, Ser219D and Val12D, while palmatine interacted at Ala10D, Leu243C, Pro241C, Ser220D and Val12D (Figure 18-20). Methyl gallate, palmatine and artesunate had binding affinity of -6.0, -8.1, and -9.0 Kcal/mol respectively (Table 4).

The compounds interacted with plasmepsin II (PDB ID: 1SME). Methyl gallate exhibited interactions at Lys326A, Lys327A, Tyr272A and Val160A while palmatine did the same with the amino acids Ala117A, Arg307C, Gln12A, Glu271C, Lys308C, Thr54A, Tyr272C and Val160C (Figures 21-23). The binding affinity of methyl gallate, palmatine and artesunate with plasmepsin II was -5.9, -8.0 and -8.6 Kcal/mol respectively (Table 4).

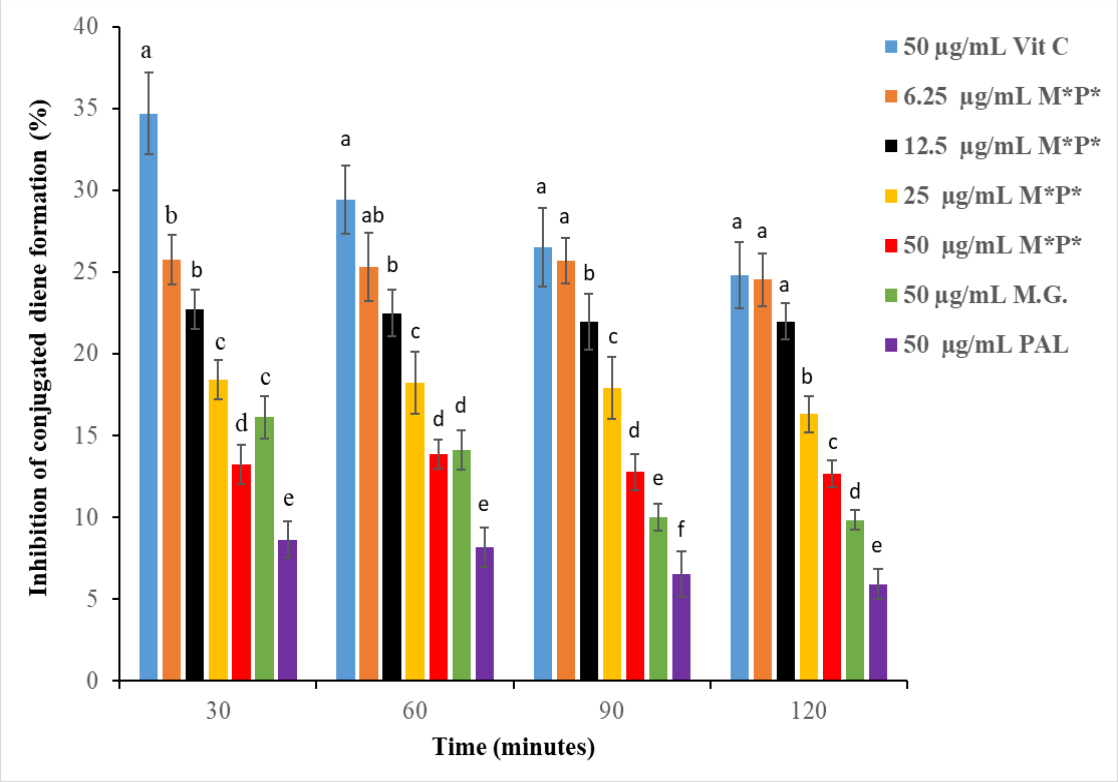

Figure 16: Inhibitory effects of methyl gallate, palmatine, and methyl gallate-palmatine combination (3:2) on conjugated diene formation by copper-induced oxidation of plasma

Values are means ± SD of three replicates. **Vit C**= Vitamin C; **M.G.** = Methyl gallate; **PAL**= Palmatine; **M*P*** = 3:2 of methyl gallate and Palmatine (most active ratio from *in vitro*antimalarial study)

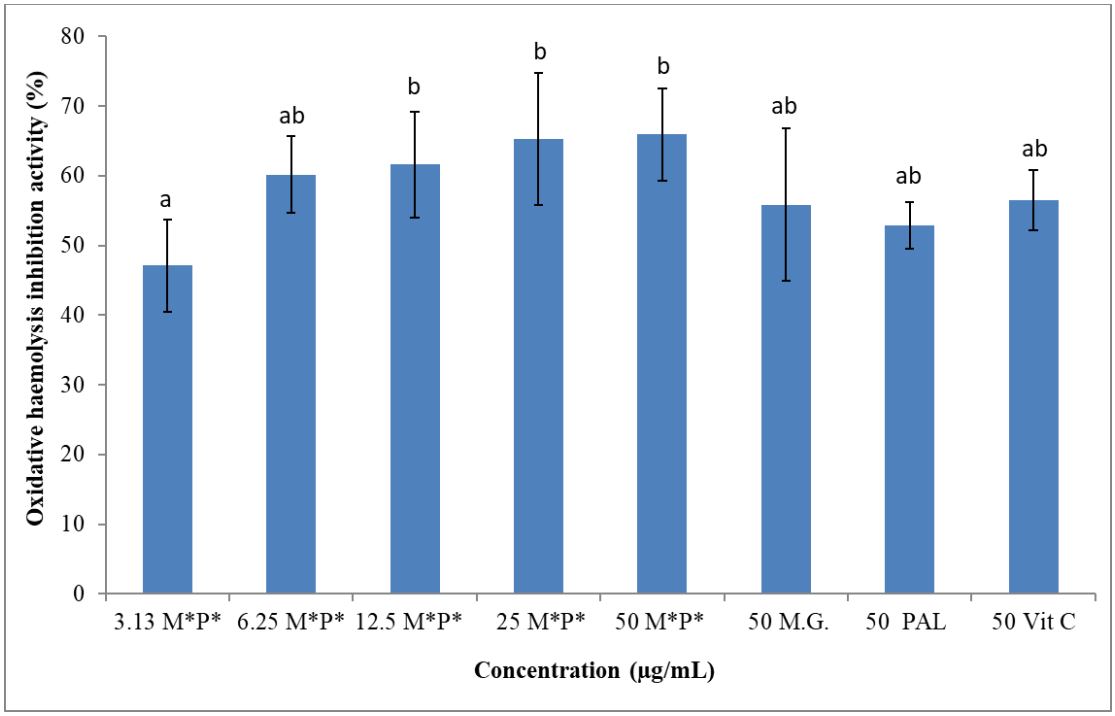

Figure 17: Antihemolytic effects of methyl gallate-palmatine combination on oxidative haemolysis induced by AAPH

Values are means ± SD of three replicates. Bars with different alphabets are significantly different ($p < 0.05$). **Vit C**= Vitamin C; **M.G.** = Methyl gallate; **PAL**= Palmatine; **M*P*** = 3:2 of methyl gallate and Palmatine (most active ratio from *in vitro* antimalarial study); **AAPH** = 2,2'-Azobis(2-amidinopropane) dihydrochloride.

Docking of the compounds into plasmepsin III (PDB ID: 3FNU) showed that methyl gallate interacted with amino acids Asn11B, Asn285B, Glu276B, Leu275B and Lys272B while palmatine interacted with Glu182D, Phe238B and Pro256B (Figures 24-26). The binding affinity was -6.0, -8.5 and -8.5 Kcal/mol for methyl gallate, palmatine and artesunate respectively (Table 4).

Methyl gallate interacted with amino acids Asn263A, Asn264A, Asp198B, Lys260B and Ser261A of plasmepsin IV (PDB ID: 2ANL) while the interaction of palmatine was with Ala118A, Asn13A, Asp34A, Leu114A and Met15A of the protein (Figure 27-29). The binding affinity was -5.5, -7.4, and -8.0 Kcal/mol for methyl gallate, palmatine and artesunate respectively (Table 4).

Docking of the compounds into plasmepsin V (PDB ID: 4ZL4) showed that methyl gallate interacted with the protein at Ala210B, Arg167A, Leu213B, Phe207B, Pro211B and Ser151A while palmatine interacted with Ala60B, Gly315B, His320B, Leu179B, Ser316B and Tyr182B (Figure 30-32). The binding affinity of methyl gallate, palmatine and artesunate was -5.5, -7.5 and -7.5 Kcal/mol respectively (Table 4).

Methyl gallate and palmatine docked into falcipain-2 (PDB ID: 1YVB) interacted in various forms with methyl gallate interacting with amino acids Arg118A, Asn115A, Leu113A and Ser28B, while palmatine interacted with Gln36A, His174A and Trp206A (Figures 33-35). The binding affinity of the compounds with falcipain-2 showed that palmatine had a lower binding energy of -7.8 Kcal/mol compared with -5.6 Kcal/mol of methyl gallate, and similar binding energy to -7.9 Kcal/mol of artesunate (Table 4).

The interaction of the compounds with *Plasmodium falciparum* lactate dehydrogenase (PDB I.D: 1T2C) showed that methyl gallate interacted with amino acids Gly29A, Gly99A, Ile31A and Thr97A, while palmatine interacted at Ala236A, Ile31A, Pro246A, Ser245A (Figure 36-38). The binding affinity of methyl gallate was -5.3 Kcal/mol, palmatine had -6.9 Kcal/mol while artesunate had -7.5 Kcal/mol (Table 4).

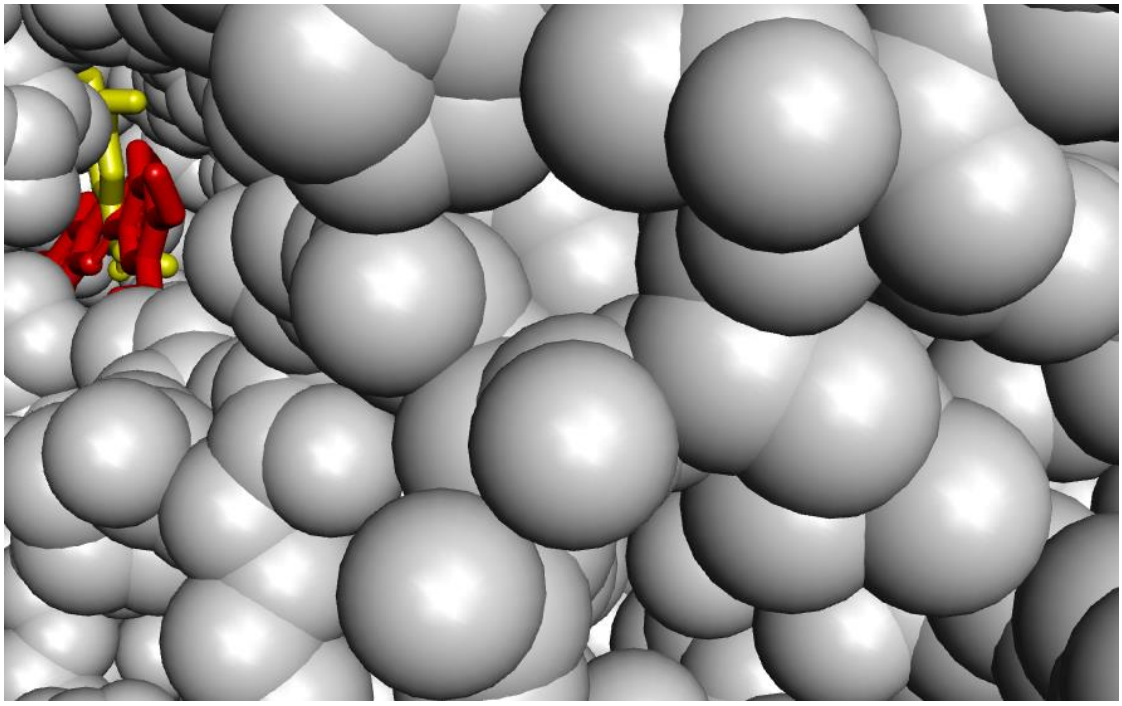

Figure 18: The most active pose of methyl gallate and palmatine in the binding pocket of plasmepsin I
Yellow stick model represents methyl gallate; Red stick model represents Palmatine; Grey molecule represents receptor

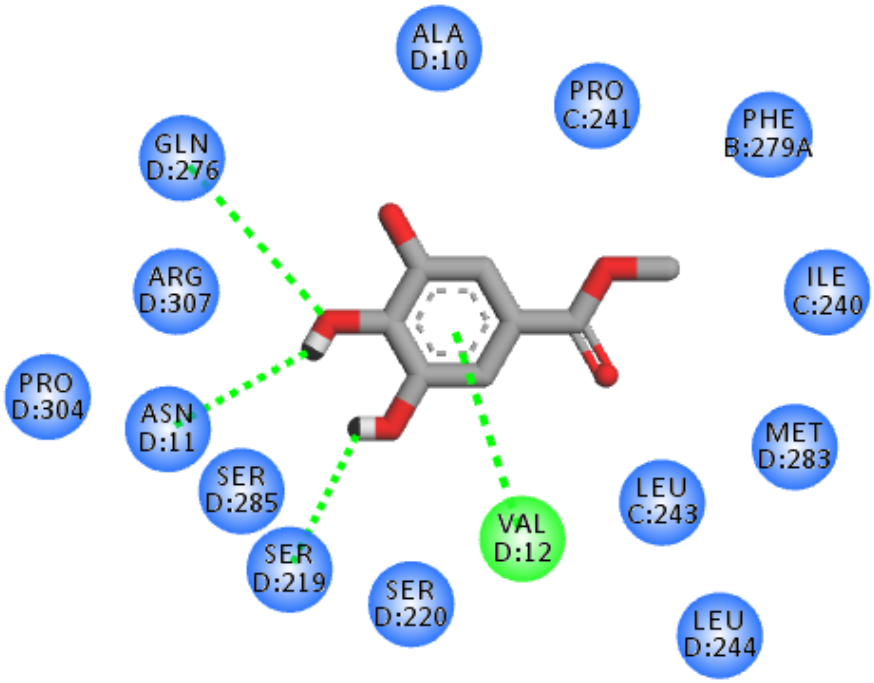

Figure 19: Interactions of methyl gallate with amino acids in the binding pocket of plasmepsin I

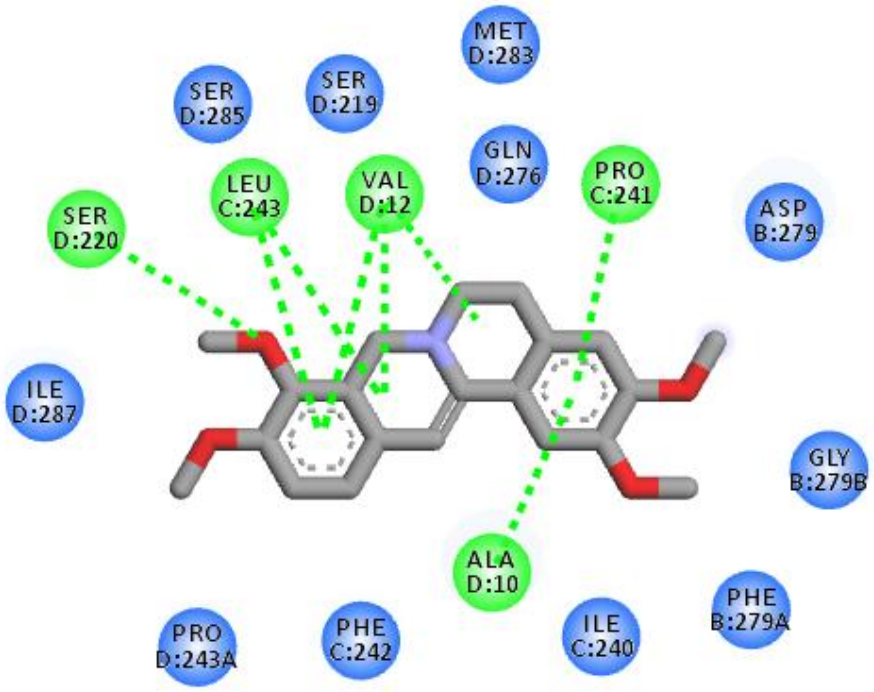

Figure 20: Interactions of palmatine with amino acids in the binding pocket of plasmepsin I

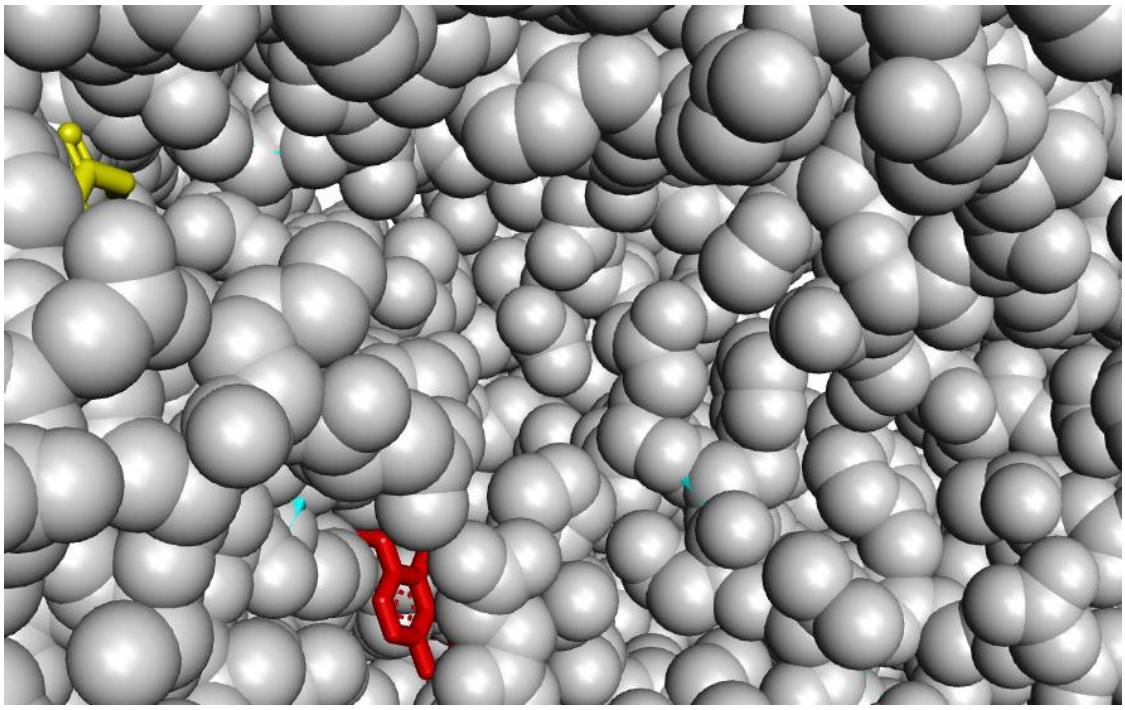

Figure 21: The most active pose of methyl gallate and palmatine in the binding pockets of plasmepsin II
Yellow stick model represents methyl gallate; Red stick model represents Palmatine; Grey molecule represents receptor

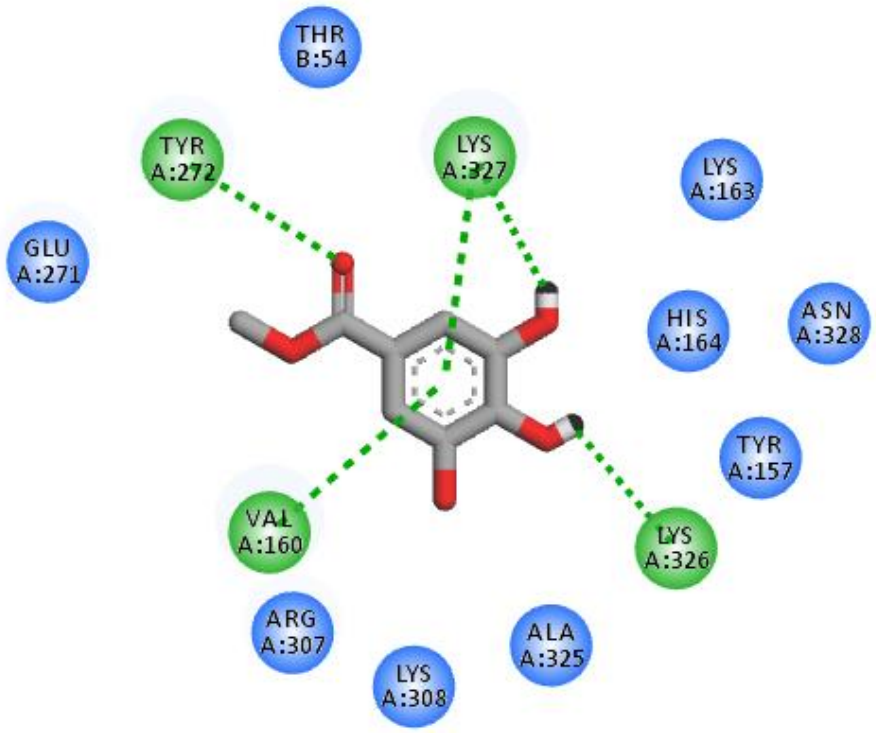

Figure 22: Interactions of methyl gallate with amino acida in the binding pocket of plasmepsin II

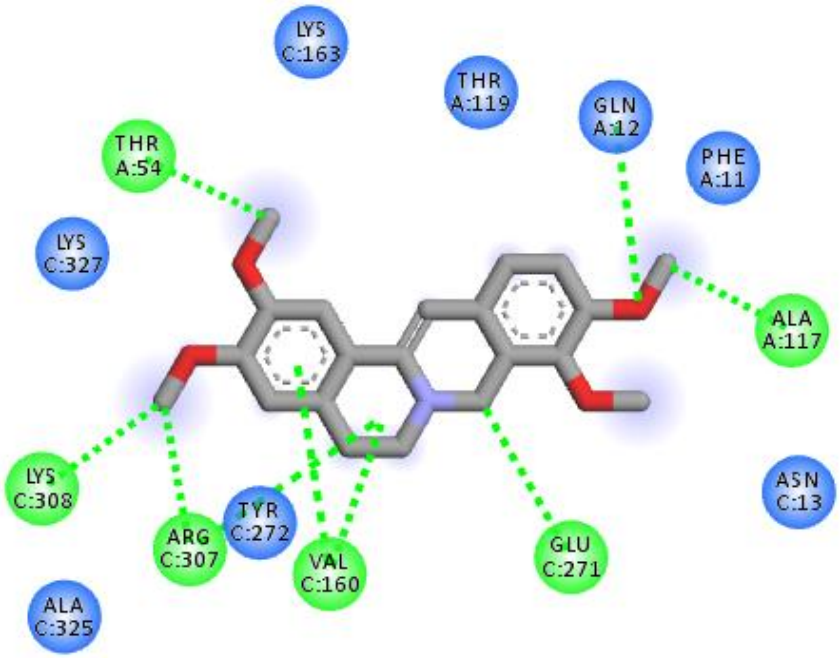

Figure 23: Interactions of palmatine with amino acids in the binding pocket of plasmepsin II

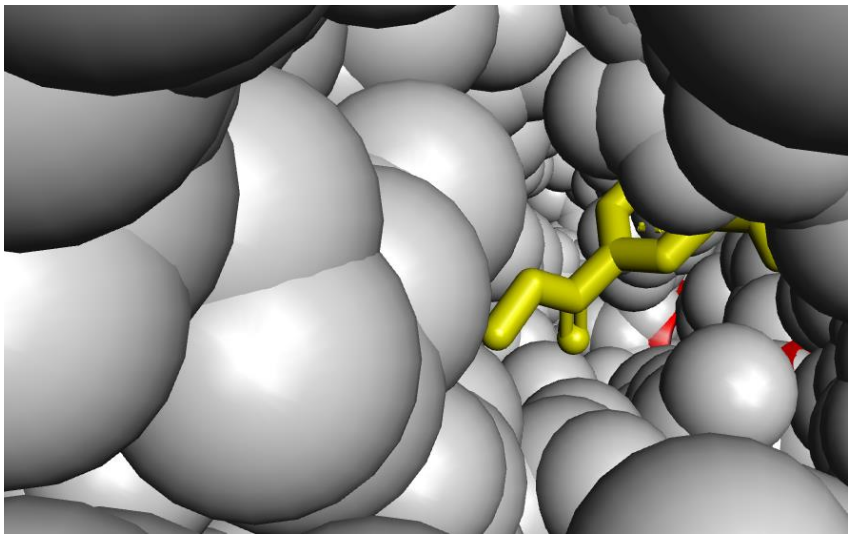

A

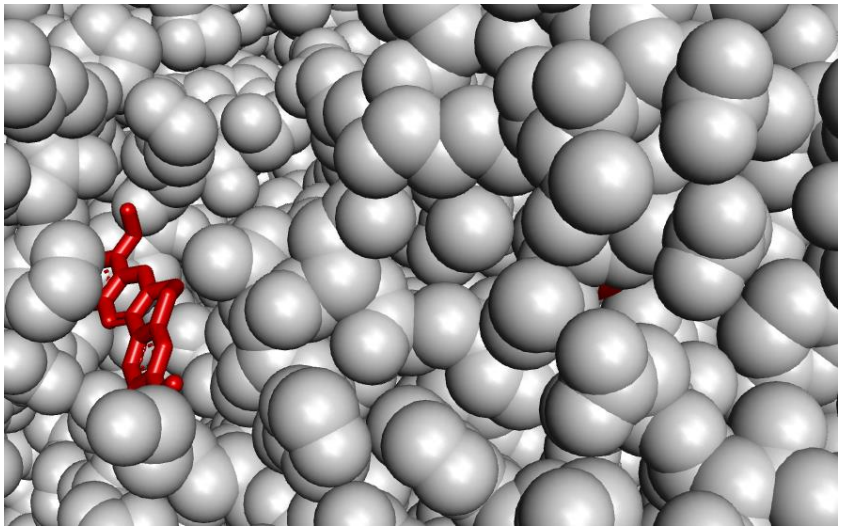

B

Figure 24: The most active pose of methyl gallate (A) and palmatine (B) in the binding pockets of plasmepsin III
Yellow stick model represents methyl gallate; Red stick model represents Palmatine; Grey molecule represents receptor

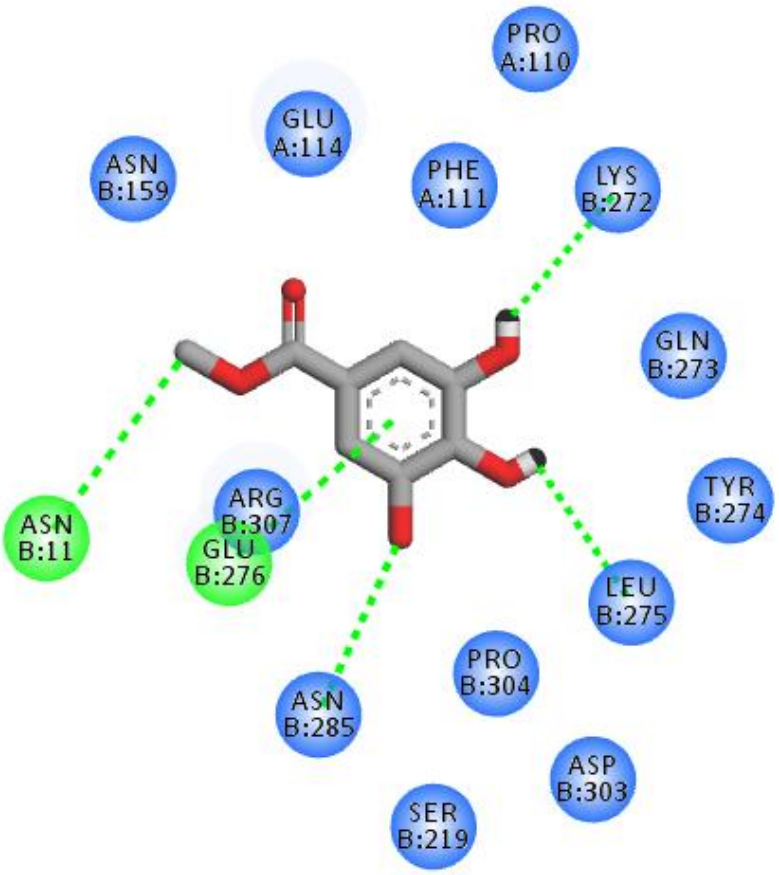

Figure 25: Interactions of methyl gallate with amino acids in the binding pocket of plasmepsin III

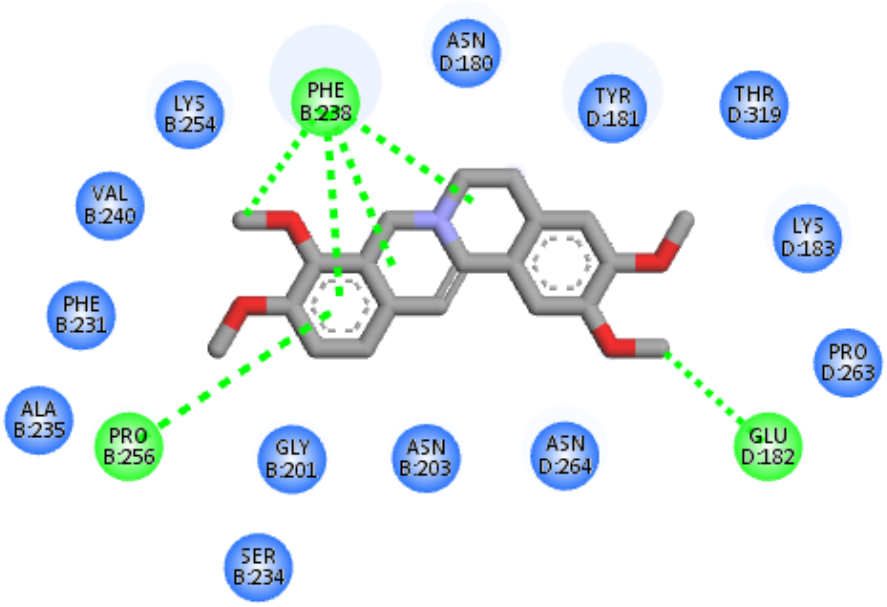

Figure 26: Interactions of palmatine with amino acids in the binding pocket of plasmepsin III

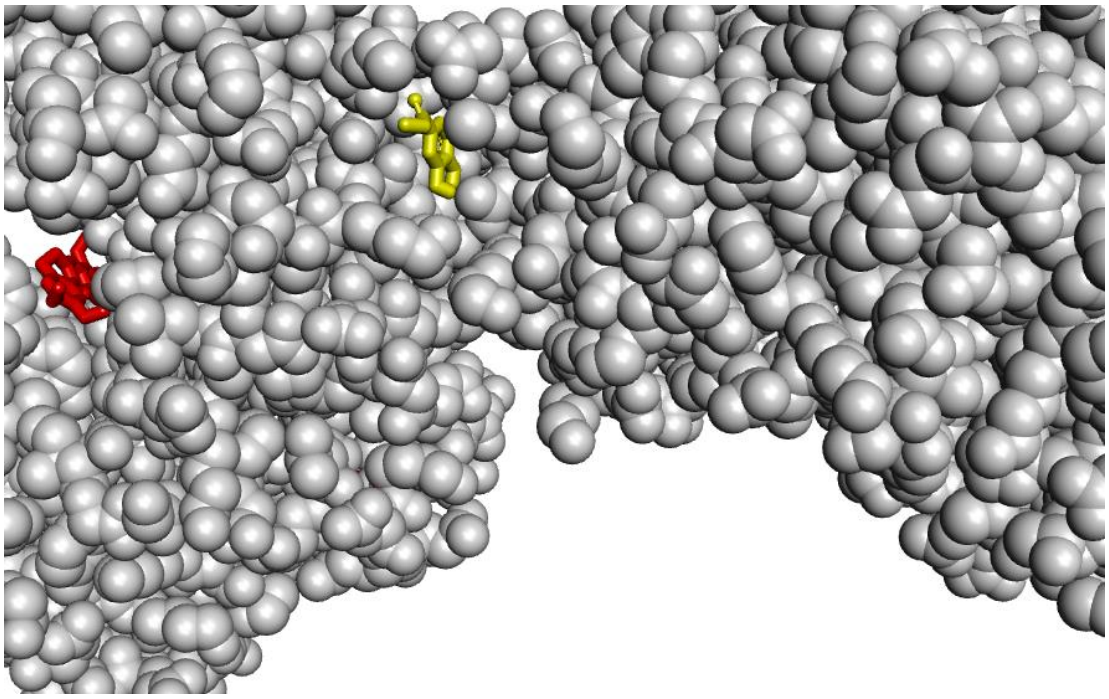

Figure 27: The most active pose of methyl gallate and palmatine in the binding pockets of plasmepsin IV
Yellow stick model represents methyl gallate; Red stick model represents Palmatine; Grey molecule represents receptor.

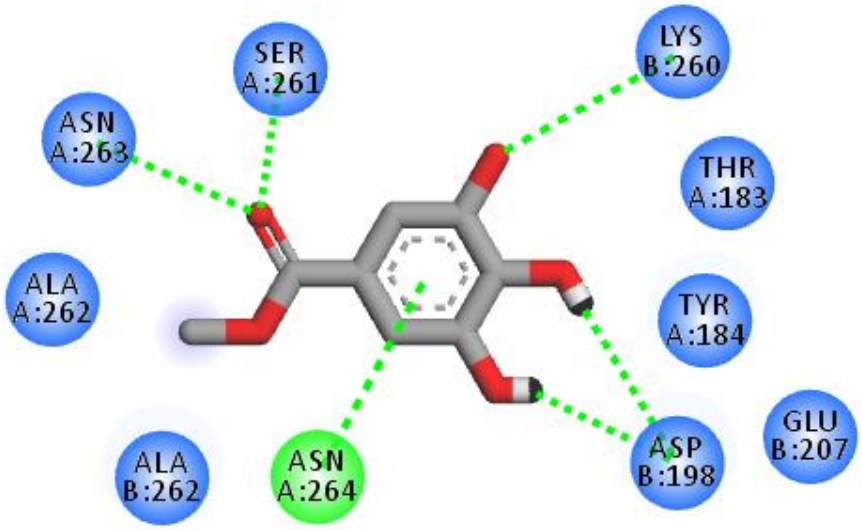

Figure 28: Interactions of methyl gallate with amino acids in the binding pocket of plasmepsin IV

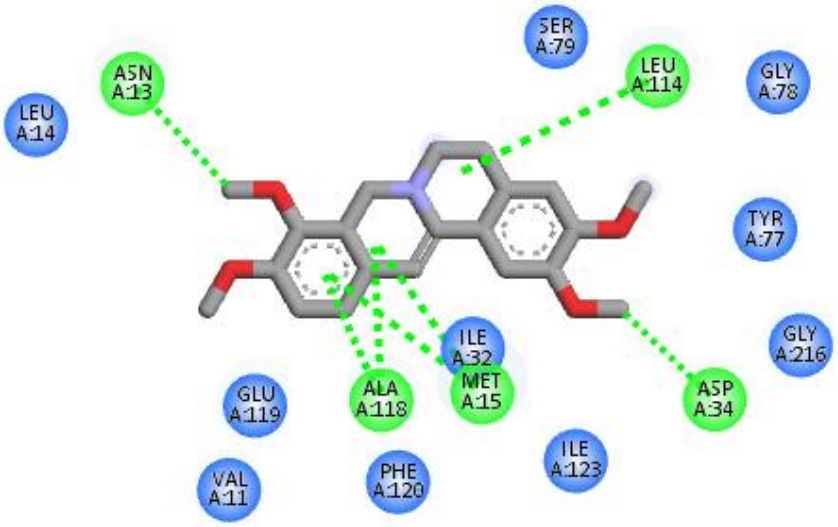

Figure 29: Interactions of palmatine with amino acids in the binding pocket of plasmepsin IV

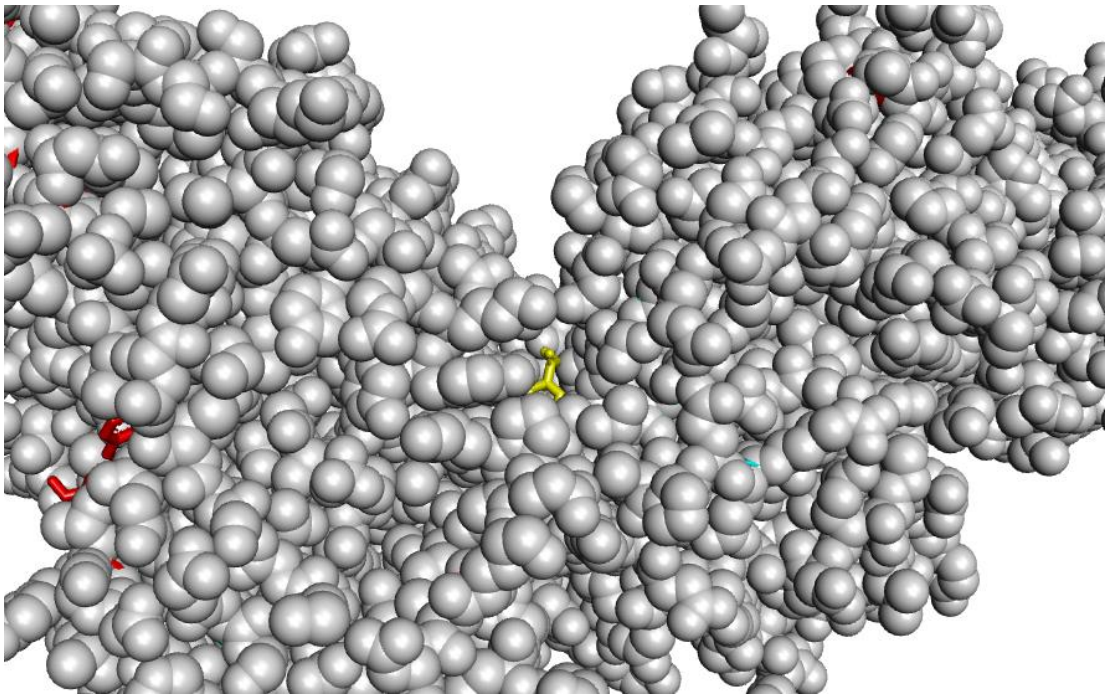

Figure 30: The most active pose of methyl gallate and palmatine in the binding pockets of plasmepsin V
Yellow stick model represents methyl gallate; Red stick model represents Palmatine; Grey molecule represents receptor.

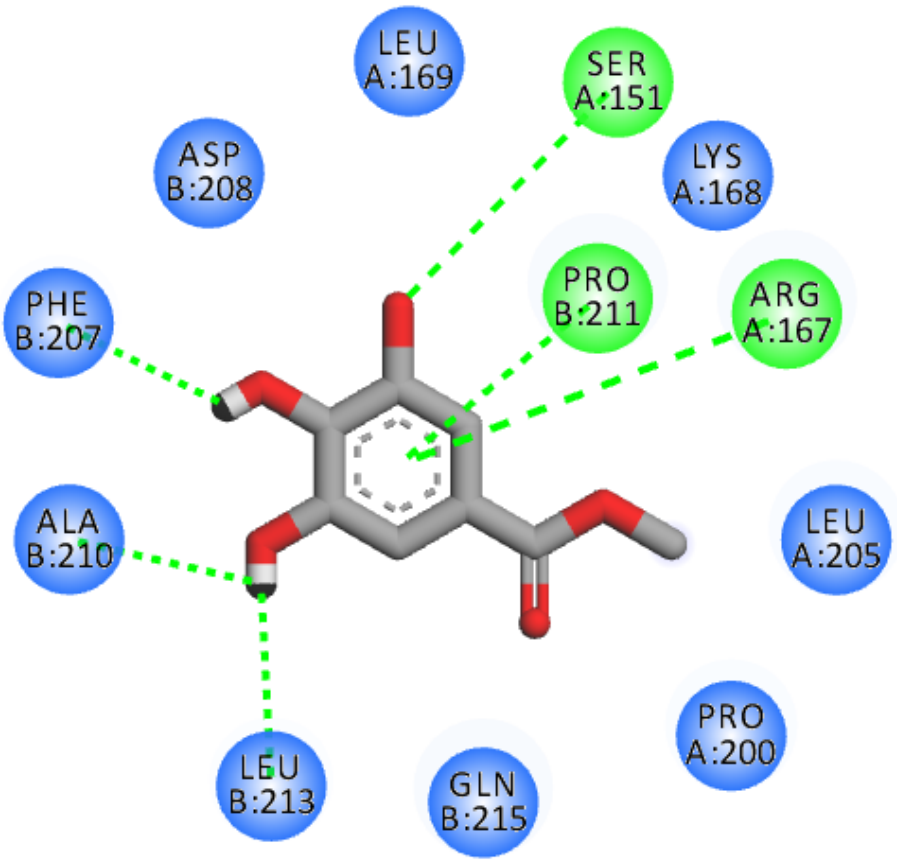

Figure 31: Interactions of methyl gallate with amino acids in the binding pocket of plasmepsin V

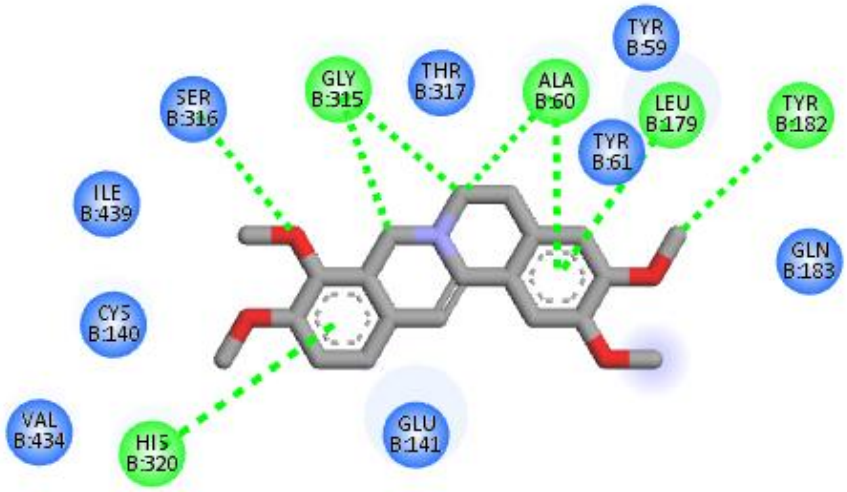

Figure 32: Interactions of palmatine with amino acids in the binding pocket of plasmepsin V

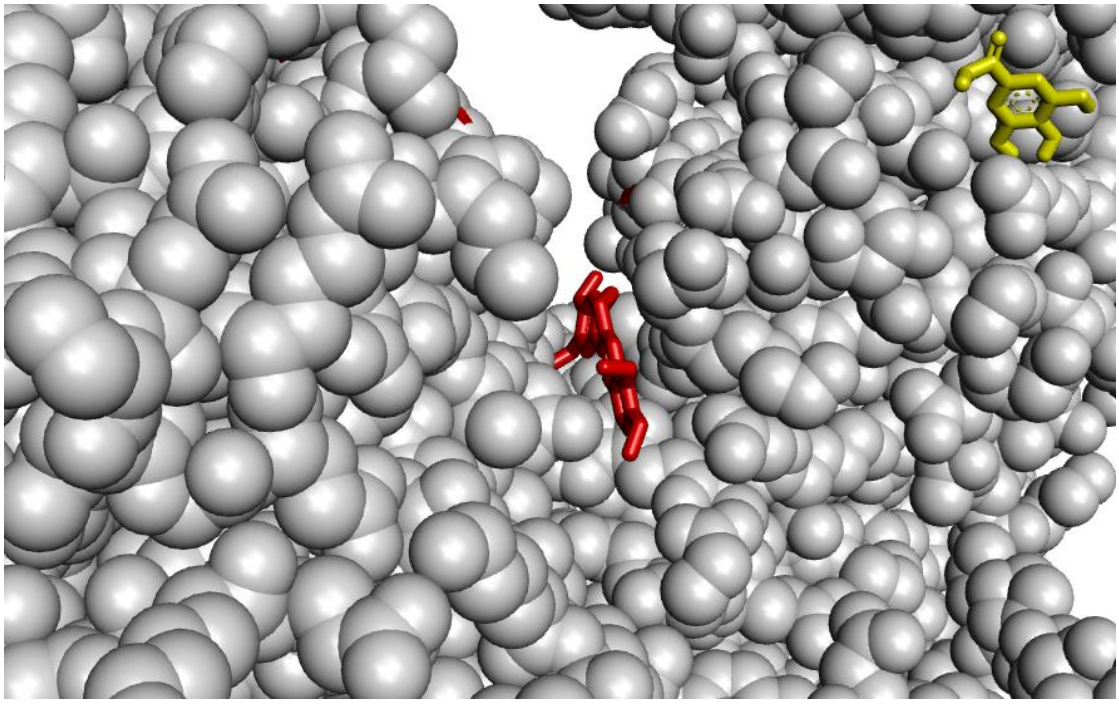

Figure 33: The most active pose of methyl gallate and palmatine in the binding pockets of falcipain-2
Yellow stick model represents methyl gallate; Red stick model represents Palmatine; Grey molecule represents receptor

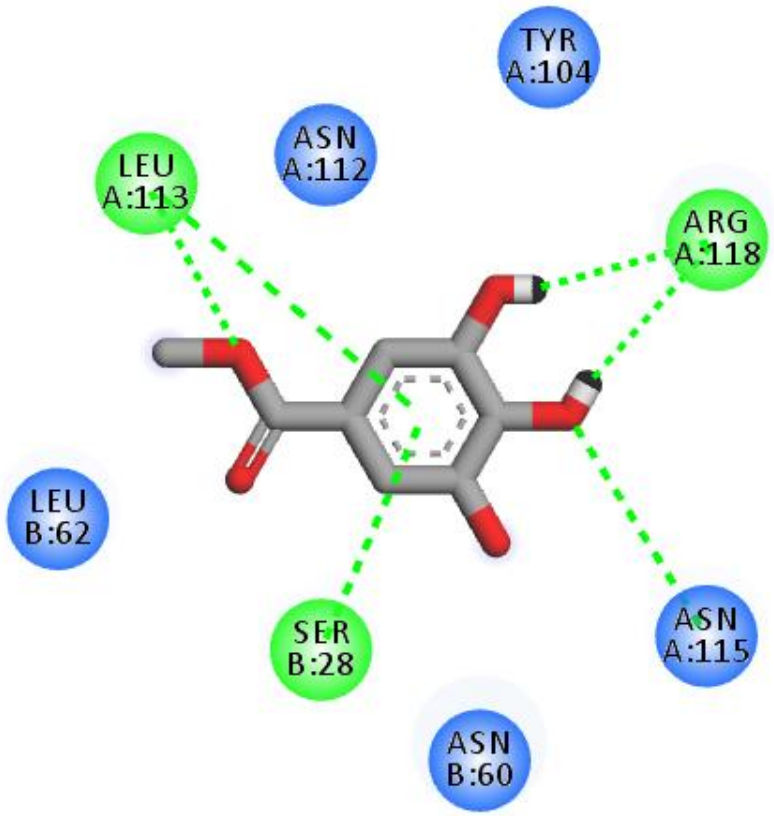

Figure 34: Interactions of methyl gallate with amino acids in the binding pocket of Falcipain-2

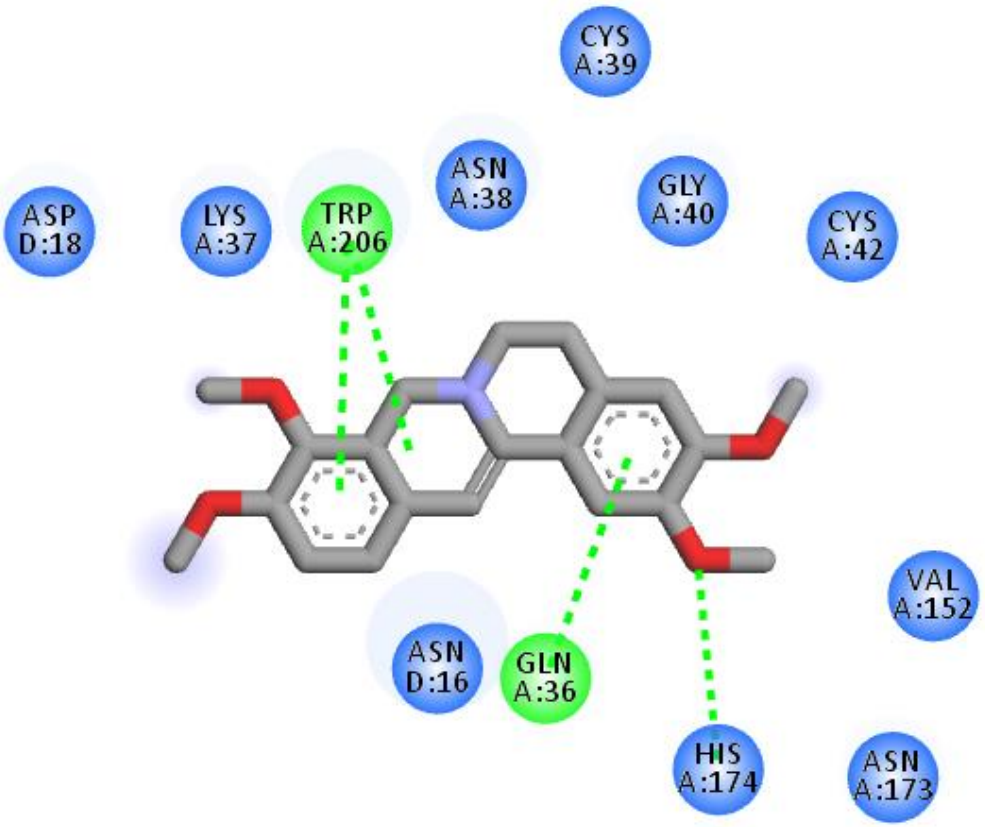

Figure 35: Interactions of Palmatine with amino acids in the binding pocket of Falcipain-2

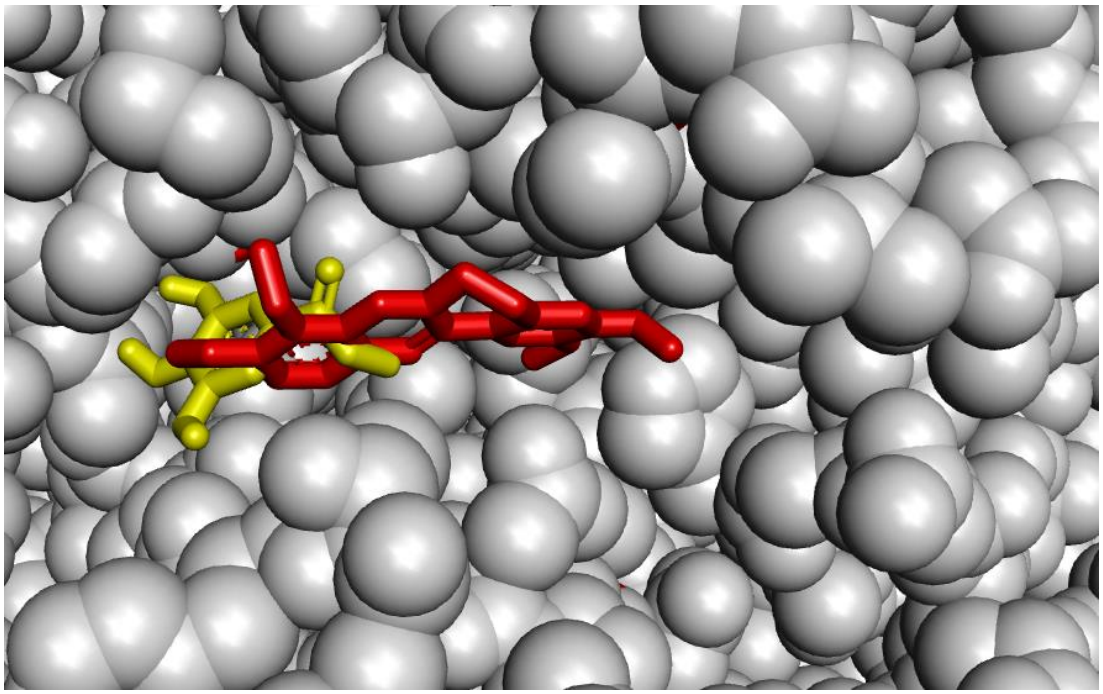

Figure 36: The most active pose of methyl gallate and palmatine in the binding pocket of *Plasmodium falciparum* lactate dehydrogenase
Yellow stick model represents methyl gallate; Red stick model represents Palmatine; Grey molecule represents receptor

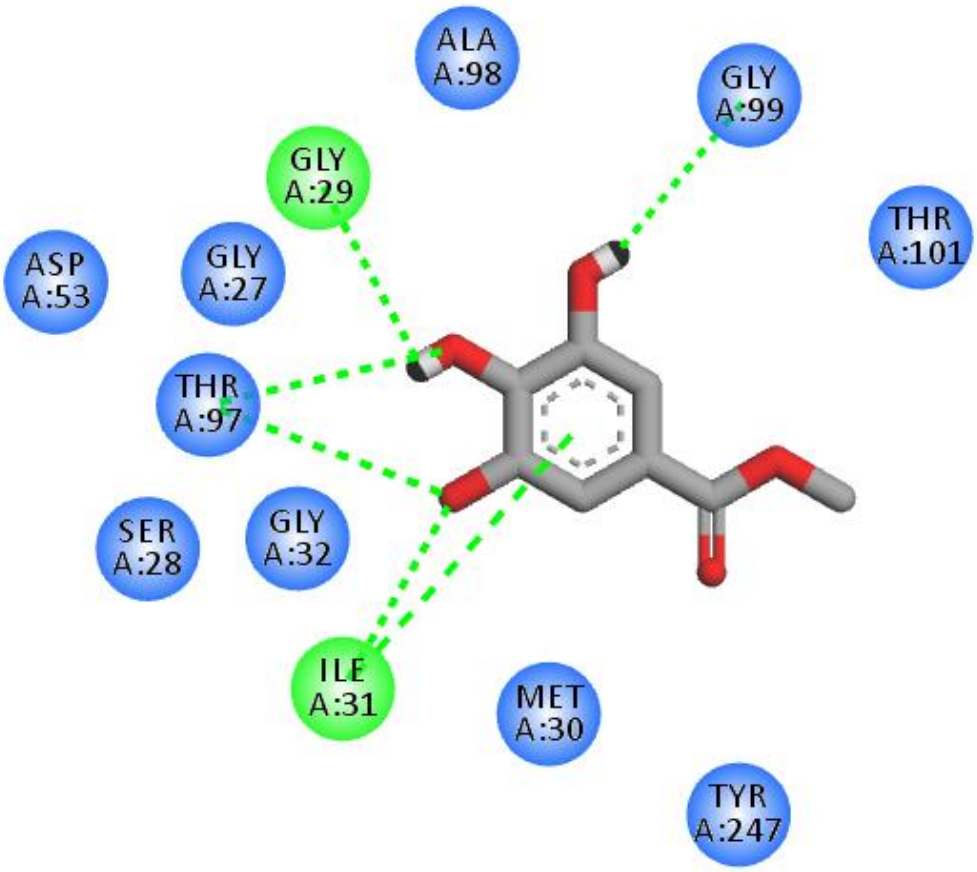

Figure 37: Interactions of methyl gallate with amino acids in the binding pocket of *Plasmodium falciparum* lactate dehydrogenase

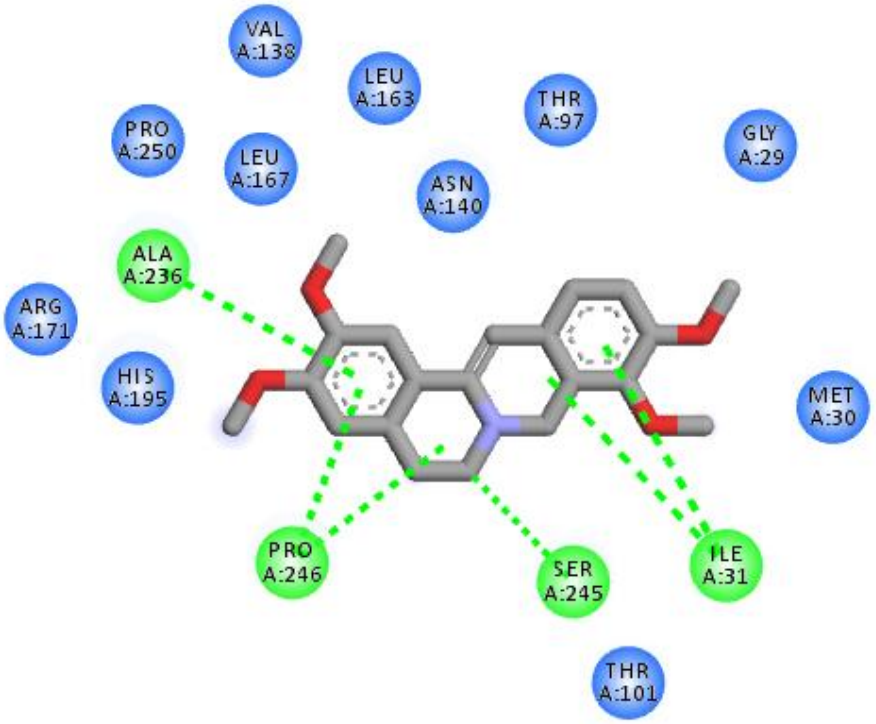

Figure 38: Interactions of palmatine with amino acids in the binding pocket of *Plasmodium falciparum* lactate dehydrogenase

Table 3: Summary of ligand-amino acid interactions in various *in silico* studies

Protein	Methyl gallate	Palmatine
Plasmepsin I	Asn11D, Gln276D, Ser219D, Val12D	Ala10D, Leu243C, Pro241C, Ser220D, Val12D
Plasmepsin II	Lys326A, Lys327A, Tyr272A, Val160A	Ala117A, Arg307C, Gln12A, Glu271C, Lys308C, Thr54A, Tyr272C, Val160C
Plasmepsin III	Asn11B, Asn285B, Glu276B, Leu275B, Lys272B	Glu182D, Phe238B, Pro256B
Plasmepsin IV	Asn263A, Asn264A, Asp198B, Lys260B, Ser261A	Ala118A, Asn13A, Asp34A, Leu114A, Met15A
Plasmepsin V	Ala210B, Arg167A, Leu213B, Phe207B, Pro211B, Ser151A	Ala60B, Gly315B, His320B, Leu179B, Ser316B, Tyr182B
Falcipain-2	Arg118A, Asn115A, Leu113A, Ser28B	Gln36A, His174A, Trp206A
*Pf*LDH	Gly29A, Gly99A, Ile31A, Thr97A	Ala236A, Ile31A, Pro246A, Ser245A

*Pf*LDH = *Plasmodium falciparum* lactate dehydrogenase

Table 4: Summary of Binding affinities of methyl gallate, palmatine and artesunate in various *in silico* studies

	Binding Affinities (Kcal/mol)		
Protein	**Methyl gallate**	**Palmatine**	**Artesunate**
Plasmepsin I	-6.0	-8.1	-9.0
Plasmepsin II	-5.9	-8.0	-8.6
Plasmepsin III	-6.0	-8.5	-8.5
Plasmepsin IV	-5.5	-7.4	-8.0
Plasmepsin V	-5.5	-7.5	-7.5
Falcipain-2	-5.6	-7.8	-7.9
*Pf*LDH	-5.3	-6.9	-7.5

4.3 *In vivo* Studies

4.3.1 *In vivo* Antimalarial Studies

4.3.1.1 Suppressive Antimalarial Study

Methyl gallate and palmatine administered separately were inactive (causing less than 30% reduction in parasitaemia) against *P. berghei* NK65 (Table 5). Moreover, the combination of methyl gallate and palmatine at different doses were also inactive against *P. berghei* NK65 (Table 6). However, 12.5 mg/Kg body weight of the combination of methyl gallate and palmatine, in the presence of piperine was partially active (>30% but <40% reduction in parasitemia) and active (>40% reduction in parasitaemia) against *P. berghei* NK65 on days 6 and 8 post-inoculation respectively (Table 6). Furthermore, 25 mg/Kg body weight of the combination of methyl gallate and palmatine, in the presence of piperine, was partially active against *P. berghei* NK65 on day 4 post-inoculation and was active against the parasite on days 6 and 8 post-inoculation. The combination at 50 mg/Kg body weight, in the presence of piperine, was partially active against the parasite on day 8 post-inoculation (Table 6).

4.3.1.2 Curative Antimalarial Study

Methyl gallate and palmatine administered separately exhibited no curative antimalarial activity at 100 mg/kg body weight. Also, methyl gallate and palmatine combination (3:2) administred at various doses was inactive against *P. berghei* NK65. However, 12.5 and 25 mg/Kg body weight of the combination of methyl gallate and palmatine in the presence of piperine (a bio-enhancer) were partially active (34.3% reduction in parasitemia) and active (41.29% reduction in parasitemia) against *P. berghei* NK65 respectively on day 10 post-inoculation, though the latter dose was also

partially active against the parasite on day 8 post-inoculation. These doses also increased the mean survival time of the mice compared to the untreated control (Table 7).

4.3.1.3 Prophylactic Antimalarial Study

Methyl gallate, palmatine and their combination (3:2) were inactive against the *P. berghei* NK65, in the prophylactic antimalarial test, at the doses considered in this study. Likewise, the administration of methyl gallate and palmatine, in the presence of piperine caused less than 30% parasitaemia reduction; hence, they were considered inactive. On the contrary, chloroquine caused 30% reduction in parasitemia on day 3 post-inoculation and above 50% reduction on days 5 and 7 post-inoculation, thus considered active (Table 8).

Table 5: Effects of methyl gallate and palmatine on parasitaemia and mean survival time of *P. berghei* NK65-infected mice assessed by suppressive test

Treatment	Parasitaemia, % (% Reduction)			MST (Days)
	Day 4 º	Day 6 º	Day 8 º	
5% DMSO	4.27	5.87	7.44	13
10 mg/Kg bwt Chloroquine	1.77 (58.55)	1.42 (75.81)	1.23 (83.47)	27
20 mg/Kg bwt Piperine	4.26 (0.23)	5.84 (0.51)	7.37 (0.94)	13
6.25 mg/Kg bwt Methyl gallate	4.24 (0.70)	5.70 (2.89)	7.21 (3.09)	15
12.5 mg/Kg bwt Methyl gallate	4.20 (1.64)	5.59 (4.77)	7.05 (5.24)	16
25 mg/Kg bwt Methyl gallate	4.25 (0.47)	5.29 (9.88)	6.70 (9.95)	16
50 mg/Kg bwt Methyl gallate	4.19 (1.87)	5.54 (5.62)	6.91 (7.12)	16
100 mg/Kg bwt Methyl gallate	4.15 (2.81)	5.30 (9.71)	6.82 (8.33)	15
6.25 mg/Kg bwt Palmatine	4.21 (1.41)	5.52 (5.96)	7.10 (4.57)	15
12.5 mg/Kg bwt Palmatine	4.17 (2.34)	5.28 (10.05)	6.64 (10.75)	15
25 mg/Kg bwt Palmatine	4.20 (1.64)	5.36 (8.69)	6.76 (9.14)	15
50 mg/Kg bwt Palmatine	4.18 (2.11)	5.49 (6.47)	6.86 (7.79)	15
100 mg/Kg bwt Palmatine	4.13 (3.28)	5.25 (10.56)	6.74 (9.41)	15

Values are mean of 5 determinations. Values in parenthesis represent the percentage parasitaemia reduction. **º =** post-inoculation; **MST** = Mean survival time; **20 Pip** = 20 mg/Kg bwt Piperine;

Table 6: Effects of methyl gallate and palmatine combination on parasitaemia and mean survival time of P. berghei NK65-infected mice assessed by suppressive test

Treatment	Parasitaemia, % (% Reduction)			MST (Days)
	Day 4 º	Day 6 º	Day 8 º	
5% DMSO	4.27	5.87	7.44	13
10 mg/Kg bwt Chloroquine	1.77 (58.55)	1.42 (75.81)	1.23 (83.47)	27
20 mg/Kg bwt Piperine	4.26 (0.23)	5.84 (0.51)	7.37 (0.94)	13
6.25 mg/Kg bwt M*P*	4.17 (2.34)	5.39 (8.18)	6.77 (9.01)	15
12.5 mg/Kg bwt M*P*	4.11 (3.75)	5.20 (11.41)	6.60 (11.29)	16
25 mg/Kg bwt M*P*	4.09 (4.22)	5.18 (11.75)	6.52 (12.37)	17
50 mg/Kg bwt M*P*	4.12 (3.51)	5.30 (9.71)	6.62 (11.02)	16
100 mg/Kg bwt M*P*	4.14 (3.04)	5.28 (10.05)	6.64 (10.75)	15
6.25 mg/Kg bwt M*P* + 20 Pip	3.90 (8.67)	4.68 (20.27)	5.73 (22.98)	20
12.5 mg/Kg bwt M*P* + 20 Pip	3.41 (20.14)	3.89 (33.73)	4.00 (46.24)	22
25 mg/Kg bwt M*P* + 20 Pip	2.90 (32.08)	3.50 (40.37)	3.31 (55.51)	23
50 mg/Kg bwt M*P* + 20 Pip	3.54 (17.09)	4.22 (28.11)	4.58 (38.44)	22
100 mg/Kg bwt M*P* + 20 Pip	3.82 (10.54)	4.61 (21.47)	5.66 (23.92)	20

Values are means of 5 determinations. Values in parenthesis represent the percentage parasitaemia reduction. **º =** post-inoculation; **MST** = Mean survival time; **20 Pip** = 20 mg/Kg bwt Piperine; **M*P*** = 3:2 of Methyl gallate and palmatine (most active ratio from *in vitro* antimalarial study)

Table 7: Effects of methyl gallate and palmatine combination on parasitaemia and mean survival time of *P. berghei* NK65-infected mice assessed by curative test

Treatment	Parasitaemia, % (% Reduction)			MST (Days)
	Day 6 º	Day 8 º	Day 10 º	
5% DMSO	5.17	8.23	9.93	13
10 mg/Kg bwt Chloroquine	2.52 (51.26)	2.29 (72.17)	1.21 (87.81)	29
20 mg/Kg bwt Piperine	5.11 (1.16)	8.12 (1.34)	9.80 (1.31)	14
100 mg/Kg bwt Methyl gallate	5.07 (1.93)	7.88 (4.25)	9.24 (6.95)	15
100 mg/Kg bwt Palmatine	5.06 (2.13)	7.83 (4.86)	9.21 (7.25)	15
6.25 mg/Kg bwt M*P*	5.11 (1.16)	7.77 (5.59)	9.20 (7.35)	15
12.5 mg/Kg bwt M*P*	4.92 (4.84)	7.63 (7.29)	8.90 (10.37)	16
25 mg/Kg bwt M*P*	4.88 (5.61)	7.40 (10.09)	8.70 (12.39)	16
50 mg/Kg bwt M*P*	5.00 (3.29)	7.66 (6.93)	9.00 (9.37)	16
100 mg/Kg bwt M*P*	5.05 (2.32)	7.76 (5.71)	9.10 (8.36)	16
6.25 mg/Kg bwt M*P* + 20 Pip	4.87 (5.80)	7.45 (9.48)	8.60 (13.39)	19
12.5 mg/Kg bwt M*P* + 20 Pip	4.72 (8.70)	6.24 (24.18)	6.52 (34.34)	20
25 mg/Kg bwt M*P* + 20 Pip	4.50 (12.96)	5.12 (37.79)	5.83 (41.29)	21
50 mg/Kg bwt M*P* + 20 Pip	4.79 (7.35)	6.88 (16.40)	7.44 (25.08)	20
100 mg/Kg bwt M*P* + 20 Pip	4.85 (6.19)	7.13 (13.37)	8.20 (17.42)	19

Values are mean of 5 determinations. Values in parenthesis represent the percentage parasitaemia reduction. **º =** post-inoculation; **MST** = Mean survival time; **20 Pip** = 20 mg/Kg bwt Piperine;**M*P*** = 3:2 of Methyl gallate and palmatine (most active ratio from *in vitro* antimalarial study)

Table 8: Effects of methyl gallate and palmatine combination on parasitaemia and mean survival time of *P. berghei* NK65-infected mice assessed by prophylactic test

Treatment	Parasitaemia, % (% Reduction)			MST (Days)
	Day 3 º	Day 5 º	Day 7 º	
5% DMSO	3.10	4.68	6.75	12
10 mg/Kg bwtChloroquine	2.17	2.23	2.09	26
	(30.00)	(52.35)	(69.04)	
20 mg/Kg bwt Piperine	3.07	4.57	6.64	12
	(0.97)	(2.35)	(1.63)	
100 mg/Kg bwtMethyl gallate	3.06	4.43	6.20	14
	(1.29)	(5.34)	(8.15)	
100 mg/Kg bwtPalmatine	3.02	4.31	6.12	14
	(2.58)	(7.91)	(9.33)	
100 mg/Kg bwtM*P*	2.96	4.21	5.81	15
	(4.52)	(10.04)	(13.93)	
100 mg/Kg bwtM*P* + 20 Pip	2.51	3.40	5.05	19
	(19.03)	(27.35)	(25.19)	

Values are means of 5 determinations. Values in parenthesis represent the percentage parasitaemia reduction. **º =** post-inoculation; **MST** = Mean survival time; **20 Pip** = 20 mg/Kg bwt Piperine;**M*P*** = 3:2 of Methyl gallate and palmatine (most active ratio from *in vitro* antimalarial study)

4.3.2 *In vivo* Antioxidant Studies

4.3.2.1 Malondialdehyde Concentration

On days 4 and 8 post-inoculation, the malondialdehyde levels in erythrocyte, liver and kidney were significantly increased ($p<0.05$) in the untreated infected mice compared to the uninfected control (Figures 39, 40 and 42). However, malondialdehyde levels in the heart and brain were only significantly increased ($p<0.05$) on day 8 post- inoculation compared to the uninfected control (Figures 41 and 43).

The increased malondialdehyde levels in the erythrocyte and liver on day 4 post-inoculation caused by the infection was reverted to the range of the uninfected control ($p>0.05$) at doses higher than 6.25 mg/kg body weight of bio-enhanced methyl gallate and palmatine combination (Figures 39-43). On day 8 post-inoculation, the bio-enhanced compound combination at doses higher than 6.25 mg/kg body weight significantly reduced ($p<0.05$) erythrocyte and liver malonaldehyde concentrations compared to the untreated infected controls, though not to the range of the uninfected control in the erythrocyte but to the range of the uninfected control in the liver at doses higher than 12.5 mg/kg body weight.

The increased malondialdehyde levels in the heart and kidney on day 4 post-inoculation caused by the infection was reverted to the range of the uninfected controls ($p>0.05$) at all doses of the bio-enhanced methyl gallate and palmatine combination. The same trend was observed on day 8 post-inoculation, in which the reduction was to the range of the uninfected control at doses higher than 6.25 mg/kg body weight for the heart, 12.5 mg/kg body weight for the kidney and at all doses for the brain (Figs. 39-43).

Generally, chloroquine did not alleviate the increase in MDA concentrations in the tissues caused by the infection on days 4 and 8 post-inoculation, except in the kidney on day 4 post-inoculation and in the heart on day 8 post-inoculation (Figures 39-43).

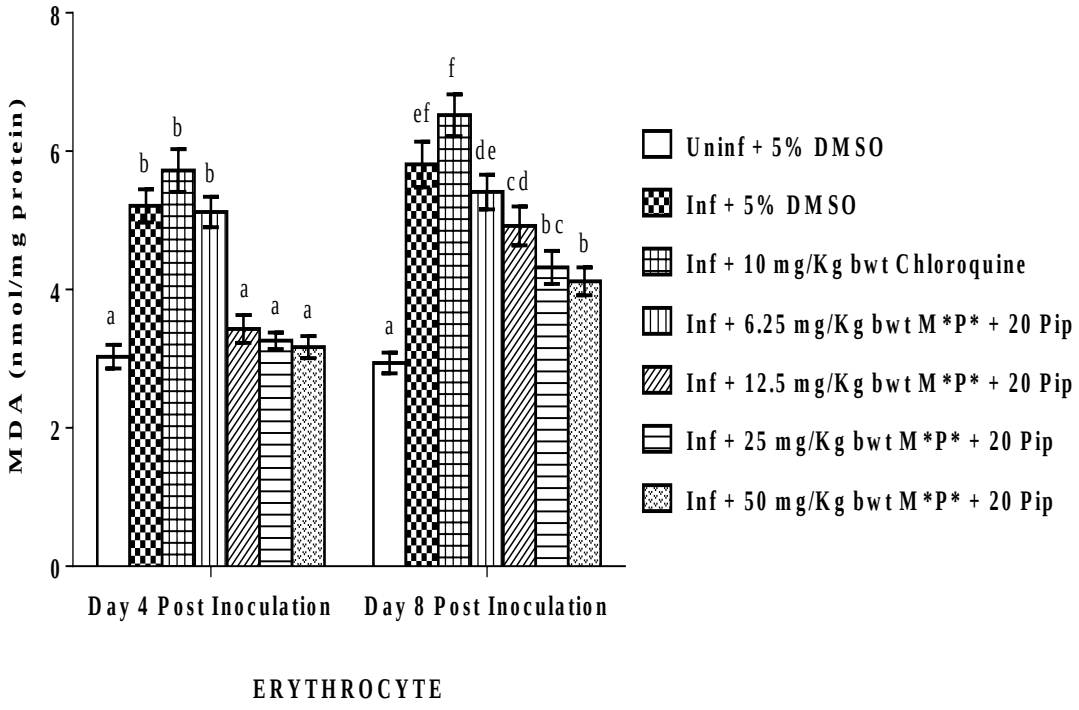

Figure 39: Effects of methyl gallate and palmatine combination in the presence of piperine on malondialdehyde level in the erythrocyte of *P. berghei* NK65-infected mice on days 4 and 8 post-inoculation

Values are means ± SEM of 5 determinations. Bars for each day with different alphabets are significantly different ($p<0.05$). **Uninf** = Uninfected; **Inf** = infected; **DMSO** = Dimethyl sulfoxide; **bwt** = body weight; **M*P*** = 3:2 Methyl gallate and Palmatine (most active ratio from *in vitro* antimalarial study); **20 Pip** = 20 mg/Kg bwt Piperine

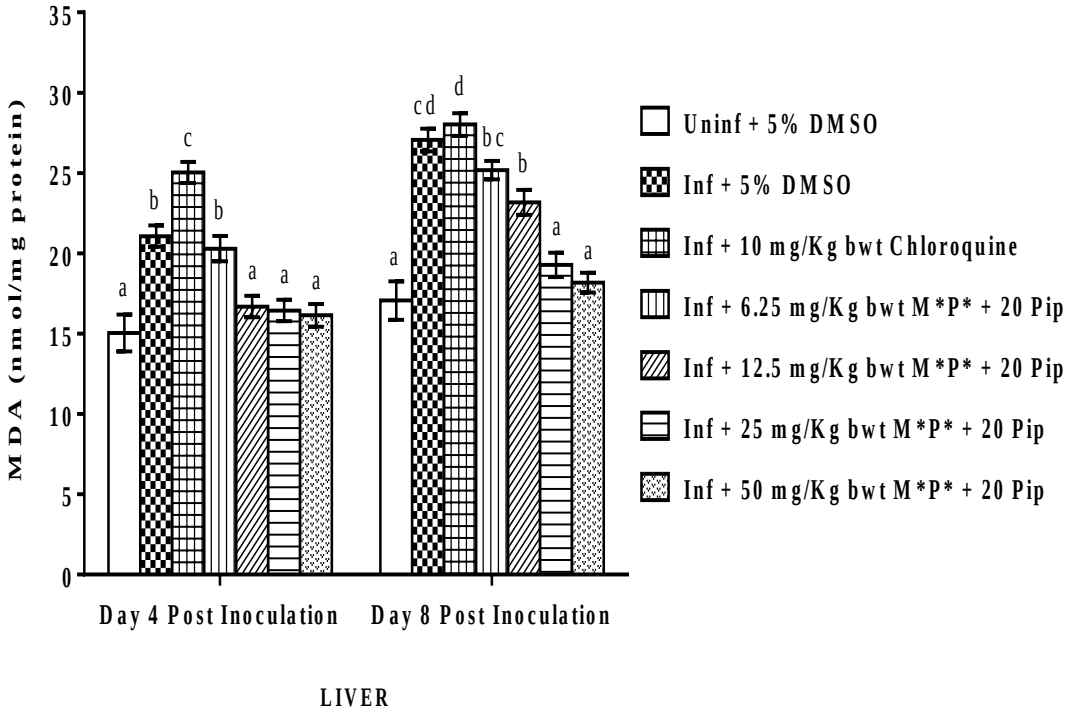

Figure 40: Effects of methyl gallate and palmatine combination in the presence of piperine on malondialdehyde level in the liver of *P. berghei* NK65-infected mice on days 4 and 8 post-inoculation

Values are means ± SEM of 5 determinations. Bars for each day with different alphabets are significantly different ($p<0.05$). **Uninf** = Uninfected; **Inf** = infected; **DMSO** = Dimethyl sulfoxide; **bwt** = body weight; **M*P*** = 3:2 Methyl gallate and Palmatine (most active ratio from *in vitro* antimalarial study); **20 Pip** = 20 mg/Kg bwt Piperine.

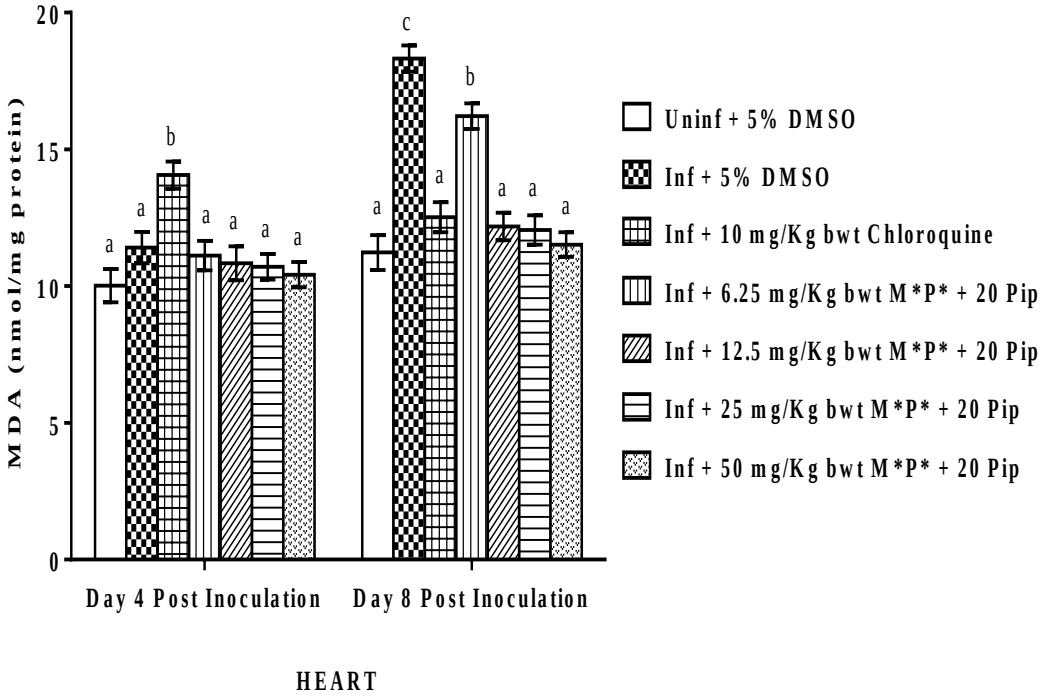

Figure 41: Effects of methyl gallate and palmatine combination in the presence of piperine on malondialdehyde level in the heart of *P. berghei* NK65-infected mice on days 4 and 8 post inoculation

Values are means ± SEM of 5 determinations. Bars for each day with different alphabets are significantly different ($p<0.05$). **Uninf** = Uninfected; **Inf** = infected; **DMSO** = Dimethyl sulfoxide; **bwt** = body weight; **M*P*** = 3:2 Methyl gallate and Palmatine (most active ratio from *in vitro* antimalarial study); **20 Pip** = 20 mg/Kg bwt Piperine

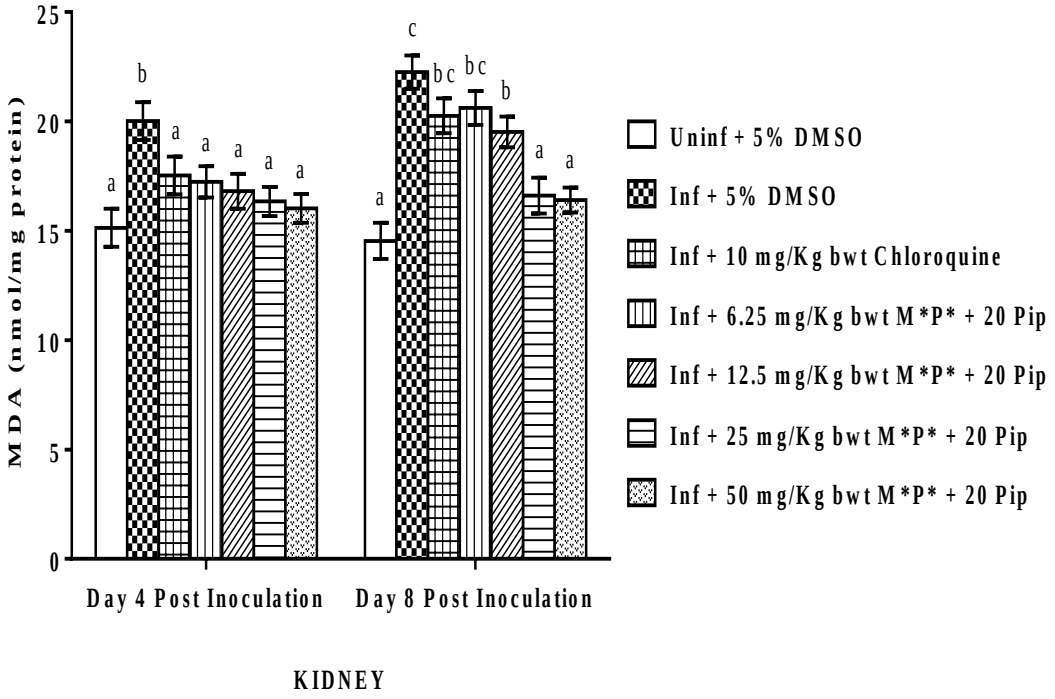

Figure 42: Effects of methyl gallate and palmatine combination in the presence of piperine on malondialdehyde level in the kidney of *P. berghei* NK65-infected mice on days 4 and 8 post inoculation

Values are means ± SEM of 5 determinations. Bars for each day with different alphabets are significantly different ($p<0.05$). **Uninf** = Uninfected; **Inf** = infected; **DMSO** = Dimethyl sulfoxide; **bwt** = body weight; **M*P*** = 3:2 Methyl gallate and Palmatine (most active ratio from *in vitro* antimalarial study); **20 Pip** = 20 mg/Kg bwt Piperine

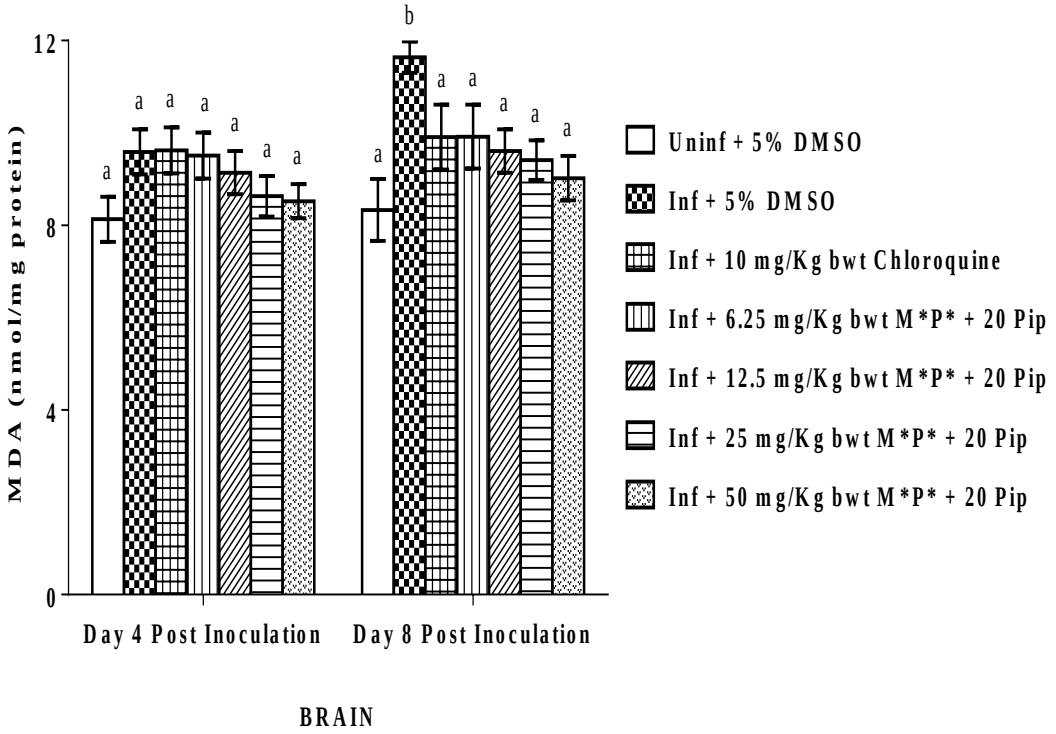

Figure 43: Effects of methyl gallate and palmatine combination in the presence of piperine on malondialdehyde level in the brain of *P. berghei* NK65-infected mice on days 4 and 8 post inoculation

Values are means ± SEM of 5 determinations. Bars for each day with different alphabets are significantly different ($p<0.05$). **Uninf** = Uninfected; **Inf** = infected; **DMSO** = Dimethyl sulfoxide; **bwt** = body weight; **M*P*** = 3:2 Methyl gallate and Palmatine (most active ratio from *in vitro* antimalarial study); **20 Pip** = 20 mg/Kg bwt Piperine

4.3.2.2 Superoxide Dismutase Activity

On days 4 and 8 post-inoculation, the activities of superoxide dismutase in erythrocyte, liver, heart, kidney and brain were significantly reduced ($p<0.05$) in the untreated infected control compared to the uninfected control except in the heart, where there was no significant change ($p>0.05$) in enzyme activity on day 4 post-inoculation (Figures 44-48).

Treatment with bio-enhanced combination of methyl gallate and palmatine at doses higher than 6.25 mg/Kg body weight yielded significant increase ($p<0.05$) in the superoxide dismutase activities in erythrocyte, liver, heart, kidney and brain compared with those of untreated infected control on days 4 and 8 post-inoculation (Figures 44-48). In most cases, these doses of bio-enhanced combination of methyl gallate and palmatine were able to revert the reduction in SOD activities in the heart, kidney and brain caused by the infection to the range of the uninfected controls ($p>0.05$) (Figures 46-48).

Considering SOD activities in the tissues and erythrocyte studied on days 4 and 8 post-inoculation, it was observed that the bio-enhanced combination of methyl gallate and palmatine at doses higher than 6.25 mg/Kg body weight was more potent in reverting the reduced SOD activities caused by the infection than chloroquine (Figures 44-48).

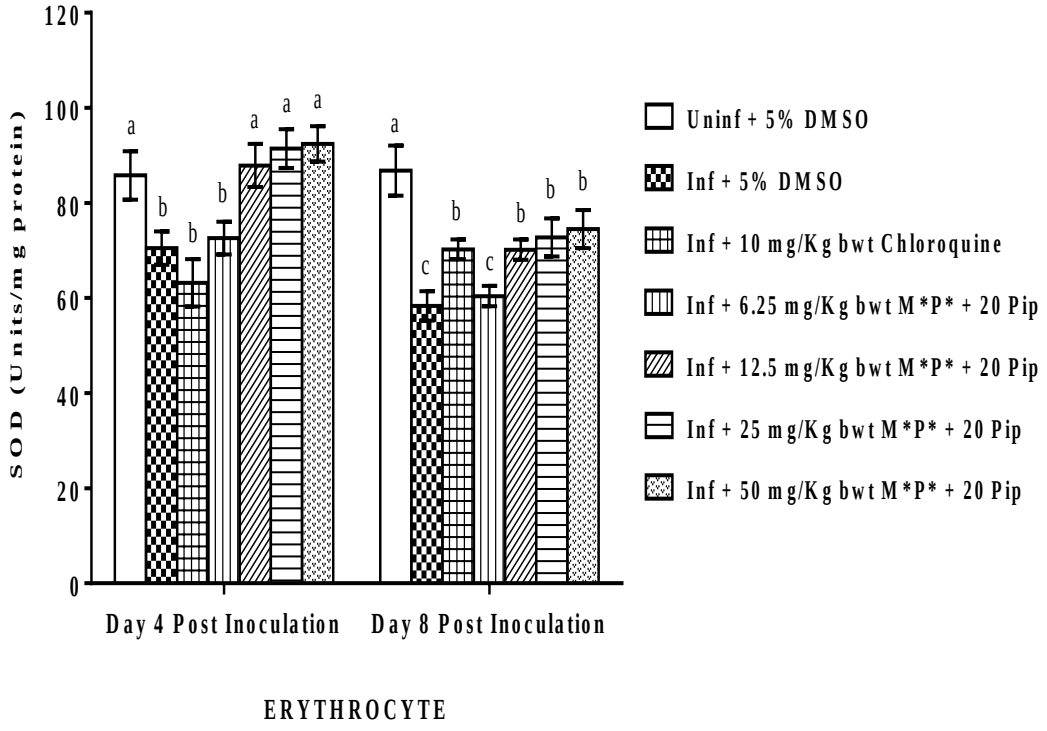

Figure 44: Effects of methyl gallate and palmatine combination in the presence of piperine on superoxide dismutase activity in the erythrocyte of *P. berghei* NK65-infected mice on days 4 and 8 post inoculation

Values are means ± SEM of 5 determinations. Bars for each day with different alphabets are significantly different ($p<0.05$). **Uninf** = Uninfected; **Inf** = infected; **DMSO** = Dimethyl sulfoxide; **bwt** = body weight; **M*P*** = 3:2 Methyl gallate and Palmatine (most active ratio from *in vitro* antimalarial study); **20 Pip** = 20 mg/Kg bwt Piperine.

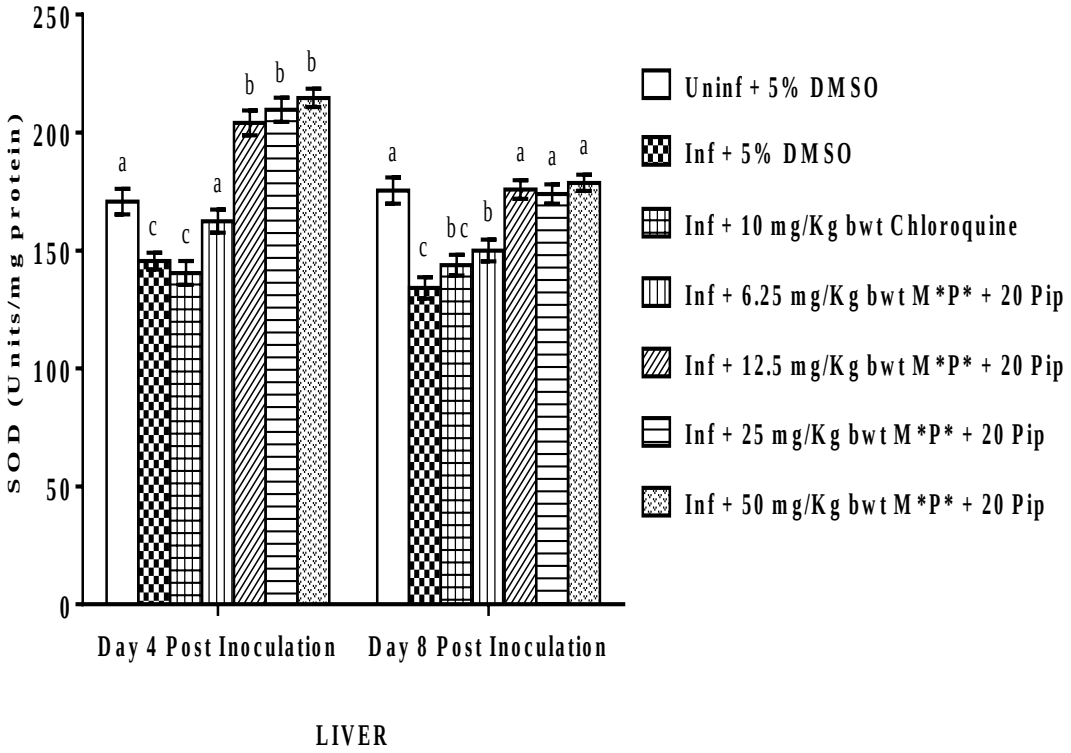

Figure 45: Effects of methyl gallate and palmatine combination in the presence of piperine on superoxide dismutase activity in the liver of *P. berghei* NK65-infected mice on days 4 and 8 post inoculation

Values are means ± SEM of 5 determinations. Bars for each day with different alphabets are significantly different ($p<0.05$). **Uninf** = Uninfected; **Inf** = infected; **DMSO** = Dimethyl sulfoxide; **bwt** = body weight; **M*P*** = 3:2 Methyl gallate and Palmatine (most active ratio from *in vitro* antimalarial study); **20 Pip** = 20 mg/Kg bwt Piperine

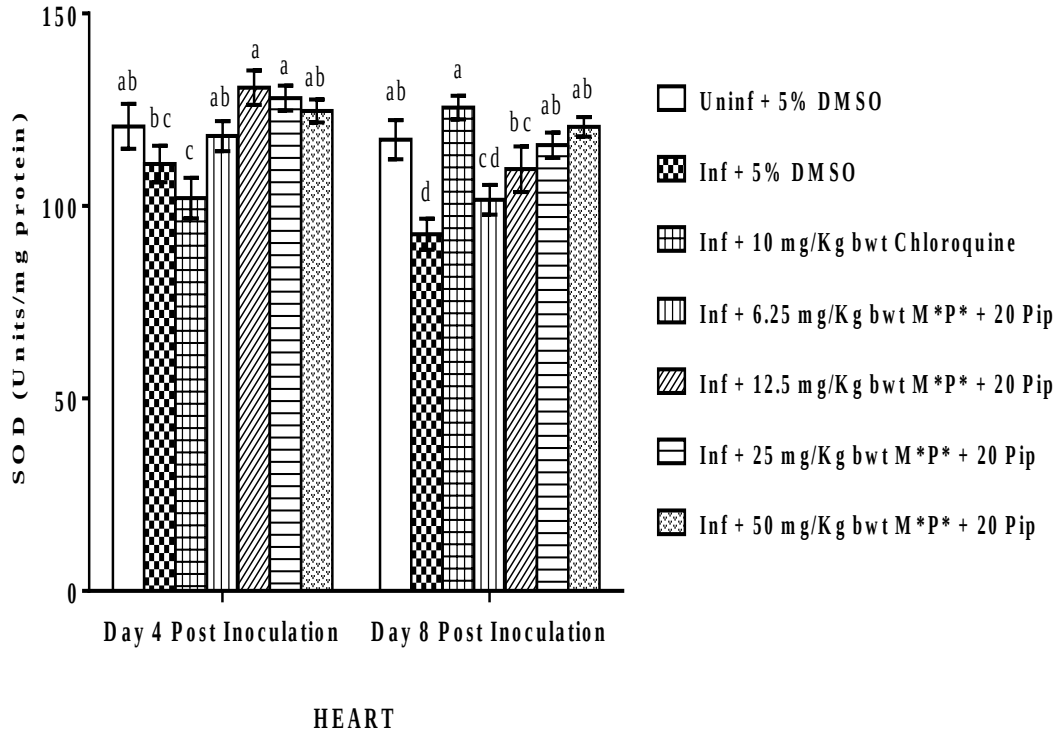

Figure 46: Effects of methyl gallate and palmatine combination in the presence of piperine on superoxide dismutase activity in the heart of *P. berghei* NK65-infected mice on days 4 and 8 post inoculation

Values are means ± SEM of 5 determinations. Bars for each day with different alphabets are significantly different ($p<0.05$). **Uninf** = Uninfected; **Inf** = infected; **DMSO** = Dimethyl sulfoxide; **bwt** = body weight; **M*P*** = 3:2 Methyl gallate and Palmatine (most active ratio from *in vitro* antimalarial study); **20 Pip** = 20 mg/Kg bwt Piperine

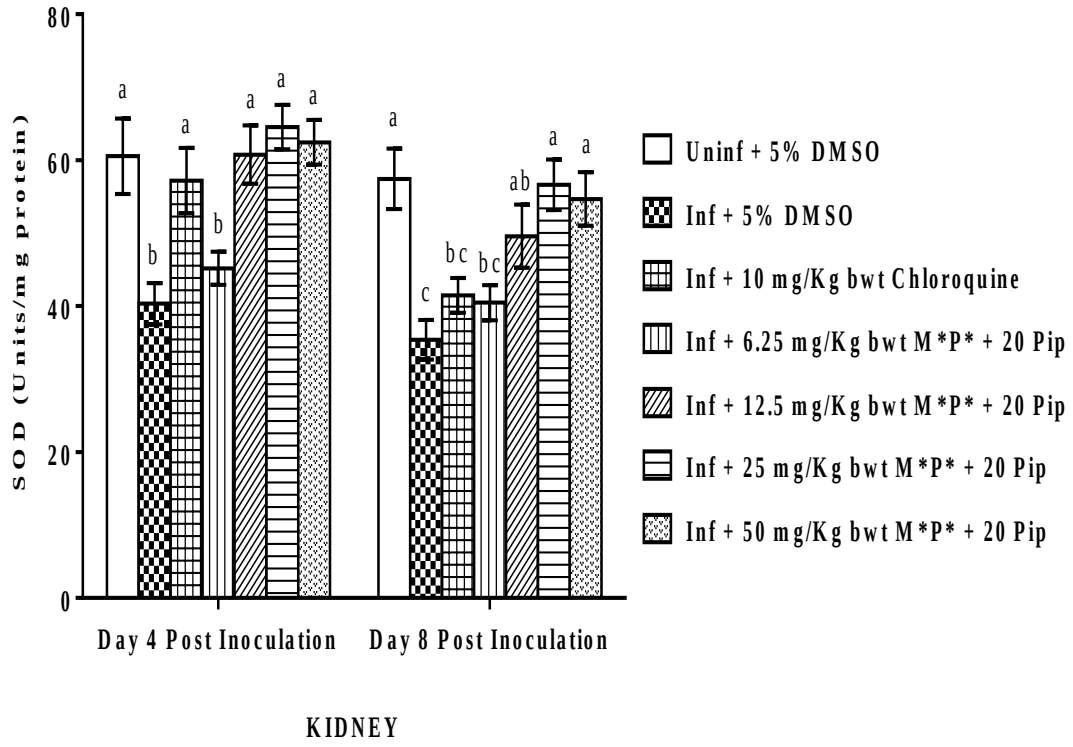

Figure 47: Effects of methyl gallate and palmatine combination in the presence of piperine on superoxide dismutase activity in the kidney of *P. berghei* NK65-infected mice on days 4 and 8 post inoculation

Values are means ± SEM of 5 determinations. Bars for each day with different alphabets are significantly different ($p<0.05$). **Uninf** = Uninfected; **Inf** = infected; **DMSO** = Dimethyl sulfoxide; **bwt** = body weight; **M*P*** = 3:2 Methyl gallate and Palmatine (most active ratio from *in vitro* antimalarial study); **20 Pip** = 20 mg/Kg bwt Piperine

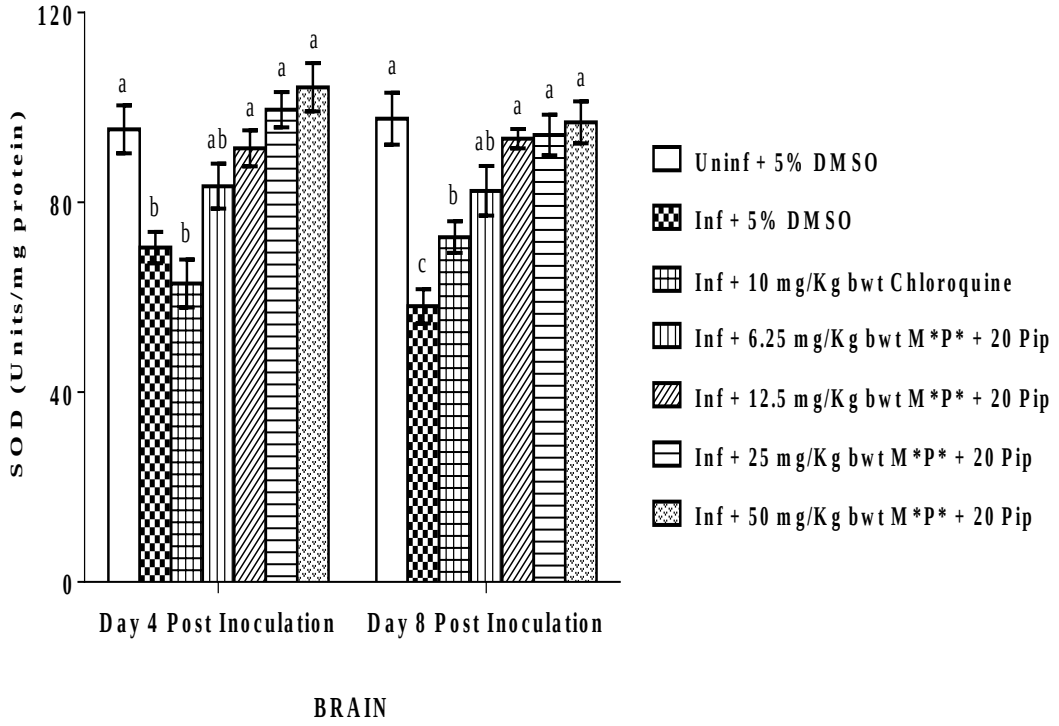

Figure 48: Effects of methyl gallate and palmatine combination in the presence of piperine on superoxide dismutase activity in the brain of *P. berghei* NK65-infected mice on days 4 and 8 post inoculation

Values are means ± SEM of 5 determinations. Bars for each day with different alphabets are significantly different ($p<0.05$). **Uninf** = Uninfected; **Inf** = infected; **DMSO** = Dimethyl sulfoxide; **bwt** = body weight; **M*P*** = 3:2 Methyl gallate and Palmatine (most active ratio from *in vitro* antimalarial study); **20 Pip** = 20 mg/Kg bwt Piperine

4.3.2.3 Catalase Activity

The activities of catalase (CAT) in the erythrocyte, liver, kidney and brain on days 4 and 8 post-inoculation were significantly reduced ($p<0.05$) in the untreated infected controls compared to the uninfected controls. However, heart CAT activity was not significantly changed ($p>0.05$) on day 4 post-inoculation but was significantly reduced ($p<0.05$) on day 8 post-inoculation in the untreated infected controls compared to the uninfected controls (Figures 49-53).

Treatment with bio-enhanced combination of methyl gallate and palmatine at doses above 6.25 mg/kg body weight significantly reverted ($p< 0.05$) the reduction in CAT activities in the tissues and erythrocyte caused by the infection on days 4 and 8 post-inoculation to the range of uninfected controls in most cases and even above the range in some cases (Figures 49-53). At all doses administered, the bio-enhanced compound combination was able to significantly revert ($p< 0.05$) the reduction in CAT activity in the brain caused by the infection to the range of unifected controls (Fig. 53).

Also, the bio-enhanced combination of methyl gallate and palmatine at doses higher than 12.5 mg/kg body weight was more potent in significantly reverting ($p< 0.05$) the reduction in CAT activities in erythrocyte and tissues caused by the infection to the range of the uninfected controls and above the range in some cases compared to chloroquine (Figures 49-53).

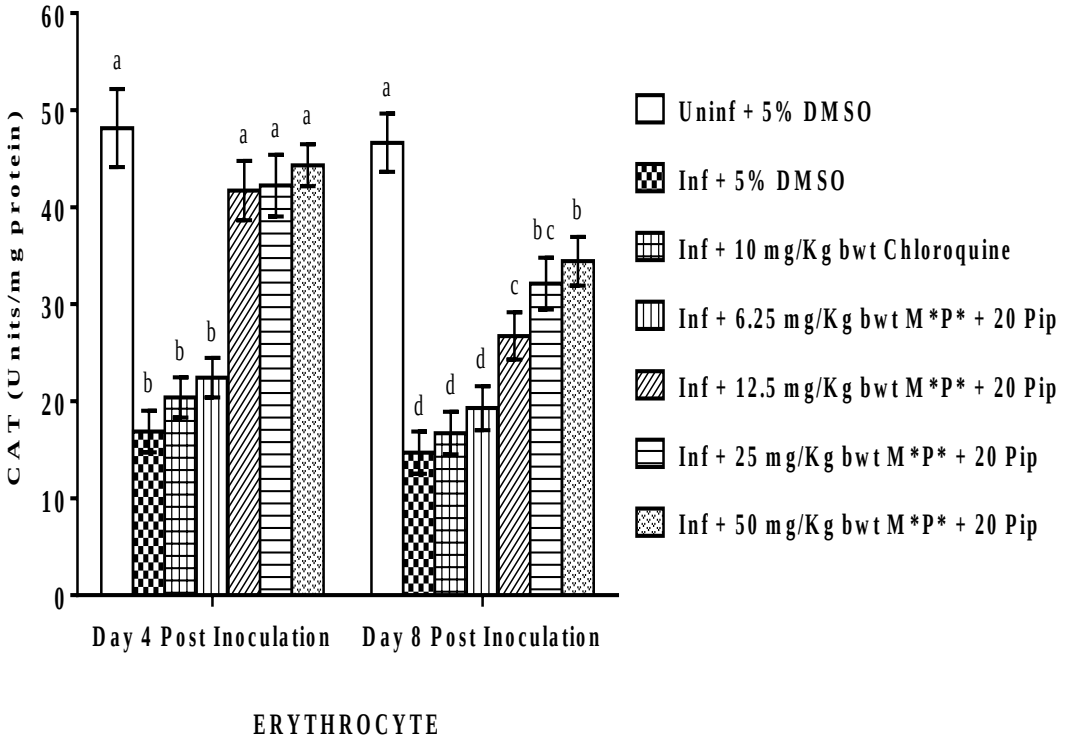

Figure 49: Effects of methyl gallate and palmatine combination in the presence of piperine on catalase activity in the erythrocyte of *P. berghei* NK65-infected mice on days 4 and 8 post-inoculation

Values are means ± SEM of 5 determinations. Bars for each day with different alphabets are significantly different ($p<0.05$). **Uninf** = Uninfected; **Inf** = infected; **DMSO** = Dimethyl sulfoxide; **bwt** = body weight; **M*P*** = 3:2 Methyl gallate and Palmatine (most active ratio from *in vitro* antimalarial study); **20 Pip** = 20 mg/Kg bwt Piperine

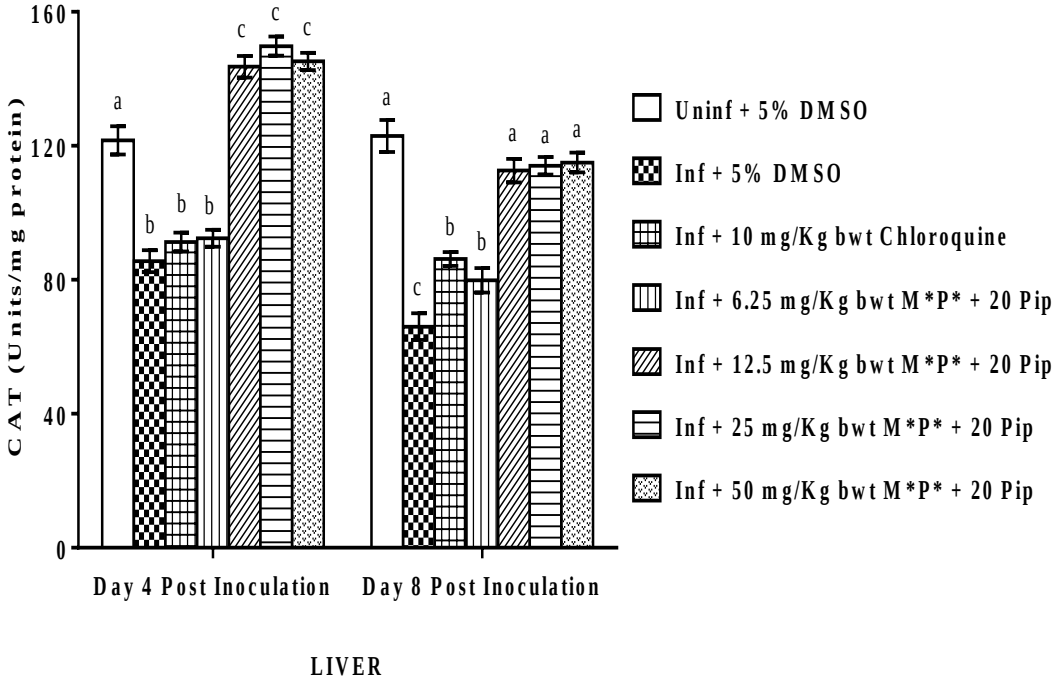

Figure 50: Effects of methyl gallate and palmatine combination in the presence of piperine on catalase activity in the liver of *P. berghei* NK65-infected mice on days 4 and 8 post inoculation

Values are means ± SEM of 5 determinations. Bars for each day with different alphabets are significantly different ($p<0.05$). **Uninf** = Uninfected; **Inf** = infected; **DMSO** = Dimethyl sulfoxide; **bwt** = body weight; **M*P*** = 3:2 Methyl gallate and Palmatine (most active ratio from *in vitro* antimalarial study); **20 Pip** = 20 mg/Kg bwt Piperine

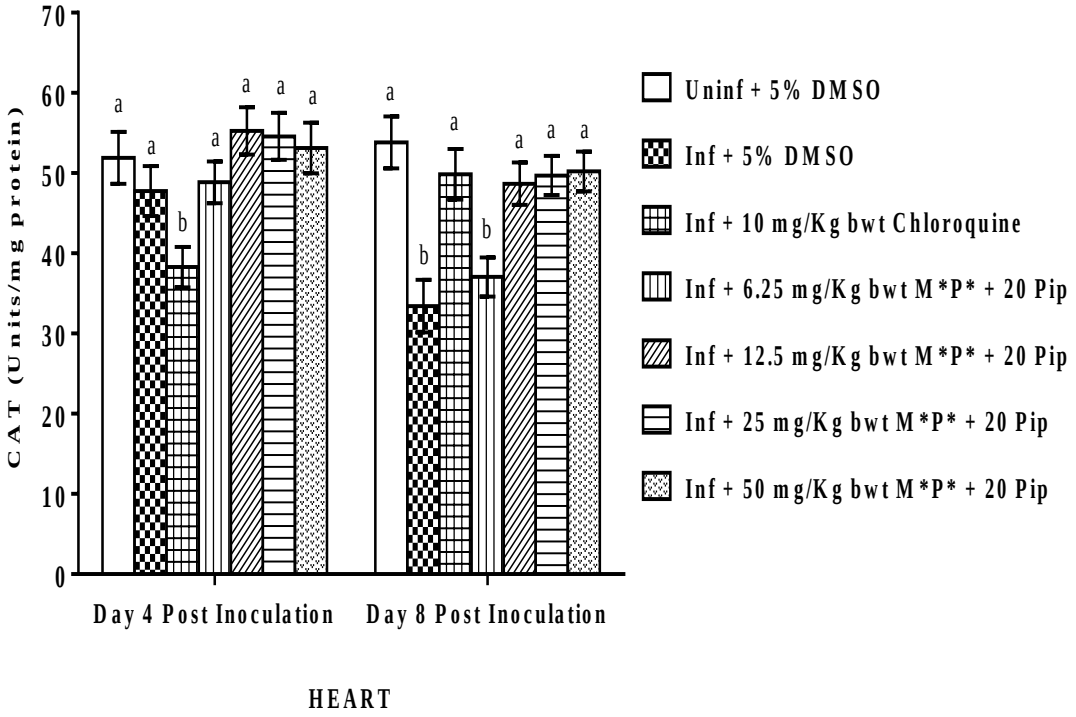

Figure 51: Effects of methyl gallate and palmatine combination in the presence of piperine on catalase activity in the heart of *P. berghei* NK65-infected mice on days 4 and 8 post inoculation

Values are means ± SEM of 5 determinations. Bars for each day with different alphabets are significantly different ($p<0.05$). **Uninf** = Uninfected; **Inf** = infected; **DMSO** = Dimethyl sulfoxide; **bwt** = body weight; **M*P*** = 3:2 Methyl gallate and Palmatine (most active ratio from *in vitro* antimalarial study); **20 Pip** = 20 mg/Kg bwt Piperine

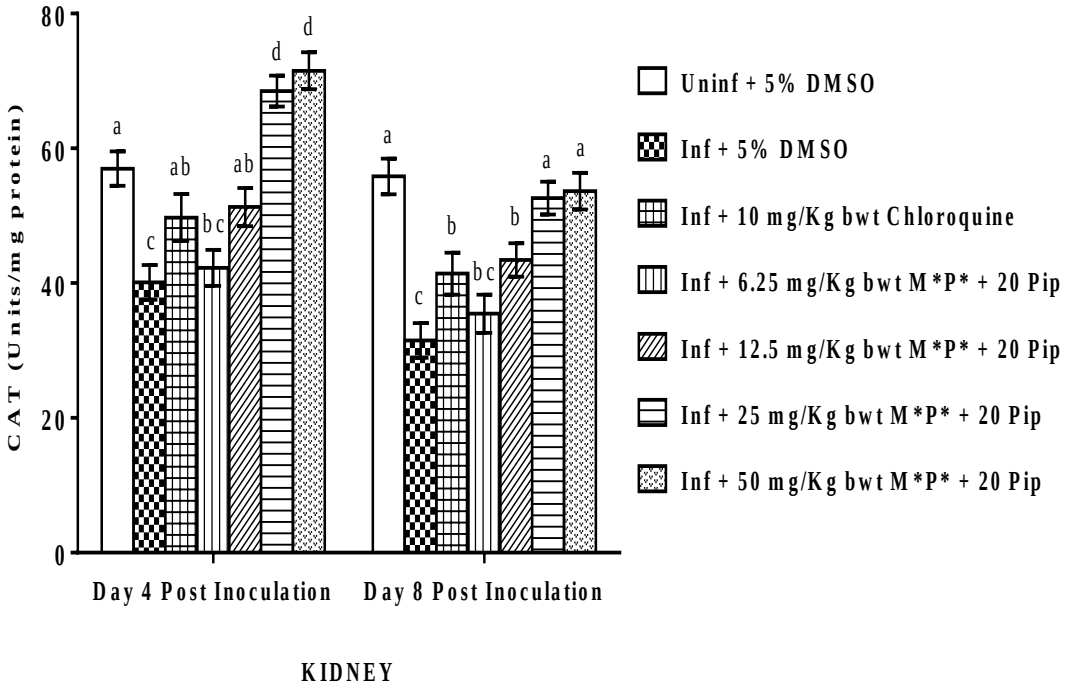

KIDNEY

Figure 52: Effects of methyl gallate and palmatine combination in the presence of piperine on catalase activity in the kidney of *P. berghei* NK65-infected mice on days 4 and 8 post inoculation

Values are means ± SEM of 5 determinations. Bars for each day with different alphabets are significantly different ($p<0.05$). **Uninf** = Uninfected; **Inf** = infected; **DMSO** = Dimethyl sulfoxide; **bwt** = body weight; **M*P*** = 3:2 Methyl gallate and Palmatine (most active ratio from *in vitro* antimalarial study); **20 Pip** = 20 mg/Kg bwt Piperine

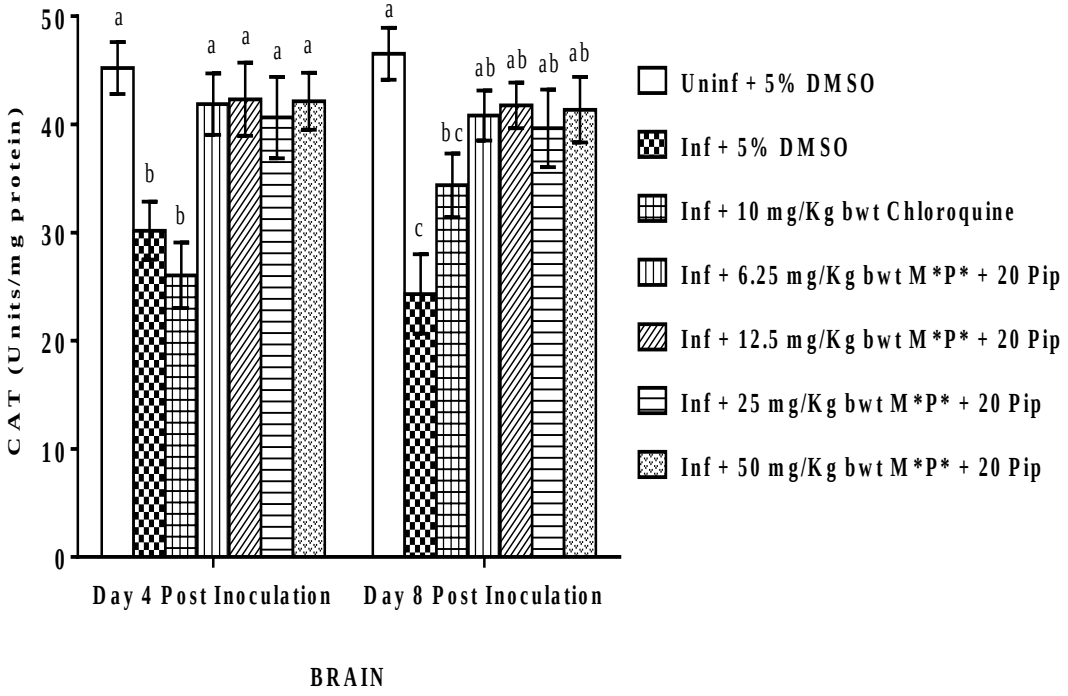

Figure 53: Effects of methyl gallate and palmatine combination in the presence of piperine on catalase activity in the brain of *P. berghei* NK65-infected mice on days 4 and 8 post inoculation

Values are means ± SEM of 5 determinations. Bars for each day with different alphabets are significantly different ($p<0.05$). **Uninf** = Uninfected; **Inf** = infected; **DMSO** = Dimethyl sulfoxide; **bwt** = body weight; **M*P*** = 3:2 Methyl gallate and Palmatine (most active ratio from *in vitro* antimalarial study); **20 Pip** = 20 mg/Kg bwt Piperine

4.3.2.4 Glutathione Peroxidase Activity

Plasmodium berghei NK65 infection in mice brought about significant decrease ($p<0.05$) in glutathione peroxidase (GPx) activities in the erythrocyte, liver, heart, kidney and brain on days 4 and 8 post-inoculation compared to the uninfected control, except the activities of GPx in the heart and brain on day 4 post-inoculation, which were not significantly altered ($p>0.05$) (Figures 54-58).

Treatment with bio-enhanced combination of methyl gallate and palmatine at doses higher than 6.25 mg/Kg body weight caused significant increase ($p<0.05$) in glutathione peroxidase activities in the various tissues studied compared to untreated infected controls on days 4 and 8 post-inoculation, except that heart and brain GPx activities on day 4 post-inoculation were not significant changed ($p>0.05$) at all doses administered compared to untreated infected controls (Figures 54-58). These treatments, especially at doses higher than 12.5 mg/kg body weight, caused no significant alteration ($p>0.05$) in glutathione peroxidase activities in all tissues studied on days 4 and 8 post-inoculation compared to those of uninfected controls (Figures 54-58).

Also, treatment with doses above 6.25 mg/Kg body weight of bio-enhanced combination of methyl gallate and palmatine caused significant increase ($p<0.05$) in glutathione peroxidase activities of the erythrocyte, liver and heart while those of the kidney and brain were not significantly changed ($p>0.05$) on day 4 post-inoculation compared to those of chloroquine-treated group. On day 8 post-inoculation, the compound combination caused significant increase ($p<0.05$) in glutathione peroxidase activities in the liver and kidney at doses above 12.5 mg/kg body weight compared to those of chloroquine-treated group (Figures 54-58).

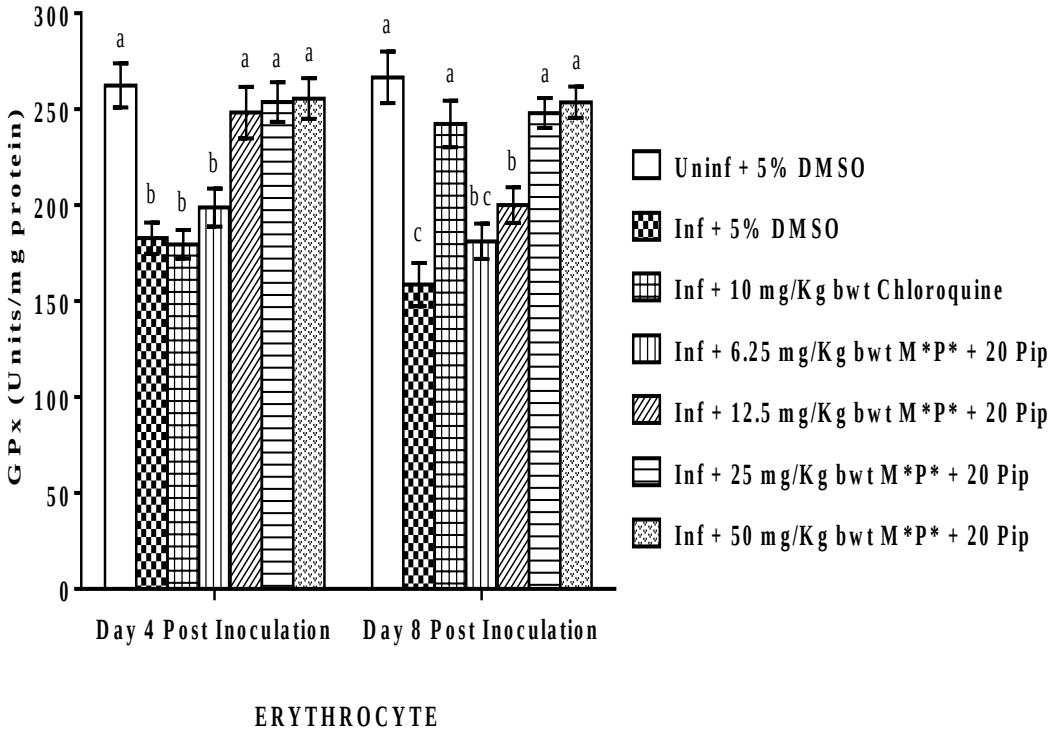

Figure 54: Effects of methyl gallate and palmatine combination in the presence of piperine on glutathione peroxidase activity in the erythrocyte of *P. berghei* NK65-infected mice on days 4 and 8 post-inoculation

Values are means ± SEM of 5 determinations. Bars for each day with different alphabets are significantly different ($p<0.05$). **Uninf** = Uninfected; **Inf** = infected; **DMSO** = Dimethyl sulfoxide; **bwt** = body weight; **M*P*** = 3:2 Methyl gallate and Palmatine (most active ratio from *in vitro* antimalarial study); **20 Pip** = 20 mg/Kg bwt Piperine.

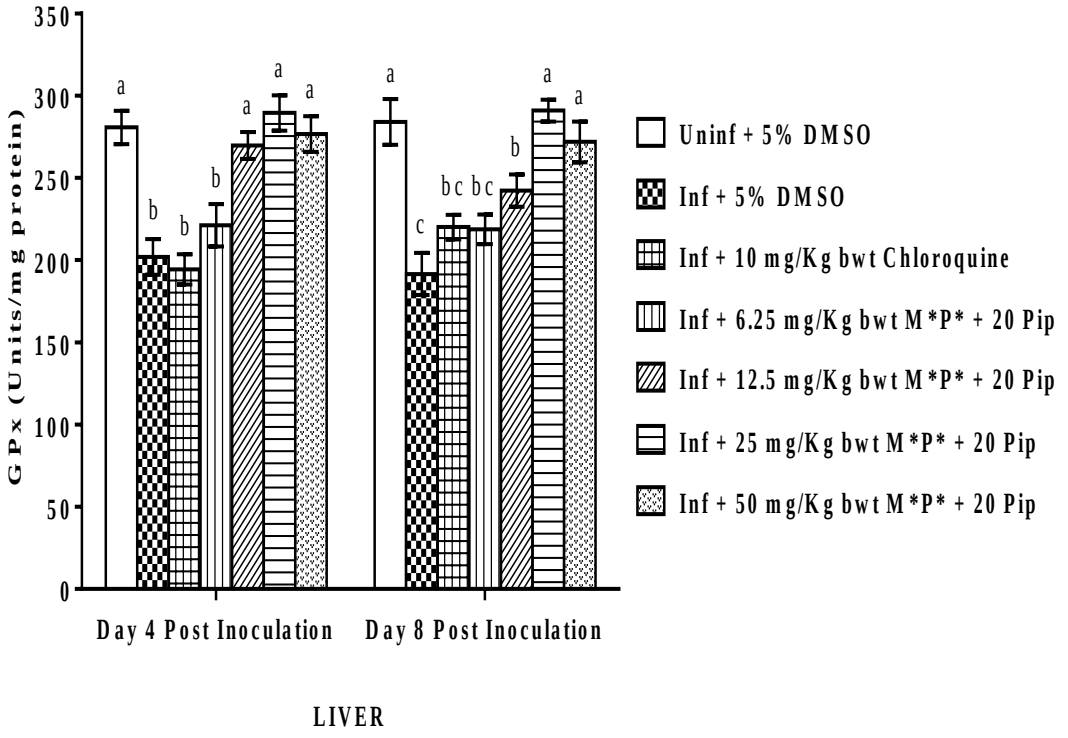

Figure 55: Effects of methyl gallate and palmatine combination in the presence of piperine on glutathione peroxidase activity in the liver of *P. berghei* NK65-infected mice on days 4 and 8 post inoculation

Values are means ± SEM of 5 determinations. Bars for each day with different alphabets are significantly different ($p<0.05$). **Uninf** = Uninfected; **Inf** = infected; **DMSO** = Dimethyl sulfoxide; **bwt** = body weight; **M*P*** = 3:2 Methyl gallate and Palmatine (most active ratio from *in vitro* antimalarial study); **20 Pip** = 20 mg/Kg bwt Piperine

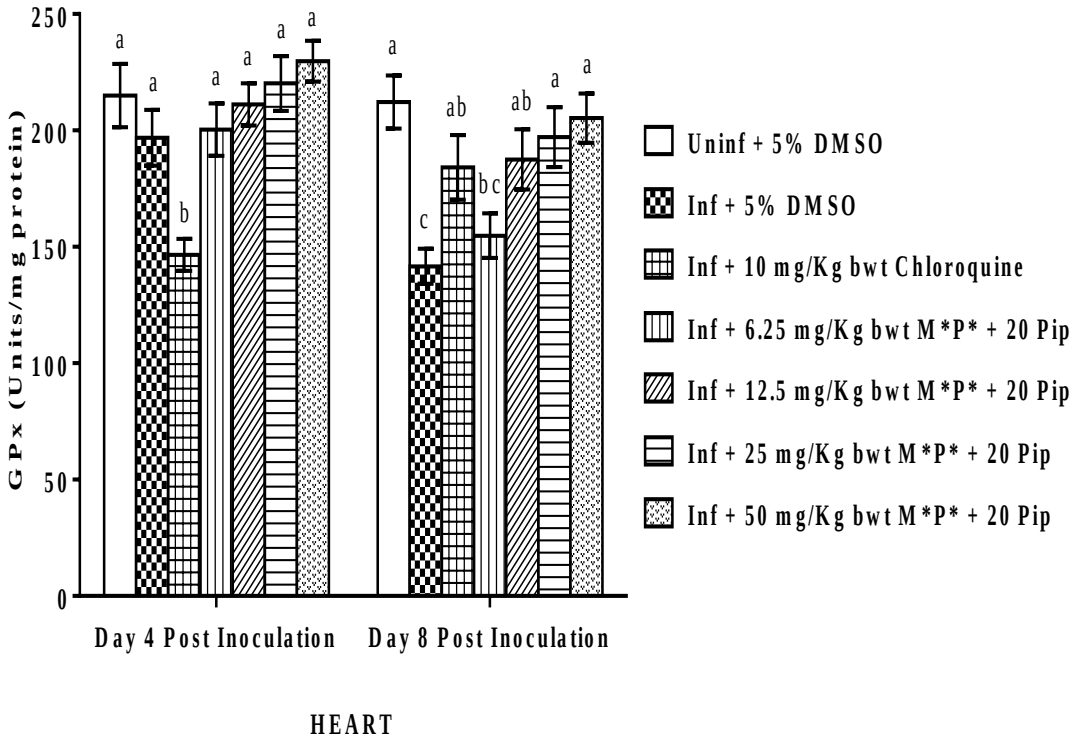

Figure 56: Effects of methyl gallate and palmatine combination in the presence of piperine on glutathione peroxidase activity in the heart of *P. berghei* NK65-infected mice on days 4 and 8 post inoculation

Values are means ± SEM of 5 determinations. Bars for each day with different alphabets are significantly different ($p<0.05$). **Uninf** = Uninfected; **Inf** = infected; **DMSO** = Dimethyl sulfoxide; **bwt** = body weight; **M*P*** = 3:2 Methyl gallate and Palmatine (most active ratio from *in vitro* antimalarial study); **20 Pip** = 20 mg/Kg bwt Piperine.

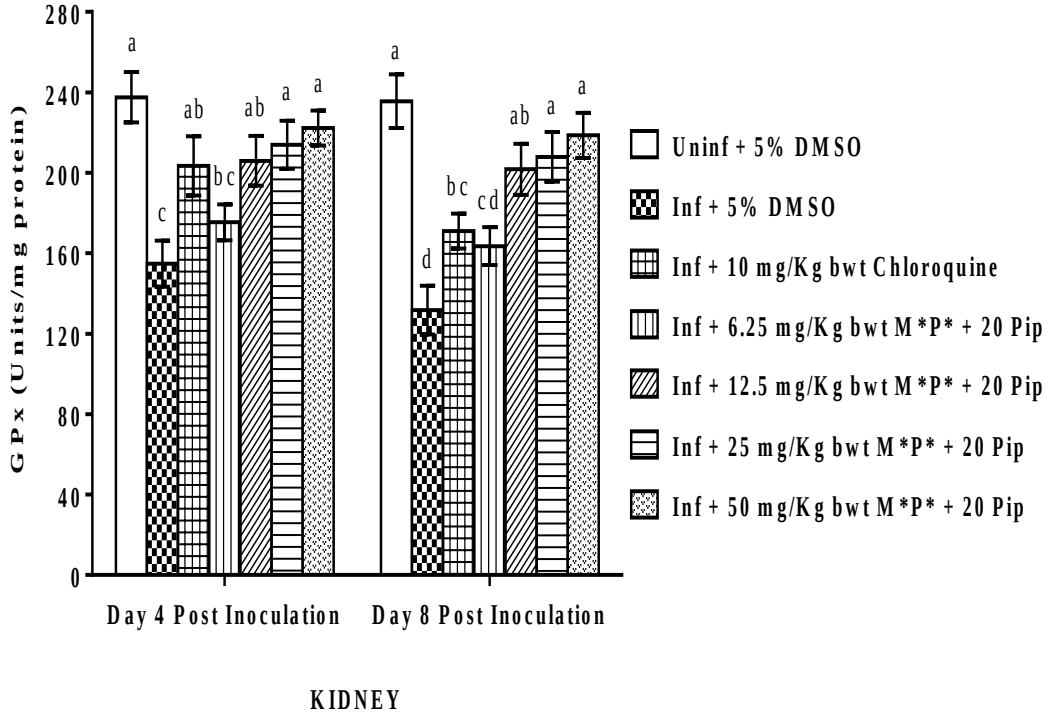

Figure 57: Effects of methyl gallate and palmatine combination in the presence of piperine on glutathione peroxidase activity in the kidney of *P. berghei* NK65-infected mice on days 4 and 8 post inoculation

Values are means ± SEM of 5 determinations. Bars for each day with different alphabets are significantly different ($p<0.05$). **Uninf** = Uninfected; **Inf** = infected; **DMSO** = Dimethyl sulfoxide; **bwt** = body weight; **M*P*** = 3:2 Methyl gallate and Palmatine (most active ratio from *in vitro* antimalarial study); **20 Pip** = 20 mg/Kg bwt Piperine.

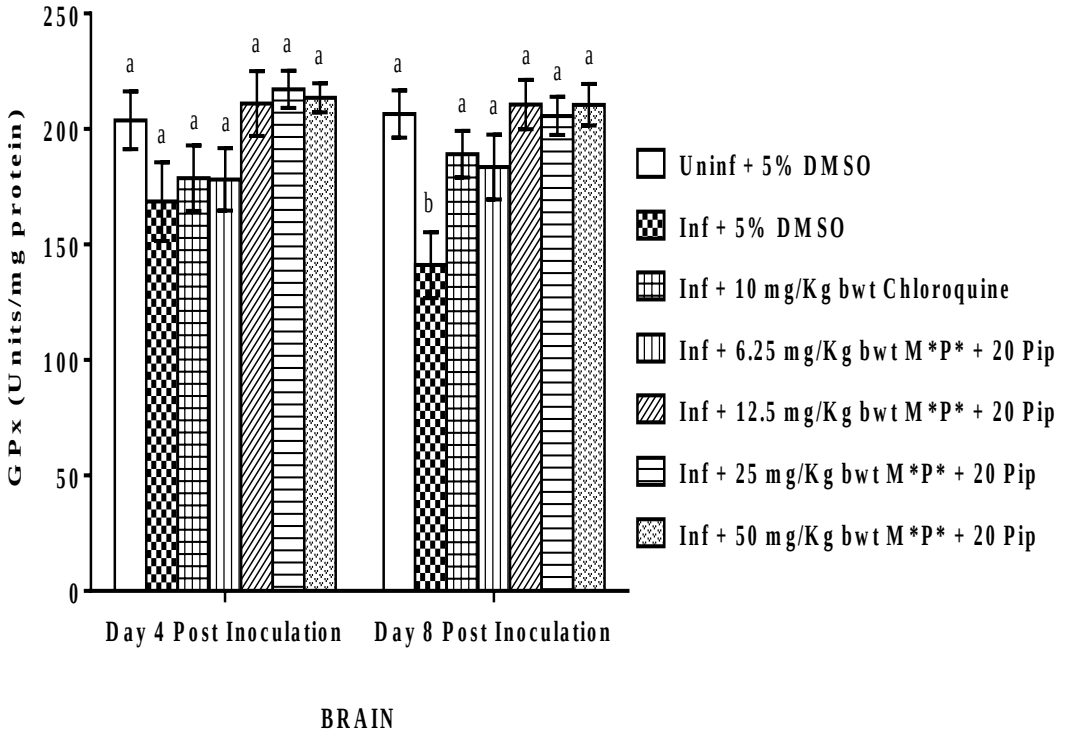

Figure 58: Effects of methyl gallate and palmatine combination in the presence of piperine on glutathione peroxidase activity in the brain of *P. berghei* NK65-infected mice on days 4 and 8 post inoculation

Values are means ± SEM of 5 determinations. Bars for each day with different alphabets are significantly different ($p<0.05$). **Uninf** = Uninfected; **Inf** = infected; **DMSO** = Dimethyl sulfoxide; **bwt** = body weight; **M*P*** = 3:2 Methyl gallate and Palmatine (most active ratio from *in vitro* antimalarial study); **20 Pip** = 20 mg/Kg bwt Piperine

4.3.2.5 Glutathione Reductase Activity

There was significant reduction ($p<0.05$) in glutathione reductase (GR) activities on days 4 and 8 post-inoculation in erythrocyte and various tissues of infected mice compared to uninfected controls, except for the heart and brain on day 4 post-inoculation, in which glutathione reductase activities were not significantly altered ($p>0.05$) (Figures 59-63).

Treatment with bio-enhanced methyl gallate and palmatine combination at doses higher than 6.25 mg/Kg body weight caused significant increase ($p<0.05$) in glutathione reductase activities in the erythrocyte and tissues studied compared to untreated infected controls on days 4 and 8 post-inoculation, except that GR activities in the heart and brain were not significantly changed ($p>0.05$) on day 4 post-inoculation (Figures 59-63).

At doses of 25 and 50 mg/Kg body weight, the bio-enhanced compound combination caused no significant change ($p>0.05$) in glutathione reductase activities in the various tissues studied on days 4 and 8 post-inoculation compared to uninfected controls, except kidney GR activity which was significantly increased ($p< 0.05$) on day 8 post-inoculation (Figures 59-63). Also, treatment with 25 and 50 mg/kg body weight of the bio-enhanced compound combination caused significant increase ($p< 0.05$) in glutathione reductase activities of erythrocyte, liver and heart on day 4 post-inoculation while on day 8 post-inoculation, it led to significant increase ($p<0.05$) in glutathione reductase activities in the erythrocyte, liver, brain and kidney compared to those of chloroquine-treated mice (Figures 59-63).

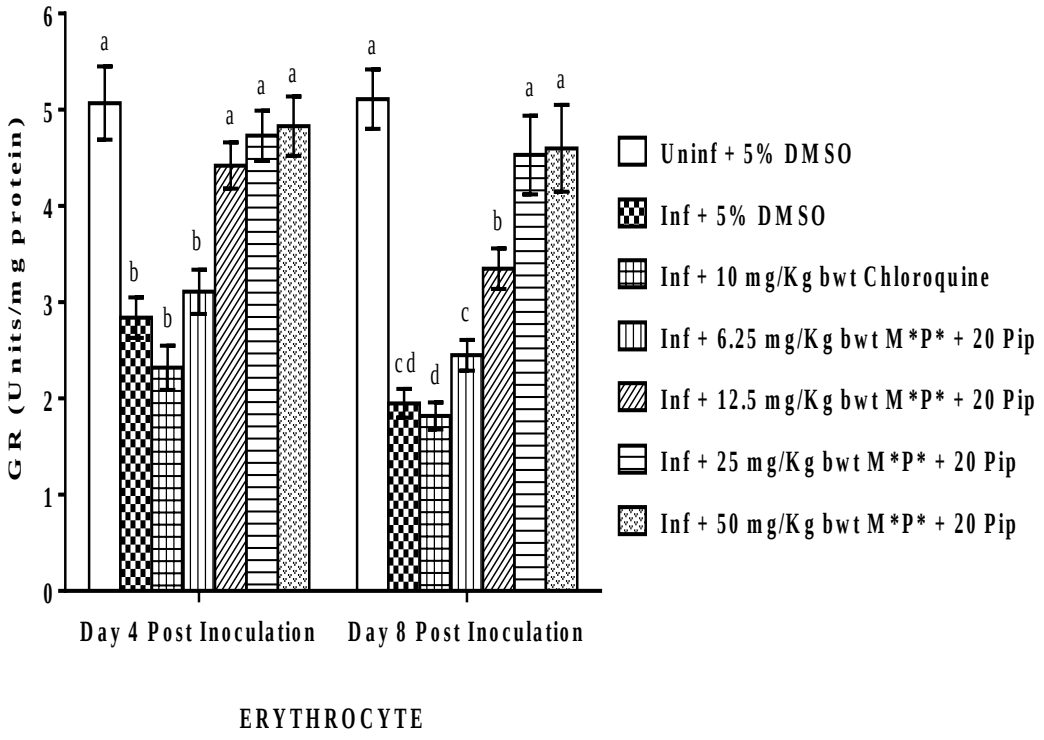

Figure 59: Effects of methyl gallate and palmatine combination in the presence piperine on glutathione reductase activity in the erythrocyte of *P. berghei* NK65-infected mice on days 4 and 8 post inoculation

Values are means ± SEM of 5 determinations. Bars for each day with different alphabets are significantly different ($p<0.05$). **Uninf** = Uninfected; **Inf** = infected; **DMSO** = Dimethyl sulfoxide; **bwt** = body weight; **M*P*** = 3:2 Methyl gallate and Palmatine (most active ratio from *in vitro* antimalarial study); **20 Pip** = 20 mg/Kg bwt Piperine.

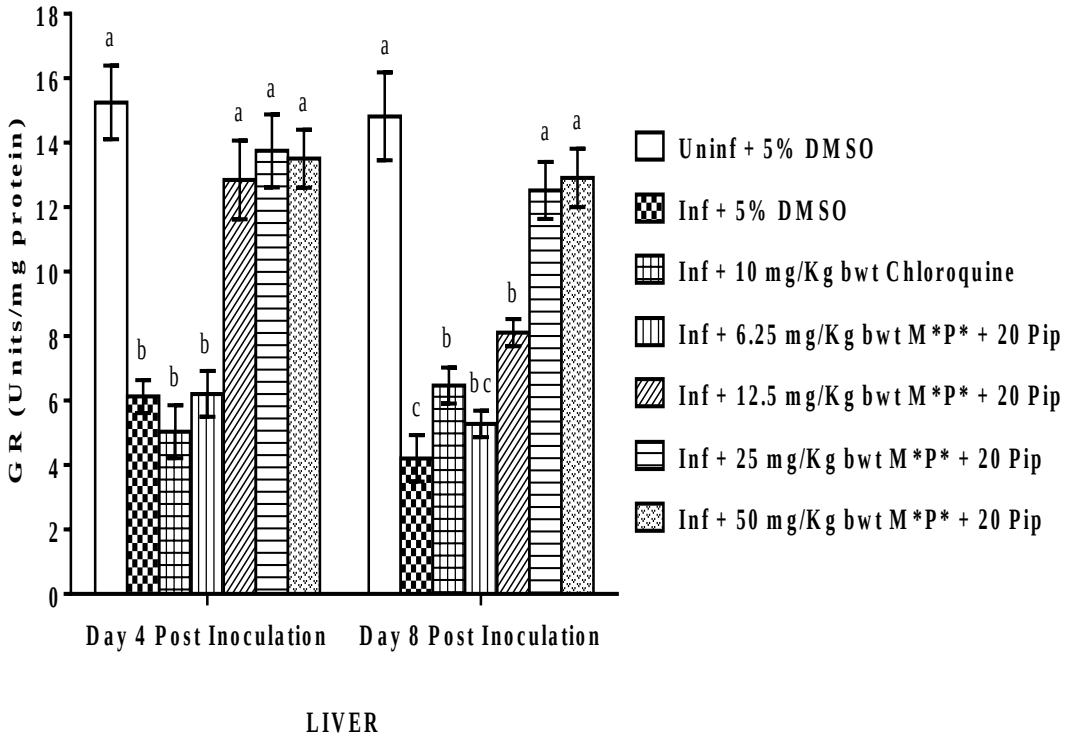

LIVER

Figure 60: Effects of methyl gallate and palmatine combination in the presence piperine on glutathione reductase activity in the liver of *P. berghei* NK65-infected mice on days 4 and 8 post inoculation

Values are means ± SEM of 5 determinations. Bars for each day with different alphabets are significantly different ($p<0.05$). **Uninf** = Uninfected; **Inf** = infected; **DMSO** = Dimethyl sulfoxide; **bwt** = body weight; **M*P*** = 3:2 Methyl gallate and Palmatine (most active ratio from *in vitro* antimalarial study); **20 Pip** = 20 mg/Kg bwt Piperine.

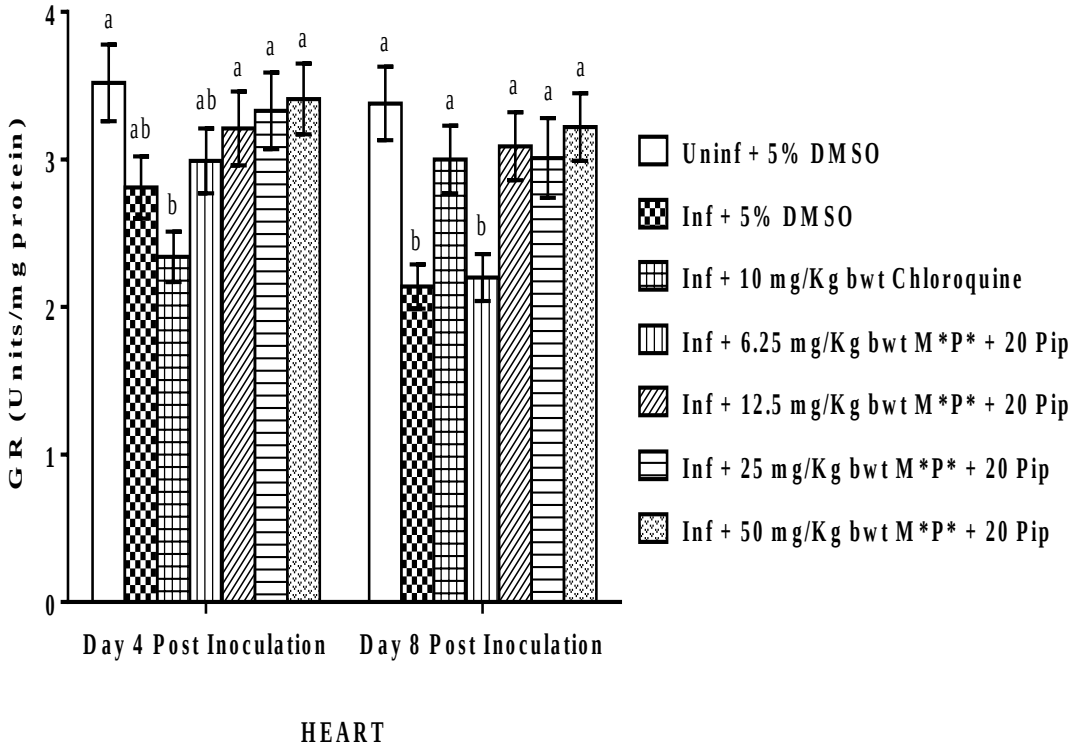

Figure 61: Effects of methyl gallate and palmatine combination in the presence piperine on glutathione reductase activity in the heart of *P. berghei* NK65-infected mice on days 4 and 8 post inoculation

Values are means ± SEM of 5 determinations. Bars for each day with different alphabets are significantly different ($p<0.05$). **Uninf** = Uninfected; **Inf** = infected; **DMSO** = Dimethyl sulfoxide; **bwt** = body weight; **M*P*** = 3:2 Methyl gallate and Palmatine (most active ratio from *in vitro* antimalarial study); **20 Pip** = 20 mg/Kg bwt Piperine.

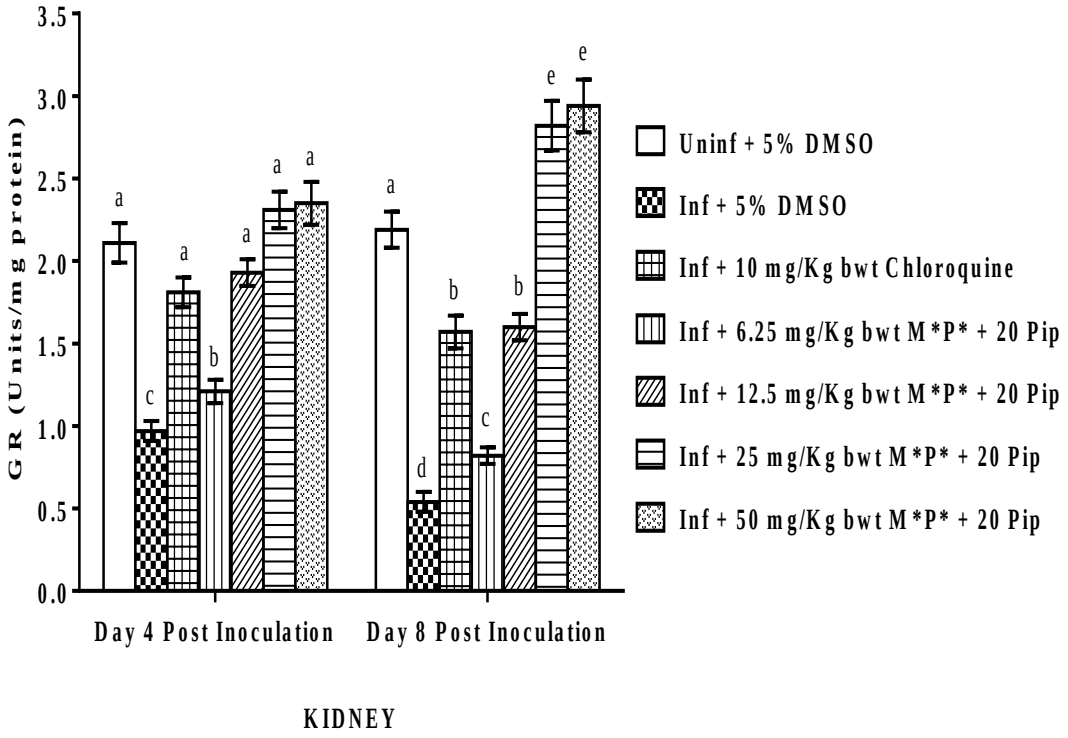

Figure 62: Effects of methyl gallate and palmatine combination in the presence piperine on glutathione reductase activity in the kidney of *P. berghei* NK65-infected mice on days 4 and 8 post inoculation

Values are means ± SEM of 5 determinations. Bars for each day with different alphabets are significantly different ($p<0.05$). **Uninf** = Uninfected; **Inf** = infected; **DMSO** = Dimethyl sulfoxide; **bwt** = body weight; **M*P*** = 3:2 Methyl gallate and Palmatine (most active ratio from *in vitro* antimalarial study); **20 Pip** = 20 mg/Kg bwt Piperine.

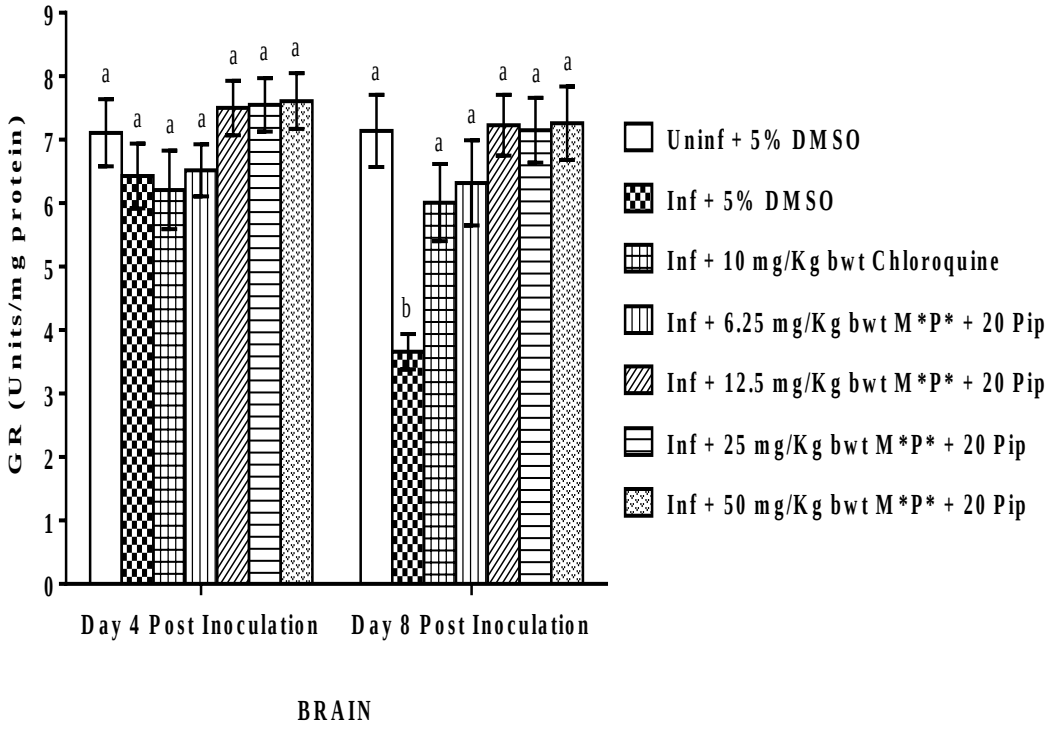

Figure 63: Effects of methyl gallate and palmatine combination in the presence piperine on glutathione reductase activity in the brain of *P. berghei* NK65-infected mice on days 4 and 8 post inoculation

Values are means ± SEM of 5 determinations. Bars for each day with different alphabets are significantly different ($p<0.05$). **Uninf** = Uninfected; **Inf** = infected; **DMSO** = Dimethyl sulfoxide; **bwt** = body weight; **M*P*** = 3:2 Methyl gallate and Palmatine (most active ratio from *in vitro* antimalarial study); **20 Pip** = 20 mg/Kg bwt Piperine.

4.3.2.6 Reduced Glutathione Concentration

P. berghei NK65 infection led to significant decrease ($p< 0.05$) in reduced glutathione concentration in the erythrocyte and various tissues considered on days 4 and 8 post-inoculation compared to uninfected controls, except the concentrations of reduced glutathione in the heart and brain on day 4 post-inoculation which were not significantly changed ($p>0.05$) (Figures 64-68).

Treatment of infected mice with bio-enhanced methyl gallate and palmatine combination at doses higher than 6.25 mg/Kg body weight caused significant increase ($p<0.05$) in concentrations of reduced glutathione in erythrocyte, liver and kidney on day 4 post-inoculation compared to untreated infected controls. Doses higher than 12.5 mg/kg body weight brought about significant increase ($p<0.05$) in concentrations of reduced glutathione in erythrocyte, heart and kidney compared to untreated infected controls on day 8 post-inoculation (Figures 64-68). All doses of the bio-enhanced compound combination caused significant increase ($p<0.05$) in the concentration of reduced glutathione in the brain compared to untreated infected control (Figure 68).

The bio-enhanced compound combination at doses higher than 6.25 mg/kg body weight did not significantly change ($p>0.05$) the concentrations of reduced glutathione in all tissues studied on day 4 post-inoculation compared to those of uninfected control while doses higher than 12.5 mg/kg body weight did not significantly alter ($p>0.05$) the concentrations of reduced glutathione in the erythrocyte, heart and kidney compared to uninfected controls, on day 8 post-inoculation (Figures 64-68). All doses of the bio-enhanced compound combination did not significantly alter ($p>0.05$) the concentration of reduced glutathione in the brain on day 8 post-inoculation compared to uninfected control (Figures 68).

Also, the bio-enhanced methyl gallate and palmatine combination at doses higher than 6.25 mg/kg body weight caused significant increase ($p< 0.05$) in the concentrations of reduced glutathione in the erythrocyte, liver and heart on day 4 post-inoculation compared to those of chloroquine-treated mice. The bio-enhanced compound combination at doses higher than 12.5 mg/kg body weight caused significant increase ($p<0.05$) in the concentrations of reduced glutathione in the erythrocyte and kidney on day 8 post-inoculation compared to those of the chloroquine-treated mice (Figures 64 and 67).

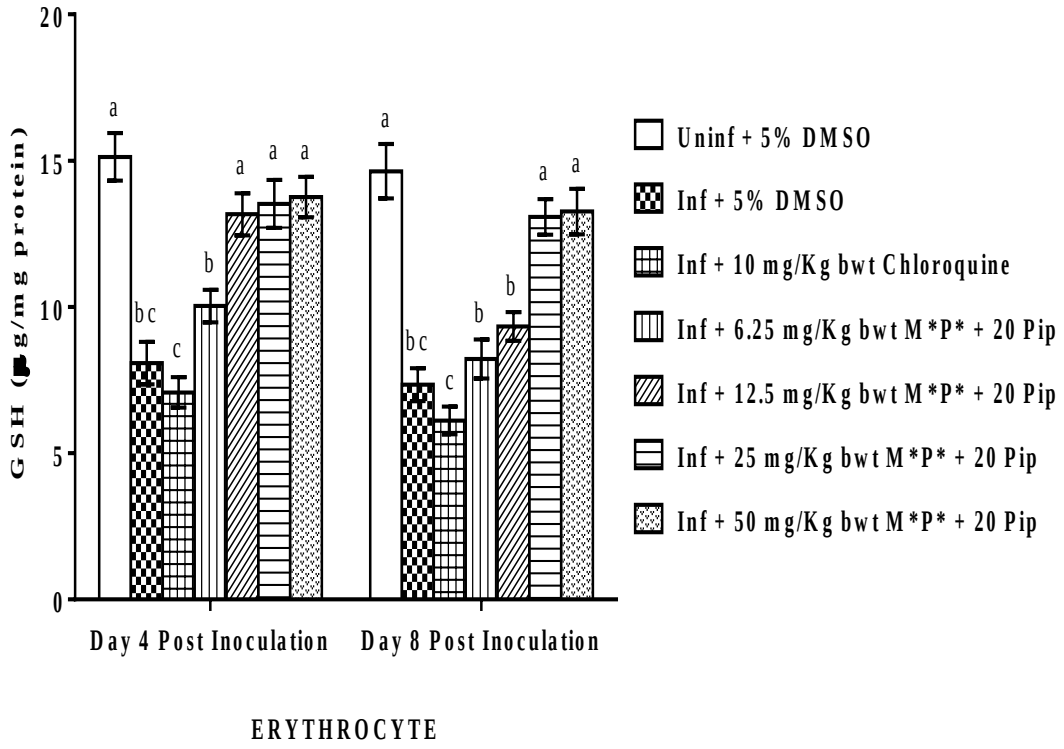

Figure 64: Effects of methyl gallate and palmatine combination in the presence of piperine on reduced glutathione concentration in the erythrocyte of *P. berghei* NK65-infected mice on days 4 and 8 post inoculation

Values are means ± SEM of 5 determinations. Bars for each day with different alphabets are significantly different ($p<0.05$). **Uninf** = Uninfected; **Inf** = infected; **DMSO** = Dimethyl sulfoxide; **bwt** = body weight; **M*P*** = 3:2 Methyl gallate and Palmatine (most active ratio from *in vitro* antimalarial study); **20 Pip** = 20 mg/Kg bwt Piperine.

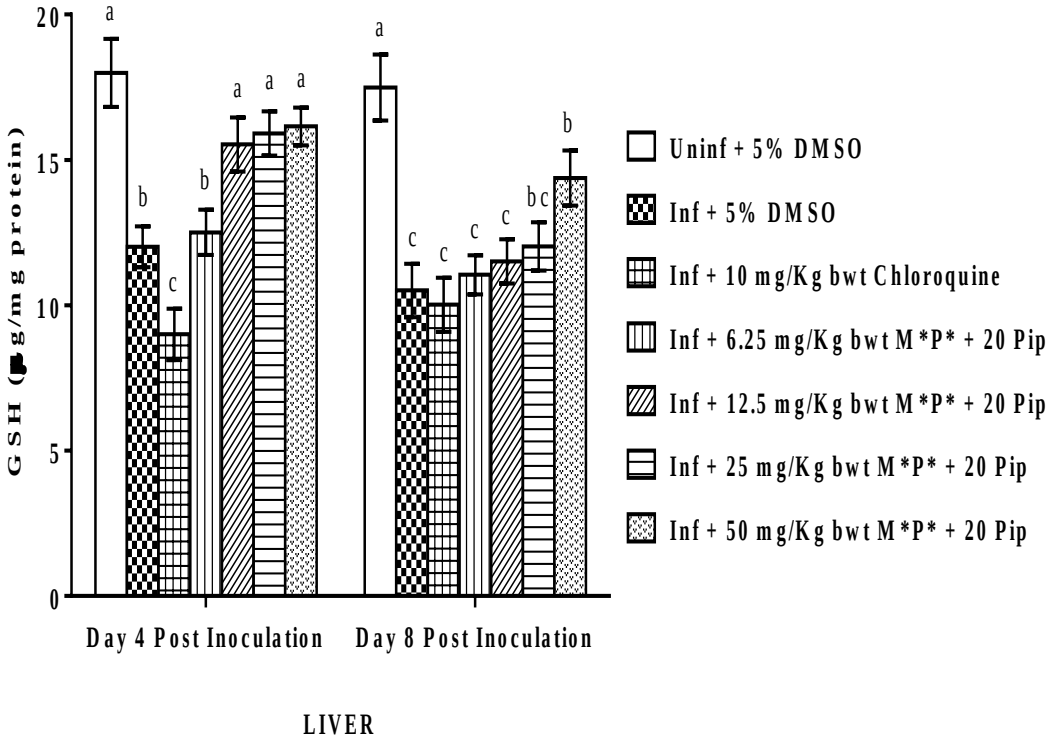

LIVER

Figure 65: Effects of methyl gallate and palmatine combination in the presence of piperine on reduced glutathione concentration in the liver of *P. berghei* NK65-infected mice on days 4 and 8 post inoculation

Values are means ± SEM of 5 determinations. Bars for each day with different alphabets are significantly different ($p<0.05$). **Uninf** = Uninfected; **Inf** = infected; **DMSO** = Dimethyl sulfoxide; **bwt** = body weight; **M*P*** = 3:2 Methyl gallate and Palmatine (most active ratio from *in vitro* antimalarial study); **20 Pip** = 20 mg/Kg bwt Piperine.

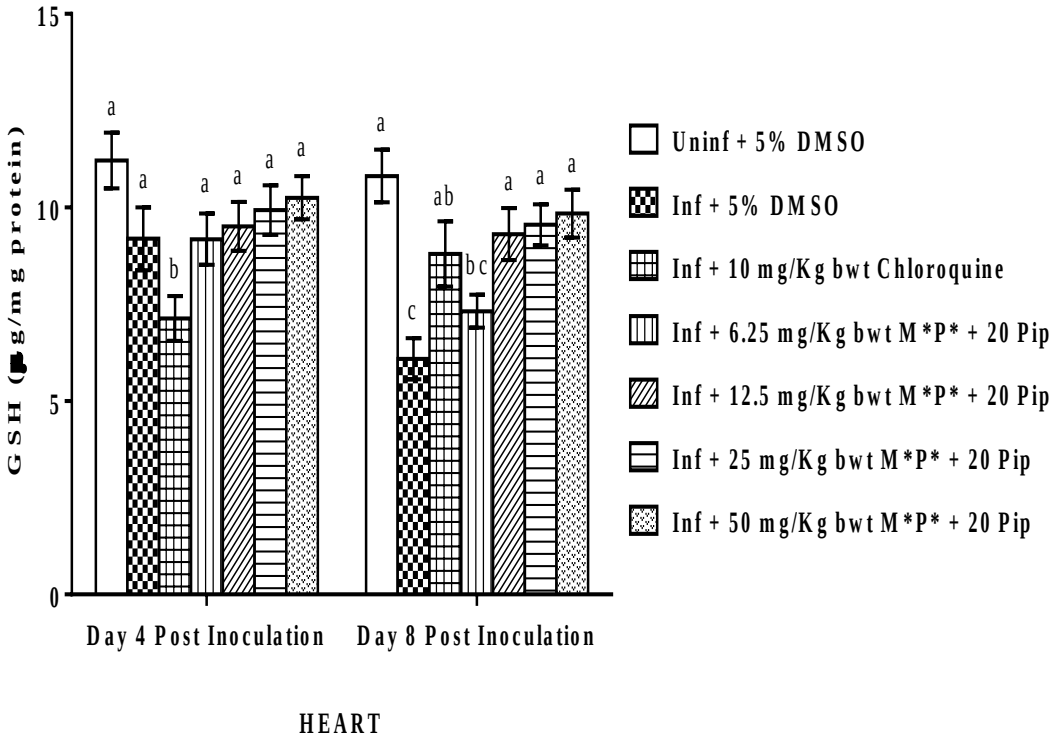

Figure 66: Effects of methyl gallate and palmatine combination in the presence of piperine on reduced glutathione concentration in the heart of *P. berghei* NK65-infected mice on days 4 and 8 post inoculation

Values are means ± SEM of 5 determinations. Bars for each day with different alphabets are significantly different ($p<0.05$). **Uninf** = Uninfected; **Inf** = infected; **DMSO** = Dimethyl sulfoxide; **bwt** = body weight; **M*P*** = 3:2 Methyl gallate and Palmatine (most active ratio from *in vitro* antimalarial study); **20 Pip** = 20 mg/Kg bwt Piperine

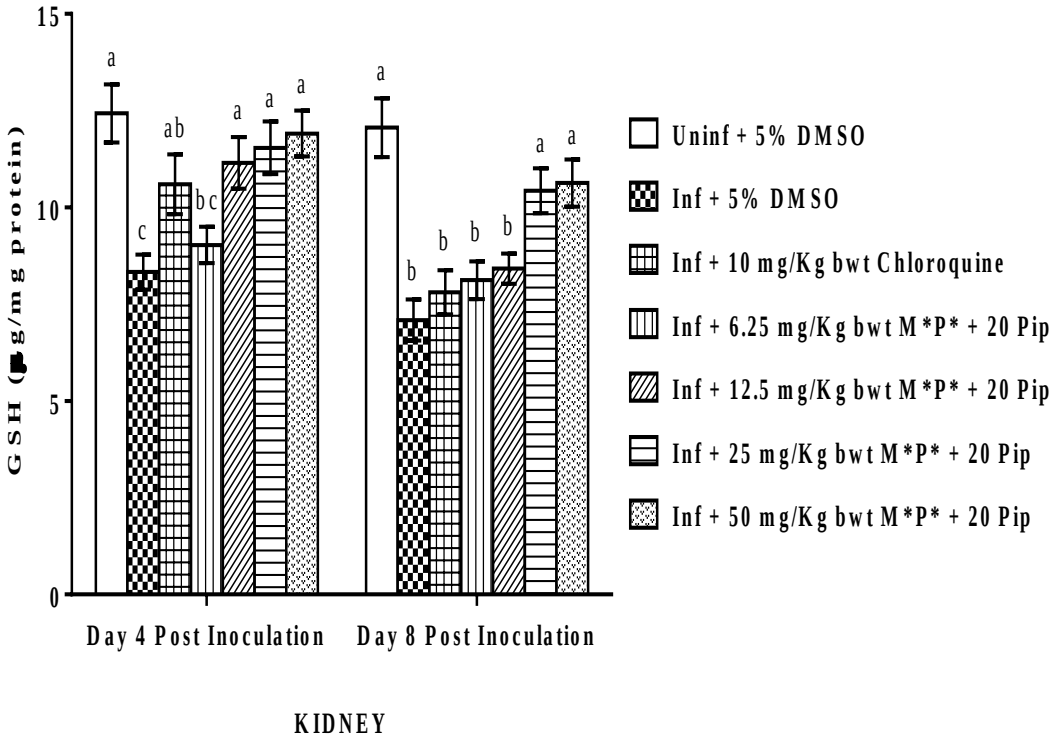

Figure 67: Effects of methyl gallate and palmatine combination in the presence of piperine on reduced glutathione concentration in the kidney of *P. berghei* NK65-infected mice on days 4 and 8 post inoculation

Values are means ± SEM of 5 determinations. Bars for each day with different alphabets are significantly different ($p<0.05$). **Uninf** = Uninfected; **Inf** = infected; **DMSO** = Dimethyl sulfoxide; **bwt** = body weight; **M*P*** = 3:2 Methyl gallate and Palmatine (most active ratio from *in vitro* antimalarial study); **20 Pip** = 20 mg/Kg bwt Piperine.

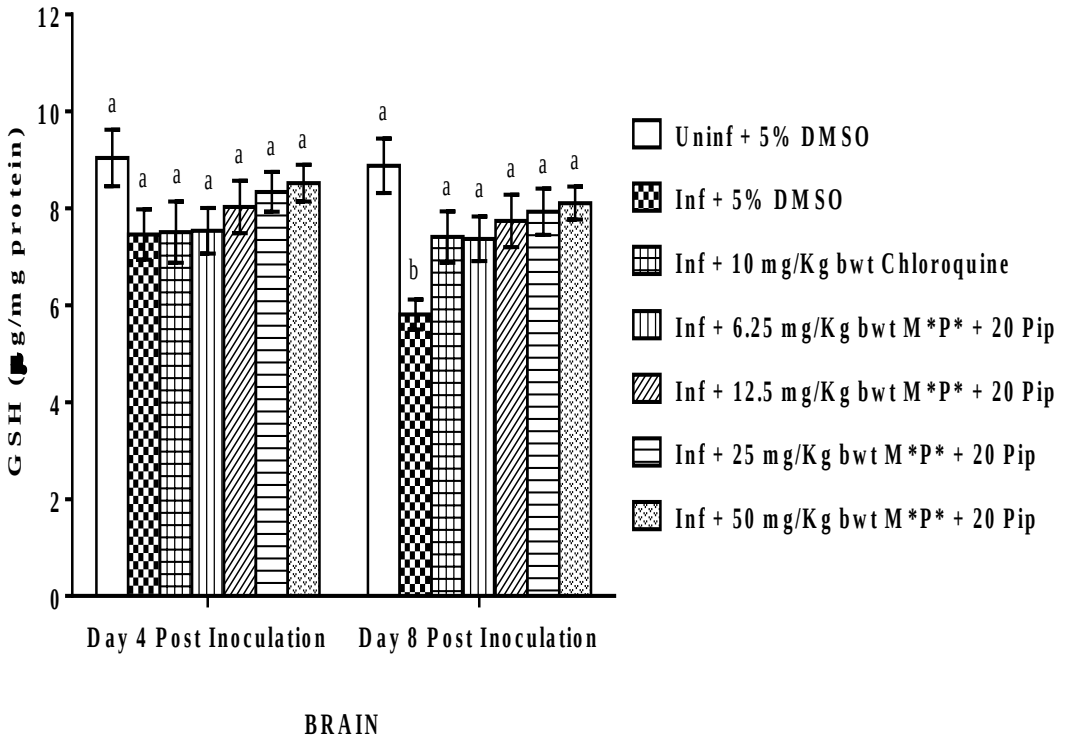

Figure 68: Effects of methyl gallate and palmatine combination in the presence of piperine on reduced glutathione concentration in the brain of *P. berghei* NK65-infected mice on days 4 and 8 post inoculation

Values are means ± SEM of 5 determinations. Bars for each day with different alphabets are significantly different ($p<0.05$). **Uninf** = Uninfected; **Inf** = infected; **DMSO** = Dimethyl sulfoxide; **bwt** = body weight; **M*P*** = 3:2 Methyl gallate and Palmatine (most active ratio from *in vitro* antimalarial study); **20 Pip** = 20 mg/Kg bwt Piperine.

4.3.2.7 Glutathione-S-Transferase Activity

There was significant reduction ($p<0.05$) in glutathione-S-transferase activities in erythrocyte, liver, heart and kidney of untreated infected mice on days 4 and 8 post-inoculation, compared to those of uninfected mice, though heart glutathione-S-transferase activity on day 4 post-inoculation was not significantly altered ($p>0.05$) (Figures 69-72). Brain glutathione-S-transferase activity of the untreated infected control was only significantly reduced ($p<0.05$) on day 8 post-inoculation compared to uninfected control (Figure 73).

The bio-enhanced compound combination at doses higher than 6.25 mg/kg body weight caused significant increase ($p<0.05$) in glutathione-S-transferase (GST) activities in the erythrocyte and tissues studied on days 4 and 8 post-inoculation compared to untreated infected controls, except that the activities of GST in the heart (on day 4 post-inoculation) and erythrocyte (on day 8 post-inoculation) were not significantly altered ($p>0.05$) at the dose of 12.5 mg/Kg body weight (Figures 69-72). At all doses of the bio-enhanced compound combination, the activity of glutathione-S-transferase in the brain was not significantly changed ($p>0.05$) compared to untreated infected control (Figure 73).

The bio-enhanced methyl gallate and palmatine combination at the doses of 25 and 50 mg/Kg body weight did not significantly change ($p>0.05$) the activities of glutathione-S-transferase in the liver, kidney and brain on day 4 post-inoculation compared to uninfected control (Figures 70, 72 and 73). There was also no significant alteration ($p>0.05$) in the activities of the enzyme in the erythrocyte, heart and brain at these doses on day 8 post-inoculation (Figures 69, 71 and 73).

Also, the bio-enhanced compound combination at doses higher than 6.25 mg/Kg body weight caused significant increase ($p<0.05$) in glutathione-S-transferase activities in the erythrocyte and liver on day 4 post-inoculation compared to those of chloroquine-treated group (Figures 69-70). On day 8 post-inoculation, the bio-enhanced compound combination at doses higher than 12.5 mg/Kg body weight caused significant increase ($p<0.05$) in glutathione-S-transferase activities in the erythrocyte and kidney compared to those of chloroquine-treated group (Figures 69 and 72). On day 8 post-inoculation, the bio-enhanced compound combination at doses higher than 6.25 mg/kg body weight caused significant increase ($p<0.05$) in glutathione-S-transferase activities in the liver compared to those of chloroquine-treated group (Figures 70).

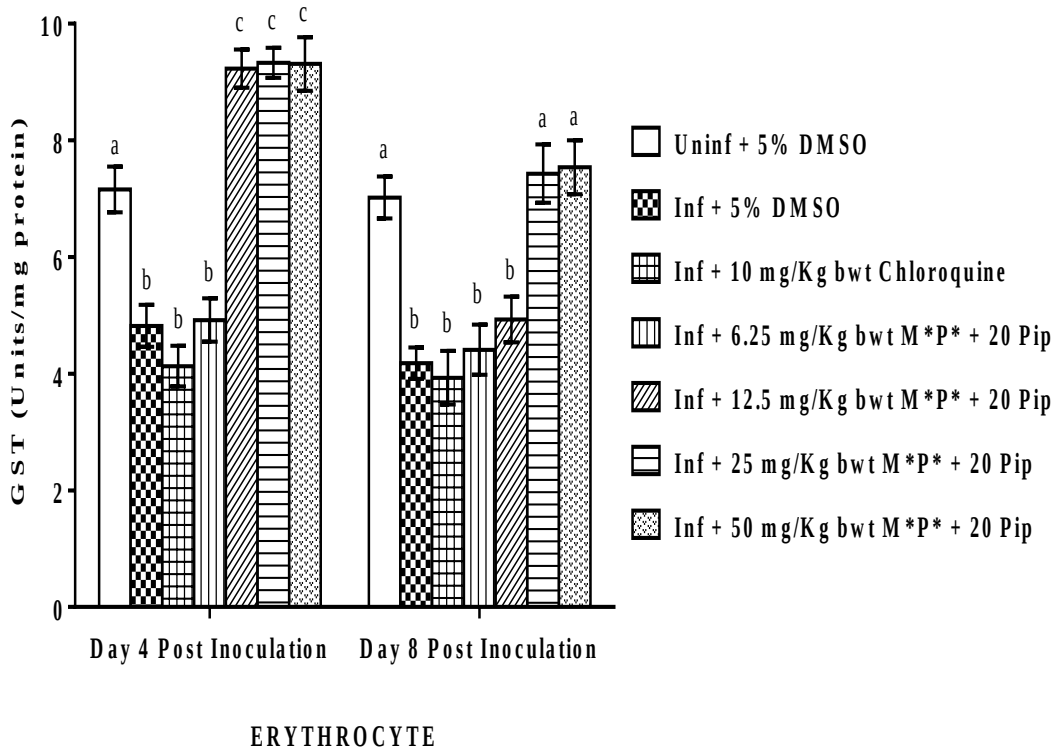

Figure 69: Effects of methyl gallate and palmatine combination in the presence of piperine on glutathione-S-transferase activity in the erythrocyte of *P. berghei* NK65-infected mice on days 4 and 8 post-inoculation

Values are means ± SEM of 5 determinations. Bars for each day with different alphabets are significantly different ($p<0.05$). **Uninf** = Uninfected; **Inf** = infected; **DMSO** = Dimethyl sulfoxide; **bwt** = body weight; **M*P*** = 3:2 Methyl gallate and Palmatine (most active ratio from *in vitro* antimalarial study); **20 Pip** = 20 mg/Kg bwt Piperine.

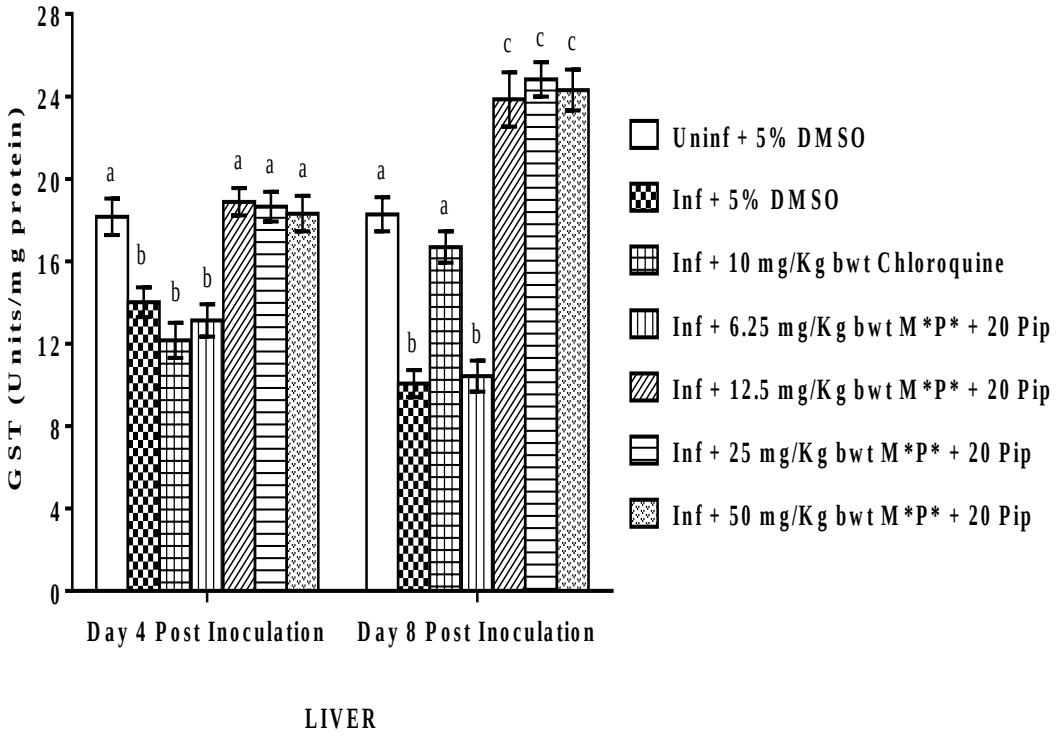

Figure 70: Effects of methyl gallate and palmatine combination in the presence of piperine on glutathione-S-transferase activity in the liver of *P. berghei* NK65-infected mice on days 4 and 8 post inoculation

Values are means ± SEM of 5 determinations. Bars for each day with different alphabets are significantly different ($p<0.05$). **Uninf** = Uninfected; **Inf** = infected; **DMSO** = Dimethyl sulfoxide; **bwt** = body weight; **M*P*** = 3:2 Methyl gallate and Palmatine (most active ratio from *in vitro* antimalarial study); **20 Pip** = 20 mg/Kg bwt Piperine.

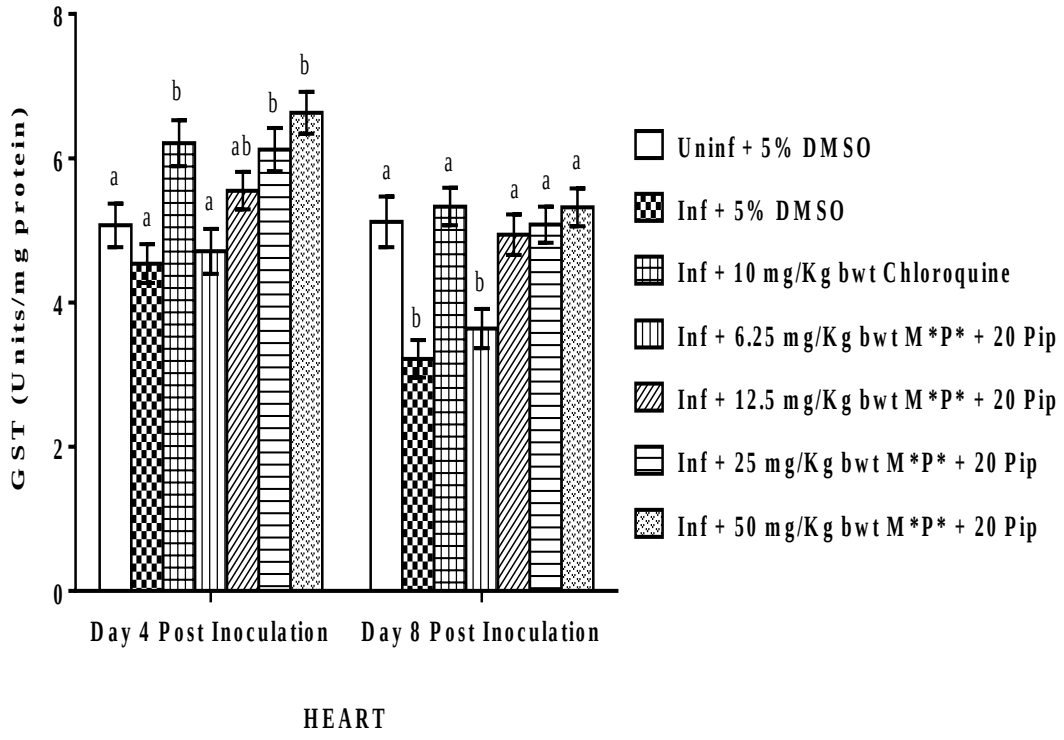

Figure 71: Effects of methyl gallate and palmatine combination in the presence of piperine on glutathione-S-transferase activity in the heart of *P. berghei* NK65-infected mice on days 4 and 8 post inoculation

Values are means ± SEM of 5 determinations. Bars for each day with different alphabets are significantly different ($p<0.05$). **Uninf** = Uninfected; **Inf** = infected; **DMSO** = Dimethyl sulfoxide; **bwt** = body weight; **M*P*** = 3:2 Methyl gallate and Palmatine (most active ratio from *in vitro* antimalarial study); **20 Pip** = 20 mg/Kg bwt Piperine.

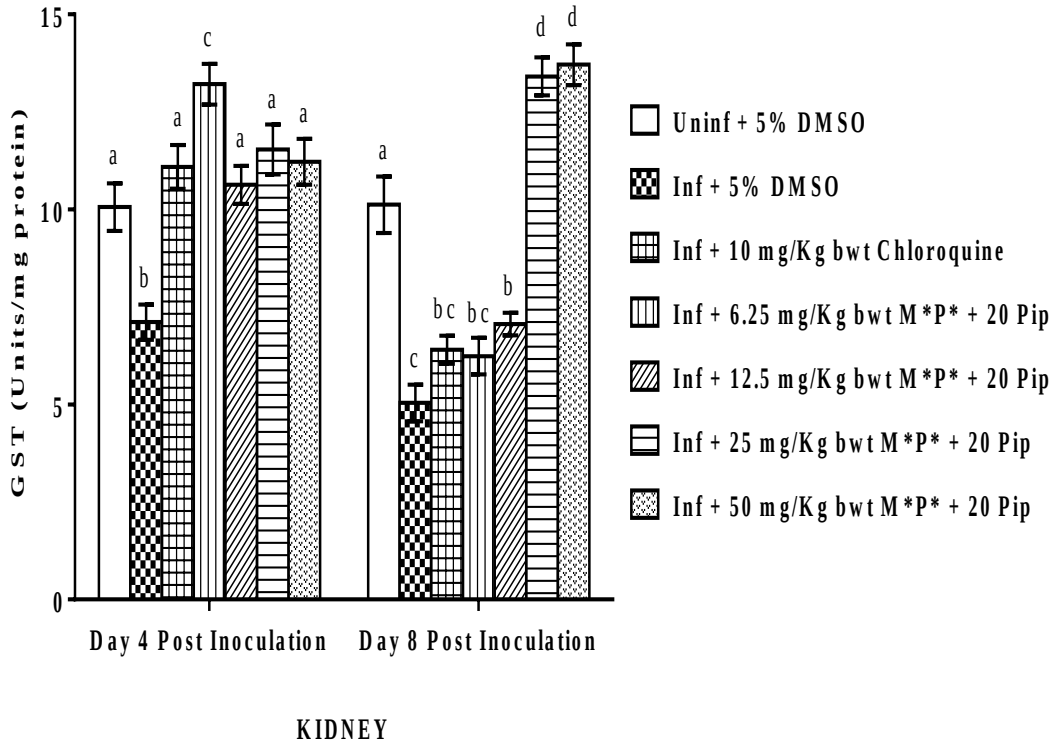

Figure 72: Effects of methyl gallate and palmatine combination in the presence of piperine on glutathione-S-transferase activity in the kidney of *P. berghei* NK65-infected mice on days 4 and 8 post inoculation

Values are means ± SEM of 5 determinations. Bars for each day with different alphabets are significantly different ($p<0.05$). **Uninf** = Uninfected; **Inf** = infected; **DMSO** = Dimethyl sulfoxide; **bwt** = body weight; **M*P*** = 3:2 Methyl gallate and Palmatine (most active ratio from *in vitro* antimalarial study); **20 Pip** = 20 mg/Kg bwt Piperine.

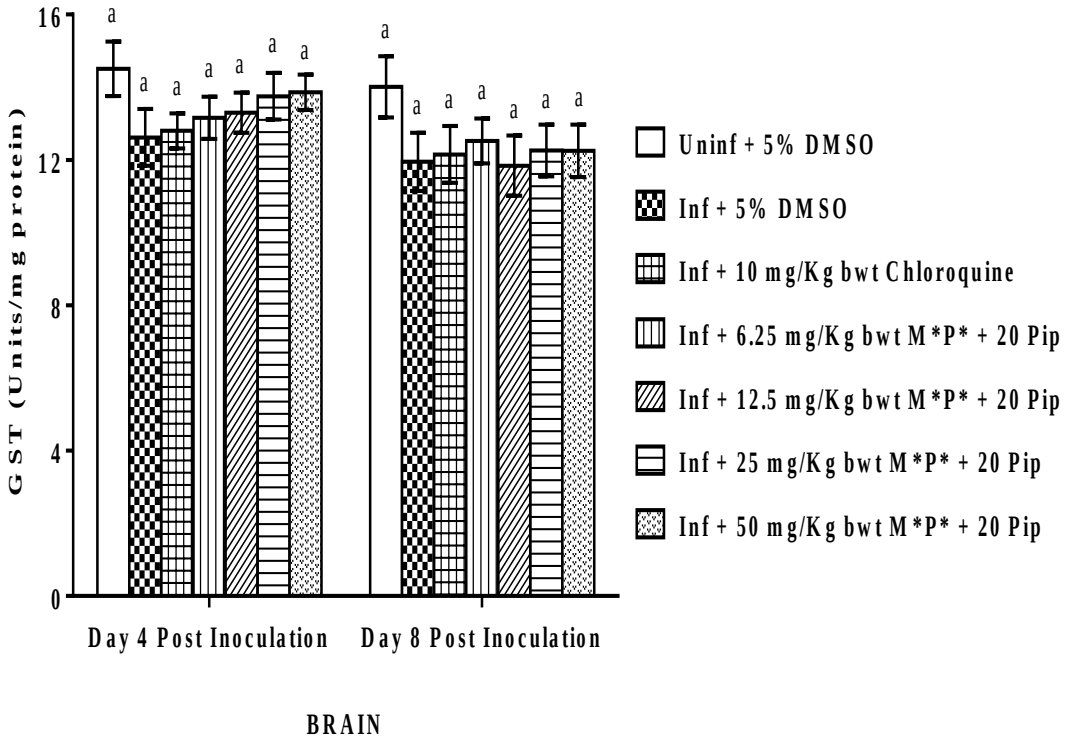

Figure 73: Effects of methyl gallate and palmatine combination in the presence of piperine on glutathione-S-transferase activity in the brain of *P. berghei* NK65-infected mice on days 4 and 8 post inoculation

Values are means ± SEM of 5 determinations. Bars for each day with different alphabets are significantly different ($p<0.05$). **Uninf** = Uninfected; **Inf** = infected; **DMSO** = Dimethyl sulfoxide; **bwt** = body weight; **M*P*** = 3:2 Methyl gallate and Palmatine (most active ratio from *in vitro* antimalarial study); **20 Pip** = 20 mg/Kg bwt Piperine.

4.3.3 Toxicological Studies

4.3.3.1 Organ-Body Weight Ratio

Compared to those in control groups, the 28-day administration of bio-enhanced methyl gallate and palmatine combination did not significantly alter ($p>0.05$) the weight of selected organs relative to the rat's body weight (Table 9).

4.3.3.2 Haematological Analysis

4.3.3.2.1 Red Blood Cell Indices

The 28-day administration of bio-enhanced combination of methyl gallate and palmatine did not significantly alter ($p>0.05$) the red blood cell count, haemoglobin concentration, packed cell volume, mean corpuscular volume, mean corpuscular haemoglobin and mean corpuscular haemoglobin concentration compared to controls (Table 10).

4.3.3.2.2 White Blood Cell Indices and Platelet Count

The administration of bio-enhanced combination of methyl gallate and palmatine did not significantly alter ($p>0.05$) the platelet count, white blood cell count and percentage lymphocyte compared to the controls (Table 11). Also, there was no significant change ($p>0.05$) in percentage neutrophil and the percentage of other myeloid cells (basophils, eosinophils and monocytes) at the doses administered compared to controls except the significant reduction ($p<0.05$) in percentage neutrophil and corresponding significant increase ($p<0.05$) in the percentage of other myeloid cells observed at 50 mg/Kg body weight of the bio-enhanced compound combination (Table 11).

Table 9: Effects of bio-enhanced methyl gallate and palmatine combination on selected organ-body weight ratios of rats

Treatment	Organ-Body weight ratio (%)			
	Brain	**Heart**	**Kidney**	**Liver**
5% DMSO	1.35 ± 0.17[a]	0.56 ± 0.06[a]	1.17 ± 0.05[a]	3.24 ± 0.12[a]
6.25 mg/Kg bwt M*P* + 20 Pip	1.41 ± 0.16[a]	0.54 ± 0.05[a]	1.21 ± 0.04[a]	3.27 ± 0.15[a]
12.5 mg/Kg bwt M*P* + 20 Pip	1.33 ± 0.14[a]	0.59 ± 0.06[a]	1.21 ± 0.06[a]	3.26 ± 0.12[a]
25 mg/Kg bwt M*P* + 20 Pip	1.38 ± 0.15[a]	0.57 ± 0.05[a]	1.18 ± 0.05[a]	3.31 ± 0.14[a]
50 mg/Kg bwt M*P* + 20 Pip	1.40 ± 0.17[a]	0.58 ± 0.06[a]	1.22 ± 0.07[a]	3.30 ± 0.12[a]
100 mg/Kg bwt M*P* + 20 Pip	1.39 ± 0.16[a]	0.57 ± 0.05[a]	1.20 ± 0.05[a]	3.32 ± 0.16[a]

Values are means ± SD of 5 replicates. Values in the same column with different superscripts are significantly different ($p<0.05$). **DMSO** = Dimethyl sulfoxide; **bwt** = body weight; **20 Pip** = 20 mg/Kg bwt Piperine; **M*P*** = 3:2 Methyl gallate and Palmatine (most active ratio from *in vitro* antimalarial study)

Table 10: Effects of bio-enhanced methyl gallate and palmatine combination on selected red blood cells indices of rats

Treatment	RBC ($x10^{12}$/L)	PCV(%)	Hb (g/L)	MCV (%)	MCH (ρg)	MCHC (g/L)
5% DMSO	9.20 ± 0.52^{a}	51.20 ± 3.12^{a}	169.60 ± 5.88^{a}	55.65 ± 2.41^{a}	18.43 ± 0.58^{a}	33.13 ± 0.89^{a}
6.25 mg/Kg bwt M*P* + 20 Pip	9.30 ± 0.44^{a}	51.80 ± 2.35^{a}	172.00 ± 6.21^{a}	55.69 ± 2.18^{a}	18.49 ± 0.62^{a}	33.20 ± 0.57^{a}
12.5 mg/Kg bwt M*P* + 20 Pip	8.82 ± 0.48^{a}	49.40 ± 3.29^{a}	161.60 ± 7.11^{a}	56.01 ± 1.98^{a}	18.32 ± 0.72^{a}	32.71 ± 0.85^{a}
25 mg/Kg bwt M*P* + 20 Pip	8.84 ± 0.53^{a}	52.20 ± 3.01^{a}	170.20 ± 5.26^{a}	59.05 ± 3.22^{a}	19.25 ± 0.71^{a}	32.61 ± 0.91^{a}
50 mg/Kg bwt M*P* + 20 Pip	8.60 ± 0.36^{a}	49.80 ± 2.84^{a}	163.60 ± 7.05^{a}	57.91 ± 2.31^{a}	19.02 ± 0.84^{a}	32.85 ± 0.83^{a}
100 mg/Kg bwt M*P* + 20 Pip	8.31 ± 0.58^{a}	48.40 ± 3.61^{a}	161.20 ± 6.91^{a}	58.24 ± 2.18^{a}	19.39 ± 0.88^{a}	33.31 ± 0.76^{a}

Values are means ± SEM of 5 replicates. Values in the same column with different superscripts are significantly different ($p<0.05$). **DMSO** = Dimethyl sulfoxide; **bwt** = body weight; **20 Pip** = 20 mg/Kg bwt Piperine; **M*P*** = 3:2 Methyl gallate and Palmatine (most active ratio from *in vitro* antimalarial study); **RBC** = Red blood cell; **Hb** = Haemoglobin; **PCV** = Packed cell volume; **MCV** = Mean corpuscular volume; **MCH** = Mean corpuscular haemoglobin; **MCHC** = Mean corpuscular haemoglobin concentration

Table 11: Effects of bio-enhanced methyl gallate and palmatine combination on platelet count and white blood cell indices of rats

Treatment	Platelet Count($x10^9$/L)	WBC ($x10^9$/L)	Lymphocytes (%)	Neutrophils (%)	Other myeloid cells (%)
5% DMSO	745.69 ± 61.83[a]	10.42 ± 3.13[a]	64.21 ± 7.03[a]	32.67 ± 2.16[a]	3.12 ± 0.41[a]
6.25 mg/Kg bwt M*P* + 20 Pip	804.82 ± 72.33[a]	9.65 ± 2.57[a]	63.05 ± 5.31[a]	34.06 ± 3.08[a]	2.89 ± 0.37[a]
12.5 mg/Kg bwt M*P* + 20 Pip	810.04 ± 65.96[a]	11.37 ± 1.98[a]	68.21 ± 6.74[a]	29.07 ± 2.47[ab]	2.72 ± 0.29[a]
25 mg/Kg bwt M*P* + 20 Pip	783.27 ± 49.71[a]	11.14 ± 2.41[a]	70.47 ± 6.17[a]	26.70 ± 2.91[ab]	2.83 ± 0.36[a]
50 mg/Kg bwt M*P* + 20 Pip	818.13 ± 68.25[a]	12.08 ± 3.24[a]	72.13 ± 6.83[a]	22.94 ± 2.01[b]	4.93 ± 0.21[b]
100 mg/Kg bwt M*P* + 20 Pip	771.62 ± 45.06[a]	10.99 ± 2.75[a]	69.05 ± 5.03[a]	28.16 ± 2.33[ab]	2.79 ± 0.40[a]

Values are means ± SEM of 5 replicates. Values in the same column with different superscripts are significantly different ($p<0.05$). **DMSO** = Dimethyl sulfoxide; **bwt** = body weight; **20 Pip** = 20 mg/Kg bwt Piperine; **M*P*** = 3:2 Methyl gallate and Palmatine (most active ratio from *in vitro* antimalarial study); **WBC** = White blood cells; **Other myeloid cells** = basophils, eosinophils and monocytes.

4.3.3.3 Plasma Electrolytes

The administration of bio-enhanced methyl gallate and palmatine combination at various doses had no significant impact ($p>0.05$) on the plasma concentrations of Na^+, K^+, Cl^-, HCO_3^- and PO_4^{3-} compared to controls (Table 9). Likewise, the administration of the bio-enhanced combination at doses of lower than 100 mg/Kg body weight had no effect ($p>0.05$) on the plasma concentration of Ca^{2+} compared to control. However, the administration of the bio-enhanced combination at the dose of 100 mg/Kg body weight brought about significant decrease ($p<0.05$) in plasma Ca^{2+} concentration compared to control (Table 12).

4.3.3.4 Plasma Biomolecules

The administration of bio-enhanced methyl gallate and palmatine combination at all doses had no significant effect ($p>0.05$) on the plasma concentrations of creatinine and uric acid compared to controls (Table 13). Likewise, no significant alteration ($p>0.05$) in plasma urea concentration was observed in groups administered 6.25, 12.5, 25 and 100 mg/Kg body weight of bio-enhanced methyl gallate and palmatine combination. However, the administration of the bio-enhanced combination at the dose of 50 mg/Kg body weight brought about significant increase ($p<0.05$) in plasma concentration of urea (Table 13).

Bio-enhanced methyl gallate and palmatine combination administered at various doses had no significant effect ($p>0.05$) on the plasma concentrations of total protein, albumin, globulin and bilirubin compared to controls (Table 14). Also, administration of the combination at doses lower than 100 mg/Kg body weight caused no significant alteration ($p>0.05$) in the plasma concentration of conjugated bilirubin. However, 100 mg/Kg body weight of the bio-enhanced combination caused significant

increase ($p<0.05$) in plasma concentration of conjugated bilirubin compared to control (Table 14).

Table 12: Effects of bio-enhanced methyl gallate and palmatine combination on plasma concentrations of selected electrolytes of rats

Treatment	Na^+ (mmol/L)	K^+ (mmol/L)	Ca^{2+} (mmol/L)	Cl^- (mmol/L)	HCO_3^- (mmol/L)	PO_4^{3-} (mmol/L)
5% DMSO	141.37 ± 7.78[a]	5.14 ± 0.31[a]	3.43 ± 0.17[a]	107.44 ± 6.12[a]	25.83 ± 1.22[a]	2.15 ± 0.18[a]
6.25 mg/Kg bwt M*P* + 20 Pip	139.57 ± 8.24[a]	5.20 ± 0.44[a]	3.39 ± 0.13[a]	112.10 ± 5.62[a]	23.97 ± 1.06[a]	2.18 ± 0.15[a]
12.5 mg/Kg bwt M*P* + 20 Pip	138.21 ± 8.09[a]	5.08 ± 0.28[a]	3.32 ± 0.11[a]	109.68 ± 3.97[a]	26.04 ± 1.61[a]	2.20 ± 0.15[a]
25 mg/Kg bwt M*P* + 20 Pip	131.11 ± 7.11[a]	5.02 ± 0.36[a]	3.27 ± 0.10[a]	106.31 ± 5.76[a]	25.51 ± 1.01[a]	2.38 ± 0.13[a]
50 mg/Kg bwt M*P* + 20 Pip	127.83 ± 7.42[a]	4.89 ± 0.42[a]	3.20 ± 0.13[ab]	103.92 ± 6.81[a]	24.86 ± 1.37[a]	2.40 ± 0.11[a]
100 mg/Kg bwt M*P* + 20 Pip	129.46 ± 9.14[a]	4.95 ±0.49[a]	2.79 ± 0.10[b]	101.84 ± 6.29[a]	24.94 ± 1.45[a]	2.37 ± 0.10[a]

Values are means ± SEM of 5 replicates. Values in the same column with different superscripts are significantly different ($p<0.05$). **DMSO** = Dimethyl sulfoxide; **bwt** = body weight; **20 Pip** = 20 mg/Kg bwt Piperine; **M*P*** = 3:2 Methyl gallate and Palmatine (most active ratio from *in vitro* antimalarial study)

Table 13: Selected kidney function indices of rats administered bio-enhanced methyl gallate and palmatine combination

Treatment	Urea concentration (mmol/L)	Creatinine concentration (µmol/L)	Uric acid concentration (µmol/L)
5% DMSO	5.59 ± 0.38[a]	104.53 ± 13.61[a]	350.28 ± 32.31[a]
6.25 mg/Kg bwt M*P* + 20 Pip	5.69 ± 0.27[a]	110.28 ± 15.32[a]	372.43 ± 28.68[a]
12.5 mg/Kg bwt M*P* + 20 Pip	5.74 ± 0.31[a]	117.31 ± 12.61[a]	368.61 ± 31.07[a]
25 mg/Kg bwt M*P* + 20 Pip	5.71 ± 0.34[a]	115.49 ± 9.37[a]	381.42 ± 25.74[a]
50 mg/Kg bwt M*P* + 20 Pip	7.62 ± 0.50[b]	121.01 ± 15.18[a]	389.45 ± 36.88[a]
100 mg/Kg bwt M*P* + 20 Pip	5.95 ± 0.41[ab]	119.36 ± 14.45[a]	385.20 ± 29.72[a]

Values are means ± SEM of 5 replicates. Values in the same column with different superscripts are significantly different ($p<0.05$). **DMSO** = Dimethyl sulfoxide; **bwt** = body weight; **20 Pip** = 20 mg/Kg bwt Piperine; **M*P*** = 3:2 Methyl gallate and Palmatine (most active ratio from *in vitro* antimalarial study)

Table 14: Selected liver function indices of rats administered bio-enhanced methyl gallate and palmatine combination

Treatment	Total Protein concentration (g/L)	Albumin concentration (g/L)	Globulin concentration (g/L)	Total bilirubin concentration (µmol/L)	Conjugated bilirubin concentration (µmol/L)
5% DMSO	25.56 ± 2.32[a]	16.83 ± 1.84[a]	8.73 ± 0.95[a]	18.83 ± 1.04[a]	5.17 ± 0.85[a]
6.25 mg/Kg bwt M*P* + 20 Pip	25.94 ± 2.61[a]	17.46 ± 1.71[a]	8.48 ± 0.87[a]	18.88 ± 1.11[a]	5.25 ± 0.71[a]
12.5 mg/Kg bwt M*P* + 20 Pip	26.48 ± 2.02[a]	16.92 ± 1.52[a]	9.56 ± 1.10[a]	18.72 ± 1.08[a]	5.45 ± 0.68[a]
25 mg/Kg bwt M*P* + 20 Pip	26.57 ± 1.86[a]	16.78 ± 1.66[a]	9.79 ± 1.08[a]	19.43 ± 1.17[a]	5.39 ± 0.75[a]
50 mg/Kg bwt M*P* + 20 Pip	27.14 ± 1.92[a]	17.43 ± 1.58[a]	9.71 ± 1.04[a]	19.32 ± 1.14[a]	5.81 ± 0.56[a]
100 mg/Kg bwt M*P* + 20 Pip	27.32 ± 2.17[a]	17.52 ± 1.69[a]	9.80 ± 1.21[a]	19.57 ± 1.16[a]	8.89 ± 0.79[b]

Values are means ± SEM of 5 replicates. Values in the same column with different superscripts are significantly different ($p<0.05$). **DMSO** = Dimethyl sulfoxide; **bwt** = body weight; **20 Pip** = 20 mg/Kg bwt Piperine; **M*P*** = 3:2 Methyl gallate and Palmatine (most active ratio from *in vitro* antimalarial study).

4.3.3.5 Cardiovascular Disease Indices

The administration of bio-enhanced methyl gallate and palmatine combination at various doses caused no significant alteration ($p>0.05$) in plasma concentrations of total cholesterol and triacylglycerol compared to controls (Table 15). The bio-enhanced compound combination at doses higher than 6.25 mg/kg body weight caused significant reduction ($p<0.05$) in plasma LDL cholesterol concentration and atherogenic index compared to controls (Table 15). However, there was significant increase ($p<0.05$) in plasma HDL cholesterol concentration at doses higher than 12.5 mg/kg body weight of the bio-enhanced compound combination compared to control (Table 15).

4.3.3.6 Cellular Enzymes

4.3.3.6.1 Alkaline Phosphatase Activity

There was no significant alteration ($p>0.05$) in alkaline phosphatase activities in the brain, heart, kidney, liver and plasma of rats administered various doses of the bio-enhanced methyl gallate and palmatine combination compared to controls (Figures 74-75).

4.3.3.6.2 Gamma Glutamyl Transferase Activity

The administration of bio-enhanced combination of methyl gallate and palmatine at various doses had no significant effect ($p>0.05$) on gamma glutamyl transferase activities in the kidney, liver and plasma compared to controls (Figure 76).

Table 15: Effects of bio-enhanced methyl gallate and palmatine combination on selected cardiovascular disease indices of rats

Treatment	Total Chol (mmol/L)	TAG (mmol/L)	LDL-C (mmol/L)	HDL-C (mmol/L)	A.I
5% DMSO	4.41 ± 0.27[a]	1.58 ± 0.07[a]	2.38 ± 0.08[a]	1.30 ± 0.11[a]	3.38 ± 0.15[a]
6.25 mg/Kg bwt M*P* + 20 Pip	4.39 ± 0.29[a]	1.55 ± 0.06[a]	2.21 ± 0.06[a]	1.47 ± 0.08[a]	2.99 ± 0.13[a]
12.5 mg/Kg bwt M*P* + 20 Pip	4.21 ± 0.27[a]	1.51 ± 0.07[a]	1.87 ± 0.05[b]	1.65 ± 0.17[ab]	2.55 ± 0.12[b]
25 mg/Kg bwt M*P* + 20 Pip	4.15 ± 0.24[a]	1.48 ± 0.05[a]	1.70 ± 0.08[b]	1.77 ± 0.08[b]	2.35 ± 0.18[b]
50 mg/Kg bwt M*P* + 20 Pip	4.23 ± 0.32[a]	1.46 ± 0.07[a]	1.76 ± 0.06[b]	1.79 ± 0.07[b]	2.35 ± 0.11[b]
100 mg/Kg bwt M*P* + 20 Pip	4.10 ± 0.31[a]	1.47 ± 0.06[a]	1.66 ± 0.09[b]	1.77 ± 0.08[b]	2.31 ± 0.29[b]

Values are means ± SEM of 5 replicates. Values in the same column with different superscripts are significantly different ($p<0.05$). **DMSO** = Dimethyl sulfoxide; **bwt** = body weight; **20 Pip** = 20 mg/Kg bwt Piperine; **M*P*** = 3:2 Methyl gallate and Palmatine (most active ratio from *in vitro* antimalarial study); **A.I =** Atherogenic index; **TAG** = Triacylglycerol; **Total Chol** = Total cholesterol; **HDL-C** = High density lipoprotein cholesterol; **LDL-C** = Low density lipoprotein cholesterol.

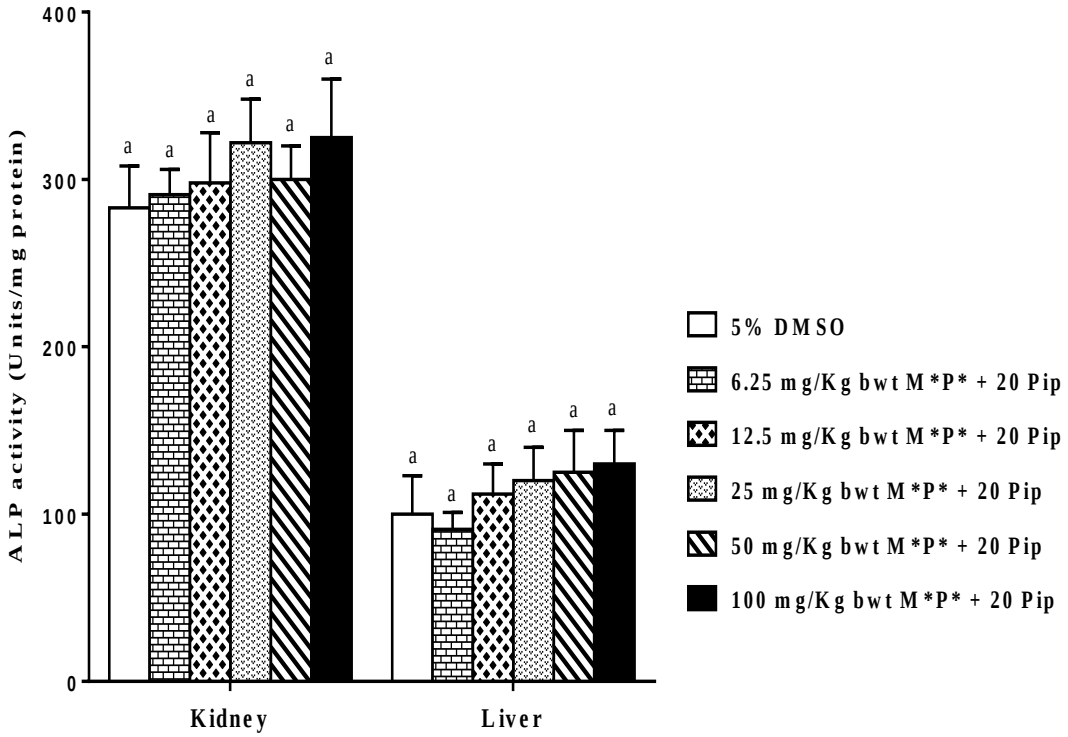

Figure 74: Effects of bio-enhanced methyl gallate and palmatine combination on alkaline phosphatase activities in kidney and liver of rats

Values are means ± SEM of 5 replicates. Bars for each organ with similar alphabets are not significantly different ($p>0.05$). **DMSO** = Dimethyl sulfoxide; **bwt** = body weight; **20 Pip** = 20 mg/Kg bwt Piperine; **M*P*** = 3:2 Methyl gallate and Palmatine (most active ratio from *in vitro* antimalarial study)

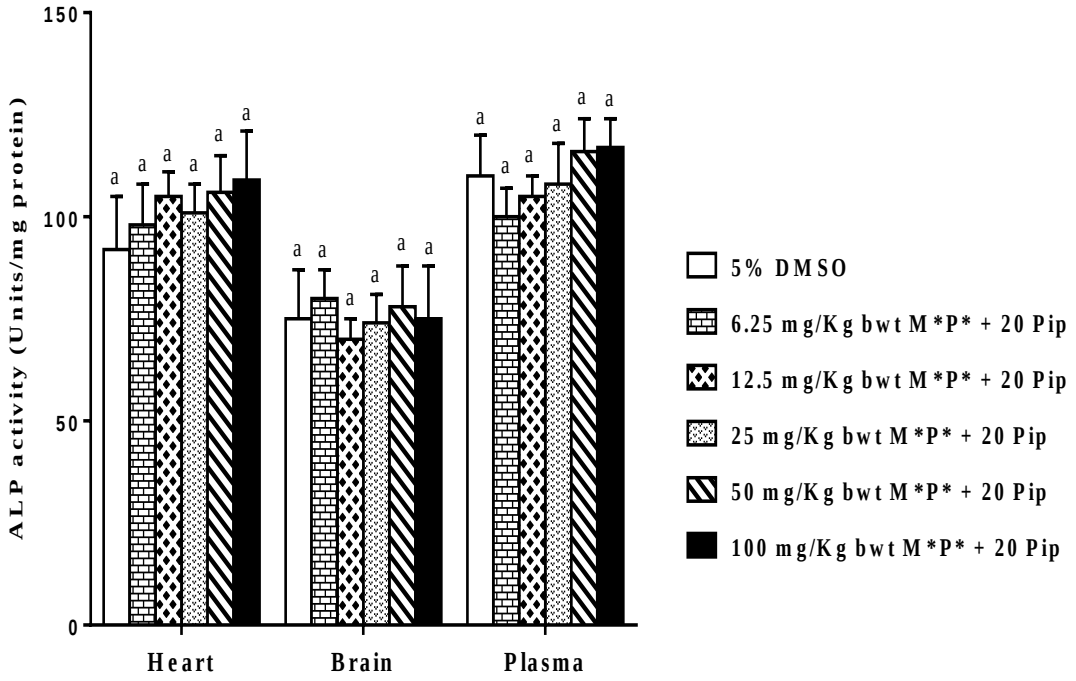

Figure 75: Effects of bio-enhanced combination of methyl gallate and palmatine on alkaline phosphatase activities in heart, brain and plasma of rats

Values are means ± SEM of 5 replicates. Bars for each organ/plasma with similar alphabets are not significantly different ($p>0.05$). **DMSO** = Dimethyl sulfoxide; **bwt** = body weight; **20 Pip** = 20 mg/Kg bwt Piperine; **M*P*** = 3:2 Methyl gallate and Palmatine (most active ratio from *in vitro* antimalarial study)

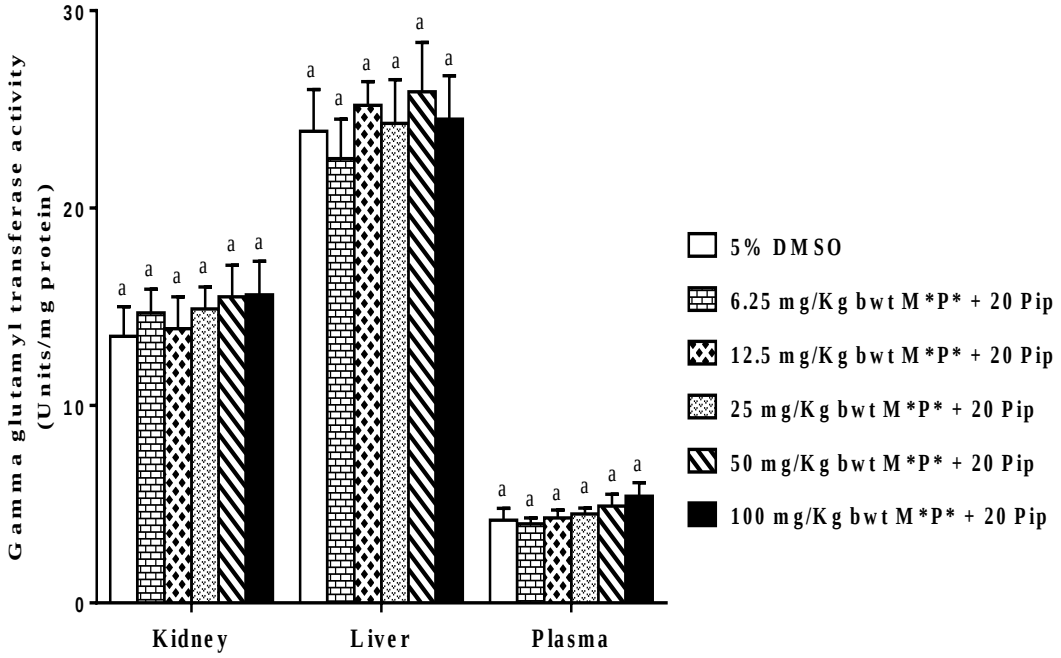

Figure 76: Effects of bio-enhanced combination of methyl gallate and palmatine on gamma glutamyl transferase activities in kidney, liver and plasma of rats
Values are means ± SEM of 5 replicates. Bars for each organ/plasma with similar alphabets are not significantly different ($p>0.05$). **DMSO** = Dimethyl sulfoxide; **bwt** = body weight; **20 Pip** = 20 mg/Kg bwt Piperine; **M*P*** = 3:2 Methyl gallate and Palmatine (most active ratio from *in vitro* antimalarial study)

4.3.3.6.3 Aspartate Aminotransferase Activity

The bio-enhanced combination of methyl gallate and palmatine at various doses had no significant effect ($p>0.05$) on aspartate aminotransferase activities in the heart and plasma compared to controls (Figure 77). Likewise, at the doses of 6.25, 12.5 and 25 mg/kg body weight, the bio-enhanced compound combination caused no significant alteration ($p>0.05$) in aspartate aminotransferase activity in the liver but brought about significant increase ($p<0.05$) in aspartate aminotransferase activity in the liver at the doses of 50 and 100 mg/kg body weight compared to control (Figure 77).

4.3.3.6.4 Alanine Aminotransferase Activity

The bio-enhanced combination of methyl gallate and palmatine at all doses did not significantly affect ($p>0.05$) alanine aminotransferase (ALT) activity in the plasma compared to control (Figure 78). Also, ALT activity in the liver was not significantly altered ($p>0.05$) by the bio-enhanced compound combination at doses lower than 100 mg/kg body weight but caused significant increase ($p<0.05$) in liver ALT activity at 100 mg/kg body weight compared to control (Figure 78).

4.3.3.6.5 Lactate Dehydrogenase Activity

The bio-enhanced combination of methyl gallate and palmatine at all doses caused no significant alteration ($p>0.05$) in lactate dehydrogenase activities in the heart and plasma compared to controls (Figure 79).

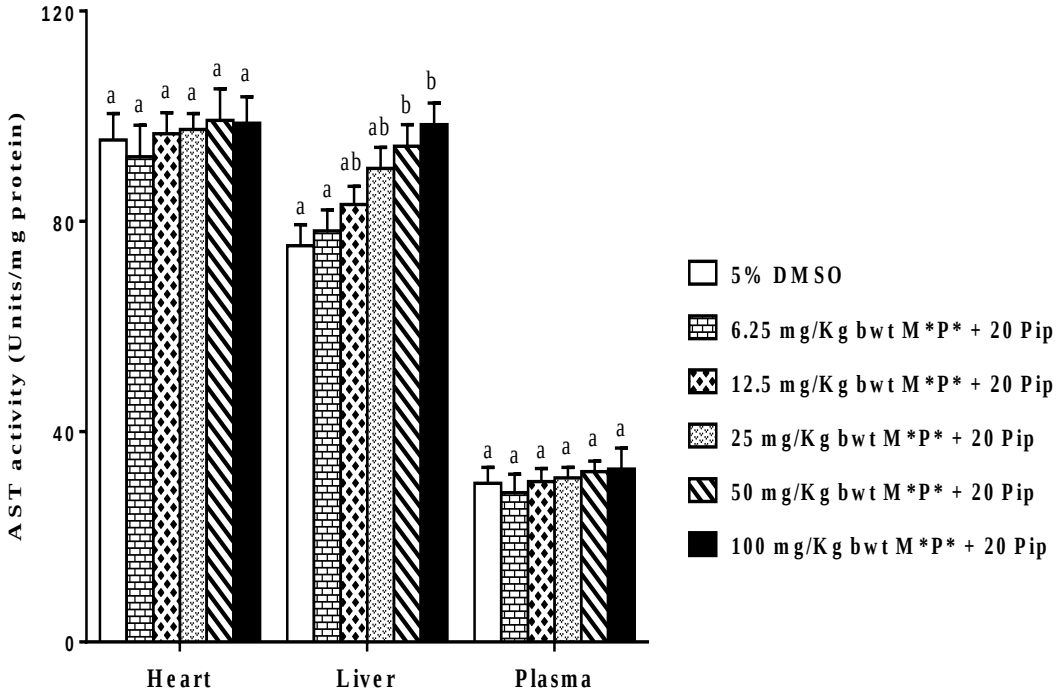

Figure 77: Effects of bio-enhanced combination of methyl gallate and palmatine on aspartate aminotransferase activities in heart, liver and plasma of rats
Values are means ± SEM of 5 replicates. Bars for each organ/plasma with different alphabets are significantly different ($p<0.05$). **DMSO** = Dimethyl sulfoxide; **bwt** = body weight; **20 Pip** = 20 mg/Kg bwt Piperine; **M*P*** = 3:2 Methyl gallate and Palmatine (most active ratio from *in vitro* antimalarial study).

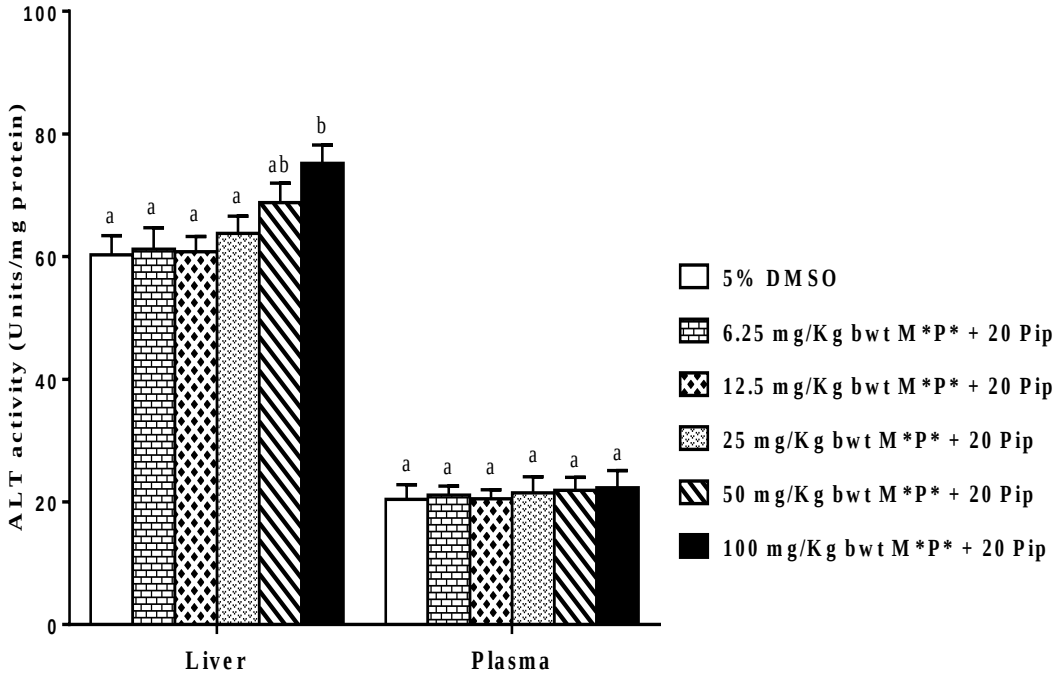

Figure 78: Effects of bio-enhanced combination of methyl gallate and palmatine on alanine aminotransferase activities in liver and plasma of rats

Values are means ± SEM of 5 replicates. Bars for liver/plasma with different alphabets are significantly different ($p<0.05$). **DMSO** = Dimethyl sulfoxide; **bwt** = body weight; **20 Pip** = 20 mg/Kg bwt Piperine; **M*P*** = 3:2 Methyl gallate and Palmatine (most active ratio from *in vitro* antimalarial study)

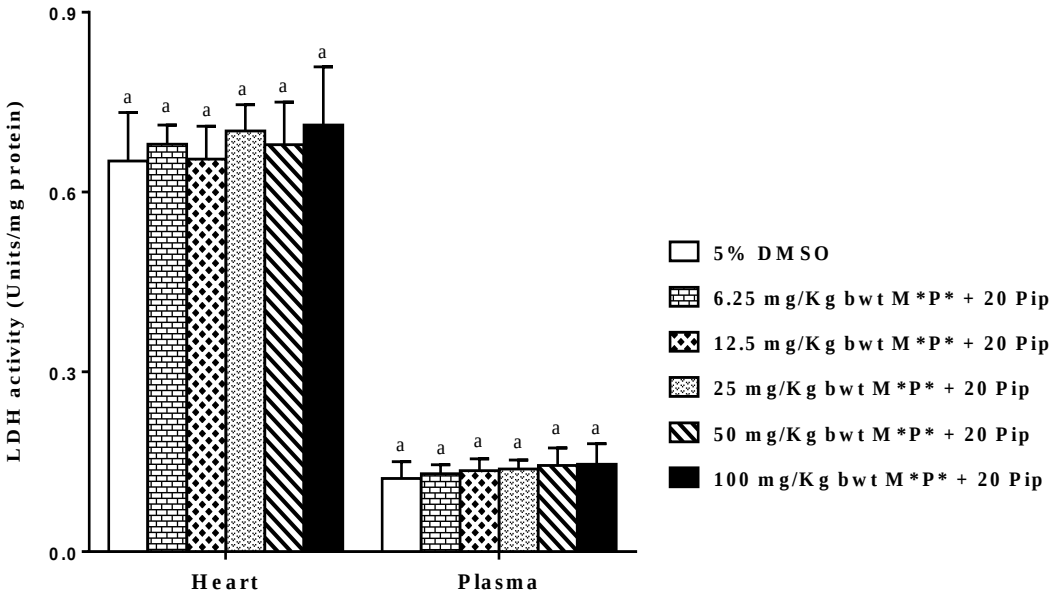

Figure 79: Effects of bio-enhanced combination of methyl gallate and palmatine on lactate dehydrogenase activities in heart and plasma of rats

Values are means ± SEM of 5 replicates. Bars for heart/plasma with similar alphabets are not significantly different ($p>0.05$). **DMSO** = Dimethyl sulfoxide; **bwt** = body weight; **20 Pip** = 20 mg/Kg bwt Piperine; **M*P*** = 3:2 Methyl gallate and Palmatine (most active ratio from *in vitro* antimalarial study)

4.3.3.6.6 Glutamate Dehydrogenase Activity

The glutamate dehydrogenase activities in the liver and plasma were not significantly altered ($p>0.05$) by the bio-enhanced combination of methyl gallate and palmatine at all doses compared to controls (Figure 80).

4.3.3.6.7 Malate Dehydrogenase Activity

The bio-enhanced combination of methyl gallate and palmatine at all doses caused no significant alteration ($p>0.05$) in malate dehydrogenase activity in the liver compared to control (Figure 81).

4.3.3.6.8 Creatine kinase Activity

The creatine kinase activities in the brain, heart and plasma were not significantly changed ($p>0.05$) by the bio-enhanced combination of methyl gallate and palmatine at all doses administered compared to controls (Figure 82).

4.3.3.6.9 Acetylcholinesterase Activity

Acetylcholinesterase activity in the brain of rats administered various doses of bio-enhanced combination of methyl gallate and palmatine was not significantly altered ($p>0.05$) compared to control (Figure 83).

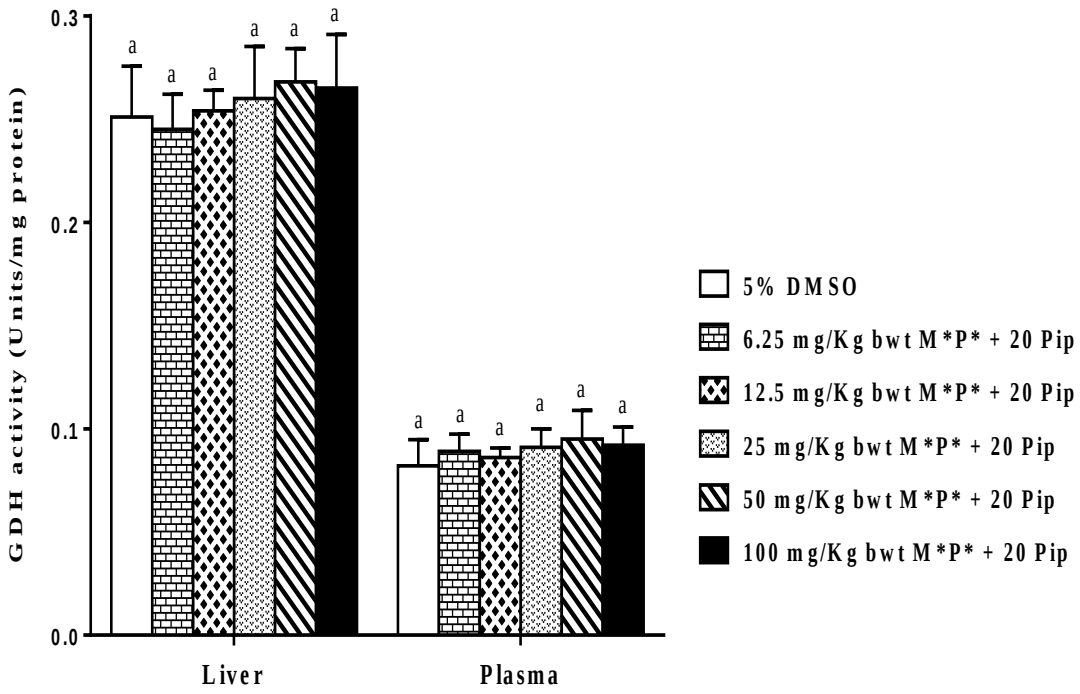

Figure 80: Effects of bio-enhanced combination of methyl gallate and palmatine on glutamate dehydrogenase activities in liver and plasma of rats

Values are means ± SEM of 5 replicates. Bars for liver/plasma with similar alphabets are not significantly different ($p>0.05$). **DMSO** = Dimethyl sulfoxide; **bwt** = body weight; **20 Pip** = 20 mg/Kg bwt Piperine; **M*P*** = 3:2 Methyl gallate and Palmatine (most active ratio from *in vitro* antimalarial study)

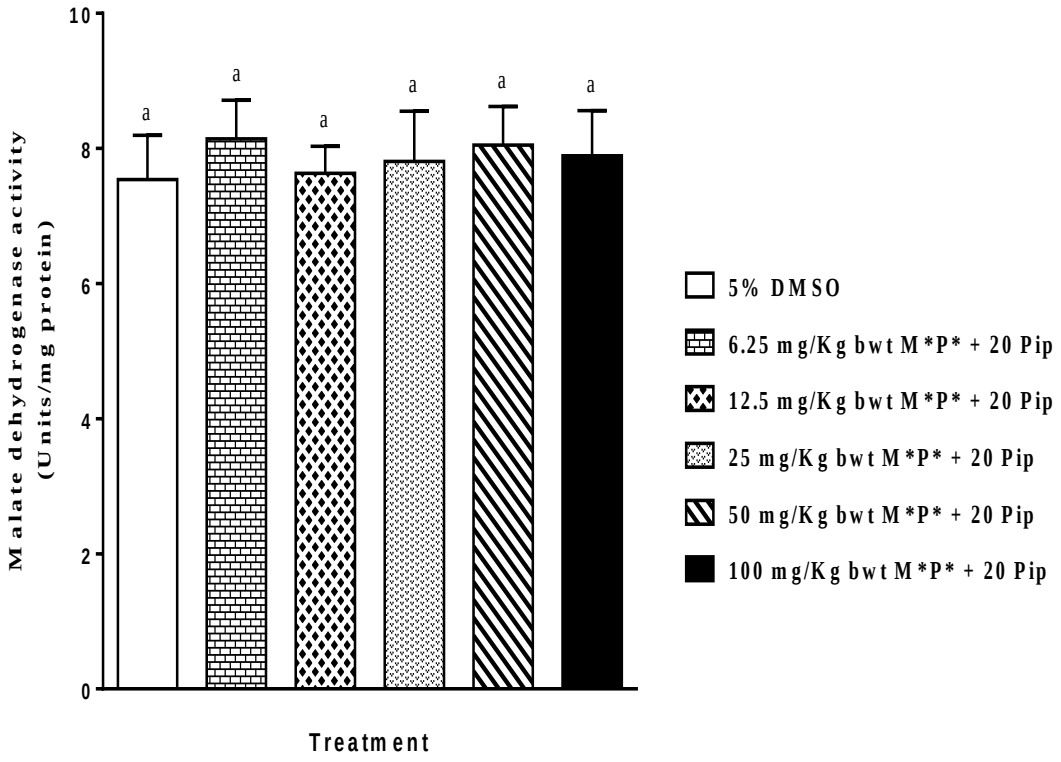

Figure 81: Effects of bio-enhanced combination of methyl gallate and palmatine on malate dehydrogenase activities in liver of rats

Values are means ± SEM of 5 replicates. Bars with similar alphabets are not significantly different ($p>0.05$). **DMSO** = Dimethyl sulfoxide; **bwt** = body weight; **20 Pip** = 20 mg/Kg bwt Piperine; **M*P*** = 3:2 Methyl gallate and Palmatine (most active ratio from *in vitro* antimalarial study)

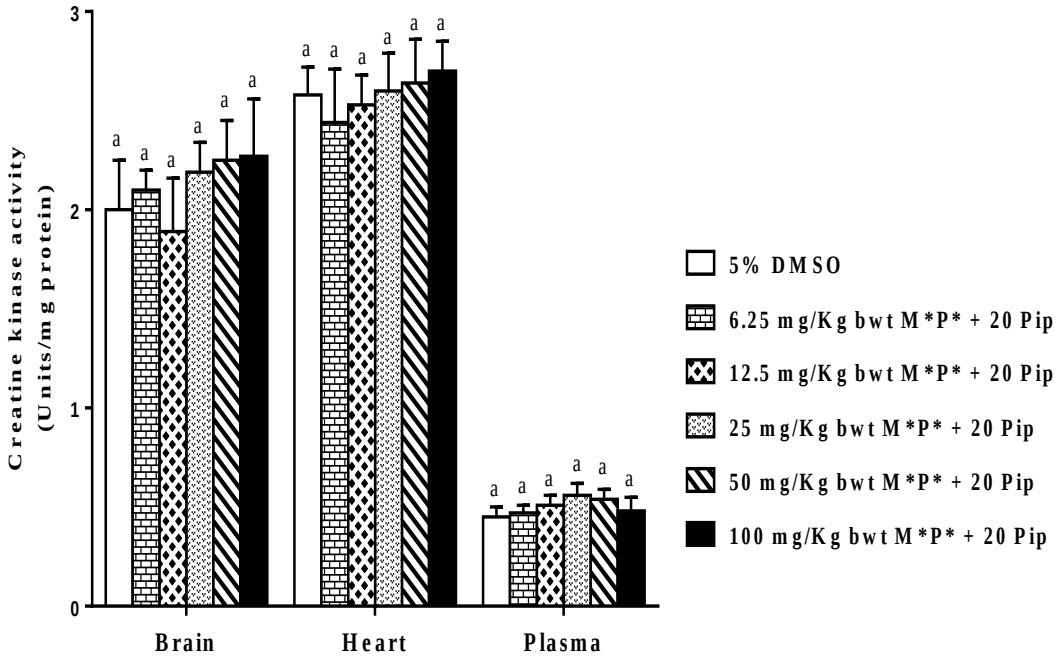

Figure 82: Effects of bio-enhanced combination of methyl gallate and palmatine on creatine kinase activities in brain, heart and plasma of rats

Values are means ± SEM of 5 replicates. Bars for each organ/plasma with similar alphabets are not significantly different ($p>0.05$). **DMSO** = Dimethyl sulfoxide; **bwt** = body weight; **20 Pip** = 20 mg/Kg bwt Piperine; **M*P*** = 3:2 Methyl gallate and Palmatine (most active ratio from *in vitro* antimalarial study)

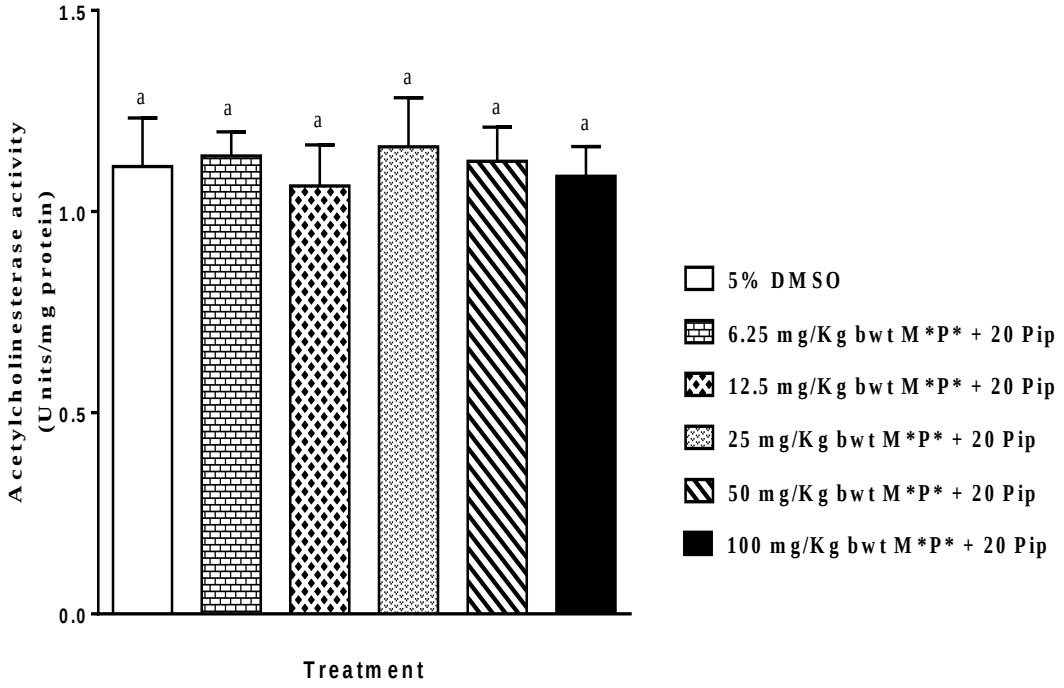

Figure 83: Effects of bio-enhanced combination of methyl gallate and palmatine on acetylcholinesterase activity in brain of rats

Values are means ± SEM of 5 replicates. Bars with similar alphabets are not significantly different ($p>0.05$). **DMSO** = Dimethyl sulfoxide; **bwt** = body weight; **20 Pip** = 20 mg/Kg bwt Piperine; **M*P*** = 3:2 Methyl gallate and Palmatine (most active ratio from *in vitro* antimalarial study)

4.3.3.6.10 ATPase Activities

4.3.3.6.10.1 4.3.3.6.10.1 Na^+,K^+-ATPase Activity

There was no significant change ($p>0.05$) in the activities of Na^+,K^+-ATPase in the kidney, heart and brain of rats administered various doses of bio-enhanced combination of methyl gallate and palmatine compared to controls (Figure 84).

4.3.3.6.10.2 Ca^{2+},Mg^{2+}-ATPase Activity

The bio-enhanced combination of methyl gallate and palmatine at various doses did not significantly alter ($p>0.05$) Ca^{2+},Mg^{2+}-ATPase activities in the kidney and brain compared to controls. Likewise, the bio-enhanced compound combination at doses lower than 100 mg/kg body weight caused no significant change ($p>0.05$) in Ca^{2+},Mg^{2+}-ATPase activity in the heart compared to control. However, 100 mg/kg body weight of the bio-enhanced compound combination significantly increased ($p<0.05$) heart Ca^{2+},Mg^{2+}-ATPase activity compared to control (Figure 85).

4.3.3.6.10.3 Mg^{2+}-ATPase Activity

The activities of Mg^{2+}-ATPase in the kidney, heart and brain of rats administered various doses of bio-enhanced combination of methyl gallate and palmatine were not significantly altered ($p>0.05$) compared to controls (Figure 86).

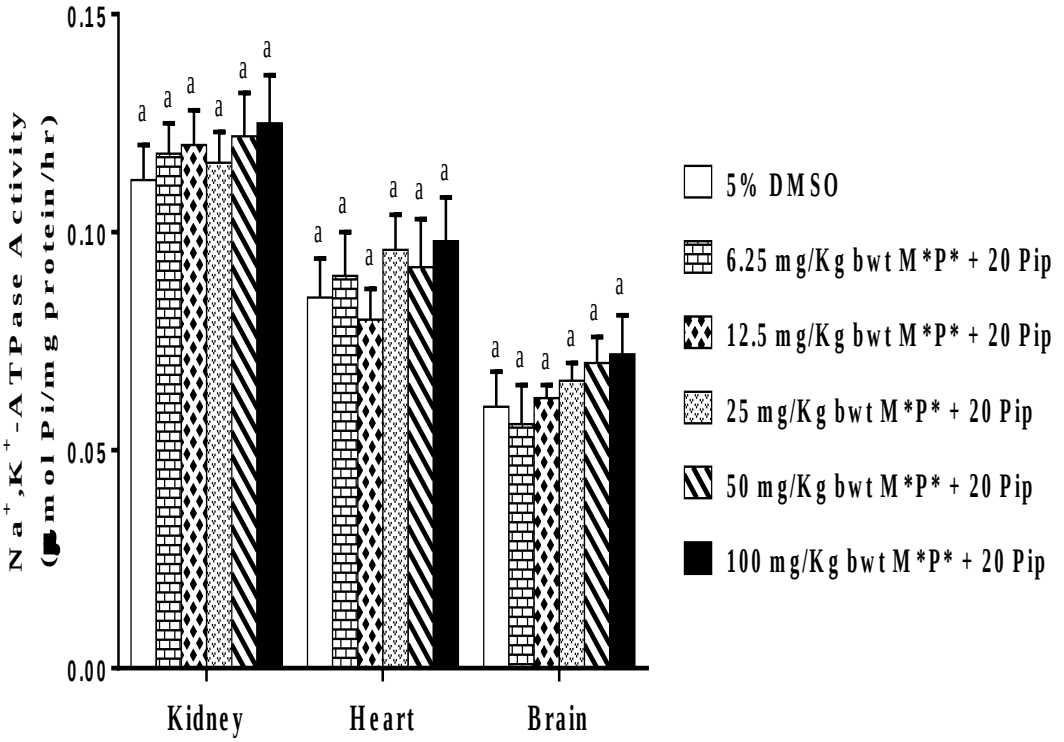

Figure 84: Effects of bio-enhanced combination of methyl gallate and palmatine on Na^+,K^+-ATPase activities in kidney, heart and brain of rats

Values are means ± SEM of 5 replicates. Bars for each organ with similar alphabets are not significantly different ($p>0.05$). **DMSO** = Dimethyl sulfoxide; **bwt** = body weight; **20 Pip** = 20 mg/Kg bwt Piperine; **M*P*** = 3:2 Methyl gallate and Palmatine (most active ratio from *in vitro* antimalarial study)

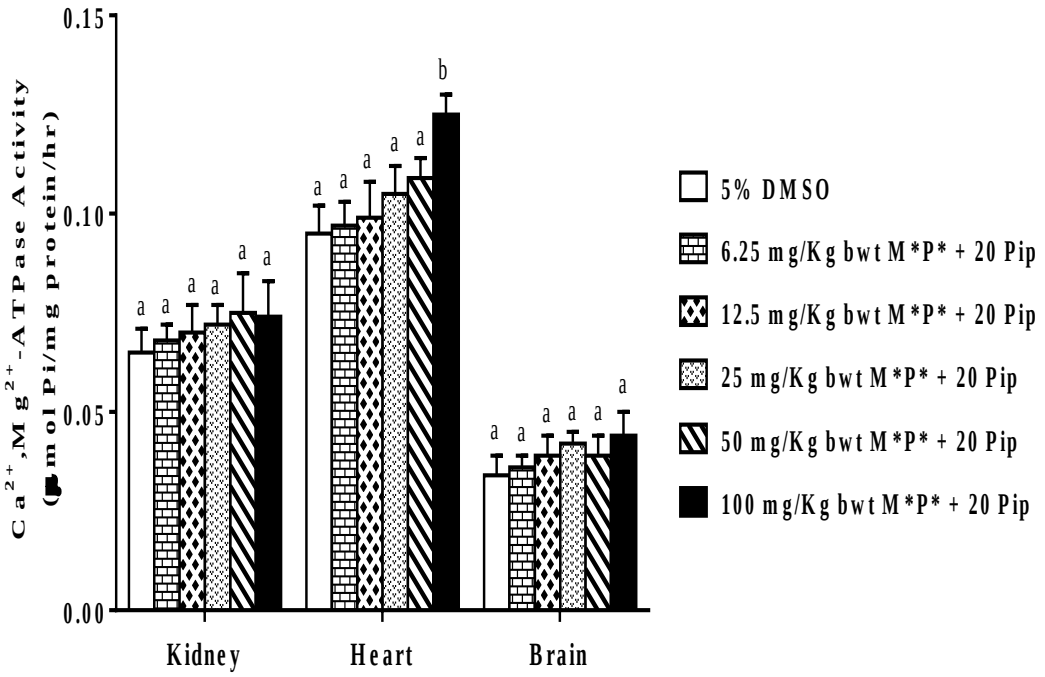

Figure 85: Effects of bio-enhanced combination of methyl gallate and palmatine on Ca^{2+},Mg^{2+}-ATPase activities in kidney, heart and brain of rats

Values are means ± SEM of 5 replicates. Bars for each organ with different alphabets are significantly different ($p<0.05$). **DMSO** = Dimethyl sulfoxide; **bwt** = body weight; **20 Pip** = 20 mg/Kg bwt Piperine; **M*P*** = 3:2 Methyl gallate and Palmatine (most active ratio from *in vitro* antimalarial study)

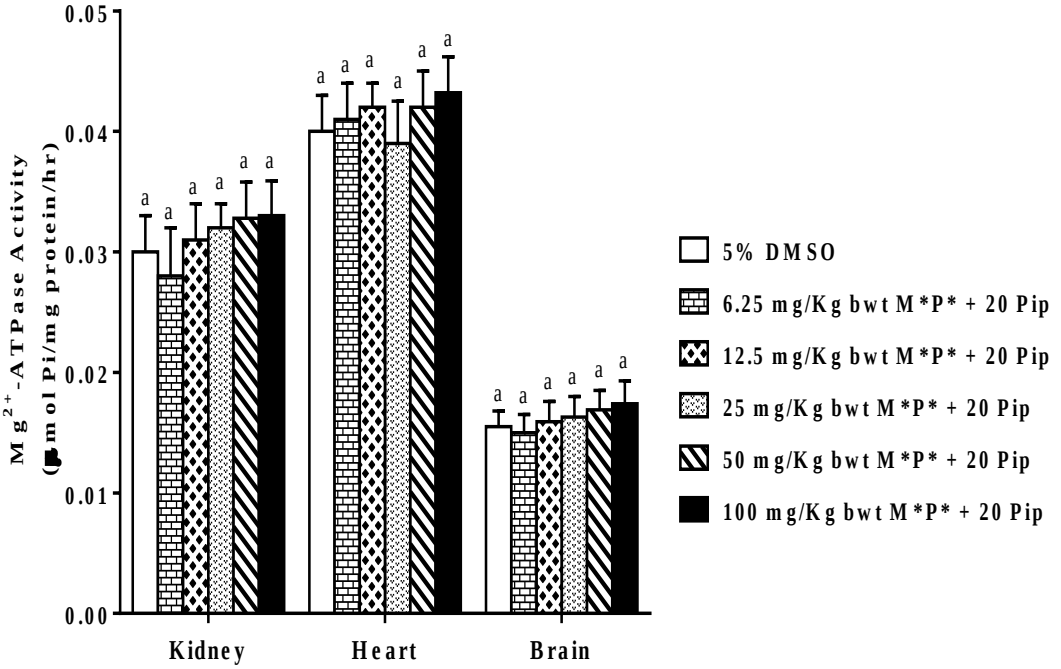

Figure 86: Effects of bio-enhanced combination of methyl gallate and palmatine on Mg^{2+}-ATPase activities in kidney, heart and brain of rats

Values are means ± SEM of 5 replicates. Bars for each organ with similar alphabets are not significantly different ($p>0.05$). **DMSO** = Dimethyl sulfoxide; **bwt** = body weight; **20 Pip** = 20 mg/Kg bwt Piperine; **M*P*** = 3:2 Methyl gallate and Palmatine (most active ratio from *in vitro* antimalarial study)

CHAPTER FIVE

5.0 DISCUSSION

5.1 Antimalarial Activity of Methyl gallate and Palmatine Combination

5.1.1 5.1.1 *In vitro* Antimalarial Activity and Interactions

The active degradation of erythrocyte's haemoglobin by *Plasmodium spp*. is to ensure the necessary supply of parasite with amino acids needed for protein synthesis. Haem, being the by-product of haemoglobin degradation, is toxic to the parasite, hence, its polymerization by the parasite to form hemozoin (Egan, 2008; e Silva *et al.*, 2015). Therefore, the inhibition of this process has been considered as a key mechanism of action of some clinically used antimalarial drugs. The ability of chemotherapeutic agents to inhibit the formation of β-hematin, the synthetic equivalent of hemozoin, therefore provides useful information regarding the mechanism of action of such compounds. Methyl gallate and palmatine, separately, inhibited the polymerization of hemin into β-haematin and this was synergistically so when combined at the ratio of 3:2 and 2:3 with more inhibition obtained at ratio 3:2. This goes to demonstrate that methyl gallate and palmatine combination could cause the build-up of haem within the food vacuole of *Plasmodium* spp., hence its toxicity to the parasite. Due to the fact that this metabolic process of haem polymerization is only essential to the parasite but not to the human host (Miller *et al.*, 2013), the synergistic inhibition of this process by the combination of methyl gallate and palmatine is noteworthy.

5.1.2 *In vivo* antimalarial Activity

The *in vitro* activities of methyl gallate and palmatine against multi-drug resistant strains of *Plasmodium* have been reported (Malebo *et al*., 2013; Zofou *et al*., 2013), but studies on their *in vivo* antimalarial activities yielded no significant result (Vennerstrom and Klayman, 1988) which prevented them from being considered for further antimalarial studies. Thus, the inactivity of methyl gallate and palmatine combination against *P. berghei* NK65 *in vivo* in the absence of a bio-enhancer in this study corroborates earlier findings of Vennerstrom and Klayman (1988). However, it was observed that the bio-enhanced form of the combination yielded significant antimalarial activity, especially in the suppressive antimalarial test. The improved *in vivo* activity of the combination of the pure molecules in the presence of piperine suggests that piperine was effective in increasing the bioavailability of the pure compounds. Synergism between components of a medicinal plant (e.g. propolis) extract has been suggested as the key reason why the unrefined extract has higher therapeutic activity than its individual active components (Amoros *et al*., 1992; Wagner and Ulrich-Merzenich, 2009). The results of the *in vitro* antimalarial studies revealed synergism as the nature of interaction between methyl gallate and palmatine at ratio 3:2. This finding therefore suggests an effective strategy of obtaining novel antimalarial combination therapies (apart from the artemisinin based combination therapies) which are potent and may delay the development of resistance by malaria parasite.

5.1.3 *In silico* interaction of compounds with selected proteins of *Plasmodium* species

Plasmodium sp. utilises proteases to degrade haemoglobin for its amino acids, and for detoxification. Plasmepsin I – V are some of these proteases which are found in the

digestive vacuole of the parasite. Plasmepsin I, II, IV and V are aspartic proteases while plasmepsin III is a histo-aspartic protease (Coronado *et al*., 2014). About 60% to 80% of globin degradation by *Plasmodium* species is carried out by aspartic proteases while 20–40% is performed by cysteine proteases (Francis *et al.,* 1997b). The degradation of haemoglobin by proteases is initiated by plasmepsin I which attacks the globin residue between α33Phe and 34Leu. This cleavage leads to the uncoiling of haemoglobin thereby opening sites where other aspartic proteases and cysteine proteases can attack (Goldberg *et al*., 1991). Compounds that inhibit these proteases interfere with the parasite's ability to degrade haemoglobin, consequently limiting the availability of amino acids necessary for parasite growth, and eventually causing the death of the parasite (Olson *et al.,* 1999; Jiang *et al.,* 2001). Results of these study revealed that palmatine has better binding affinity than methyl gallate and could be a better inhibitor of these proteases. While artesunate has better affinity for plasmepsin I, II, and IV compared to methyl gallate and palmatine, the affinity of artesunate and palmatine for plasmepsin III and V are similar. Both methyl gallate and palmatine interacted with various amino acids of plasmepsin I, II, III, IV, and V with strong binding affinities. These suggest that both methyl gallate and palmatine can bind tightly to these proteases and can consequently inhibit the activities of the enzymes degrading haemoglobin. This may limit the availability of amino acids needed for parasite growth and may cause early lysis of infected red blood cell resulting from colloid osmotic pressure exerted by the impermeant solutes, mostly haemoglobin, in the host cell cytoplasm (Ginsburg, 1990; Coronado *et al.,* 2014).

Peptides which are already cleaved by plasmepsins are further broken down into smaller fragments and amino acids by falcipain-2, a cysteine protease, of the parasite (Gluzman *et al.,* 1994). This action of falcipain-2 ensures availability of amino

acids for parasite growth and ensures that excess peptides from haemoglobin degradation are sufficiently small to be freely removed from the food vacuole, thereby creating space within the parasite and prevent osmotic swelling (Francis *et al.,* 1996). In this study, palmatine binds to falcipain-2 with similar affinity as artesunate and demonstrated better binding compared to methyl gallate. Both methyl gallate and palmatine interacted strongly with this cysteine protease and may cause inhibition of this enzyme. This could bring about accumulation of haemoglobin and peptides in the infected red blood cell, thereby causing osmotic swelling, lysis of the cell and the death of the parasite.

Plasmodium species relies on glycolysis for its supply of energy because its cytochromes are not functionally well organized to ensure oxidative phosphorylation (Planche *et al.*, 2005). Also, since host erythrocytes lack mitochondria, *Plasmodium* species depends on its lactate dehydrogenase (LDH) to regenerate NAD^+ which it needs to keep glycolysis ongoing (Mi-Ichi *et al.,* 2003). Therefore, inhibition of *Plasmodium* LDH results in limited or complete stoppage of ATP production and therefore the death of the parasite. Both methyl gallate and palmatine showed good interactions with *Plasmodium* lactate dehydrogenase, though with poorer binding relative to artesunate. Also, both methyl gallate and palmatine interacted with Ile31A which is one of the amino acids that NAD^+ present in the native *Pf*LDH (PDB ID: 1T2C) interacts with. These suggest that the compounds could inhibit the enzymes of the parasite, thereby limiting the generation of energy in the parasites.

5.2 Antioxidant Activities of Bio-enhanced Methyl gallate and Palmatine Combination

5.2.1 *In vitro* Antioxidant Activity

During oxidative phosphorylation, in metabolic processes, electrons do leak from the electron transport chain. These electrons interact with molecular oxygen to generate radical oxygen which further generates reactive oxygen species, such as hydroxyl radical, superoxide anion radical, peroxyl radical, which can cause oxidative damage to biomolecules like lipids, proteins and DNA (Speakman and Garratt, 2013). Though a biological system has ways of rendering reactive species harmless and has necessary mechanisms to prevent or repair damage resulting from these reactive species, they are sometimes overwhelmed by the rate of production of additional reactive species arising from pathological conditions such as malaria (Becker *et al*., 2004; Guha *et al*., 2006; Percário *et al*., 2012). This results in systemic complications, which could be salvaged by the antioxidant activity of administered compounds.

Based on type of chemical reactions involved, the *in vitro* antioxidant assays tend to measure the radical (or oxidant) scavenging capacity, rather than preventive antioxidant capacity of a sample and can loosely be categorised as hydrogen transfer reaction-based and electron transfer reaction-based (Huang *et al.,* 2005). The *in vitro* study revealed that the combination of methyl gallate and palmatine can scavenge DPPH (2,2-diphenyl-1-picrylhydrazyl) radicals better than butylated hydroxytoluene. On the contrary, ability of the 3:2 combination ratio of methyl gallate and palmatine to scavenge hydroxyl oxidant was lower compared to the reference compound. However, the ferric ion reducing power of the combination compared favourably well with that of the reference compound. These suggest that the combination of methyl gallate and palmatine can function to reduce oxidants via transfer of electrons and hydrogen

transfer reaction models. The radical scavenging capacity exhibited by the combination of methyl gallate and palmatine could serve to protect the host cells from effects of excessive radical while allowing sufficient radical availability to destroy the parasite.

Nitric oxide has been reported to serve in dual capacity as protective or harmful molecule in *Plasmodium* species-infected individual. High amounts of nitric oxide production could promote the death of the parasites, maintenance of blood brain barrier integrity, and resistance to severe malaria (Gramaglia *et al.,* 2006; Ong *et al*., 2013; Weinberg *et al*., 2014; Olivera *et al*., 2016) and in contrast could cause immune-suppression and cellular damage (Jaramillo *et al.,* 2003). The results of this study showed that the 3:2 combination ratio of methyl gallate and palmatine exhibited lower nitric oxide scavenging activity compared to butylated hydroxytoluene. Therefore, the compound combination could ensure that nitric oxide production is not excessive, and still preserve the role of nitric oxide in destroying malaria parasite.

Haemolysis results from malaria and this contributes to severe pathologies, including endothelial dysfunction (Kuhn *et al*., 2017). The combination of methyl gallate and palmatine demonstrated effective ability to protect from oxidative attack against erythrocyte and could possibly maintain the integrity of plasma membrane as revealed by its ability to inhibit conjugated diene formation induced by copper and prevent oxidative haemolysis induced by 2,2'-Azobis (2-amidinopropane) dihydrochloride. This suggest that severe pathologies associated with malaria could be attenuated by the combination of methyl gallate and palmatine.

5.2.2 *In vivo* Antioxidant Activity

Large number of oxidative by-products is produced in *Plasmodium* species - infected cells due to increased metabolic rate of rapidly multiplying parasite,

consequently resulting in antioxidant enzymes such as glutathione peroxidase, catalase and superoxide dismutase being reduced over time (Araujo *et al*., 2008; Steinbrenner and Sies, 2009). If the antioxidant system is overwhelmed, then the biological system goes into state of oxidative stress. Oxidative stress in malaria can be caused by activities of the parasite such as reproduction and degradation of host haemoglobin. Also, the host immune response which initiate series of defense mechanisms through release of radicals can also result in oxidative stress (Kawazu *et al.*, 2008; Kapoor and Banyal, 2009; Fabbri *et al*., 2013).

Increased lipid peroxidation, resulting from oxidative damage of cells by reactive oxygen species, is usually associated with cases of malaria (Das and Nanda, 1999) and this may affect the membrane of both infected and uninfected erythrocytes (Omodeo-Sale *et al*., 2003). Results from this study revealed that lipid peroxidation, measured by the level of malondialdehyde, increased in erythrocyte, liver, heart and kidney of *Plasmodium berghei* NK65-infected mice, on day 8 post-inoculation, suggesting the damaging effect of the infection on host cell plasma membrane. Also, these results corroborate an earlier report that chloroquine (another antimalarial) induces lipid peroxidation in cells (Farombi *et al.,* 2003). However, treatment of *Plasmodium berghei* NK65-infected mice with bio-enhanced combination of methyl gallate and palmatine significantly protected against the peroxidation caused by the parasite in the selected tissues. Erythrocyte membrane is particularly susceptible to reactive oxygen species attack given its high content of polyunsaturated fatty acids (Niki, 2009). The increased levels of malondialdehyde in the tissues of *Plasmodium berghei* NK65-infected mice is an indication of reactive oxygen species attack on the plasma membrane of cells in these tissues. The malondialdehyde generated can react with protein thiols in membrane to induce more damage (Niki, 2009), thereby

adversely affecting the integrity of plasma membrane which may result in cellular dysfunction and leakage of cellular contents. The bio-enhanced compound combination was able to revert the increased malondialdehyde concentrations in the tissues of infected mice to the range of the controls in most cases. This suggests that the bio-enhanced combination of methyl gallate and palmatine may be well suited for alleviating the oxidative stress associated with malaria, due to its free radical scavenging activities (Fig. 12-15).

Superoxide dismutase forms the first line of enzymatic antioxidant defense mechanism against reactive species. While superoxide dismutase catalyses the dismutation of superoxide into oxygen and hydrogen peroxide, catalase catalyses the formation oxygen and water from the hydrogen peroxide, and glutathione peroxidase utilises reducing equivalents from reduced glutathione (GSH) to catalyse the two-electron reduction of peroxides into water (Lei *et al*., 2016). While the removal of hydrogen peroxide from cells by catalase requires high intracellular concentration of hydrogen peroxide for substantial activities, glutathione peroxidase can effectively function even at lower concentration of hydrogen peroxide (Makino *et al.*, 1994). The activities of superoxide dismutase, catalase and glutathione peroxidase in the erythrocyte and tissues were reduced by *P. berghei* NK65-infection in this study. However, treatment with bio-enhanced combination of methyl gallate and palmatine increased the activities of these antioxidant enzymes in the various tissues studied compared to untreated infected controls, restoring the antioxidant enzyme activities to the range of the uninfected controls, especially at higher doses. The activities of catalase and glutathione peroxidase limit the accumulation of hydrogen peroxide in cells. Hydrogen peroxide, being a product of superoxide dismutase activity, could be utilised in a Fenton reaction to generate hydroxyl radical which is highly reactive.

However, the activities of catalase and glutathione peroxidase prevent/limit this by catalysing the conversion of hydrogen peroxide into water and oxygen (Panduru *et al*., 2010; Kavishe *et al.,* 2017). Treatment of *P. berghei* NK65-infected mice with bio-enhanced combination of methyl gallate and palmatine augmented the activities of superoxide dismutase, catalase and glutathione peroxidase in the various tissues studied, either by activating the enzymes *in situ* or inducing their synthesis. These suggest that both superoxide radical and hydrogen peroxide, which are capable of oxidising biological molecules, thereby causing alteration in normal cell functions (Raza *et al*., 2015), are scavenged by the bio-enhanced compound combination. Therefore, the bio-enhanced combination of methyl gallate and palmatine appears to be able to preserve the antioxidant capacity of the tissues, especially at higher doses.

The functionality of glutathione peroxidase is in close association with those of glutathione reductase (Flohe *et al*., 2011). Glutathione reductase maintains a reduced intracellular environment by regenerating reduced glutathione (GSH) from oxidized glutathione (GSSG) utilising NADPH. While glutathione reductase does not scavenge reactive species, its activity is essential for the regeneration of reduced glutathione which, in turn, is essential for defense against oxidative stress in cells (Muller, 2004; Kim *et al.,* 2010; Flohe *et al*., 2011; Tripathy *et al.,* 2014). The infection of mice with *P. berghei* NK65 caused reduction in the activities of glutathione reductase in tissues studied compared to uninfected controls. Likewise, treatment of infected mice with chloroquine resulted in reduction in the activities of this enzyme in the erythrocyte, liver, heart and kidney. However, treatment with bio-enhanced combination of methyl gallate and palmatine protected against this reduction in enzyme activity in the erythrocyte, liver, heart and kidney, especially at the higher doses of 12.5, 25, and 50 mg/Kg body weight. The activity of glutathione reductase is usually increased by the

presence of small quantity of oxidants as a way of maintaining homeostasis (Kim *et al.,* 2010). However, this observed reduction in the activities of enzymes of *P. berghei* NK65-infected mice and chloroquine-treated mice suggest reduction in the level of its substrate (GSH), inactivation of the enzyme *in situ* or suppression of the synthesis of the enzyme.

Reduced glutathione (GSH) is an essential cofactor of glutathione peroxidase whose function is detoxification of peroxides. It is important to biological systems both as component of their antioxidant defense systems and as direct scavenger of reactive species (Tripathy *et al.,* 2014). In this study, the levels of GSH in cell/tissues, especially erythrocytes, liver and kidney, of *P. berghei* NK65-infected mice were reduced compared to uninfected control. This result corroborates earlier findings that the presence of *Plasmodium* species cause significant reduction in the concentration of GSH, which is one of the main antioxidants in biological systems (Zanini *et al.,* 2012). This reduction in GSH level was also observed in *P. berghei*-infected mice treated with chloroquine. This is fairly expected as antimalarial agents such as chloroquine and primaquine are known to act by oxidative stress through production of high amount of reactive oxygen species, causing depletion of reduced glutathione and consequently opposing effects of antioxidants that depend on reduced glutathione (Beutler, 1994; Platel *et al*., 1999). However, with bio-enhanced combination of methyl gallate and palmatine maintained the reduced glutathione concentration in tissues in the range of uninfected controls. The reduced level of GSH observed in tissues of *P. berghei*-infected mice and chloroquine-treated mice may be due to the increased lipid oxidation occasioned by increased generation of reactive oxygen species, leading to possible reduction in the level of NADPH which glutathione reductase requires for its activity to form GSH. However, treatment with bio-enhanced

combination of methyl gallate and palmatine reverted the reduced GSH level back to the range of the uninfected controls, suggesting that the bio-enhanced compound combination may be able to maintain the ratio of GSH to GSSG in a direction that favours GSH, hence the availability of this antioxidant to perform its cellular functions.

Glutathione-S-transferase is involved in phase II xenobiotic metabolism and responsible for catalysing conjugation of GSH thiolate anions to electrophiles, to yield compounds which are more soluble and can easily be excreted (Gemma *et al*., 2006). Hence, toxic electrophiles in cells are detoxified by activities of this enzyme during reductive reactions and oxidised glutathione (GSSG) is produced (Sampayo-Reyes and Zakharyan, 2006; Tripathy *et al.*, 2014). In this study, *P. berghei*-infection and its treatment with chloroquine caused reduction in activities of glutathione-S-transferase. Due to the reduced ability to properly manage oxidative stress induced by *Plasmodium species*, impaired activity of glutathione-S-transferase is said to influence severity of malaria (Kavishe *et al*., 2006). Glutathione S-transferases have been reported to reduce lipid hydroperoxides through their Se-independent glutathione-peroxidase activity and can also detoxify lipid peroxidation end-products such as 4-hydroxy-2-trans-nonenal (Singhal *et al*, 2015). Treatment of *Plasmodium* species infection with bio-enhanced combination of methyl gallate and palmatine, however, protected against the observed reduction in GST activities in the tissues of infected mice. This therefore suggests that the bio-enhanced combination may preserve the detoxification and antioxidant functions of glutathione-S-transferase in cases of malaria.

In summary, the observed alterations in concentration/activities of antioxidant proteins during malaria episodes and treatment suggest that they are essential for biological systems to bear the burden of elevated oxidative stress associated with

Plasmodium species infection. This further suggests that the change in concentrations/activities of antioxidant proteins may indictate the severity of malaria. The reduction observed in the concentrations/activities of antioxidants in the erythrocyte and tissues of *P. berghei*-infected mice suggest impaired antioxidant defense arising from the multiplication and metabolic activities of the parasite, resulting in overwhelming production of oxidants. However, the antioxidants in tissues of infected mice treated with bio-enhanced combination of methyl gallate and palmatine were augmented, especially at higher doses, suggesting the ability of the compound combination to handle oxidative stress which could arise from malaria.

5.3 Toxicological Studies

The use of some potent chemotherapeutic agents is limited due to their toxic side effects (Prasaja *et al*., 2015). The safety or toxicity of bio-enhanced combination of methyl gallate and palmatine was therefore assessed using animal model.

5.3.1 Organ-Body Weight Ratio

Change in organ-body weight ratio is a sensitive indication of chemically or pathologically induced alterations in organs and determination of this ratio enables the assessment of alteration in size of an organ relative to the body weight of the biological subject (Adebayo *et al*., 2003; Michael *et al.*, 2007; Sellers *et al*., 2007). Increase in organ body weight ratios of liver and heart may suggest hepatocellular hypertrophy and myocardial hypertrophy respectively while kidney weight increase may suggest renal toxicity, or tubular hypertrophy (Amacher *et al*., 2006; Juberg *et al*., 2006; Greaves, 2012). The bio-enhanced methyl gallate and palmatine combination caused no significant alteration in organ- body weight ratios of brain, heart, kidney and liver. This suggest that the bio-enhanced compound combination neither caused inflammation nor constriction of these organs.

5.3.2 Haematological indices

Anaemia is a pathological condition characterized by decrease in the number of circulating erythrocytes and defined by low haemoglobin (Hb) concentrations in whole blood (WHO, 2011). Anaemia could arise from increased rate of erythrocyte destruction and/or impaired synthesis of haem (Shah *et al.,* 2010). While erythrocyte destruction could result from haemoglobin oxidation by compounds, inhibition of enzymes essential for haematopoiesis could cause impaired synthesis of haem (Sharma *et al*., 2012; Azab *et al.*, 2013). Change in haematological parameters could alter the functions of blood components. In this study, the RBC, haemoglobin concentration, PCV, MCHC, MCH and MCV were not altered by administration of the bio-enhanced combination of methyl gallate and palmatine. The RBC, Hb and PCV are indices associated with the total population of erythrocytes in the blood while MCHC, MCH and MCV are indices that are associated with individual erythrocyte (Adebayo *et al*., 2005). The results suggest that the compound combination neither impaired the synthesis of haemoglobin nor resulted in anaemia and did not alter the morphology and osmostic fragility of erythrocyte. Hence the respiratory gas-carrying capacity of the blood was not altered.

White blood cells also called leucocytes develop from undifferentiated stem cells in the bone marrow and provide immunity to the biological system (Houseman *et al.,* 2012). Their production is regulated by growth factors such as granulocyte- and granulocyte-macrophage colony-stimulating factors (Hercus *et al.,* 2009). The composition of white blood cell population mirrors the disease states and/or exposures of a biological system to toxicant (Houseman *et al.,* 2012). The results from this study revealed that there was no change in the white blood cell count of rats administered bio-enhanced combination of methyl gallate and palmatine compared to control. This

suggest that production of white blood cells was not impaired and the ability of the biological system to fight infections was not compromised. Also, lymphocytes and neutrophils play crucial roles in chronic (or adaptive) and acute inflammation respectively (Shrivastava and Bhatia, 2010). The administration of the bio-enhanced combination resulted in no alteration in the levels of lymphocytes and neutrophils in the blood except at 50 mg/kg body weight of the combination, where increased level of lymphocytes was observed with a corresponding reduction in the level of neutrophils. These suggest that adaptive and innate immune systems were conserved except at 50 mg/kg body weight of the compound combination, at which the immune system of the rats appeared to shift from phagocytic immune response to humoral immune response.

Platelets function to stop haemorrhage at the site of broken endothelium by contributing to vessel constriction and repair and host defense (Paniccia *et al*., 2015). Anaemia, inflammation, or infection may cause elevated platelet level while reduction in platelet level could result from inhibition of platelet synthesis by drugs, foods, kidney infections or dysfunction (George, 2000). Platelets are connected to the pathogenesis of inflammatory diseases such as malaria and atherosclerosis (Morrell *et al.,* 2014) and its reduction and elevation have been reported in cases of malaria (Kakar *et al.,* 1999; McMorran *et al.,* 2009). The administration of bio-enhanced combination of methyl gallate and palmatine did not alter the platelet count. This suggests that the compound combination did not inhibit platelet formation, neither did it adversely affect its roles in host defense. Hence, its immune effects both locally at activation sites and systemically at locations away from activation sites (Morrell *et al.,* 2014) were preserved.

5.3.3 Liver Function Indices

The liver function indices evaluated in this study are routine biochemical indices used in the diagnosis of liver pathologies resulting from exposure to drugs and chemicals. They are elevated or reduced in plasma following hepatic dysfunction.

The total protein content of the plasma is majorly made up of albumin and globulin. Alteration in the level of total protein of a tissue gives insight into functional changes that possibly occurred in such tissue. Reduction in the level of total protein in organs with corresponding rise in plasma could imply cellular damage or toxicity in those organs (Kaneko *et al.,* 1997). Plasma albumin binds and transport many sparingly soluble metabolic products such as fatty acids, unconjugated bilirubin and xenobiotics in blood and helps in maintaining the osmotic pressure of cells (Metzler, 2003; Snider *et al.,* 2010). Reduction in plasma level of albumin is an indication of impaired synthesis of albumin arising from weakened liver function (Zargar *et al.,* 2016) and such reduction causes accumulation of fluids in interstitial spaces resulting in oedema (Arneson and Brickell, 2007a). Globulins act as transport molecules and perform immune functions. The plasma level of globulin (especially the immunoglobulin fraction) is raised after a biological system is exposed to antigen, thereby acting as an indicator of immune response (Timbrell, 2009). In this study, the administration of bio-enhanced combination of methyl gallate and palmatine, at various doses, caused no significant alteration in the plasma concentrations of total protein, albumin and globulin compared to controls. These suggest that the synthetic capability of the liver was preserved as well as the availability of these biomolecules to perform their cellular roles of immunity, transport and osmotic pressure control.

The degradation of iron-free porphyrin portion of haem in the reticuloendothelial cells yields bilirubin which is a lipid-soluble pigment that binds noncovalently to albumin to increase its solubility in the plasma and serves as a biomarker of hepatic function (Awad Jr., 2010). Bilirubin remains in cells until rendered water-soluble through conjugation by a specific transferase which is primarily located in the endoplasmic reticulum and the conjugated bilirubin is readily excreted in the bile (Vítek and Ostrow, 2009). Elevated plasma levels of bilirubin could be due to overproduction resulting from excessive degradation of haem (prehepatic hyperbilirubinemia) or decreased conjugation culminating in failure of its excretion due to liver damage caused by diseases or xenobiotics (hepatic hyperbilirubinemia). Likewise, obstruction of the excretory ducts of the liver (extrahepatic cholestasis) can also result in hyperbilirubinemia, that is posthepatic hyperbilirubinemia (Ferrier, 2014). The administration of bio-enhanced combination of methyl gallate and palmatine, at various doses, caused no alteration in plasma concentrations of total bilirubin and conjugated bilirubin except at the dose of 100 mg/kg body weight at which there was increase in conjugated bilirubin concentration compared to controls. These suggest that the compound combination did not cause haem degradation and that the conjugation functions of hepatic cells were not altered. However, obstruction of hepatobiliary ducts may not be the reason for the increase in conjugated bilirubin concentration in the plasma at 100 mg/Kg body weight of the compound combination, because hepatobiliary obstruction which is primarily signified by increased conjugated bilirubin level is always accompanied with an increase in the activities of gamma-glutamyl transferase and alkaline phosphatase in the plasma (Arneson and Brickell, 2007a). The increased conjugated bilirubin level suggests that its synthesis in the liver occurs at a faster rate than its secretion into the bile duct.

Tissue damage results in the release of some enzymes into the plasma. A mild and reversible cellular alteration such as inflammation results in increased permeability of cell membrane, hence, cytoplasmic enzymes could be released into extracellular fluid whereas a much higher alteration or cellular death could result in release of organelle-based enzymes such as mitochondrial enzymes into extracellular fluid (Brickell *et al.*, 2007).

Alkaline phosphatase is a membrane-bound enzyme found in hepatobiliary tissues and cytoplasmic membranes of cells. It generates inorganic phosphate ions from organic phosphate esters and can serve as biomarker in assessing the integrity of membrane (Panteghini and Bais, 2008; Johnson-Davis and McMillin, 2010). Gamma-glutamyl transferase catalyses the transfer of gamma-glutamyl functional group from glutathione to an acceptor, such as amino acid. They are concentrated in hepatobiliary ducts cells and endoplasmic reticulum of hepatocytes and their activities are elevated in plasma in various hepatobiliary diseases (Murray, 2012). The results from this study revealed that the administration of bio-enhanced combination of methyl gallate and palmatine, at various doses, caused no alteration in the activities of alkaline phosphatase and gamma-glutamyltransferase both in the liver and plasma of rats. These suggest that membranes of the hepatocytes were not damaged, and the compound combination may not cause hepatobiliary obstruction.

Aminotransferases are intracellular enzymes with alanine aminotransferase being more hepatocyte-specific than aspartate aminotransferase. They are pyridoxal phosphate-requiring enzymes that function in amino acid biosynthesis, catalysing the transfer of amino group from an amino acid to an α-keto acid, thereby forming another amino acid (Metzler, 2003). Hepatic damage results in their elevated activities in the blood. Hence, decreased activities of these enzymes in liver with concomitant rise in

blood suggest damage of hepatic cells (Honda *et al*., 2010; Rosenthal and Glew, 2011). The bio-enhanced combination of methyl gallate and palmatine, at various doses, caused no alteration in the activities of aspartate and alanine aminotransferases both in the liver and plasma except at 50 and 100 mg/kg body weight compared to controls. The compound combination caused increased aspartate aminotransferase activity in liver at 50 and 100 mg/kg body weight and caused increased alanine aminotransferase activity in liver at 100 mg/kg body weight compared to controls. The elevation of the activities of these enzymes in the liver at the higher doses without corresponding change in their activities in the plasma suggest that this compound combination may induce synthesis of the enzymes or activate them *in situ* at higher dosages rather than causing their leakage into the plasma from the liver.

The amino group of glutamate is removed as NH_4^+ during oxidative deamination reaction catalysed by glutamate dehydrogenase, a mitochondrial enzyme. The enzyme also catalyses the reductive amination of α-ketoglutarate to form glutamate (Rosenthal and Glew, 2011) which is favoured by high cellular energy level while low cellular energy level favours the oxidative deamination reaction to form α-ketoglutarate (Coomes, 2010). The activity of the enzyme could serve to supply the tricarboxylic acid cycle with α-keto acids, and to remove ammonia from circulation for synthesis of urea. Meanwhile, malate dehydrogenase is both cytosolic and mitochondrial enzyme that catalyses reversible conversion of malate and oxaloacetate. Mitochondrial malate dehydrogenase is essential for both gluconeogenesis and the tricarboxylic acid cycle with corresponding drift of metabolites in reverse directions in the two processes (Nelson and Cox, 2013). The bio-enhanced combination of methyl gallate and palmatine at various doses did not cause alteration in glutamate dehydrogenase activities in the liver and plasma, suggesting that the compound

combination did not cause mitochondrial damage in the liver. Likewise, the malate dehydrogenase activity in liver was not altered, suggesting that the roles of its product (oxaloacetate) in the TCA cycle and gluconeogenesis in the liver were not be compromised by the compound combination. This still lends credence to the submission that the integrity of the mitochondria in the liver may not be compromised by the compound combination.

5.3.4 Renal Function Indices

Renal function can be evaluated through indicators such as plasma creatinine, urea and uric acid levels. Due to lack of arginase, the kidney cannot synthesise urea (Rosenthal and Glew, 2011). However, they are synthesized in the liver from nitrogenous compounds and transported to the kidney for elimination in urine. Also eliminated by the kidney are creatinine and uric acid which are nitrogenous breakdown products of muscle creatine phosphate and purine catabolism respectively (Rosenthal and Glew, 2011). Therefore, plasma creatinine and urea levels are biomarkers for assessing filtration functionality of the kidney with creatinine levels being a more sensitive tool (Sharma *et al*., 2011; Mohamed and Wakwak, 2014) because elevated urea level could be influenced by increased protein breakdown or amplified conversion of ammonia to urea. Compromised functionality of the kidney could result in excessive build-up of creatinine, urea and uric acid in the circulatory system (Laskshmi and Sudhakar, 2010; Sefidan and Mohajeri, 2013). The bio-enhanced combination of methyl gallate and palmatine, at various doses, had no effect on the plasma concentrations of creatinine, urea and uric acid compared to controls except at the dose of 50 mg/kg body weight at which plasma concentration of urea was increased. These suggest that the glomerular filtration in the kidney was not compromised by the compound combination. However, the observed increase in urea level at the dose of 50

mg/kg body weight of the compound combination suggest amplified conversion of ammonia to urea rather than renal dysfunction since creatinine and uric acid, which are other sensitive indicators of glomerular filtration, were not altered.

The kidney regulates the electrolyte composition of blood and imbalance of these electrolytes may signal renal insufficiency (Kirk and Horner, 1995). In this study, administration of bio-enhanced combination of methyl gallate and palmatine caused no alteration in plasma levels of Na^+, K^+, Cl^-, HCO_3^- and PO_4^{3-} at all doses considered compared to controls. Likewise, the compound combination did not cause alteration in plasma levels of Ca^{2+} at doses lower than 100 mg/kg body weight but reduced it at 100 mg/kg body weight compared to control. These suggest that the administration of the bio-enhanced compound combination may not alter the osmoregulatory function of the kidney especially at the lower doses. The results also suggest that the combination may not complicate reduction in plasma electrolytes levels which are associated with malaria (Tiffert *et al*., 2000; Yoel, 2007; Jasani *et al*., 2012). However, the highest dose considered in this study may pose a threat to Ca^{2+} homeostasis as the observed reduction may lead to elevated neuromuscular excitability and muscle paralysis (Faridi and Weisberg, 2008; Schafer and Shoback, 2013).

The presence of alkaline phosphatase and gamma-glutamyltransferase in the plasma membrane of renal tubular cells (Murray, 2012) could serve as a “marker” of integrity of the renal cells. The administration of bio-enhanced combination of methyl gallate and palmatine, at various doses, did not cause any change in activities of alkaline phosphatase and gamma-glutamyltransferase in both kidney and plasma. These suggest that the cellular membranes of the kidney cells were not disrupted. Hence, the compound combination may not affect the role of alkaline phosphatase in releasing inorganic phosphate which is essential for proper functioning of renal cells.

Likewise, the function of renal gamma-glutamyl transferase in the metabolism of glutathione may not be compromised.

The Na^+-K^+ ATPase is a plasma membrane-bound pump, that maintains the gradient of sodium and potassium ions between extracellular and intracellular settings, thereby serving to control cellular resting membrane potential (Doi and Iwasaki, 2008). When Na^+-K^+ ATPase is inhibited by compounds such as ouabain, Mg^{2+} ATPase swaps their action by utilising magnesium ion to sustain energy metabolism and maintain membrane potential (Ravindran *et al.*, 2012). Similarly, the Ca^{2+}-Mg^{2+} ATPase is a membrane-bound enzyme responsible for maintaining intracellular calcium ion homeostasis through active transport (Gutierres *et al.*, 2014). Inhibition of the activities of these enzymes could result in renal abnormalities and cell death (Geering, 1994; Ravindran *et al.*, 2012). The administration of bio-enhanced combination of methyl gallate and palmatine, at various doses, did not cause alteration in the activities of Mg^{2+} ATPase, Ca^{2+}-Mg^{2+} ATPase, and Na^+-K^+ ATPase in the kidney compared to controls. These suggest that the compound combination may not impair ATP metabolism and membrane potential of the kidney. Therefore, the compound combination may not compromise the active transport of sodium and calcium ions in the kidney. Na^+-K^+ ATPase plays a very important role at the brush border membrane in the kidney during the reabsorption of Na^+ into the blood.

5.3.5 Cardiovascular Indices

Plasma lipoproteins are mixed clusters of lipid–protein complexes which are synthesized in both intestine and liver (Snider *et al.*, 2010). Alterations in the levels of total cholesterol, LDL cholesterol, HDL cholesterol and triacylglycerol are primary risk factors of atherosclerosis (As *et al.*, 2013; Nemati *et al.*, 2013). Increased rate of

triacylglycerol synthesis and VLDL production results in reduced level of HDL and increased level of LDL and density (Toledo *et al.*, 2006). Meanwhile, reduction in HDL cholesterol concentration and concomitant rise in LDL cholesterol level increase the risk of coronary heart disease (Nader *et al.*, 2008). Atherogenic index computed as ratio of total cholesterol to HDL-cholesterol is also a vital pointer to cardiovascular disease predisposition (Naghii *et al*., 2011; Adebayo *et al*., 2013). The bio-enhanced combination of methyl gallate and palmatine, at different doses, did not cause alteration in plasma concentrations of total cholesterol and triacylglycerol, but caused reduction in plasma LDL cholesterol concentration with corresponding elevation in plasma HDL cholesterol concentration compared to controls. It also caused reduction in atherogenic index, at various doses above 6.25 mg/kg body weight compared to controls. These suggest that the bio-enhanced combination of methyl gallate and palmatine may not predispose subjects to cardiovascular diseases.

Assessment of the membrane integrity via evaluation of alkaline phosphatase activity showed that the bio-enhanced combination of methyl gallate and palmatine did not bring about alteration in the activities of this enzyme both in the heart and plasma compared to controls. This suggests that the structural integrity of the membranes of heart cells were not compromised.

When the flow of blood to heart tissue is limited, the amount of oxygen that gets to heart is also restricted and this can cause pain while complete stoppage of blood flow to the heart muscle results in cell death, necrosis and myocardial infarction (Gorman, 2007). Elevated activity of creatine kinase in plasma is a marker of myocardial infarction (Rosenthal and Glew, 2011). Cellular damage to heart muscle fibres brings about release of creatine kinase, lactate dehydrogenase and aspartate aminotransaminase into the bloodstream (Costa *et al.*, 2001; Gorman, 2007). In this

study, the activities of creatine kinase, lactate dehydrogenase and aspartate aminotransferase, both in the heart and plasma, were not changed by the bio-enhanced combination of methyl gallate and palmatine at various doses compared to controls. These suggest that the compound combination may not cause in cellular damage and leakage of these enzymes into the bloodstream. Thus, it may not cause myocardial infarction.

The effects of the bio-enhanced ccmpound ombination on activities of plasma membrane-bound ATPases of cardiac cells were also evaluated. The bio-enhanced combination of methyl gallate and palmatine, at the various doses considered, did not alter the activities of Mg^{2+} ATPase, Ca^{2+}-Mg^{2+} ATPase, and Na^{+}-K^{+} ATPase in the heart except at the dose of 100 mg/Kg body weight at which Ca^{2+}-Mg^{2+} ATPase activity was elevated. These suggest that the compound combination had no inhibitory effects on ATPases especially at lower doses; therefore, the ion concentration gradients across membrane may not be adversely affected. Hence, the ability of the cardiac cells to respond to electrical impulses and contract may not be compromised by the compound combination. However, the elevated activity of Ca^{2+}-Mg^{2+} ATPase at the highest dose suggests an attempt by the cells to restore resting membrane potential, by pumping the second messenger, calcium ion, out of intracellular environment (Mata and Sepulveda, 2010; Yamaguchi, 2012).

5.3.6 Brain Function Indices

The bio-enhanced combination of methyl gallate and palmatine did not alter the activities of alkaline phosphatase in the brain. Likewise, the activity of creatine kinase which is normally high in the skeletal muscle, heart and brain, was not altered by the bio-enhanced compound combination. Creatine kinase plays a crucial function in

maintaining ATP homeostasis. Reversibly, it activates creatine by transferring a high-energy phosphate group from ATP, hence, enabling the storage of cellular energy as phosphocreatine (Gorman, 2007; Hettling and van Beek, 2011). The results suggest that the bio-enhanced compound combination may not adversely affect the architectural integrity of the plasma membrane of the brain cells. Also, the bio-enhanced compound combination may not adversely affect energy homeostasis in the cells of the brain.

Binding of acetylcholine to its receptor at postsynaptic membrane of neurons causes opening of its ion channel, and this leads to movement of ions which depolarise the membrane and consequently triggering stimulation via electric signals. The hydrolyses of acetylcholine, at the postsynaptic membrane, to acetate and choline by acetylcholinesterase ensures that the action of acetylcholine is terminated (Smith, 2010). Neurotoxic effects of chemical agents could result from inhibition of acetylcholinesterase activity, thereby causing alteration in synaptic transmission, metabolism of acetylcholine and muscle contraction (El-Demerdash, 2011). In this study, the administration of bio-enhanced combination of methyl gallate and palmatine, at various doses, caused no alteration in acetylcholinesterase activities of the brain. This suggest that the compound combination may not adversely affect cholinergic neurotransmission in subjects.

Brain Mg^{2+} ATPase, Ca^{2+}-Mg^{2+} ATPase and Na^{+}-K^{+} ATPase are membrane-bound pumps essential for neuronal homeostasis of ions and synaptic neurotransmission (Gutierres *et al.*, 2014). Oedema, cognitive deficits and cell death could arise from inhibition of Na^{+}-K^{+}ATPase activity in brain (Sato *et al*., 2004). Likewise, inhibition of Ca^{2+}-Mg^{2+} ATPase activities could result in production of reactive oxygen species and neurodegenerative diseases (Skou and Esmann, 1992; Clarke and Fan, 2011). The

bio-enhanced combination of methyl gallate and palmatine, at various doses, caused no alteration in activities of Mg^{2+} ATPase, Ca^{2+}-Mg^{2+} ATPase and Na^{+}-K^{+} ATPase in the brain compared to controls. These suggest that the compound combination may not derange ions homeostasis which is essential for neurotransmission. Furthermore, the compound combination may not cause impairment of mitochondrial function or reduction in ATP levels which are pathologically associated with neurodegenerative diseases and cognitive decline (Ferrer, 2009; Hauptmann *et al.,* 2009).

CONCLUSION

The results from this study revealed that;

i. Methyl gallate and palmatine, separately and in combination exhibited antimalarial activity *in vitro*, inhibiting β-haematin formation, hence revealing a key mechanism of action;

ii. Methyl gallate and palmatine showed synergistic interaction when combined in ratio 3:2;

iii. The combination of methyl gallate and palmatine exhibited ligand-protein interactions in plasmepsins I, II, III, IV and V; falcipain-2, and *Pf*LDH;

iv. The administration of methyl gallate and palmatine separately had no *in vivo* antimalarial activity;

v. The combined administration of methyl gallate and palmatine, in ratio 3:2, in the presence of piperine had delayed *in vivo* antimalarial activity;

vi. Methyl gallate and palmatine combination in the ratio 3:2 demonstrated antioxidant activity *in vitro* and may not damage the membrane of red blood cells;

vii. The combined administration of methyl gallate and palmatine, in ratio 3:2, in the presence of piperine induced antioxidant defense system in murine malaria;

viii. The combination of methyl gallate and palmatine in the ratio 3:2, in the presence of piperine, may not adversely affect liver functions;

ix. The combination of methyl gallate and palmatine in the ratio 3:2, in the presence of piperine, may not impair kidney osmoregulatory function, though may cause reduction in plasma Ca^{2+} concentration at the highest dose;

x. The combination of methyl gallate and palmatine in the ratio 3:2, in the presence of piperine, may not predispose subject to cardiovascular diseases.

These results therefore suggest that, in the presence of piperine, the combination of methyl gallate and palmatine in ratio 3:2 has some antimalarial activity, may ameliorate the ROS-mediated secondary complications of malaria, may not predispose subjects to cardiovascular diseases, and may not adversely affect the functions of the liver and kidney, especially at lower doses.

RECOMMENDATIONS

From the findings and the limitations of this study, further studies are recommended to:

i. Elucidate other possible mechanisms of action of the combination.
ii. Investigate the modulation of immune responses by the compound combination during malaria treatment.
iii. Investigate the activities of the compound combination against different resistant strains of *Plasmodium* species.

REFERENCES

Abtahi, N.S., Shahriari, A., Talaiezadeh, A. and Fathizadeh, P. (2017). Kinetic characterization of malate dehydrogenase in normal and malignant human breast tissues. *Biomedical Research*, 28(10), 4329-4334.

Acharyya, S., Patra, A. and Bag, P.K. (2012). A comparative study on antioxidant potential of nine indian medicinal plants. *CIBTech Journal of Pharmaceutical Sciences*, 1 (2), 16-23.

Adebayo, J. O., Santana, A. E. G. and Krettli, A. U. (2012). Evaluation of the antiplasmodial and cytotoxicity potentials of husk fiber extracts from Cocos nucifera, a medicinal plant used in Nigeria to treat human malaria. *Human & experimental toxicology*, *31*(3), 244-249.

Adebayo, J.O. and Krettli, A.U. (2011). Potential antimalarials from Nigerian plants: A review. *Journal of Ethnopharmacology*, 133(2), 289–302.

Adebayo, J.O., Adesokan, A.A., Olatunji, L.A., Buoro, D.O. and Soladoye, A.O. (2005). Effect of ethanolic extract of *Bougainvillea spectabilis* leaves on haematological and serum lipid variables in rats. *Biokemistri*, 17(1), 45-50.

Adebayo, J.O., Balogun, E.A., Malomo, S.O., Soladoye, A.O., Olatunji, L.A., Kolawole, O.M., Oguntoye, O.S., Babatunde, A.S., Akinola, O.B., Aguiar A.C.C., Andrade, I.M., Souza, N.B. and Krettli, A.U. (2013). Antimalarial activity of Cocos nucifera husk fibre: further studies. *Evidence-Based Complementary and Alternate Medicine*, 2013.

Adebayo, J.O., Yakubu, M.T., Egwim, E.C., Owoyele, V.B. and Enaibe, B.U. (2003). Effect of ethanolic extract of Khaya senegalensis on some biochemical parameters of rat kidney. *Journal of Ethnopharmacology*, 88(1), 69-72.

Adler, S. (2010). Novel Kidney Injury Biomarkers. *Journal of Renal Nutrition*, 20(5), S15–S18.

Agnandji, S.T., Lell, B., Fernandes, J.F., Abossolo, B.P., Methogo, B.G., Kabwende, A.L., Adegnika, A.A., Mordmüller, B., Issifou, S., Kremsner, P.G. and Sacarlal, J. (2012). A phase 3 trial of RTS, S/AS01 malaria vaccine in African infants. The New England journal of medicine, 367(24), 2284-2295.

Aldred, E.M., Buck, C. and Vall, K. (2009). Free radicals. In: Aldred, E.M. (ed.), *Pharmacology; A Handbook for Complementary Healthcare Professionals*, Churchill-Livingston, Philadelphia, pp. 41–52.

Aldunate, R., Casar, J.C., Brandan, E. and Inestrosa, N.C. (2004). Structural and functional organization of synaptic acetylcholinesterase. *Brain Research Reviews*, 47, 96–104.

Amacher, D.E., Schomaker, S.J., Boldt, S.E. and Mirsky, M. (2006). The relationship among microsomal enzyme induction, liver weight, and histological change in cynomolgus monkey toxicology studies. *Food and chemical toxicology*, 44(4), 528-537.

Amar, S., Pawar, V.K., Vikash, J., Parabia, M.H., Rajendra, A. and Gaurav, S. (2010). In-vivo assessment of enhanced bioavailability of metronidazole with piperine in rabbits. *Research Journal of Pharmaceutical, Biological and Chemical Sciences*, 1(4), 273-278.

Amino, R., Thiberge, S., Martin, B., Celli, S., Shorte, S., Frischknecht, F. and Ménard, R. (2006). Quantitative imaging of Plasmodium transmission from mosquito to mammal. *Nature medicine, 12*(2), 220-224.

Amoros, M., Simoes, C.M., Girre, L., Sauvager, F. and Cormier, M. (1992). Synergistic effect of flavones and flavonols against herpes simplex virus type 1 in cell culture. Comparison with the antiviral activity of propolis. *J Nat Prod.* 55, 1732-1740.

Andres, R.H., Ducray, A.D., Schlattner, U., Wallimann, T. and Widmer, H.R. (2008). Functions and effects of creatine in the central nervous system. *Brain Research Bulletin*, 76, 329–343.

Arama, C. and Troye-Blomberg, M. (2014). The path of malaria vaccine development: challenges and perspectives. *Journal of internal medicine, 275*(5), 456-466.

Araujo, C.F., Lacerda, M.V.G., Abdalla, D.S.P. and Lima, E.S. (2008). The role of platelet and plasma markers of antioxidant status and oxidative stress in thrombocytopenia among patients with vivax malaria. *Mem Inst Oswaldo Cruz*, 103, 517–521.

Arneson, W.L. and Brickell, J.M. (2007a). Assessment of liver function. In: Arneson, W.L. and Brickell, J.M. (eds.), *Clinical Chemistry: A Laboratory Perspective*, F.A. Davis Company, Philadelphia, pp. 233.

Arneson, W.L. and Brickell, J.M. (2007b). Assessment of renal function. In: Arneson, W.L. and Brickell, J.M. (eds.), *Clinical Chemistry: A Laboratory Perspective*, F.A. Davis Company, Philadelphia, pp. 218.

As, S., Sahukar, S., Murthy, J. and Kumar, K. (2013). A study of serum apolipoprotein A1, apolipoprotein B and lipid profile in stroke. *J Clin Diagn Res*, 7(7), 1303–6.

Ashley, E.A., Dhorda, M., Fairhurst, R.M., Amaratunga, C., Lim, P., Suon, S., Sreng, S., Anderson, J.M., Mao, S., Sam, B. and Sopha, C. (2014). Spread of artemisinin resistance in *Plasmodium falciparum* malaria. *New England Journal of Medicine*, 371(5), 411-423.

Asnaashari, M., Farhoosh, R. and Sharif, A. (2014). Antioxidant activity of gallic acid and methyl gallate in triacylglycerols of Kilka fish oil and its oil-in-water emulsion. *Food chemistry*, 159, 439-444.

Atawodi, S.E., Atawodi, J.C., Idakwo, P., Pfundstein, B., Haubner, R., Wurtele, G., Spiegelhalder, B., Bartsch, H. and Owen, R.W. (2009). Evaluation of the polyphenol composition and antioxidant activity of African variety of Dacryodes edulis (G.Don) H.J Lam Fruit. *Journal of Medicinal Food*, 12(6), 1321-1325.

Aulbach, A.D. and Amuzie, C.J. (2017). Biomarkers in Nonclinical Drug Development. In: Faqi, A.S. (ed.), *A Comprehensive Guide to Toxicology in Nonclinical Drug Development*, 2nd edition, Academic Press, San Diego, pp. 447–471.

Auron, A. and Brophy, P.D. (2012). Hyperammonemia in review: pathophysiology, diagnosis, and treatment. *Pediatric nephrology*, 27(2), 207-222.

Autino, B., Corbett, Y., Castelli, F. and Taramelli, D. (2012). Pathogenesis of malaria in tissues and blood. *Mediterranean journal of hematology and infectious diseases*, 4(1), e2012061.

Awad Jr., W.M. (2010). Iron and Heme Metabolism. In: Devlin, T.M. (Ed.), *Textbook of Biochemistry with Clinical Correlations*, 7th edition, Wiley, Hoboken,

Ayala, A., Muñoz, M.F. and Argüelles, S. (2014). Lipid Peroxidation: Production, Metabolism, and Signaling Mechanisms of Malondialdehyde and 4-Hydroxy-2-Nonenal. *Oxidative Medicine and Cellular Longevity*, 2014, 1-31.

Azab, A.E.A., El-Dakhly, A.T., Alrawi, Q.K. and Albasha, M.O. (2013). Protective effects of sesame oil against lead acetate induced haemato-biochemical toxicity in albino mice. *Int. J. Sci. Res.*, 4(2), 2053-2063.

Bafana, A., Dutt, S., Kumar, A., Kumar, S. and Ahuja, P.S. (2011). The basic and applied aspects of superoxide dismutase. *Journal of Molecular Catalysis B: Enzymatic*, 68(2), 129-138.

Bagchi, K. and Puri, S. (1998). Free radicals and antioxidants in health and disease. *Eastern Mediterranean Health Journal*, 4(2), 350–360.

Bailly, E., Jambou, R., Savel, J. and Jaureguiberry, G. (1992). *Plasmodium falciparum*: differential sensitivity *in vitro* to E-64 (cysteine protease inhibitor) and Pepstatin A (aspartyl protease inhibitor). *Journal of Eukaryotic Microbiology*, 39(5), 593-599.

Banerjee, R. and Goldberg, D.E. (2001). The Plasmodium Food Vacuole. In: Rosenthal, P.J. (ed.), *The Antimalarial Chemotherapy: Mechanisms of Action,*

Resistance and New Directions in Drug Discovery, Humana Press, New Jersey, pp. 43-64.

Banerjee, R., Francis, S.E. and Goldberg, D.E. (2003). Food vacuole plasmepsins are processed at a conserved site by an acidic convertase activity in *Plasmodium falciparum*. *Molecular and biochemical parasitology*, 129(2), 157-165.

Banerjee, R., Liu, J., Beatty, W., Pelosof, L., Klemba, M. and Goldberg, D.E. (2002). Four plasmepsins are active in the *Plasmodium falciparum* food vacuole, including a protease with an active-site histidine. *Proceedings of the National Academy of Sciences*, 99(2), 990-995.

Barrett, K.E., Brooks, H.L., Boitano, S. and Barman, S.M. (2010). Ganong's Review of Medical Physiology. 23rd edition, McGraw-Hill, New York, pp. 639-662.

Bartels, H. and Bohmer, M. (1972). Kinetic determination of creatinine concentration. *Clinica Chimica Acta*, 37, 193–197.

Beare, N.A., Taylor, T.E., Harding, S.P., Lewallen, S. and Molyneux, M.E. (2006). Malarial retinopathy: a newly established diagnostic sign in severe malaria. *The American journal of tropical medicine and hygiene*, 75(5), 790-797.

Becker, B.F. (1993). Towards the physiological function of uric acid. *Free Radical Biology and Medicine*, 14(6), 615-631.

Becker, K., Tilley, L., Vennerstrom, J.L., Roberts, D., Rogerson, S. and Ginsburg, H. (2004). Oxidative stress in malaria parasite-infected erythrocytes: host–parasite interactions. *International journal for parasitology*, 34(2), 163-189.

Bedu-Addo, G., Meese, S. and Mockenhaupt, F.P. (2013). An ATP2B4 polymorphism protects against malaria in pregnancy. *The Journal of infectious diseases*, 207(10), 1600-1603.

Berg, J.M., Tymoczko, J.L. and Stryer, L. (2002). Important Derivatives of Cholesterol Include Bile Salts and Steroid Hormones. In: *Biochemistry*, 5th edition, W.H Freeman, New York.

Berry, C., Humphreys, M.J., Matharu, P., Granger, R., Horrocks, P., Moon, R.P., Certa, U., Ridley, R.G., Bur, D. and Kay, J. (1999). A distinct member of the aspartic proteinase gene family from the human malaria parasite *Plasmodium falciparum*. *FEBS letters*, 447(2-3), 149-154.

Beutler, E. (1994). G6PD deficiency. *Blood*, 84, 3613-3636.

Beutler, E., Duron, O. and Kelly, B. M. (1963). Improved method for the determination of blood glutathione. *Journal of laboratory and Clinical Medicine*, 61, 882-888.

Bewaji, C.O., Olorunsogo, O.O. and Bababunmi, E.A. (1985). Comparison of the membrane-bound (Ca^{2+},Mg^{2+})-ATPase in erythrocyte ghosts from some mammalian species. Comparative Biochemistry and Physiology Part B: *Comparative Biochemistry*, 82(1), 117-122.

Bhardwaj, R.K., Glaeser, H., Becquemont, L., Klotz, U., Gupta, S.K. and Fromm, M.F. (2002). Piperine, a major constituent of black pepper, inhibits human P-glycoprotein and CYP3A4. *Journal of Pharmacology and Experimental Therapeutics*, 302(2), 645-650.

Bhatnagar, D., Soran, H. and Durrington, P.N. (2008). Hypercholesterolaemia and its management. *Bmj*, 337, 503-508.

Bhatt, S., Weiss, D.J., Cameron, E., Bisanzio, D., Mappin, B., Dalrymple, U., Battle, K., Moyes, C.L., Henry, A.,Eckhoff, P.A., Wenger, E.A., Briët, O., Penny, M.A., Smith, T.A., Bennett, A., Yukich, J., Eisele, T.P., Griffin, J.T. Fergus, C.A., Lynch, M., Lindgren, F., Cohen, J.M., Murray, C.L.J., Smith, D.L., Hay, S.I., Cibulskis, R.E. and Gething, P.W. (2015). The effect of malaria control on *Plasmodium falciparum* in Africa between 2000 and 2015. *Nature,* 526(7572), 207–211.

Biggs, H.G. and Moorehead, W.R. (1974). 2-Amino-2-methyl-1-propanol as the alkalizing agent in an improved continuous-flow cresolphthalein complexone procedure for calcium in serum. *Clinical Chemistry,* 20(11), 1458-1460.

Birkett, A.J. (2016). Status of vaccine research and development of vaccines for malaria. *Vaccine*, 34, 2915–2920.

Boddey, J.A. and Cowman, A.F. (2013). Plasmodium nesting: remaking the erythrocyte from the inside out. *Annual review of microbiology*, 67, 243-269.

Bogaczewicz, A. and Sobów, T. (2017). Psychiatric adverse effects of chloroquine. *Psychiatria i Psychologia Kliniczna*, 17(2).

Boni, M.F., Smith, D.L. and Laxminarayan, R. (2008). Benefits of using multiple first-line therapies against malaria. *Proceedings of the National Academy of Sciences*, 105(37), 14216-14221.

Bos, M.J., Koudstaal, P.J., Hofman, A., Witteman, J.C. and Breteler, M.M. (2006). Uric acid is a risk factor for myocardial infarction and stroke. *Stroke*, 37(6), 1503-1507.

Boss, C., Richard-Bildstein, S., Weller, T., Fischli, W., Meyer, S. and Binkert, C. (2003). Inhibitors of the *Plasmodium falciparum* parasite aspartic protease plasmepsin II as potential antimalarial agents. *Current medicinal chemistry*, 10(11), 883-907.

Bousema, T. and Drakeley, C. (2011). Epidemiology and infectivity of *Plasmodium falciparum* and Plasmodium vivax gametocytes in relation to malaria control and elimination. *Clinical microbiology reviews*, 24(2), 377-410.

Bozdech, Z. and Ginsburg, H. (2004). Antioxidant defense in *Plasmodium falciparum*–data mining of the transcriptome. *Malaria journal*, 3(1), 23.

Bray, P.G., Martin, R.E., Tilley, L., Ward, S.A., Kirk, K. and Fidock, D.A. (2005). Defining the role of PfCRT in *Plasmodium falciparum* chloroquine resistance. *Molecular microbiology*, 56(2), 323-333.

Briani, C., Zaninotto, M., Forni, M. and Burra, P. (2003). Macroenzymes: too often overlooked. *Journal of hepatology*, 38(1), 119.

Brickell, J.M., Arneson, W.L. and Mass, D. (2007). Overview of clinical chemistry. In: Arneson, W.L. and Brickell, J.M. (eds.), *Clinical Chemistry: A Laboratory Perspective*, F.A. Davis Company, Philadelphia, pp. 22.

Brini, M. and Carafoli, E. (2011). The plasma membrane Ca^{2+} ATPase and the plasma membrane sodium calcium exchanger cooperate in the regulation of cell calcium. *Cold Spring Harb Perspect Biol*, 3, a004168.

Caldwell, J.E. (2009). Clinical limitations of acetylcholinesterase antagonists. *Journal of Critical Care*, 24, 21–28.

Cameron, A., Read, J., Tranter, R., Winter, V.J., Sessions, R.B., Brady, R.L., Vivas, L., Easton, A., Kendrick, H., Croft, S.L. and Barros, D. (2004). Identification and activity of a series of azole-based compounds with lactate dehydrogenase-directed anti-malarial activity. *Journal of Biological Chemistry*, 279(30), 31429-31439.

Campbell, T.W. and Ellis, C.K. (2013). Avian and Exotic Animal Hematology and Cytology, 3rd edition, John Wiley & Sons, New Jersey.

Celermajer, D.S., Chow, C.K., Marijon, E., Anstey, N.M. and Woo, K.S. (2012). Cardiovascular disease in the developing world: prevalences, patterns, and the potential of early disease detection. *Journal of the American College of Cardiology*, 60(14), 1207-1216.

Cerwenka, A. and Lanier, L.L. (2001). Natural killer cells, viruses and cancer. *Nature Reviews Immunology*, 1(1), 41-49.

Chabory, E., Damon, C., Lenoir, A., Kauselmann, G., Kern, H., Zevnik, B., Garrel, C., Saez, F., Cadet, R., Henry-Berger, J. and Schoor, M. (2009). Epididymis seleno-independent glutathione peroxidase 5 maintains sperm DNA integrity in mice. *The Journal of clinical investigation*, 119(7), 2074.

Chanda, S. and Dave, R. (2009). *In vitro*models for antioxidant activity evaluation and some medicinal plants possessing antioxidant properties: An overview. *African Journal of Microbiology Research*, 3(13), 981-996.

Chao, J., Liao, J., Peng, W., Lee, M., Pao, L. and Cheng, H. (2013). Antioxidant, Analgesic, Anti-Inflammatory, and Hepatoprotective Effects of the Ethanol Extract of Mahonia oiwakensis Stem. *International Journal of Molecular Sciences*, 14, 2928-2945.

Chatterjee, C. and Sparks, D.L. (2011). Hepatic lipase, high density lipoproteins, and hypertriglyceridemia. *The American journal of pathology*, 178(4), 1429-1433.

Chaubal, R., Deshpande, V.H. and Deshpande, N.R. (2005). Methyl gallate, the medicinally important compound: a review. *Electron J. Environ. Agric. Food Chem*., 4, 956–962.

Chaudhary, K.K. and Mishra, N. (2016). A Review on Molecular Docking: Novel Tool for Drug Discovery. *JSM Chem*, 4(3), 1029.

Cheeseman, K.H. and Slater, T.F. (1993). An introduction to free radical biochemistry. *British medical bulletin*, 49(3), 481-493.

Chelikani, P., Fita, I. and Loewen, P.C. (2004). Diversity of structures and properties among catalases. *Cellular and molecular life sciences*, 61(2), 192-208.

Chen, N.X. and Moe, S.M. (2015). Pathophysiology of vascular calcification. *Current osteoporosis reports*, 13(6), 372-380.

Cheng, C., Kuo, E. and Huang, C. (2013). Extracellular Potassium Homeostasis: Insights from Hypokalemic Periodic Paralysis. *Semin Nephrol.*, 33(3), 237–247.

Cheung, L.M., Cheung, P.C. and Ooi, V.E. (2003). Antioxidant activity and total phenolics of edible mushroom extracts. *Food Chem*., 81, 249–255.

Cho, H.J. and Yoon, I.S. (2015). Pharmacokinetic interactions of herbs with cytochrome p450 and p-glycoprotein. *Evidence-Based Complementary and Alternative Medicine*, 2015, 736431.

Cho, H.J. and Yoon, I.S. (2015). Pharmacokinetic interactions of herbs with cytochrome p450 and p-glycoprotein. *Evidence-Based Complementary and Alternative Medicine*, 2015, 736431.

Choi, C.S., Lee, F.N., McDonough, A.A. and Youn, J.H. (2002). Independent regulation of *in vivo* insulin action on glucose versus K(+) uptake by dietary fat and K(+) content. *Diabetes*, 51, 915–920.

Choi, J.G., Mun, S.H., Chahar, H.S., Bharaj, P., Kang, O.H., Kim, S.G., Shin, D.W. and Kwon, D.Y. (2014). Methyl gallate from Galla rhois successfully controls clinical isolates of Salmonella infection in both *in vitro* and *in vivo* systems. *PloS one*, 9(7), e102697.

Chonchol, M., Shlipak, M.G., Katz, R., Sarnak, M.J., Newman, A.B., Siscovick, D.S., Kestenbaum, B., Carney, J.K. and Fried, L.F. (2007). Relationship of uric acid with progression of kidney disease. *American Journal of Kidney Diseases*, 50(2), 239-247.

Cilingiroglu, M. and Ballantyne, C. (2004). Endothelial lipase and cholesterol metabolism. *Current atherosclerosis reports*, 6(2), 126-130.

Clark, V.L. and Kruse, J.A. (1990). Clinical methods: the history, physical, and laboratory examinations. *The Journal of American Medical Association*, 264(21), 2808-2809.

Clarke, R.J. and Fan, X. (2011). Pumping ions. *Clin. Exp. Pharmacol. Physiol.*, 38, 726-733.

Clausen, T. (1998). Clinical and therapeutic significance of the Na^+,K^+ pump. *Clin Sci (Lond)*, 95, 3–17.

Clausen, T. (2003). Na^+-K^+ pump regulation and skeletal muscle contractility. *Physiol Rev.*, 83, 1269–1324.

Cohee, L.M. and Laufer, M.K. (2017). Malaria in Children. *Pediatric Clinics of North America*, 64, 851–866.

Cohen, D.E. (2008). Balancing cholesterol synthesis and absorption in the gastrointestinal tract. *Journal of clinical lipidology*, 2(2), S1-S3.

Coleman, R.A. and Lee, D.P. (2004). Enzymes of triacylglycerol synthesis and their regulation. *Progress in lipid research*, 43(2), 134-176.

Coleman, R.A. and Mashek, D.G. (2011). Mammalian triacylglycerol metabolism: synthesis, lipolysis, and signaling. *Chemical reviews*, 111(10), 6359-6386.

Coombs, G.H., Goldberg, D.E., Klemba, M., Berry, C., Kay, J. and Mottram, J.C. (2001). Aspartic proteases of *Plasmodium falciparum* and other parasitic protozoa as drug targets. *Trends in parasitology*, 17(11), 532-537.

Coomes, M.W. (2010). Amino Acid Metabolism. In: Devlin, T.M. (Ed.), *Textbook of Biochemistry with Clinical Correlations*, 7th edition, Wiley, Hoboken,

Coronado, L.M., Nadovich, C.T. and Spadafora, C. (2014). Malarial hemozoin: from target to tool. *Biochimica et Biophysica Acta*, 1840(6), 2032-2041.

Corrado, A., D'Onofrio, F., Santoro, N., Melillo, N. and Cantatore, F.P. (2006). Pathogenesis, clinical findings and management of acute and chronic gout. *Minerva medica*, 97(6), 495-509.

Costa, M.A., Carere, R.G., Lichtenstein, S.V., Foley, D.P., De Valk, V., Lindenboom, W., Roose, P.C., Van Geldorp, T.R., Macaya, C., Castanon, J.L. and Fernandez-Avilèz, F. (2001). Incidence, predictors, and significance of abnormal cardiac enzyme rise in patients treated with bypass surgery in the arterial revascularization therapies study (ARTS). *Circulation*, 104(22), 2689-2693.

Costedoat-Chalumeau, N., Dunogué, B., Leroux, G., Morel, N., Jallouli, M., Le Guern, V., Piette, J.C., Brézin, A.P., Melles, R.B. and Marmor, M.F. (2015). A critical review of the effects of hydroxychloroquine and chloroquine on the eye. *Clinical reviews in allergy and immunology*, 49(3), 317-326.

Cowman, A.F., Healer, J., Marapana, D. and Marsh, K. (2016). Malaria: biology and disease. *Cell*, 167(3), 610-624.

Cowman, A.F., Tonkin, C.J., Tham, H. and Duraisingh, M.T. (2017). The Molecular Basis of Erythrocyte Invasion by Malaria Parasites. *Cell Host & Microbe*, 22(2), 232-245.

Crook, M.A. (2013). Clinical Biochemistry and Metabolic Medicine. 8th edition, CRC Press, pp. 270-281.

Cummings, M. (2008). Human Heredity: Principles and Issues. 8th edition, pp. 230-257.

Cunningham-Rundles, C. (1998). Gammaglobulin. In: Delves, P.I. and Roitt, I.M.C.E. (eds.), *Encyclopedia of Immunology*, 2nd edition, Academic Press, San Diego, pp. 964–966.

Dahl, E.L., Shock, J.L., Shenai, B.R., Gut, J., DeRisi, J.L. and Rosenthal, P.J. (2006). Tetracyclines specifically target the apicoplast of the malaria parasite *Plasmodium falciparum*. *Antimicrobial agents and chemotherapy,* 50(9), 3124-3131.

Dai, J. and Mumper, R.J. (2010). Plant Phenolics: Extraction, Analysis and Their Antioxidant and Anticancer Properties. *Molecules*, 15, 7313-7352.

Dalton, R.N. (2010). Serum Creatinine and Glomerular Filtration Rate: Perception and Reality. *Clinical Chemistry,* 56(5), 687-689.

Dame, J.B., Reddy, G.R., Yowell, C.A., Dunn, B.M., Kay, J. and Berry, C. (1994). Sequence, expression and modeled structure of an aspartic proteinase from the human malaria parasite *Plasmodium falciparum*. *Molecular and biochemical parasitology,* 64(2), 177-190.

Dancygier, H. (2010). Clinical hepatology: Principles and practice of hepatobiliary diseases (Vol. 2). Springer Science, New York, pp. 319-330.

Das, B.S. and Nanda, N.K. (1999). Evidence for erythrocyte lipid peroxidation in acute falciparum malaria. *Trans. R. Soc. Trop. Med. Hyg*., 93, 58–62.

Dasgupta, A. and Klein, K. (2014). Introduction to Free Radicals and the Body's Antioxidant Defense. In: *Antioxidants in Food, Vitamins and Supplements: Prevention and Treatment of Diseas,* Academic Press, San Diego, pp. 1–18.

Dasika, S.K., Vinnakota, K.C. and Beard, D.A. (2015). Determination of the Catalytic Mechanism for Mitochondrial Malate Dehydrogenase. *Biophysical Journal*, 108, 408–419.

David, S.B. (1999). Endogenous nitric oxide synthesis: biological functions and pathophysiology. *Free Radic. Res.*, 31 (6), 577–596.

Davis, T.M.E., Pukrittayakamee, S., Woodhead, J.S., Holloway, P., Chaivisuth, B. and White, N.J. (1991). Calcium and phosphate metabolism in acute falciparum malaria. *Clinical Science*, 81(3), 297-304.

de Dominguez, N.G. and Rosenthal, P.J., (1996). Cysteine proteinase inhibitors block early steps in hemoglobin degradation by cultured malaria parasites. *Blood*, 87(10), 4448-4454.

De Man, F.H., Jonkers, I.J., Schwedhelm, E., Smelt, A.H., Onkenhout, W., van Duyvenvoorde, W., Buytenhek, R., Leuven, J.A.G., Troost, R., van der Laarse, A. and Princen, H.M. (2000). Normal oxidative stress and enhanced lipoprotein resistance to *in vitro* oxidation in hypertriglyceridemia. *Arteriosclerosis, thrombosis, and vascular biology*, 20(11), 2434-2440.

DeFronzo, R. A., Davidson, J. A., and Del Prato, S. (2012). The role of the kidneys in glucose homeostasis: a new path towards normalizing glycaemia. *Diabetes, Obesity and Metabolism*, 14(1), 5-14.

Degenhardt, L., Mathers, B., Vickerman, P., Rhodes, T., Latkin, C. and Hickman, M. (2010). Prevention of HIV infection for people who inject drugs: why individual, structural, and combination approaches are needed. *The Lancet*, 376(9737), 285-301.

Demir, E., Kaya, B., Soriano, C., Creus, A. and Marcos, R. (2011). Genotoxic analysis of four lipid peroxidation products in the mouse lymphoma assay. Mutat Res., 726, 98–103.

Deshmukh, R. and Trivedi, V. (2014). Role of Pro-Oxidants from Infected RBCS in Disturbing Homeostasis and Pathogenesis During Malaria. *Austin Journal of Biotechnology & Bioengineering*, 1(7), 1-5.

Deshpande, S., Durdagi, S. and Noskov, S.Y. (2013). Potassium in Biological Systems. In: Kretsinger, R.H., Uversky, V.N. and Permyakov, E.A. (eds.), *Encyclopedia of Metalloproteins*, Springer, New York, pp. 1799-1804.

Dhingra, D. and Bhankher, A. (2014). Behavioral and biochemical evidences for antidepressant-like activity of palmatine in mice subjected to chronic unpredictable mild stress. *Pharmacological Reports*, 66, 1–9.

Dhingra, D. and Kumar, V. (2012). Memory-Enhancing Activity of Palmatine in Mice Using Elevated Plus Maze and Morris Water Maze. *Advances in Pharmacological Sciences*, 2012, 357368.

Di Witt, C. and Trendelenburg, J. (1982). Quantitative determination of creatine kinase in serum. *Journal of Clinical Chemistry and Clinical Biochemistry*, 20, 235.

Doi, M. and Iwasaki, K. (2008). Na^+/K^+ ATPase regulates the expression and localization of acetylcholine receptors in a pump activity-independent manner. *Molecular and Cellular Neuroscience*, 38(4), 548-558.

Dondorp, A.M., Fairhurst, R.M., Slutsker, L., MacArthur, J.R., Guerin, P.J., Wellems, T.E., Ringwald, P., Newman, R.D. and Plowe, C.V. (2011). The threat of

artemisinin-resistant malaria. *New England Journal of Medicine*, 365(12), 1073-1075.

Dondorp, A.M., Smithuis, F.M., Woodrow, C. and Seidlein, L.V. (2017). How to Contain Artemisinin and Multidrug Resistant Falciparum Malaria. *Trends in parasitology*, 33(5), 353-363.

Doumas, B.T., Watson, W.A. and Biggs, H.G. (1971). Albumin standards and the measurement of serum albumin with bromcresol green. *Clinica Chimica Acta*, 31(1), 87–92.

Dröge, W. (2002). Free radicals in the physiological control of cell function. *Physiological reviews*, 82(1), 47-95.

Drury, R.A.B. and Wallington, E.A. (1973). In: Carleton's Histological Techniques. 4th edn. Oxford University Press, NY. Pp. 58.

e Silva, L.F.R., Nogueira, K.L., da Silva Pinto, A.C., Katzin, A.M., Sussmann, R.A., Muniz, M.P., de Andrade Neto, V.F., Chaves, F.C.M., Coutinho, J.P., Lima, E.S. and Krettli, A.U. (2015). *In vivo* antimalarial activity and mechanisms of action of 4-nerolidylcatechol derivatives. *Antimicrobial agents and chemotherapy*, 59(6), 3271-3280.

Eckersall, P.D. (2008). Proteins, Proteomics, and the Dysproteinemias. In: Kaneko, J.J., Harvey, J.W. and Bruss, M.L. (eds.), *Clinical Biochemistry of Domestic Animals*, 6th edition, Academic press, San Diego, pp. 117–155.

Egan, T.J. (2003). Haemozoin (malaria pigment): a unique crystalline drug target. *Targets*, 2(3), 115-124.

Egan, T.J. (2008). Haemozoin formation. *Mol Biochem Parasitol*, 157, 127-136.

Egan, T.J. and Ncokazi, K.K. (2005). Quinoline antimalarials decrease the rate of β-hematin formation. *Journal of inorganic biochemistry*, 99(7), 1532-1539.

Ekaprasada, M.T, Nurdin, H., Ibrahim, S. and Dachriyanus, A. (2009). Antioxidant activity of methyl gallate isolated from the leaves of Toona sureni. *Indo. J. Chem.*, 9(3), 457–460.

Elchuri, S., Oberley, T.D., Qi, W., Eisenstein, R.S., Roberts, L.J., Van Remmen, H., Epstein, C.J. and Huang, T.T. (2005). CuZnSOD deficiency leads to persistent and widespread oxidative damage and hepatocarcinogenesis later in life. *Oncogene*, 24(3), 367-380.

El-Demerdash, F.M. (2011). Lipid peroxidation, oxidative stress and acetylcholinesterase in rat brain exposed to organophosphate and pyrethroid insecticides. *Food Chem Toxicol*, 49, 1346-1352.

Elwess, N.L., Filoteo, A.G., Enyedi, A. and Penniston, J.T. (1997). Plasma membrane Ca^{2+} pump isoforms 2a and 2b are unusually responsive to calmodulin and Ca^{2+}. *J Biol Chem*, 272, 17981–17986.

Endres, D.B. and Rude, R.K. (2008). Disorders of bone. In: Burtis, C.A., Ashwood, E.R. and Bruns, D.E. (eds.), *Tietz fundamentals of clinical chemistry*, 6th edition, Saunders Elsevier, St. Louis. pp. 711-734.

English, M.C., Waruiru, C., Lightowler, C., Murphy, S.A., Kirigha, G. and Marsh, K. (1996). Hyponatraemia and dehydration in severe malaria. *Archives of disease in childhood*, 74(3), 201-205.

Enyedi, A., Flura, M., Sarkadi, B., Gardos, G. and Carafoli, E. (1987). The maximal velocity and the calcium affinity of the red cell calcium pump may be regulated independently. *J Biol Chem,* 262, 6425–6430.

Ercal, N., Gurer-Orhan, H. and Aykin-Burns, N. (2001). Toxic metals and oxidative stress part I: mechanisms involved in metal-induced oxidative damage. *Current topics in medicinal chemistry*, 1(6), 529-539.

Eren, E., Yilmaz, N. and Aydin, O. (2012). High density lipoprotein and it's dysfunction. *The open biochemistry journal*, 6, 78-93

Ersmark, K., Samuelsson, B. and Hallberg, A. (2006). Plasmepsins as potential targets for new antimalarial therapy. *Medicinal research reviews*, 26(5), 626-666.

Evans, T.W. (2002). Albumin as a drug: biological effects of albumin unrelated to oncotic pressure. *Alimentary pharmacology & therapeutics*, 16(5), 6-11.

Evans, W.C. (2009). Alkaloids. In: Evans, W.C. (ed.), *Trease and Evans's pharmacognosy*, 16th edition, Elsevier, Edinburgh, pp. 353–415.

Everds, N.E. (2007). Hematology of the Laboratory Mouse. In: Fox, J.G., Barthold, S., Davisson, M., Newcomer, C.E., Quimby, F.W. and Smith, A. (eds.), The Mouse in Biomedical Research, 2nd edition, Academic press, San Diego, pp. 133–170.

Fabbri, C., Mascarenhas-Netto, R.D., Lalwani, P., Melo, G.C., Magalhães, B.M.L., Alexandre, M.A.A., Lacerda, M.V.G. and Lima, E.S. (2013). Lipid peroxidation and antioxidant enzymes activity in Plasmodium vivax malaria patients evolving with cholestatic jaundice. *Malaria Journal*, 12, 315-321.

Faridi, A.B. and Weisberg, L.S. (2008). Acid-Base, Electrolyte, and Metabolic Abnormalities. In: Parrillo, J.E. and Dellinger, R.P. (eds), *Critical Care Medicine: Principles of Diagnosis and Management in the Adult*, 3d edition, Mosby Elsevier, Philadelphia, pp. 1203-1243.

Fan, W., Yuan, G., Li, Q. and Lin, W. (2014). Antibacterial mechanisms of methyl gallate against *Ralstonia solanacearum*. *Australasian Plant Pathology*, 43 (1), 1-7.

Fang, Y.Z., Yang, S. and Wu, G. (2002). Free radicals, antioxidants, and nutrition. *Nutrition*, 18, 872–879.

Farombi, E.O., Shyntum, Y. and Emerole, G.O. (2003). Influence of chloroquine treatment and Plasmodium, falciparum malaria infection on some enzymatic and non-enzymatic antioxidant defense indices in humans. *Drug Chem Toxicol*, 26(1), 59–71.

Farrell, G.C. (2002). Liver disease caused by drugs, anesthetics, and toxins. In: Feldman, M., Friedman, L.S. and Sleisenger, M.H. (eds.), *Sleisenger & Fordtran's Gastrointestinal and Liver Disease: pathophysiology, Diagnosis, Management*, 7th edition, Saunders, Philadelphia, pp. 1403–1447.

Fatehi, M., Saleh, T.M., Fatehi-Hassanabad, Z., Farrokhfal, K., Jafarzadeh, M. and Davodi, S. (2005). A pharmacological study on Berberis vulgaris fruit extract. *Journal of ethnopharmacology*, 102(1), 46-52.

Fausto, N. (2000). Liver regeneration. *Journal of hepatology*, 32, 19-31.

Ferrari, C. and Mondelli, M (2009). Immune mechanisms of viral clearance and disease pathogenesis during viral hepatitis. In: Arias, I.M., Wolkoff, A.W.,

Boyer, J.L., Shafritz, D.A., Fausto, N., Alter, H.J. and Cohen, D.E. (eds.), *The liver: biology and pathobiology*, 5th edition, John Wiley & Sons, Oxford, pp. 835-858.

Ferrer, I. (2009). Altered mitochondria, energy metabolism, voltage-dependent anion channel, and lipid rafts converge to exhaust neurons in Alzheimer's disease. *J. Bioenerg. Biomembr.*, 41, 425–431.

Ferrier, D.R. (2014). Conversion of Amino Acids to Specialized Products. In: Harvey, R.A. (Ed.) *Biochemistry: Lippincott's Illustrated Reviews*, 6th edition, Lippincott Williams & Wilkins, pp. 277.

Fidock, D.A., Rosenthal, P.J., Croft, S.L., Brun, R. and Nwaka, S. (2004). Antimalarial Drug Discovery: Efficacy Models for Compound Screening. *Nat. Rev. Drug Discov.*, 3(6), 509–520.

Fivelman, Q. L., Adagu, I. S., and Warhurst, D. C. (2004). Modified fixed-ratio isobologram method for studying *in vitro* interactions between atovaquone and proguanil or dihydroartemisinin against drug-resistant strains of *Plasmodium falciparum*. *Antimicrobial agents and chemotherapy*, *48*(11), 4097-4102.

Flegg, J.A., Guerin, P.J., White, N.J. and Stepniewska, K. (2011). Standardizing the measurement of parasite clearance in falciparum malaria: the parasite clearance estimator. *Malaria journal, 10*(1), 339.

Fleschner, C.R. and Kraus-Friedmann, N. (1986). The effect of Mg^{2+} on hepatic microsomal Ca^{2+} and Sr^{2+} transport. *European Journal of Biochemistry,* 154(2), 313-320.

Flohe, L., Toppo, S., Cozza, G. and Ursini, F. (2011). A comparison of thiol peroxidase mechanisms. *Antioxid Redox Signal*, 15, 763–780.

Foley, M. and Tilley, L. (1998). Quinoline antimalarials: mechanisms of action and resistance and prospects for new agents. *Pharmacology & therapeutics*, 79(1), 55-87.

Forrester, R.L., Wataji, L.J., Silverman, D.A. and Pierre, K.J. (1976). Enzymatic method for determination of CO2 in serum. *Clinical Chemistry*, 22(2), 243-245.

Fossati, P., Prencipe, L. and Berti, G. (1980). Use of 3, 5-dichloro-2-hydroxybenzenesulfonic acid/4-aminophenazone chromogenic system in direct enzymic assay of uric acid in serum and urine. *Clinical chemistry*, 26(2), 227-231.

Francis, S.E., Banerjee, R. and Goldberg, D.E. (1997a). Biosynthesis and maturation of the malaria aspartic hemoglobinases plasmepsins I and II. *J Biol Chem.*, 272, 14961–14968.

Francis, S.E., Gluzman, I.Y., Oksman, A., Banerjee, D. and Goldberg, D.E. (1996). Characterization of native falcipain, an enzyme involved in *Plasmodium falciparum* hemoglobin degradation. *Molecular and biochemical parasitology*, 83(2), 189-200.

Francis, S.E., Sullivan Jr, D.J. and Goldberg, A.D.E. (1997b). Hemoglobin metabolism in the malaria parasite *Plasmodium falciparum*. *Annual Reviews in Microbiology*, 51(1), 97-123.

Friedwald, W.T., Levey, R.I. and Friedrickson, D.S. (1972). Estimation of the concentration of LDL in plasma without the use of preparative concentrating. *Clinical Chemistry,* 18, 499-502.

Fuchs, P., Perez-Pinzon, M.A. and Dave, K.R. (2014). Cerebral Ischemia in Diabetics and Oxidative Stress. In: Preedy, V.R. (ed.), *Diabetes: Oxidative Stress and Dietary Antioxidants*, Elsevier, Amsterdam, pp. 15–23.

Fujii, T., Mashimo, M., Moriwaki, Y., Misawa, H., Ono, S., Horiguchi, K. and Kawashima, K. (2017). Physiological functions of the cholinergic system in immune cells. *Journal of Pharmacological Sciences*, 134, 1-21.

Gadalla, N.B., Abdallah, T.M., Atwal, S., Sutherland, C.J. and Adam, I. (2013). Selection of pfdhfr/pfdhps alleles and declining artesunate/sulphadoxine-pyrimethamine efficacy against *Plasmodium falciparum* eight years after deployment in eastern Sudan. *Malaria journal*, 12(1), 255.

Galati, G. and O'Brien, P.J. (2004). Potential toxicity of flavonoids and other dietary phenolics: significance for their chemopreventive and anticancer properties. *Free Radical Biology and Medicine,* 37(3), 287-303.

Gallego-Delgado, J. and Rodriguez, A. (2017). Rupture and Release: A Role for Soluble Erythrocyte Content in the Pathology of Cerebral Malaria. *Trends in parasitology*.

Gallo, V., Schwarzer, E., Rahlfs, S., Schirmer, R.H., van Zwieten, R., Roos, D., Arese, P. and Becker, K. (2009). Inherited glutathione reductase deficiency and *Plasmodium falciparum* malaria—a case study. *PLoS One*, 4(10), e7303.

Garcia, S.C., Grotto, D., Bulcão, R.P., Moro, A.M., Roehrs, M., Valentini, J., de Freitas, F.A., Paniz, C., Bubols, G.B. and Charão, M.F. (2013). Evaluation of lipid damage related to pathological and physiological conditions. *Drug and chemical toxicology*, 36(3), 306-312.

Gavigan, C.S., Dalton, J.P. and Bell, A. (2001). The role of aminopeptidases in haemoglobin degradation in *Plasmodium falciparum*-infected erythrocytes. *Molecular and biochemical parasitology*, 117(1), 37-48.

Geering, K. (1994). Na, K-ATPase. *Curr Opin Nephrology Hypertension*, 6, 434.

Gemma, S., Vichi, S. and Testai, E. (2006). Individual susceptibility and alcohol effects: biochemical and genetic aspects. *Ann. Ist. Super. Sanita.*, 42, 8-16.

George, J.N. (2000). Platelets. *Lancet*, 355, 1531-1539

Gilbert, B. and Alves, L.F. (2003). Synergy in plant medicines. *Current medicinal chemistry*, 10, 13-20.

Gill, S.S. and Tuteja, N. (2010). Reactive oxygen species and antioxidant machinery in abiotic stress tolerance in crop plants. *Plant physiology and biochemistry*, 48(12), 909-930.

Ginsburg, H. (1990). Some reflections concerning host erythrocyte-malarial parasite interrelationships. *Blood Cells*, 16, 225–235.

Ginsburg, H. (2005). Should chloroquine be laid to rest? *Acta tropica*, 96(1), 16-23.

Giovannini, C. and Masella, R. (2012). Role of polyphenols in cell death control. *Nutritional Neuroscience*, 15(3), 134–149.

Giri, P., Hossain, M. and Kumar, G.S. (2006). RNA specific molecules: cytotoxic plant alkaloid palmatine binds strongly to poly(A). *Bioorganic and Medicinal Chemistry Letters*, 16(9), 2364–2368.

Glavind, E., Aagaard, N.K., Grønbæk, H., Møller, H.J., Orntoft, N.W., Vilstrup, H. and Thomsen, K.L. (2016). Alcoholic Hepatitis Markedly Decreases the Capacity for Urea Synthesis. *PloS one*, 11(7), e0158388.

Gluzman, I.Y., Francis, S.E., Oksman, A., Smith, C.E., Duffin, K.L. and Goldberg, D.E. (1994). Order and specificity of the *Plasmodium falciparum* hemoglobin degradation pathway. *Journal of Clinical Investigation*, 93(4), 1602-1608.

Goel, A., Danni, V. and Dhawan, D.K. (2005). Protective effects of zinc on lipid peroxidation, antioxidant enzymes and hepatic histoarchitecture in chlorpyrifos-induced toxicity. Chem Biol Interact, 156, 131–140.

Goldberg, D.E. (1993). Hemoglobin degradation in Plasmodium-infected red blood cells. *Semin Cell Biol*, 4, 355–361.

Goldberg, D.E., Slater, A.F., Beavis, R., Chait, B., Cerami, A. and Henderson, G.B. (1991). Hemoglobin degradation in the human malaria pathogen *Plasmodium falciparum*: a catabolic pathway initiated by a specific aspartic protease. *Journal of Experimental Medicine*, 173(4), 961-969.

Goldberg, D.M. and Spooner, R.J (1983). In: Methods of enzymatic analysis. Bergmeyen, H.V. (Ed). 3rd edition, Verlog Chemie, Deerfield Beach, Florida, 3, pp. 258-265.

Goldstein-Fuchs, D.J. and LaPierre, A.F. (2014). Nutrition and Kidney Disease., In: Gilbert, S.J. and Weiner, D.E. (eds.), *National Kidney Foundation Primer on Kidney Diseases*, 6th edition, Elsevier Saunders, St. Louis, pp. 467–475.

Gorman, L.S. (2007). Assessment of Cardiovascular Disorders. In: Arneson, W.L. and Brickell, J.M. (eds.), *Clinical Chemistry: A Laboratory Perspective*, F.A. Davis Company, Philadelphia, pp. 267.

Gornall, A.G., Bardawill, C.T. and David, M.M. (1949). Determination of serum protein by means of Biuret reaction. *Journal of Biological Chemistry*, 177, 751.

Gourley, G.R. (2004). Bilirubin metabolism. In: Walker, W.A., Goulet, O.J. and Kleinman, R.E. (eds.), *Pediatric gastrointestinal disease: pathophysiology, diagnosis, management*, 4th edition, BC Decker Inc., Ontario, pp. 1344-1362.

Gowda, S., Desai, P.B., Hull, V.V., Math, A.A.K., Vernekar, S.N. and Kulkarni, S.S. (2009). A review on laboratory liver function tests. *The Pan African Medical Journal*, 3, 17.

Gowda, S., Desai, P.B., Kulkarni, S.S., Hull, V.V., Math, A.A. and Vernekar, S.N. (2010). Markers of renal function tests. *North American journal of medical sciences*, 2(4), 170-173.

Gramaglia, I. Sobolewski, P. Meays, D. Contreras, R. Nolan, J.P. and Frangos, J.A. (**2006).** Low nitric xide bioavailability contributes to the genesis of experimental cerebral malaria. *Nat. Med.*, *12*, 1417–1422.

Grauer, G.F. (2005). Canine glomerulonephritis: new thoughts on proteinuria and treatment. *Journal of small animal practice*, 46(10), 469-478.

Greaves, P. (2012). Histopathology of preclinical toxicity studies: interpretation and relevance in drug safety evaluation. 4th edition, Academic Press, San Diego.

Greenwood, B. (2017).New tools for malaria control-using them wisely. *Journal of Infection*, 74, S23-S26.

Greisen, J., Grofte, T., Hansen, P.O., Jensen, T.S. and Vilstrup, H. (1999). Acute non-traumatic pain increases the hepatic amino- to urea-N conversion in normal man. *Journal of hepatology*, 31(4), 647–55.

Griffith, O.W. (1999). Biologic and pharmacologic regulation of mammalian glutathione synthesis. *Free Radical Biology and Medicine*, 27(9), 922-935.

Grochowalska, A. and Bernat, R. (1997). Adaptation of ATP-ase activity in synaptosomes of various cerebral regions in hypoxia, modified by adrenergic and gabaergic influences). *Nowiny Lekarskie*, 66, 397-412.

Grycova´, L., Dosta´l, J. and Marek, R. (2007). Quaternary protoberberine alkaloids. *Phytochemistry*, 68, 150–175.

Guerini, D., Zecca-Mazza, A. and Carafoli, E. (2000). Single amino acid mutations in transmembrane domain 5 confer to the plasma membrane Ca^{2+}pump properties typical of the Ca^{2+} pump of endo(sarco)plasmic reticulum. *J Biol Chem*, 275, 31361–31368.

Guerra, E.M.L. and Porbén, S.S. (2015). T-Cell Number, Nutritional Status, and HIV: The Cuban Experience in the Provision of Food and Nutrition Care to People with HIV/AIDS. In: Watson, R.R. (ed.), *Health of HIV Infected People*, Academic press, San Diego, pp. 367–387.

Guha, M., Kumar, S., Choubey, V., Maity, P. and Bandyopadhyay, U. (2006). Apoptosis in liver during malaria: role of oxidative stress and implication of mitochondrial pathway. *The FASEB Journal*, 20(8), 1224-1226.

Guilbride, D.L., Guilbride, P.D.L. and Gawlinski, P. (2012). Malaria's deadly secret: a skin stage. *Trends in Parasitology*. 28(4), 142-150.

Gupta, S., Pandey, R., Katyal, R., Aggarwal, H.K., Aggarwal, R.P. and Aggarwal, S.K. (2005). Lipid peroxide levels and antioxidant status in alcoholic liver disease. *Indian Journal of Clinical Biochemistry*, 20(1), 67-71.

Gutierres, J.M., Carvalho, F.B., Schetinger, M.R.C., Agostinho, P., Marisco, P.C., Vieira, J.M., Rosa, M.M., Bohnert, C., Rubin, M.A., Morsch, V.M. and Spanevello, R. (2014). Neuroprotective effect of anthocyanins on acetylcholinesterase activity and attenuation of scopolamine-induced amnesia in rats. *International Journal of Developmental Neuroscience*, 33, 88-97.

Guyton, J.R. (2008). Lipoproteins in diabetes: Risk and opportunity. In: Feinglos, M.N. and Bethel, M.A. (eds.), *Type 2 Diabetes Mellitus: An Evidence-Based Approach to Practical Management*, Springer Science & Business Media, New Jersey, pp. 265-288.

Habig, W.H., Pabst, M.J. and Jacoby, W.B. (1974). Glutathione-S-transferases. The first enzymatic step in mercapturic acid formation. *Journal of Biological Chemistry*, 249, 7130-7139.

Hagerman, A.E., Riedl, K.M., Jones, G.A., Sovik, K.N., Ritchard, N.T., Hartzfeld, P.W. and Riechel, T.L. (1998). High molecular weight plant polyphenolics

(tannins) as biological antioxidants. *Journal of Agricultural and Food Chemistry*, 46(5), 1887-1892.

Hall, J.E. (2011). Guyton and Hall Textbook of Medical Physiology. 12th edition, Saunders Elsevier, Philadelphia, pp. 101-120, 303-321, 413-432.

Halliwell, B. and Gutteridge, J.M. (1995). The definition and measurement of antioxidants in biological systems. *Free Radical Biology and Medicine*, 18(1), 125-126.

Hamilton, C.A., Miller, W.H., Sammy, A.B., Brosnan, M.J., Drummond, R.D., McBride, M.W. and Dominiczak, A.F. (2004). Strategies to reduce oxidative stress in cardiovascular disease. *Clinical Science*, 106(3), 219-234.

Hanson, J., Hossain, A., Charunwatthana, P., Hassan, M.U., Davis, T.M., Lam, S.W., Chubb, S.P., Maude, R.J., Yunus, E.B., Haque, G. and White, N.J. (2009). Hyponatremia in severe malaria: evidence for an appropriate anti-diuretic hormone response to hypovolemia. *The American journal of tropical medicine and hygiene*, 80(1), 141-145.

Hanson, J., Lee, S.J., Hossain, M.A., Anstey, N.M., Charunwatthana, P., Maude, R.J., Kingston, H.W., Mishra, S.K., Mohanty, S., Plewes, K. and Piera, K. (2015). Microvascular obstruction and endothelial activation are independently associated with the clinical manifestations of severe falciparum malaria in adults: an observational study. *BMC medicine*, 13(1), 122.

Harris, H. (1990). The human alkaline phosphatases: what we know and what we don't know. *Clinica chimica acta*, 186(2), 133-150.

Hauptmann, S., Scherping, I., Drose, S., Brandt, U., Schulz, K.L., Jendrach, M., Leuner, K., Eckert, A. and Muller, W.E. (2009). Mitochondrial dysfunction: an early event in Alzheimer pathology accumulates with age in AD transgenic mice. *Neurobiol. Aging,* 30, 1574–1586.

He, Z., Chen, L., You, J., Qin, L. and Chen, X. (2010). *In vitro* interactions between antiretroviral protease inhibitors and artemisinin endoperoxides against *Plasmodium falciparum*. *International Journal of Antimicrobial Agents,* 35, 191–193.

Hediger, M.A., Johnson, R.J., Miyazaki, H. and Endou, H. (2005). Molecular physiology of urate transport. *Physiology*, 20(2), 125-133.

Hercus, T.R., Thomas, D., Guthridge, M.A., Ekert, P.G., King-Scott, J., Parker, M.W. and Lopez, A.F. (2009). The granulocyte-macrophage colony-stimulating factor receptor: linking its structure to cell signaling and its role in disease. *Blood*, 114(7), 1289-1298.

Hettling, H. and van Beek, J.H.G. (2011). Analyzing the functional properties of the creatine kinase system with multiscale 'sloppy'modeling. *PLoS computational biology*, 7(8), e1002130.

Hink, H.U., Santanam, N., Dikalov, S., McCann, L., Nguyen, A.D., Parthasarathy, S., Harrison, D.G. and Fukai, T. (2002). Peroxidase properties of extracellular superoxide dismutase. *Arteriosclerosis, thrombosis, and vascular biology*, 22(9), 1402-1408.

Hirt, H.M., M'pia, B. and Lindsey, K. (2008). Natural medicine in the tropics. Anamed.

Honda, A., Komuro, H., Hasegawa, T., Seko, Y., Shimada, A., Nagase, H., Hozumi, I., Inuzuka, T., Hara, H., Fujiwara, Y. and Satoh, M. (2010). Resistance of metallothionein-III null mice to cadmium-induced acute hepatotoxicity. Journal of Toxicological Sciences, 35, 209-215.

Hoppe, H.C., van Schalkwyk, D.A., Wiehart, U.I., Meredith, S.A., Egan, J. and Weber, B.W. (2004). Antimalarial quinolines and artemisinin inhibit endocytosis in *Plasmodium falciparum*. *Antimicrobial agents and chemotherapy*, 48(7), 2370-2378.

Houseman, E.A., Accomando, W.P., Koestler, D.C., Christensen, B.C., Marsit, C.J., Nelson, H.H., Wiencke, J.K. and Kelsey, K.T. (2012). DNA methylation arrays as surrogate measures of cell mixture distribution. *BMC bioinformatics*, 13(1), 86.

Huang, D., Ou, B. and Prior, R.L. (2005). The Chemistry behind Antioxidant Capacity Assays. *J. Agric. Food Chem.*, 53, 1841-1856.

Huang, S.Y. and Zou, X. (2010). Advances and challenges in protein-ligand docking. *International journal of molecular sciences*, 11(8), 3016-3034.

Imlay, J.A., Chin, S.M. and Linn, S. (1988). Toxic DNA damage by hydrogen peroxide through the Fenton reaction *in vivo* and *in vitro.Science* 240, 640–642.

Isamah, G.K. and Asagba, S.O. (2003). The Effect of Acute *Plasmodium falciparum* Infection on the levels of Malondialdehyde (MDA) and Ascorbic acid on Nigerian Children. *Journal of Applied Sciences and Environmental Management*, 7(2), 59-61.

Jaffe, A.S., Babuin, L. and Apple, F.S. (2006). Biomarkers in acute cardiac disease: the present and the future. *Journal of the American College of Cardiology*, 48(1), 1-11.

Janakiraman, K. and Manavalan, R. (2011). Compatibility and stability studies of ampicillin trihydrate and piperine mixture. *International Journal of Pharmaceutical Sciences and Research,* 2(5), 1176.

Jantarat, C. (2013). Bioavailability enhancement techniques of herbal medicine: a case exampleof curcumin. *Int J Pharm Pharm Sci.* 5(1), 493-500.

Jantarat, C. (2013). Bioavailability enhancement techniques of herbal medicine: A case example of curcumin. *International Journal of Pharmacy and Pharmaceutical Science*, 5, 493-500.

Jaramillo, M., Gowda, D.C., Radzioch, D. and Oliver, M. (2003). Hemozoin increase IFN-gamma-inducible macrophage nitric oxide generation through extracellular signal-regulated kinase- and NF-Kappa B-dependent pathways. *J. Immunol*., 171, 4243-4253.

Jasani, J.H., Sancheti, S.M., Gheewala, B.S., Bhuva, K.V., Doctor, V.S., Vacchani, A.B., Patel, V.R. and Dharya, L. (2012). Association of the electrolyte disturbances (Na+, K+) with the type and severity of the malarial parasitic infection. *J Clin Diagn Res*, 6, 678-681.

Jayaprakash, G.K., Singh, R.P., Sakariah, K.K. (2001). Antioxidant activity of grape seed extracts on peroxidation models *in-vitro*. *J. Agric. Food Chem*. 55, 1018–1022.

Jayeola, C.O., Oluwadun, A., Olubamiwa, O., Effedua, H.I. and Kale, O.E. (2011). Anti-malarial activity of cocoa powder in mice. *African Journal of Biochemistry Research*, 5(11), 328-332.

Jendrassik, L. and Grof, P. (1938). Quantitative determination of total and direct bilirubin in serum and plasma. *Biochemische Zeitchrift*, 297(8).

Jialal, I. and Devaraj, S. (1996). Low-density lipoprotein oxidation, antioxidants, and atherosclerosis: a clinical biochemistry perspective. *Clinical Chemistry*, 42(4), 498-506.

Jiamboonsri, P., Pithayanukul, P., Bavovada, R., Leanpolchareanchai, J., Yin, T., Gao, S. and Hu, M. (2015). Factors influencing oral bioavailability of Thai mango seed kernel extract and its key phenolic principles. *Molecules*, 20(12), 21254-21273.

Jiamboonsri, P., Pithayanukul, P., Bavovada, R., Leanpolchareanchai, J., Gao, S. and Hu, M. (2016). *In vitro* glucuronidation of methyl gallate and pentagalloyl glucopyranose by liver microsomes. *Drug metabolism and pharmacokinetics*, 31(4), 292-303.

Jiang, S., Prigge, S.T., Wei, L., Gao, Y.E., Hudson, T.H., Gerena, L., Dame, J.B. and Kyle, D.E. (2001). New Class of Small Nonpeptidyl Compounds Blocks*Plasmodium falciparum* Development *In vitro* by Inhibiting Plasmepsins. *Antimicrobial agents and Chemotherapy*, 45(9), 2577-2584.

Johnson-Davis, K. and McMillin, G.A. (2010). Enzymes. In: Bishop, M.L., Fody, E.P. and Schoeff, L.E. (eds.), *Clinical Chemistry; Techniques, principles,*

correlations, 6th edition, Lippincott Williams & Wilkins, Philadelphia, pp. 281-308.

Jones, D.P. (2002). Redox potential of GSH/GSSG couple: Assay and biological significance. *Methods in enzymology*, 348, 93-112.

Jorgensen, P.L., Hakansson, K.O. and Karlish, S.J. (2003). Structure and mechanism of Na,K-ATPase: functional sites and their interactions. *Annu Rev Physiol.*, 65, 817–849.

Jourdan, J.P., Schneider, J., Dassonville-Klimpt, A. and Sonnet, P. (2017). Recent advances in antimalarial drugs: structures, mechanisms of action and clinical trials. In: Méndez-Vilas, A. (ed.), *Antimicrobial research: Novel bioknowledge and educational programs*, 6th edition, Formatex Research Center, pp. 599-609.

Juberg, D.R., Mudra, D.R., Hazelton, G.A. and Parkinson, A. (2006). The effect of fenbuconazole on cell proliferation and enzyme induction in the liver of female CD1 mice. *Toxicology and applied pharmacology*, 214(2), pp.178-187.

Jung, H.A., Min, B.S., Yokozawa, T., Lee, J.H., Kim, Y.S. and Choi, J.S. (2009). Anti-Alzheimer and antioxidant activities of Coptidis Rhizoma alkaloids. *Biological and Pharmaceutical Bulletin*, 32(8), 1433-1438.

Kakar, A., Bhoi, S., Prakash, V. and Kakar, S. (1999). Profound thrombocytopenia in Plasmodium vivax malaria. *Diagnostic microbiology and infectious disease*, 35(3), 243-244.

Kalhan, S.C. (2000). Protein metabolism in pregnancy. *The American Journal of Clinical Nutrition*, 71(5 Suppl), 1249S-1255S.

Kamatham, S., Kumar, N. and Gudipalli, P. (2015). Isolation and characterization of gallic acid and methyl gallate from the seed coats of Givotia rottleriformis Griff. and their anti-proliferative effect on human epidermoid carcinoma A431 cells. *Toxicology Reports*, 2, 520-529.

Kane, C.J.M., Menna, J.H and Yeh, Y. (1988). Methyl gallate, methyl-3,4,5-trihydroxy-benzoate, is a potent and highly specific inhibitor of herpes simplex virus *in vitro*. I. Purification and characterization of methyl gallate from *Sapium sebiferum*. *Bioscience Reports*, 8(1), 85-94.

Kaneko, J.J., Harvey, J.W. and Bruss, M.L. (1997). Clinical Biochemistry of Domestic Animals. 5th edition, Academic Press, San Diego.

Kapetanovic, I.M. (2008). Computer-aided drug discovery and development (CADDD): *in silico*-chemico-biological approach. *Chemico-biological interactions*, 171(2), 165-176.

Kapoor, G. and Banyal, H.S. (2009). Glutathione reductase and thioredoxin reductase: novel antioxidant enzymes from Plasmodium berghei. *Korean J Parasitol*, 47, 421–424.

Kavishe, R.A., Koenderink, J.B. and Alifrangis, M. (2017). Oxidative stress in malaria and artemisinin combination therapy: Pros and Cons. *The FEBS Journal*.

Kavishe, R.A., Koenderink, J.B., McCall, M.B., Peters, W.H., Mulder, B., Hermsen, C.C., Sauerwein, R.W., Russel, F.G. and Van der Ven, A.J. (2006). Short report: severe *Plasmodium falciparum* malaria in Cameroon: associated with the glutathione S-transferase M1 null genotype. *Am J Trop Med Hyg*, 75, 827-829.

Kawazu, S., Yasuda-Komaki, K., Oku, H. and Kano, S. (2008). Peroxiredoxins in malaria parasites: parasitologic aspects. *Parasitol Int,* 57, 1–7.

Kehrer, J.P., Robertson, J.D. and Smith, C.V. (2010). Free Radicals and Reactive Oxygen Species. In: McQueen, C.A. (ed.), Comprehensive Toxicology, 2nd edition, Elsevier, pp. 277–307.

Kerbel, R.S., Yu, J., Tran, J., Man, S., Viloria-Petit, A., Klement, G., Coomber, B.L. and Rak, J. (2001). Possible mechanisms of acquired resistance to anti-angiogenic drugs: implications for the use of combination therapy approaches. *Cancer and Metastasis Reviews*, 20(1-2), 79-86.

Kesarwani, K. and Gupta, R. (2013). Bioavailability enhancers of herbal origin: An overview. *Asian pacific journal of tropical biomedicine*, 3(4), 253-266.

Khurana, S., Hollingsworth, A., Piche, M., Venkataraman, K., Kumar, A., Ross, G.M. and Tai, T.C. (2014). Antiapoptotic actions of methyl gallate on neonatal rat cardiac myocytes exposed to H_2O_2. *Oxidative medicine and cellular longevity*, 2014.

Khurana, S., Piche, M., Hollingsworth, A., Venkataraman, K. and Tai, T.C. (2013). Oxidative stress and cardiovascular health: therapeutic potential of polyphenols. *Canadian Journal of Physiology and Pharmacology*, 91(3), 198–212.

Kim, S., Jung, H., Hyum, D., Park, E., Kim, Y. and Lim, C. (2010). Glutathione reductase plays an anti-apoptotic role against oxidative stress in human hepatoma cells. *Biochimie*, 92, 927-932.

Kirk, K. and Horner, H.A. (1995). Novel anion dependence of induced cation transport in malaria-infected erythrocytes. *J. Biol. Chem.*, 270, 24270-24275.

Kitasato, H., Sato, S., Marunaka, Y., Murayama, K. and Nishio, K. (1980). Apparent affinity changes induced by insulin of Na-K transport system in frog skeletal muscle. *Jpn J Physiol.*, 30, 603–616.

Kitchen, D.B., Decornez, H., Furr, J.R. and Bajorath, J. (2004). Docking and scoring in virtual screening for drug discovery: methods and applications. *Nature reviews Drug discovery*, 3(11), 935-949.

Kleinveld, H.A., Hak-Lemmers, H.L., Stalenhoef, A.F. and Demacker, P.N. (1992). Improved measurement of low-density-lipoprotein susceptibility to copper-induced oxidation: application of a short procedure for isolating low-density lipoprotein. *Clinical Chemistry*, 38(10):2066-2072.

Kodydková, J., Vávrová, L., Kocík, M. and Zak, A. (2014). Human catalase, its polymorphisms, regulation and changes of its activity in different diseases. *Folia biologica*, 60(4), 153-167.

Kokwaro, G., Mwai, L. and Nzila, A. (2007). Artemether/lumefantrine in the treatment of uncomplicated falciparum malaria. *Expert opinion on pharmacotherapy*, 8(1), 75-94.

Kovesdy, C.P. (2012). Significance of hypo-and hypernatremia in chronic kidney disease. *Nephrology Dialysis Transplantation*, 27(3), 891–898.

Krause, W. J. (2001). The art of examining and interpreting histologic preparations. A student handbook. Partheton Publishing group, U.K. pp. 9-10.

Krettli, A.U., Adebayo, J.O. and Krettli, L.G. (2009). Testing of natural products and synthetic molecules aiming at new antimalarials. *Current drug targets*, 10(3), 261-270.

Krudsood, S., Imwong, M., Wilairatana, P., Pukrittayakamee, S., Nonprasert, A., Snounou, G., White, N.J. and Looareesuwan, S. (2005). Artesunate—dapsone—proguanil treatment of falciparum malaria: genotypic determinants of therapeutic response. *Transactions of the Royal Society of Tropical Medicine and Hygiene*, 99(2), 142-149.

Krugliak, M., Waldman, Z. and Ginsburg, H. (1987). Gentamicin and amikacin repress the growth of *Plasmodium falciparum* in culture, probably by inhibiting a parasite acid phospolipase. *Life sciences*, 40(13), 1253-1257.

Kuhn, V., Diederich, L., Keller IV, T.C.S., Kramer, C.M., Lu¨cksta¨dt, W., Panknin, C., Suvorava, T., Isakson, B.E., Kelm, M. and Cortese-Krott, M.M. (2017). Red Blood Cell Function and Dysfunction: Redox Regulation, Nitric Oxide Metabolism, Anemia. *Antioxidants & Redox Signaling*, 26(13), 718-742.

Kukula-Koch, W.A. and Widelski, J. (2017). Alkaloids. In: Badal, S. and Delgoda, R. (eds.), *Pharmacognosy: Fundamentals, Applications and Strategies*, Academic Press, San Diego, pp. 163–198.

Kumar, S., Bhandari, C., Sharma, P. and Agnihotri, N. (2018). Role of Piperine in Chemoresistance. In: Bharti, A.C. and Aggarwal, B.B. (eds.), *Role of Nutraceuticals in Cancer Chemosensitization*, Academic Press, San Diego, pp. 259–286.

Kumar, S., Guha, M., Choubey, V., Maity, P., Srivastava, K., Puri, S.K. and Bandyopadhyay, U. (2008). Bilirubin inhibits *Plasmodium falciparum* growth through the generation of reactive oxygen species. *Free Radic Biol Med*, 44, 602–613.

Kutzing, M.K. and Firestein, B.L. (2008). Altered uric acid levels and disease states. *Journal of Pharmacology and Experimental Therapeutics*, 324(1), 1-7.

Lamarche, B., Després, J.P., Moorjani, S., Cantin, B., Dagenais, G.R., and Lupien, P.J. (1996). Triglycerides and HDL-cholesterol as risk factors for ischemic heart disease. Results from the Quebec cardiovascular study. *Atherosclerosis*, 119(2), 235-245.

Lamb, E.J. and Price, C.P. (2008). Creatinine, urea, and uric acid. In: Burtis, C.A., Ashwood, E.R. and Bruns, D.E. (eds.), *Tietz fundamentals of clinical chemistry*, 6th edition, Saunders Elsevier, St. Louis. pp. 363-371.

Lambert, J.D., Hong, J., Kim, D.H., Mishin, V.M. and Yang, C.S, (2004). Piperine enhances the bioavailability of the tea polyphenol (-)-epigallocatechin-3-gallate in mice. *J Nutr*., 134, 1948-1952.

Lambert, J.D., Hong, J., Kim, D.H., Mishin, V.M. and Yang, C.S. (2004). Piperine enhances the bioavailability of the tea polyphenol (−)-epigallocatechin-3-gallate in mice. *The Journal of nutrition*, 134(8), 1948-1952.

Larson, D. (2015). Clinical Chemistry: Fundamentals and Laboratory Techniques. Elsevier Health Sciences, pp. 289-305.

Laskshmi, B.V. and Sudhakar, M. (2010). Protective effect of Zingiber officinale on gentimicin-induced nephrotoxicity in rats. *Int J Pharmacol*, 6(1), 58-62.

Lee, J.K. (2013). Anti-depressant like effect of methyl gallate isolated from acer barbinerve in mice. *The Korean Journal of Physiology & Pharmacology*, 17(5), 441-446.

Lee, T.H., Kim, W.R. and Poterucha, J.J. (2012). Evaluation of elevated liver enzymes. *Clinics in liver disease*, 16(2), 183-198.

Lefkowitch, J.H. (2011). Anatomy and Function. In: Dooley, J.S., Lok, A., Burroughs, A.K. and Heathcote, J. (eds.), *Sherlock's diseases of the liver and biliary system*, 12th edition, Wiley Blackwell, Oxford, pp. 1-18.

Lei, X.G., Zhu, J.H., Cheng, W.H., Bao, Y., Ho, Y.S., Reddi, A.R., Holmgren, A. and Arnér, E.S. (2016). Paradoxical roles of antioxidant enzymes: basic mechanisms and health implications. *Physiological reviews*, 96(1), 307-364.

Lew, V.L., Tiffert, T. and Ginsburg, H. (2003). Excess hemoglobin digestion and the osmotic stability of *Plasmodium falciparum*-infected red blood cells. *Blood*, 101, 4189–4194.

Li, G., Chen, Y., Hu, H., Liu, L., Hu, X., Wang, J., Shi, W. and Yin, D. (2012). Association between age-related decline of kidney function and plasma malondialdehyde. *Rejuvenation research*, 15(3), 257-264.

Liu, J., Gluzman, I.Y., Drew, M.E. and Goldberg, D.E. (2005). The role of *Plasmodium falciparum* food vacuole plasmepsins. *Journal of Biological Chemistry*, 280(2), 1432-1437.

Liu, S., Chen, Y., Gu, L., Li, Y., Wang, B., Hao, J., Zhu, H., Li, H., Yang, S. and Kitanaka, S. (2013). Effects of ultrahigh pressure extraction conditions on

yields of berberine and palmatine from cortex Phellodendri amurensis. *Analytical Methods*, 5(17), 4506-4512.

Liu, T., Stern, A., Roberts, L.J. and Morrow, J.D. (1999). The isoprostanes: novel prostaglandin-like products of the free radical-catalyzed peroxidation of arachidonic acid. *Journal of biomedical science*, 6(4), 226-235.

Lo, S., Chang, Y., Tsai, K., Chang, C., Wu, T. and Ueng, Y. (2013). Inhibition of CYP1 by berberine, palmatine, and jatrorrhizine: Selectivity, kinetic characterization, and molecular modeling. *Toxicology and Applied Pharmacology*, 272, 671–680.

Lobo, V., Patil, A., Phatak, A. and Chandra, N. (2010). Free radicals, antioxidants and functional foods: Impact on human health. *Pharmacognosy reviews*, 4(8), 118-126.

Looareesuwan, S., Chulay, J.D., Canfield, C.J. and Hutchinson, D.B. (1999). Malarone (atovaquone and proguanil hydrochloride): a review of its clinical development for treatment of malaria. Malarone Clinical Trials Study Group. *The American journal of tropical medicine and hygiene*, 60(4), 533-541.

Lopez, L.R., Bliden, K.P., Chaudhary, R., Damrongwatanasuk, R., Guyer, K.E., Gesheff, M.G., Franzese, C.J., Tantry, U.S. and Gurbel, P.A. (2016). Pro-atherogenic oxidized-LDL/B2-glycoprotein I complexes in coronary artery disease patients are associated with disease severity. *Atherosclerosis*, 252, e219.

Lu, S.C. (2001). Regulation of glutathione synthesis. *Current topics in cellular regulation*, 36, 95-116.

Lu, Z., Nie, G., Belton, P.S., Tang, H. and Zhao, B. (2006). Structure–activity relationship analysis of antioxidant ability and neuroprotective effect of gallic acid derivatives. *Neurochemistry international*, 48(4), 263-274.

Lund-Katz, S. and Phillips, M.C. (2010). High density lipoprotein structure–function and role in reverse cholesterol transport. In: *Cholesterol Binding and Cholesterol Transport Proteins*, Springer, Netherlands, pp. 183-227.

Lushchak, V.I. (2014). Free radicals, reactive oxygen species, oxidative stress and its classification. *Chemico-biological interactions*, 224, 164-175.

Lütjohann, D., Breuer, O., Ahlborg, G., Nennesmo, I., Siden, A., Diczfalusy, U. and Björkhem, I. (1996). Cholesterol homeostasis in human brain: evidence for an age-dependent flux of 24S-hydroxycholesterol from the brain into the circulation. *Proceedings of the National Academy of Sciences*, 93(18), 9799-9804.

Lytton, J., Westlin, M. and Hanley, M.R. (1991). Thapsigargin inhibits the sarcoplasmic or endoplasmic reticulum Ca-ATPase family of calcium pumps. *Journal of Biological Chemistry*, 266(26), 17067-17071.

Lytton, J., Zarain-Herzberg, A., Periasamy, M. and MacLennan, D.H. (1989). Molecular cloning of the mammalian smooth muscle sarco(endo)plasmic reticulum Ca^{2+}-ATPase. *J Biol Chem*, 264, 7059–7065.

Ma, B.L. and Ma, Y.M. (2013). Pharmacokinetic properties, potential herb–drug interactions and acute toxicity of oral Rhizoma coptidis alkaloids. *Expert opinion on drug metabolism & toxicology*, 9(1), 51-61.

Mackinnon, M.J. and Marsh, K. (2010). The selection landscape of malaria parasites. *Science*, 328, 866–71.

Magnotti, R.A., Eberly, J.P., Quarm, D.E. and Mcconnell, R.S. (1987). Measurement of acetylcholinesterase in erythrocytes in the field. *Clinical chemistry*, 33(10), 1731-1735.

Maithri, G., Manasa, B., Vani, S.S., Narendra, A. and Harshita, T. (2016). Computational Drug Design and Molecular Dynamic Studies-A Review. *Biomedical Data Mining*, 5, 123.

Makino, N., Mochizuki, Y., Bannai, S. and Sugita, Y. (1994). Kinetic studies on the removal of extracellular hydrogen peroxide by cultured fibroblasts. *J Biol Chem,* 269, 1020-1025.

Malebo, H.M., Wenzler, T., Cal, M., Swaleh, S.M., Omolo, M.O., Hassanali, A., Séquin, U., Häussinger, D., Dalsgaard, P., Hamburger,M., Brun, R. and Ndiege, I.O. (2013). Anti-protozoal activity of aporphine and protoberberine alkaloids from Annickia kummeriae (Engl. & Diels) Setten &Maas (Annonaceae). BMC Complementary and Alternative Medicine, 13, 48-58.

Mangialavori, I., Ferreira-Gomes, M., Pignataro, M.F., Strehler, E.E. and Rossi, J.P. (2010). Determination of the dissociation constants for Ca^{2+} and calmodulin from the plasma membrane Ca^{2+} pump by a lipid probe that senses membrane domain changes. *J Biol Chem.*, 285, 123–130.

Marchesini, N., Vieira, M., Luo, S., Moreno, S. N. and Docampo, R. (2005). A malaria parasite-encoded vacuolar H^{+}-ATPase is targeted to the host erythrocyte. *J. Biol. Chem.*, 280, 36841-36847.

Marcocci, I., Marguire, J.J., Droy-lefaiz, M.T. and Packer, L. (1994). The nitric oxide scavenging properties of Ginkgo biloba extract. *Biochem. Biophys. Res. Commun*., 201, 748–755.

Marletta, M.A. (1989). Nitric oxide: biosynthesis and biological significance. *Trends Biochem. Sci*., 14 (12), 488–492.

Martinelli, A. Rodrigues, L.A. and Cravo, P. (2008). *Plasmodium chabaudi*: efficacy of artemisinin + curcumin combination treatment on a clone selected for artemisinin resistance in mice. *Experimental Parasitology*. 119(2), 304–307.

Martinelli, A. Rodrigues, L.A. and Cravo, P. (2008). *Plasmodium chabaudi*: efficacy of artemisinin + curcumin combination treatment on a clone selected for artemisinin resistance in mice. *Experimental Parasitology*, 119(2), 304–307.

Martyn, J.A., Standaert, F.G. and Miller, R.D. (2000). Neuromuscular physiology and pharmacology. In: Martyn, J.A (ed.), *Anesthesia*, 5th edition, Churchill Livingstone, Philadelphia, pp.735-751.

Mata, A.M. and Sepulveda, M.R. (2010). Plasma membrane Ca-ATPases in the nervous system during development and ageing. *World J. Biol. Chem.*, 1, 229–234.

Mazzetti, A.P., Fiorile, M.C., Primavera, A. and Bello, M.L. (2015). Glutathione transferases and neurodegenerative diseases. *Neurochemistry International*, 82, 10–18.

McGill, M.R. (2016). The past and present of serum aminotransferases and the future of liver injury biomarkers. *EXCLI journal*, 15, 817-828.

McGill, M.R., Staggs, V.S., Sharpe, M.R., Lee, W.M. and Jaeschke, H. (2014). Acute liver failure study group. Serum mitochondrial biomarkers and damage-associated molecular patterns are higher in acetaminophen overdose patients with poor outcome. *Hepatology*, 60, 1336-45.

McGillewie, L. and Soliman, M.E. (2015). Flap flexibility amongst plasmepsins I, II, III, IV, and V: Sequence, structural, and molecular dynamics analyses. *Proteins*, 83, 1693–1705.

McKay, P.B., Peters, M.B., Carta, G., Flood, C.T., Dempsey, E., Bell, A., Berry, C., Lloyd, D.G. and Fayne, D. (2011). Identification of plasmepsin inhibitors as selective anti-malarial agents using ligand based drug design. *Bioorganic & medicinal chemistry letters*, 21(11), 3335-3341.

McMorran, B.J., Marshall, V.M., de Graaf, C., Drysdale, K.E., Shabbar, M., Smyth, G.K., Corbin, J.E., Alexander, W.S. and Foote, S.J. (2009). Platelets kill intraerythrocytic malarial parasites and mediate survival to infection. *Science*, 323(5915), 797-800.

McPherson, R.A. and Pincus, M.R. (2011). Henry's Clinical Diagnosis and Management by Laboratory Methods. 22nd edition, Elsevier Saunders, St. Louis, pp. 180-183, 297-299.

Meng, X.Y., Zhang, H.X., Mezei, M. and Cui, M. (2011). Molecular docking: a powerful approach for structure-based drug discovery. *Current computer-aided drug design*, 7(2), 146-157.

Messner, D.J., Murray, K.F. and Kowdley, K.V. (2012). Mechanisms of Hepatocyte Detoxification. In: Johnson, L.R. (ed.), Physiology of the Gastrointestinal Tract, 5th edition, Academic Press, San Diego, pp. 1507-1527.

Metzler, D.E. (2003). Biochemistry: The chemical reactions of living cells. 2nd edition, Elsevier Academic press, San Diego.

Michael, B., Yano, B., Sellers, R.S., Perry, R., Morton, D., Roome, N., Johnson, J.K. and Schafer, K. (2007). Evaluation of organ weights for rodent and non-rodent toxicity studies: a review of regulatory guidelines and a survey of current practices. *Toxicologic pathology*, 35(5), 742-750.

Mi-Ichi, F., Takeo, S., Takashima, E., Kobayashi, T., Kim, H., Wataya, Y., Matsuda, A., Torii, M., Tsuboi, T., Kita, K. (2003). Unique Properties of Respiratory Chain in *Plasmodium falciparum* Mitochondria. In: Marzuki, S., Verhoef, J. and Snippe, H. (eds.), *Tropical diseases, from molecule to bedside*, Springer, Boston, pp 117–133.

Millan, J.L. (2006). Alkaline Phosphatases: Structure, substrate specificity and functional relatedness to other members of a large superfamily of enzymes. *Purinergic Signalling*, 2, 335-341.

Miller, A. (2012). Superoxide dismutases: Ancient enzymes and new insights. *FEBS Letters*, 586, 585–595.

Miller, L.H., Ackerman, H.C., Su, X.Z. and Wellems, T.E. (2013). Malaria biology and disease pathogenesis: insights for new treatments. *Nat Med*, 19, 156-167.

Mishra, N., Kaitholia, K., Srivastava, B., Shah, N.K., Narayan, J.P., Dev, V., Phookan, S., Anvikar, A.R., Rana, R., Bharti, R.S. and Sonal, G.S. (2014). Declining

efficacy of artesunate plus sulphadoxine-pyrimethamine in northeastern India. *Malaria journal*, 13(1), 284.

Misra, H.P. and Fridovich, I. (1972). The role of superoxide anion in the autoxidation of epinephrine and a simple assay for superoxide dismutase. *Journal of Biological Chemistry*, 247(10), 3170-3175.

Mohamed, N.E. and Wakwak, M.M. (2014). Effect of sesame seeds or oil supplementation to the feed on some physiological parameters in Japanese quail. *J. Radiat. Res. Appl. Sci*., 7, 101-109.

Mohamed, T.M., Zakeri, S.A., Baudoin, F., Wolf, M., Oceandy, D., Cartwright, E.J., Gul, S. and Neyses, L. (2013). Optimisation and validation of a high throughput screening compatible assay to identify inhibitors of the plasma membrane calcium ATPase pump-a novel therapeutic target for contraception and malaria. *Journal of Pharmacy & Pharmaceutical Sciences*, 16(2), 217-230.

Moldovan, L. and Moldovan, N.I. (2004). Oxygen free radicals and redox biology of organelles. *Histochemistry and Cell Biology*, 122(4), 395–412.

Moncada, S., Palmer Jr, R.M. and Higgs, E.A. (1989). Biosynthesis of nitric oxide from L-arginine: a pathway for the regulation of cell function and communication. *Biochem. Pharmacol.*, 38, 1709–1715.

Moody, A. (2002). Rapid diagnostic tests for malaria parasites. *Clin Microbiol Rev.*, 15, 66-78.

Moriyama, T., Nobuoka, M. and Makino, M. (1990). Incidence and properties of aspartate aminotransferase-immunoglobulin complexes in patients with a high

serum aspartate to alanine aminotransferase ratio. *Clinica Chimica Acta*, 190(1-2), 47-56.

Moriyama, Y., Hayashi, M., Yatsushiro, S. and Yamamoto, A. (2003). Vacuolar proton pumps in malaria parasite cells. *J. Bioenerg. Biomembr.*, 35, 367-375.

Mornet, E. (2008). Hypophosphatasia. *Best Practice & Research Clinical Rheumatology*, 22(1), 113–127.

Morrell, C.N., Aggrey, A.A., Chapman, L.M. and Modjeski, K.L. (2014). Emerging roles for platelets as immune and inflammatory cells. *Blood*, 123(18), 2759-2767.

Mount, D.B., Kwon, C.Y. and Zandi-Nejad, K. (2006). Renal urate transport. *Rheumatic Disease Clinics of North America*, 32(2), 313-331.

Mukherjee, S. and Gollan, J.L. (2011). Assessment of liver function. In: Dooley, J.S., Lok, A., Burroughs, A.K. and Heathcote, J. (eds.), *Sherlock's diseases of the liver and biliary system*, 12th edition, Wiley Blackwell, Oxford, pp. 20–35.

Muller, F.L., Lustgarten, M.S., Jang, Y., Richardson, A. and van Remmen, H. (2007). Trends in oxidative aging theories. Free Radic. Biol., 43, 477-503.

Muller, S. (2004). Redox and antioxidant systems of the malaria parasite *Plasmodium falciparum*. *Molecular Microbiology*, 53, 1291-1305.

Muraleedharan, K.M. and Avery, M.A. (2007). Advances in the Discovery of New Antimalarials. In: Triggle, D.J. and Taylor, J.B. (eds.), *Comprehensive Medicinal Chemistry II*, Elsevier, pp. 765–814.

Murray, R.K. (2012). Metabolism of Xenobiotics. In: Murray, R.K *et al.* (eds.), *Harpers Illustrated Biochemistry*, 29th edition, McGraw-Hill, pp. 676.

Muttigi, M.S., Kedage, V., Suvarna, R., Rao, S.S., Joshi, C., Shetty, M.S. and Prakash, M. (2009). Serum GST activity and total thiols status in patients with liver disease secondary to various disorders. *J The Open Hepatology*, 1, 5-8.

Nader, R., Russell, W. and Alan, R. (2008). Lipids, lipoproteins, apolipoproteins, and other cardiovascular risk factors. In Tiez Fundamentals of Clinical Chemistry, Carl, A., Burtis, E. and David, E.B. (eds.). Elsevier Publisher: India, 402–430.

Naghii, M.R., Almadadi, M. and Zarchi, A.A. (2011). Regular physical activity as a basic component of lifestyle modification reduces major cardiovascular risk factors among male armored force personnel of Shabestar army installation in Iran. *Work*, 40(2), 217-227.

Nam, W., Kim, S.P., Nam, S.H. and Friedman, M. (2017).Structure-Antioxidative and Anti-Inflammatory Activity Relationships of Purpurin and Related Anthraquinones in Chemical and Cell Assays. *Molecules*,22, 265-279.

Nashar, K. and Fried, L.F. (2012). Hyperuricemia and the progression of chronic kidney disease: is uric acid a marker or an independent risk factor? *Advances in chronic kidney disease*, 19(6), 386-391.

Ncokazi, K.K. and Egan, T.J. (2005). A colorimetric high-throughput β-hematin inhibition screening assay for use in the search for antimalarial compounds. *Analytical Biochemistry*, 338, 306–319.

Nedeljkovic, N., Nikezic, G., Horvat, A., Pekovic, S., Stojiljkovic, M. and Martinovic, J.V. (1998). Properties of Mg(2+)- ATPase rat brain synaptic plasma membranes. *Gen Physiol Biophys,* 17, 3-13.

Nelson, D.L. and Cox, M.M. (2013). Glycolysis, Gluconeogenesis, and the Pentose Phosphate Pathway. In: *Lehninger Principles of Biochemistry*, 6th edition, W.H. Freeman, New York, pp. 398-402, 521.

Nelson, R.H. (2013). Hyperlipidemia as a risk factor for cardiovascular disease. *Primary Care: Clinics in Office Practice,* 40(1), 195-211.

Nemati, H., Khodarahmi, R., Rahmani, A., Ebrahimi, A., Amani, M. and Eftekhari, K. (2013). Serum lipid profile in psoriatic patients: correlation between vascular adhesion protein 1 and lipoprotein (a). *Cell Biochem Funct*., 31, 36–40.

Newby, G., Bennett, A., Larson E., Cotter, C., Shretta, R., Phillips, A.A. and Feachem, R.G. (2016). The path to eradication: a progress report on the malaria-eliminating countries. *The Lancet*, 387(10029), 1775–1784.

Niki, E. (2009). Lipid peroxidation: physiological levels and dual biological effects. *Free Radical Biol Med,* 47, 469–484.

Nimse, S.B. and Pal, D. (2015). Free radicals, natural antioxidants, and their reaction mechanisms. *RSC Advances*, 5(35), 27986-28006.

Nisha, R., Kannan SR, S. and Jagatha, P. (2017). Biochemical evaluation of creatinine and urea in patients with renal failure undergoing hemodialysis. *Journal of Clinical Pathology and Laboratory Medicine,* 1(2), 1-5.

Nithitanakool, S., Pithayanukul, P. and Bavovada, R. (2009). Antioxidant and hepatoprotective activities of Thai mango seed kernel extract. *Planta medica*, 75(10), 1118-1123.

Noori, S. (2012). An overview of oxidative stress and antioxidant defensive system. *Open access scientific reports*, 1(8), 1-9.

Oakley, A. (2011). Glutathione transferases: a structural perspective. *Drug metabolism reviews*, 43(2), 138-151.

Ochei, J.O. and Kolhatkar, A.A. (2000). Medical laboratory science: theory and practice. McGraw Hill, New York, pp. 152-159.

Ochoa, S. (1955). Malic dehydrogenase in pig heart. In: Colowick, S.P., Kalpon, N.C. (eds.), Methods Enzymol., vol. I. Academic Press, New York, pp. 735– 739.

O'Donnell, C.J. and Elosua, R. (2008). Cardiovascular risk factors. Insights from framingham heart study. *Revista Espanola de Cardiologia*, 61(3), 299-310.

Odugbemi, T.O., Akinsulire, O.R., Aibinu, I.E. and Fabeku, P.O. (2007). Medicinal plants useful for malaria therapy in Okeigbo, Ondo State, Southwest Nigeria. *African Journal of Traditional, Complementary and Alternative Medicines*, 4(2), 191-198.

Ohrt, C., Willingmyre, G.D., Lee, P., Knirsch, C. and Milhous, W. (2002). Assessment of Azithromycin in Combination with Other Antimalarial Drugs against *Plasmodium falciparumIn vitro*. *Antimicrobial Agents and Chemotherapy*, 2518–2524.

Okomor, J., Ahmadu, A.A.. and Onanuga, A. (2012). Phenolic acid ester from Alchornia cordifolia leaves. *Nigerian Journal of Pharmaceutical Sciences*, 11(2), 67–72.

Olson, J.E., Lee, G.K., Semenov, A. and Rosenthal, P.J. (1999). Antimalarial effects in mice of orally administered peptidyl cysteine protease inhibitors. *Bioorganic & medicinal chemistry*, 7(4), 633-638.

Omodeo-Sale, M.F., Motti, A., Basilico, N., Parapini, S. and Olliaro, P. (2003). Accelerated senescence of human erythrocytes cultured with *Plasmodium falciparum*. *Blood*, 102, 705–711.

O'Neill, P.M., Ward, S.A., Berry, N.G., Jeyadevan, J.P., Biagini, G.A., Asadollaly, E., Park, B.K. and Bray, P.G. (2006). A medicinal chemistry perspective on 4-aminoquinoline antimalarial drugs. *Current topics in medicinal chemistry*, 6(5), 479-507.

Ong, P.K., Melchior, B., Martins, Y.C., Hofer, A., Orjuela-Sánchez, P., Cabrales, P., Zanini, G.M., Frangos, J.A. and Carvalho, L.J. (2013). Nitric oxide synthase dysfunction contributes to impaired cerebroarteriolar reactivity in experimental cerebral malaria. *PLoS pathogens*, 9(6), e1003444.

Orjih, A.U., Banyal, H.S., Chevli, R. and Fitch, C.D. (1981). Hemin lyses malaria parasites. Science, 214(4521), 667-669.

Orth, M. and Bellosta, S. (2012). Cholesterol: its regulation and role in central nervous system disorders. *Cholesterol*, 2012, 1-19.

Osman, A.G., Chittiboyina, A.G. and Khan, I.A. (2016). Cytoprotective Role of Dietary Phytochemicals Against Cancer Development via Induction of Phase II

and Antioxidant Enzymes. In: Fishbein, J.C. and Heilman, J.M. (eds.), *Advances in Molecular Toxicology*, Academic Press, San Diego, pp. 99-137.

Ota-Sullivan, K. and Blecker-Shelly, D.L. (2013). Use of the rapid BinaxNOW malaria test in a 24-hour laboratory associated with accurate detection and decreased malaria testing turnaround times in a pediatric setting where malaria is not endemic. *Journal of Clinical Microbiology*, 51(5), 1567–1569.

Oyaizu, M. (1986). Studies on products of browning reaction: Antioxidative activities of products of browning reaction prepared from glucosamine. *Journal of Nutrition,* 44, 307–315.

Ozer, J., Ratner, M., Shaw, M., Bailey, W. and Schomaker, S. (2008). The current state of serum biomarkers of hepatotoxicity. *Toxicology,* 245(3), 194-205.

Pal, D.K. and Nimse, S.B. (2006). Screening of the antioxidant activity of Hydrilla verticillata plant. *Asian Journal of Chemistry,* 18(4), 3004-3008.

Palmer, B.F. and Clegg, D.J. (2017). Electrolyte Disturbances in Patients with Chronic Alcohol-Use Disorder. *New England Journal of Medicine*, 377(14), 1368-1377.

Panduru, N.M., Cimponeriu, D., Cruce, M., Ion, D.A. and Mota, E. (2010). Association of +35A/C (intron3/exon3) polymorphism in SOD1-gene with diabetic nephropathy in type 1 diabetes. *Rom J Morphol Embryol*, 51, 37–41.

Paniccia, R., Priora, R., Liotta, A.A. and Abbate, R. (2015). Platelet function tests: a comparative review. *Vascular health and risk management*, 11, 133.

Panteghini, M. and Bais, R. (2008). Enzymes. In: Burtis, C.A., Ashwood, E.R. and Bruns, D.E. (eds.), *Tietz fundamentals of clinical chemistry*, 6th edition, Saunders Elsevier, St. Louis. pp. 317-336.

Parham, W.A., Mehdirad, A.A., Biermann, K.M. and Fredman, C.S. (2006). Hyperkalemia revisited. *Texas Heart Institute Journal*, 33(1), 40-47.

Parks, E.J. (2002). Dietary carbohydrate's effects on lipogenesis and the relationship of lipogenesis to blood insulin and glucose concentrations. *British Journal of Nutrition,* 87, 247-253.

Pedersen, P.L. and Carafoli, E. (1987). Ion motive ATPases. I. Ubiquity, properties, and significance to cell function. *Trends Biochem Sci,* 12, 146–150.

Penna-Coutinho, J., Cortopassi, W.A., Oliveira, A.A., França, T.C.C. and Krettli, A.U. (2011). Antimalarial activity of potential inhibitors of *Plasmodium falciparum* lactate dehydrogenase enzyme selected by docking studies. *PloS one,* 6(7), e21237.

Perazella, M.A. (2000). Drug-induced hyperkalemia: old culprits and new offenders. *Am J Med.*, 109, 307–314.

Percário, S., Moreira, D.R., Gomes, B.A., Ferreira, M.E., Gonçalves, A.C.M., Laurindo, P.S., Vilhena, T.C., Dolabela, M.F. and Green, M.D. (2012). Oxidative stress in malaria. *International Journal of Molecular Sciences*, 13(12), 16346-16372.

Perry, J.J.P., Shin, D.S., Getzoff, E.D. and Tainer, J.A. (2010). The structural biochemistry of the superoxide dismutases. *Biochimica et Biophysica Acta*, 1804, 245–262.

Pestov, N.B., Zhao, H., Basrur, V. and Modyanov, N.N. (2011). Isolation and characterization of BetaM protein encoded by ATP1B4--a unique member of the Na,K-ATPase β-subunit gene family. *Biochem Biophys Res Commun*., 412, 543–548.

Peters, W. (1965). Drug resistance in *Plasmodium berghei*. Vinka and lips. *Experimental Parasitology*, 17, 80-89.

Philippe, G., Christiane, D. and Isabelle, F. (2012). Advances in Antimalarial Drug Evaluation and New Targets for Antimalarials. *Malaria Parasites*, 321-351.

Phyo, A.P., Ashley, E.A., Anderson, T.J., Bozdech, Z., Carrara, V.I., Sriprawat, K., Nair, S., White, M.M., Dziekan, J., Ling, C. and Proux, S. (2016). Declining efficacy of artemisinin combination therapy against *P. falciparum* malaria on the Thai–Myanmar border (2003–2013): the role of parasite genetic factors. *Clinical Infectious Diseases*, 63(6), 784-791.

Pink, R., Hudson, A., Mouriès, M.A. and Bendig, M. (2005). Opportunities and challenges in antiparasitic drug discovery. *Nature reviews Drug discovery*, 4(9), 727-740.

Pisoschi, A.M. and Pop, A. (2015). The role of antioxidants in the chemistry of oxidative stress: A review. *European journal of medicinal chemistry*, 97, 55-74.

Plaitakis, A., Latsoudis, H. and Spanaki, C. (2011). The human *GLUD2* glutamate dehydrogenase and its regulation in health and disease. *Neurochemistry International*, 59, 495–509.

Planche, T., Dzeing, A., Ngou-Milama, E., Kombila, M. and Stacpoole, P.W. (2005). Metabolic Complications of Severe Malaria. In: Sullivan, D.J. and Krishna, S. (eds.), *Malaria: Drugs, Disease and Post-genomic Biology*, Springer Berlin Heidelberg, New York, pp. 105-128.

Platel, D.F., Mangou, F. and Tribouley-Duret, J. (1999). Role of glutathione in the detoxification of ferriprotoporphyrin IX in chloroquine resistant Plasmodium berghei. *Mol. Biochem. Parasitol.*, 98, 215-223.

Plewes, K., Kingston, H.W., Ghose, A., Maude, R.J., Herdman, M.T., Leopold, S.J., Ishioka, H., Hasan, M.M.U., Haider, M.S., Alam, S. and Piera, K.A. (2017). Cell-free hemoglobin mediated oxidative stress is associated with acute kidney injury and renal replacement therapy in severe falciparum malaria: an observational study. *BMC infectious diseases*, 17(1), 313.

Plowe, C.V. (2001). Folate Antagonists and Mechanisms of Resistance. In: Rosenthal, P.J. (ed.), *The Antimalarial Chemotherapy: Mechanisms of Action, Resistance and New Directions in Drug Discovery*, Humana Press, New Jersey, pp. 173-190.

Plowe, C.V. (2007). Combination Therapy for Malaria: Mission Accomplished? *Clinical Infectious Diseases*, 44(8), 1075–1077.

Pongponratn, E., Turner, G.D., Day, N.P., Phu, N.H., Simpson, J.A., Stepniewska, K., Mai, N.T.H., Viriyavejakul, P., Looareesuwan, S., Hien, T.T. and Ferguson, D.J. (2003). An ultrastructural study of the brain in fatal *Plasmodium falciparum* malaria. *The American journal of tropical medicine and hygiene*, 69(4), 345-359.

Prasaja, Y., Sutandyo, N. and Andrajati, R. (2015). Incidence of cisplatin-induced nephrotoxicity and associated factors among cancer patients in Indonesia. *Asian Pac J Cancer Prev.*, 16, 1117–1122.).

Prinsen, B.H. (2004). Albumin turnover: experimental approach and its application in health and renal diseases. *Clinica chimica acta*, 347(1), 1-14.

Prior, C.B. and Marshall, I.G. (2006). Neuromuscular junction physiology. In: Hemmings, H.C. and Hopkins, P.M. (eds.), *Foundations of anesthesia: basic sciences for clinical practice*, 2nd edition, Elsevier Health Sciences, Amsterdam, pp. 435-443.

Pustovidko, A.V., Rokitskaya, T.I., Severina, I.I., Simonyan, R.A., Trendeleva, T.A., Lyamzaev, K.G., Antonenko, Y.N., Rogov, A.G., Zvyagilskaya, R.A., Skulachev, V.P. and Chernyak, B.V. (2013). Derivatives of the cationic plant alkaloids berberine and palmatine amplify protonophorous activity of fatty acids in model membranes and mitochondria. *Mitochondrion*, 13(5), 520-525.

Quiroga, A.D. and Lehner, R. (2012). Liver triacylglycerol lipases. *Biochimica et Biophysica Acta*, 1821(5), 762-769.

Radi, R., Turrens, J.F., Chang, L.Y., Bush, K.M., Crapo, J.D. and Freeman, B.A. (1991). Detection of catalase in rat heart mitochondria. *Journal of Biological Chemistry*, 266(32), 22028-22034.

Rasoanaivo, P., Wright, C.W., Willcox, M.L. and Gilbert, B. (2011). Whole plant extracts versus single compounds for the treatment of malaria: synergy and positive interactions. *Malaria Journal*, 10(1), S4.

Ravindran, V.S., Kannan, L. and Venkateshvaran, K. (2012). In-vitro modulation of Na^{+} K^{+}, Mg^{++} ATPases and AchE by sea anemone toxic proteins. *Indian Journal of Geo-Marine Sciences*, 41(5), 451-456.

Rayman, M.P. (2005). Selenium in cancer prevention: a review of the evidence and mechanism of action. *Proceedings of the Nutrition Society*, 64(4), 527-542.

Raza, A., Varshney, S.K., Khan, H.M., Malik, M.A., Mehdi, A.A., Shukla, I. (2015). Superoxide dismutase activity in patients of cerebral malaria. Asian Pacific Journal of Tropical Disease, 5(Suppl 1), S51-S53.

Read, J.A., Wilkinson, K.W., Tranter, R., Sessions, R.B. and Brady, R.L. (1999). Chloroquine Binds in the Cofactor Binding Site of *Plasmodium falciparum* Lactate Dehydrogenase. *Journal of Biological Chemistry*, 274(15), 10213-10218.

Reitman, S. and Frankel, S.A. (1957). Colorimetric method for the determination of serum glutamate-oxaloacetate and pyruvate transaminases. *American Journal of Clinical Pathology*, 28, 56-63.

Reynolds, J.L., Joannides, A.J., Skepper, J.N., McNair, R., Schurgers, L.J., Proudfoot, D., Jahnen-Dechent, W., Weissberg, P.L. and Shanahan, C.M. (2004). Human vascular smooth muscle cells undergo vesicle-mediated calcification in response to changes in extracellular calcium and phosphate concentrations: a potential mechanism for accelerated vascular calcification in ESRD. *Journal of the American Society of Nephrology*, 15(11), 2857-2867.

Rizvi, A., Hasan, S., Alam, M., Zafar, A., Fatima, T., Shareef, P.A.A., Banu, N., Saleemuddin, M., Saifullah, M.K. and Abidi, S.M.A. (2012). Levels of some

antioxidant molecules and lipid peroxidation during *in vivo* transformation of the progenetic metacercaria of Clinostomum complanatum to ovigerous adult worms. *Veterinary parasitology*, 185(2), 164-167.

Robbers, J.E., Speedie, M.K. and Tyler, V.E. (1996). Alkaloids. In: Robbers, J.E., Speedie, M.K. and Tyler, V.E. (eds.), *Pharmacognosy and pharmacobiotechnology*, Williams and Wilkins, London, pp. 144–85.

Roberts, M.F. and Wink, M. (1998). Biochemistry, ecology, and medicinal applications. In: Roberts, M.F. and Wink, M. (eds.), *Alkaloids*. Plenum Press, New York, pp. 1–7.

Ronner, P., Gazzotti, P. and Carafoli, E. (1977). A lipid requirement for the (Ca2+ Mg2+)-activated ATPase of erythrocyte membranes. *Archives of Biochemistry and Biophysics*, 179(2), 578-583.

Rosenthal, M.D. and Glew, R.H. (2011). Medical biochemistry: human metabolism in health and disease. John Wiley & Sons.

Rosenthal, P.J. (1995). *Plasmodium falciparum*: effects of proteinase inhibitors on globin hydrolysis by cultured malaria parasites. *Experimental parasitology*, 80(2), 272-281.

Rosenthal, P.J. (2003). Antimalarial drug discovery: old and new approaches. *Journal of Experimental Biology*, 206(21), 3735-3744.

Rosenthal, P.J. (2004). Cysteine proteases of malaria parasites. *International Journal for Parasitology*, 34, 1489–1499.

Rosenthal, P.J. (2013). Falcipains. In: Rawlings, N.D. and Salvesen, G. (eds.), *Handbook of Proteolytic Enzymes*, Academic Press, San Diego, pp. 1907–1912.

Rotruck, J.T., Pope, A.L., Ganther, H.E., Swanson, A.B., Hafeman, D.G. and Hoekstra, W. (1973). Selenium: biochemical role as a component of glutathione peroxidase. *Science*, 179(4073), 588-590.

Rozova, O.N., Khmelenina, V.N., Bocharova, K.A., Mustakhimov, I.I. and Trotsenko, Y.A. (2015). Role of NAD^+-Dependent Malate Dehydrogenase in the Metabolism of Methylomicrobium alcaliphilum 20Z and Methylosinus trichosporium OB3b. *Microorganisms*, 3, 47-59.

Ryley, J.F. and Peters, W. (1970). The antimalarial activity of some quinolone esters. *Annals of Tropical Medicine and Parasitology*,84, 209-222.

Saks, V.A., Ventura-Clapier, R. and Aliev, M.K. (1996). Metabolic control and metabolic capacity: two aspects of creatine kinase functioning in the cells. *Biochimica et Biophysica Acta*, 1274(3), 81-88.

Salganik, R.I. (2001). The benefits and hazards of antioxidants: controlling apoptosis and other protective mechanisms in cancer patients and the human population. *Journal of the American College of Nutrition*, 20(5), 464S-472S.

Salmon, B.L., Oksman, A. and Goldberg, D.E. (2001). Malaria parasite exit from the host erythrocyte: a two-step process requiring extraerythrocytic proteolysis. *Proceedings of the National Academy of Sciences*, 98(1), 271-276.

Sampayo-Reyes, A. and Zakharyan, R.A. (2006). Tocopherol esters inhibit human glutathione S-transferase omega. *Acta Biochim Pol*, 53, 547-552.

Sanchez, C.P. and Lanzer, M. (2000). Changing ideas on chloroquine in *Plasmodium falciparum*. *Current opinion in infectious diseases*, 13(6), 653-658.

Sanui, H. and Rubin, H. (1982). The role of magnesium in cell proliferation and transformation. In: Boynton, A.L., McKochan, W.L. and Whitfield, J.P. (eds.). *Ions, Cell Proliferation and Cancer,* Academic Press, New York, pp. 517–37.

Sarwar, N., Danesh, J., Eiriksdottir, G., Sigurdsson, G., Wareham, N., Bingham, S., Boekholdt, S.M., Khaw, K.T. and Gudnason, V. (2007). Triglycerides and the risk of coronary heart disease. *Circulation*, 115(4), 450-458.

Sato, T., Tanaka, K., Ohnishi, Y., Teramoto, T., Irifune, M. and Nishikawa, T. (2004). Effects of Steroid hormones on Na^+-K^+ATPase activity inhibition induced amnesia on the step-through passive avoidance task in gonadectomized mice. *Pharmacol Res*, 49, 151-159.

Scanlon, V.C. and Sanders, T. (2007). Essentials of Anatomy and Physiology. 5th edition, F.A. Davis Company, Philadelphia, pp. 163-193, 251-287, 379, 421.

Schafer, A.L. and Shoback, D. (2013). Hypocalcemia: Definition, etiology, pathogenesis, diagnosis, and management. In: Rosen, C.J. (ed), *Primer on the metabolic bone diseases and disorders of mineral metabolism*, 8th edition, John Wiley and Sons, New Jersey, pp. 572-578.

Schlattner, U., Forstner, M., Eder, M., Stachowiak, O., Fritz-Wolf, K. and Wallimann, T. (1998). Functional aspects of the X-ray structure of mitochondrial creatine kinase: a molecular physiology approach. *Molecular and Cellular Biochemistry*, 184, 125–140.

Schlattner, U., Tokarska-Schlattner, M. and Wallimann, T. (2006). Mitochondrial creatine kinase in human health and disease. *Biochimica et Biophysica Acta,* 1762, 164–180.

Schlitzer, M. (2007). Malaria Chemotherapeutics Part I: History of Antimalarial Drug Development, Currently Used Therapeutics, and Drugs in Clinical Development. *ChemMedChem*, 2, 944-986.

Schlitzer, M. (2008). Antimalarial Drugs – What is in Use and What is in the Pipeline. Arch. Pharm. Chem. Life Sci., 341, 149-163.

Schmuck, G., Roehrdanz, E., Haynes, R.K. and Kahl, R. (2002). Neurotoxic mode of action of artemisinin. *Antimicrobial agents and chemotherapy*, 46(3), 821-827.

Schnitzer, E., Pinchuk, I., Fainaru, M., Schafer, Z. and Lichtenberg, D. (1995). Copper-induced lipid oxidation in unfractionated plasma: the lag preceding oxidation as a measure of oxidation-resistance. *Biophys. Res. Commun.*, 216, 854–861.

Schwarzer, E., Turrini, F., Ulliers, D., Giribaldi, G., Ginsburg, H. and Arese, P. (1992). Impairment of macrophage functions after ingestion of *Plasmodium falciparum*-infected erythrocytes or isolated malarial pigment. *Journal of Experimental Medicine*, 176(4), 1033-1041.

Scott, M.G. LeGrys, V.A. and Klutts, J.S. (2008). Electrolytes and blood gases. In: Burtis, C.A., Ashwood, E.R. and Bruns, D.E. (eds.), *Tietz fundamentals of clinical chemistry*, 6th edition, Saunders Elsevier, St. Louis. pp. 431-449.

Sefidan, A.M. and Mohajeri, D. (2013). Preventive Effects of Turmeric (Curcuma longa linn) on Renal Ischemia-Reperfusion Injury in Rats. *Advances in Bioresearch*, 4(4), 40-46.

Sellers, R.S., Mortan, D., Michael, B., Roome, N., Johnson, J.K., Yano, B.L., Perry, R. and Schafer, K. (2007). Society of Toxicologic Pathology position paper: organ weight recommendations for toxicology studies. *Toxicologic pathology*, 35(5), 751-755.

Sevelius, E. and Andersson, M. (1995). Serum protein electrophoresis as a prognostic marker of chronic liver disease in dogs. *The Veterinary Record*, 137(26), 663-667.

Shah, F., Kazi, T.G., Afridi, H.I., Baig, J.A., Sumaira, K., Kolachi, N.F., Wadhwa, S.K. and Shah, A.Q. (2010). Environmental exposure of lead and iron deficit anemia in children age ranged 1-5 years: A cross sectional study. *Sci. Total Environ.*, 408, 5325-5330.

Sharma, A., Hirulkar, N.B., Wadel, P. and Das, P. (2011). Influence of hyperglycemia on renal function parameters in patients with diabetes mellitus. *Int. J. Pharm. Biol. Arch*., 2(2), 734-739.

Sharma, R., Panwar, K. and Mogra, S. (2012). Effects of prenatal and neonatal exposure to lead on white blood cells in Swiss mice. *J. Cell Mol. Biol.*, 10(1), 33-40.

Shenai, B.R., Sijwali, P.S., Singh, A. and Rosenthal, P.J. (2000). Characterization of Native and Recombinant Falcipain-2, a Principal Trophozoite Cysteine

Protease and Essential Hemoglobinase of*Plasmodium falciparum*. *Journal of Biological Chemistry*, 275(37), 29000-29010.

Shenton, J.M., Henson, K.L. and Rebelatto, M.C. (2015). Consequences and Indicators of Test Article-Related Immune Suppression in Nonhuman Primates. In: *The Nonhuman Primate in Nonclinical Drug Development and Safety Assessment*, Academic press, San Diego, pp. 215–234.

Shimizu, H., Kuratsu, T. and Hirata, F. (1979). Purification and some properties of glutamate dehydrogenase from *Proteus inconstans*. *Journal of Fermentation Technology*, 57, 428.

Shoba, G., Joy, D., Joseph, T., Majeed, M., Rajendran, R. and Srinivas, P.S. (1998). Influence of piperine on the pharmacokinetics of curcumin in animals and human volunteers. *Planta Medica*, 64, 353–356.

Shrivastava, P. and Bhatia, M. (2010). Essential role of monocytes and macrophages in the progression of acute pancreatitis. *World journal of gastroenterology*, 16(32), 3995–4002.

Sijwali, P.S., Kato, K., Seydel, K.B., Gut, J., Lehman, J., Klemba, M., Goldberg, D.E., Miller, L.H. and Rosenthal, P.J. (2004). *Plasmodium falciparum* cysteine protease falcipain-1 is not essential in erythrocytic stage malaria parasites. *Proceedings of the National Academy of Sciences of the United States of America*, 101(23), 8721-8726.

Simic, M.G. and Jovanovic, S.V. (1989). Antioxidation mechanisms of uric acid. *Journal of the American Chemical Society*, 111(15), 5778-5782.

Singhal S. S., Singh, S. P., Singhal, P., Horne, D., Singhal, J., Awasthi, S. (2015). Antioxidant role of glutathione S-transferases: 4-Hydroxynonenal, a key molecule in stress-mediated signaling. Toxicol Appl Pharmacol; 289(3):361-370.

Sinha, A. K. (1972). Colorimetric assay of catalase. *Analytical Biochemistry,* 47(2), 389- 394.

Siqueira, A.M., Cavalcante, J.A., Vítor-Silva, S., Reyes-Lecca, R.C., Alencar, A.C., Monteiro, W.M., Alexandre, M.A., Maria Paula G, M., Guinovart, C., Bassat, Q. and Alecrim, M.D.G.C. (2014). Influence of age on the haemoglobin concentration of malaria-infected patients in a reference centre in the Brazilian Amazon. Memórias do Instituto Oswaldo Cruz, 109(5), 569-576.

Sitprija, V. (2008). Altered fluid, electrolyte and mineral status in tropical disease, with an emphasis on malaria and leptospirosis. *Nature Clinical Practice Nephrology*, 4(2), 91-101.

Sjøgaard, G., Adams, R.P. and Saltin, B. (1985). Water and ion shifts in skeletal muscle of humans with intense dynamic knee extension. *Am J Physiol.*, 248, R190–R196.

Skou, J.C. and Esmann, M. (1992). The Na,K-ATPase. *J. Bioenerg. Biomembr.*, 24, 249-261.

Slomianny, C. (1990). Three-dimensional reconstruction of the feeding process of the malaria parasite. *Blood Cells,* 16, 369–378.

Smirnoff, N. and Cumbes, Q.J. (1989). Hydroxyl radical scavenging activity of compatible solutes. *Phytochem*. 28, 1057-1060.

Smith, G.S. Hall, R.L. and Walker, R.M. (2002). Applied Clinical Pathology in Preclinical Toxicology Testing. In: Haschek, W.M., Rousseaux, C.G. and Wallig, M.A. (eds.), *Handbook of Toxicologic Pathology*, 2nd edition, Academic press, San Diego, pp. 123–156.

Smith, G.S., Walter, G.L. and Walker, R.M. (2013). Clinical Pathology in Non-Clinical Toxicology Testing. In: Haschek, W.M., Rousseaux, C.G., Wallig, M.A., Bolon, B. and Ochoa, R. (eds.), *Haschek and Rousseaux's handbook of toxicologic pathology*, 3rd edition, Academic Press, San Diego, pp. 565–594.

Smith, J.A. (1994). Neutrophils, host defense, and inflammation: a double-edged sword. *Journal of leukocyte biology*, 56(6), 672-686.

Smith, T.E. (2010). Molecular Cell Biology. In: Devlin, T.M. (Ed.), *Textbook of Biochemistry with Clinical Correlations*, 7th edition, Wiley, Hoboken.

Snider, M.D., McGarry, J.D. and Hanson, R.W. (2010). Lipid Metabolism I: Synthesis, Storage, and Utilization of Fatty Acids and Triacylglycerols. In: Devlin, T.M. (Ed.), *Textbook of Biochemistry with Clinical Correlations*, 7th edition, Wiley, Hoboken.

Sohocki, M.M., Sullivan, L.S., Harrison, W.R., Sodergren, E.J., Elder, F.F., Weinstock, G., Tanase, S. and Daiger, S.P. (1997). Human glutamate pyruvate transaminase (GPT): localization to 8q24. 3, cDNA and genomic sequences, and polymorphic sites. *Genomics*, 40(2), 247-252.

Sonnen, J.A., Keene, C.D., Hevner, R.F. and Montine, T.J. (2010). Molecular Pathology: Neuropathology. In: Coleman, W.B. and Tsongalis, G.J. (eds.),

Essential Concepts in Molecular Pathology, Academic Press, San Diego, pp. 373–398.

Sotil, E.U. and Jensen, D.M. (2004). Serum enzymes associated with cholestasis. *Clinics in liver disease*, 8(1), 41-54.

Sousa, S.F., Fernandes, P.A. and Ramos, M.J. (2006). Protein–ligand docking: current status and future challenges. *Proteins: Structure, Function, and Bioinformatics*, 65(1), 15-26.

Spanaki, C., Zaganas, I., Kleopa, K.A. and Plaitakis, A. (2010). Human *GLUD2* Glutamate Dehydrogenase Is Expressed in Neural and Testicular Supporting Cells. *The Journal of Biological Chemistry*, 285(22), 16748–16756.

Speakman, J.R. and Garratt, M. (2013). Oxidative stress as a cost of reproduction: Beyond the simplistic trade-off model. *Bioessays*, 36, 93–106.

Spinella, M. (2002). The importance of pharmacological synergy in psychoactive herbal medicines. *Altern Med Rev*, 7(2), 130-137.

Spring, M.D., Lin, J.T., Manning, J.E., Vanachayangkul, P., Somethy, S., Bun, R., Se, Y., Chann, S., Ittiverakul, M., Sia-ngam, P. and Kuntawunginn, W. (2015). Dihydroartemisinin-piperaquine failure associated with a triple mutant including kelch13 C580Y in Cambodia: an observational cohort study. *The Lancet Infectious Diseases*, 15(6), 683-691.

Squadrito, G.L., Cueto, R., Splenser, A.E., Valavanidis, A., Zhang, H., Uppu, R.M. and Pryor, W.A. (2000). Reaction of uric acid with peroxynitrite and implications for the mechanism of neuroprotection by uric acid. *Archives of biochemistry and biophysics*, 376(2), 333-337.

Srivastava, I.K., Morrisey, J.M., Darrouzet, E., Daldal, F. and Vaidya, A.B. (1999). Resistance mutations reveal the atovaquone-binding domain of cytochrome b in malaria parasites. *Molecular microbiology*, 33(4), 704-711.

Stafford, N., Wilson, C., Oceandy, D., Neyses, L. and Cartwright, E.J. (2017). The Plasma Membrane Calcium ATPases and Their Role as Major New Players in Human Disease. *Physiological Reviews*, 97(3), 1089-1125.

Steinbrenner, H. and Sies, H. (2009). Protection against reactive oxygen species by selenoproteins. *Biochim Biophys Acta*, 1790, 1478–1485.

Stocks, P.A., Raynes, K.J. and Ward, S.A. (2001). Novel Quinoline Antimalarials. In: Rosenthal, P.J. (ed.), *The Antimalarial Chemotherapy: Mechanisms of Action, Resistance and New Directions in Drug Discovery*, Humana Press, New Jersey, pp. 235-254.

Storm, J. and Craig, A.G. (2014). Pathogenesis of cerebralmalaria– in*fl*ammation and cytoadherence. Frontiers in Cellular and Infection Microbiology, 4, 100.

Su, C.R., Ueng, Y.F., Dung, N.X., Vijaya Bhaskar Reddy, M. and Wu, T.S. (2007). Cytochrome P3A4 inhibitors and other constituents of Fibraurea tinctoria. *Journal of natural products*, 70(12), 1930-1933.

Suhail, M. (2010). Na+, K+-ATPase: Ubiquitous Multifunctional Transmembrane Protein and its Relevance to Various Pathophysiological Conditions. *J Clin Med Res*., 2(1), 1–17.

Sullivan, D.J., Gluzman, I.Y. and Goldberg, D.E. (1996). Plasmodium hemozoin formation mediated by histidine-rich proteins. *Science*, 219-221.

Sun, H. and Wang, Z.B. (2010). Effects on exercise endurance capacity and antioxidant properties of *Astragalus membranaceus* polysaccharides (APS). *Journal of Medicinal Plants Research*, 4, 982-986.

Szasz G., (1969). A Kinetic Photometric Method for Serum γ-Glutamyl Transpeptidase. *Clinical Chemistry*, 15, 124-136.

Tachibana, H., Koga, K., Fujimura, Y. and Yamada, K. (2004). A receptor for green tea polyphenol EGCG. *Nature structural and molecular biology*, 11(4), 380.

Talarico Jr, E.F., Kennedy, B.G., Marfurt, C.F., Loeffler, K.U. and Mangini, N.J. (2005). Expression and immunolocalization of plasma membrane calcium ATPase isoforms in human corneal epithelium. *Molecular Vision*, 11, 169-178.

Tangpukdee, N., Duangdee, C., Wilairatana, P. and Krudsood, S. (2009). Malaria Diagnosis: A Brief Review. *Korean J Parasitol*., 47(2), 93-102.

Taylor, W.R.J. and White, N.J. (2004). Antimalarial drug toxicity. *Drug safety*, 27(1), 25-61.

Teke, G.N., Lunga, P.K., Wabo, H.K., Kuiate, J., Vilarem, G., Giacinti, G., Kikuchi, H. and Oshima, Y. (2011). Antimicrobial and antioxidant properties of methanol extract, fractions and compounds from the stem bark of Entada abyssinica Stend ex A. Satabie. *BMC Complementary and Alternative Medicine*, 11, 57-65.

Tesch, G.H. (2010). Serum and urine biomarkers of kidney disease: A pathophysiological perspective. *Nephrology*, 15, 609–616.

Theander, T.G. and Lusingu, J.P.A. (2015). Efficacy and safety of RTS, S/AS01 malaria vaccine with or without a booster dose in infants and children in Africa: final results of a phase 3, individually randomised, controlled trial. *Lancet*, 386(9988), 31-45.

Therien, A.G., Goldshleger, R., Karlish, S.J. and Blostein, R. (1997). Tissue-specific distribution and modulatory role of the gamma subunit of the Na,K-ATPase. *J Biol Chem*., 272(51), 32628–32634.

Thomas, C. and Lumb, A.B. (2012). Physiology of haemoglobin. *Continuing Education in Anaesthesia Critical Care & Pain*, 12(5), 251-256.

Thomsen, K.L., Grønbæk, H., Dahlerup, J.F., Aagaard, N.K., Christensen, L.A., Agnholt, J., Frystyk, J. and Vilstrup, H. (2013). Prednisolone but not infliximab aggravates the upregulated hepatic nitrogen elimination in patients with active inflammatory bowel disease. *Inflammatory bowel diseases*, 20(1), 7-13.

Tietz, N.W. (1995). Clinical Guide to Laboratory Tests, WB Saunders, Philadelphia, Pa, USA, 3rd edition.

Tiffert, T., Staines, H.M., Ellory, J.C. and Lew, V.L. (2000). Functional state of the plasma membrane Ca2+ pump in *Plasmodium falciparum*-infected human red blood cells. *The Journal of physiology*, 525(1), 125-134.

Timbrell, J.A. (2009). Principles of Biochemical Toxicology. 4th edition, Informa Healthcare, New York, pp. 248.

Timmann, C., Thye, T., Vens, M., Evans, J., May, J., Ehmen, C., Sievertsen, J., Muntau, B., Ruge, G., Loag, W. and Ansong, D. (2012). Genome-wide

association study indicates two novel resistance loci for severe malaria. *Nature*, 489(7416), 443-446.

Toledo, F.G.S., Sniderman, A.D. and Kelley, D.E. (2006). Influence of hepatic steatosis (fatty liver) on severity and composition of dyslipidemia in type 2 diabetes. *Diabetes Care*, 29(8), 1845-1850.

Tripathy, S., Das, S., Dash, S.K., Mahapatra, S.K., Chattopadhyay, S., Majumder, S. and Roy, S. (2014). A prospective strategy to restore the tissue damage in malaria infection: Approach with chitosan-trypolyphosphate conjugated nanochloroquine in Swiss mice. *European Journal of Pharmacology*, 737, 11-21.

Trosset, J.Y. and Scheraga, H.A. (1999). PRODOCK: software package for protein modeling and docking. *Journal of computational chemistry*, 20(4), 412-427.

Trott, O. and Olson, A.J. (2010). AutoDock Vina: improving the speed and accuracy of docking with a new scoring function, efficient optimization and multithreading. *Journal of Computational Chemistry*, 31, 455-461.

Tsutsumi, V., Nakamura, T., Ueno, T., Torimura, T., Aguirre-García, J. (2017). Structure and Ultrastructure of the Normal and Diseased Liver. In: Muriel, P. (ed.), *Liver Pathophysiology: Therapies and Antioxidants*, Academic Press, London, pp. 23–44.

Turner, L., Lavstsen, T., Berger, S.S., Wang, C.W., Petersen, J.E., Avril, M., Brazier, A.J., Freeth, J., Jespersen, J.S., Nielsen, M.A. and Magistrado, P. (2013). Severe malaria is associated with parasite binding to endothelial protein C receptor. *Nature*, 498(7455), 502.

Turrens, J.F. (2010). Superoxide Dismutase and Catalase. In: McQueen, C.A. (ed.), Comprehensive Toxicology, 2nd edition, Elsevier, pp. 219–227.

Twisk, J., Gillian-Daniel, D.L., Tebon, A., Wang, L., Barrett, P.H.R. and Attie, A.D. (2000). The role of the LDL receptor in apolipoprotein B secretion. *Journal of Clinical Investigation*, 105(4), 521-532.

Vaidya, A.B. and Mather, M.W. (2005). A post-genomic view of the mitochondrion in malaria parasites. *Current topics in microbiology and immunology*, 295, 233-250.

Valvona, C.J., Fillmore, H.L., Nunn, P.B. and Pilkington, G.J. (2016). The regulation and function of lactate dehydrogenase a: therapeutic potential in brain tumor. *Brain Pathology*, 26(1), 3-17.

VanPutte, C. Regan, J. and Russo, A. (2016). Seeley's Essentials of Anatomy & Physiology. 9th edition, McGraw-Hill, New York, pp. 193-237, 329-349.

Varley, H., Gowenlock, A.H., McMurray, J.R. and McLauchlan, D.M. (1988). Varley's practical clinical biochemistry. 6th edition, Heinemann Medical, London.

Vennerstrom, J.L. and Klayman, D.L. (1988). Protoberberine alkaloids as antimalarials. *Journal of medicinal chemistry*, 31(6), 1084-1087.

Vennerstrom, J.L., Nuzum, E.O., Miller, R.E., Dorn, A., Gerena, L., Dande, P.A., Ellis, W.Y., Ridley, R.G. and Milhous, W.K. (1999). 8-Aminoquinolines active against blood stage *Plasmodium falciparumin vitro* inhibit hematin polymerization. *Antimicrobial agents and chemotherapy*, 43(3), 598-602.

Ventura-Clapier, R., Kuznetsov, A., Veksler, V., Boehm, E. and Anflous, K. (1998). Functional coupling of creatine kinases in muscles: Species and tissue specificity. *Molecular and Cellular Biochemistry*, 184, 231–247.

Verhage, D. F., Telgt, D. S. C., Bousema, T., Hermsen, C. C., van Gemert, G. J. A., van der Meer, J. W. M. and Sauerwein, R. W. (2005). Clinical outcome of experimental human malaria induced by *Plasmodium falciparum*-infected mosquitoes, *The Netherlands journal of medicine*, 63, 52–58.

Viera, A.J. and Wouk, N. (2015). Potassium Disorders: Hypokalemia and Hyperkalemia. *American family physician*, 92(6), 487-495.

Vítek, L. and Ostrow, J.D. (2009). Bilirubin Chemistry and Metabolism; Harmful and Protective Aspects. *Current Pharmaceutical Design*, 15, 2869-2883.

Vrba, J., Papouskova, B., Pyszkova, M., Zatloukalova, M., Lemr, K., Ulrichova, J. and Vacek, J. (2015). Metabolism of palmatine by human hepatocytes and recombinant cytochromes P450. *Journal of Pharmaceutical and Biomedical Analysis*, 102, 193–198.

Wadhera, R.K., Steen, D.L., Khan, I., Giugliano, R.P. and Foody, J.M. (2016). A review of low-density lipoprotein cholesterol, treatment strategies, and its impact on cardiovascular disease morbidity and mortality. *Journal of clinical lipidology*, 10(3), 472-489.

Wagner, H. and Ulrich-Merzenich, G. (2009). Synergy research: approaching a new generation of phytopharmaceuticals. *Phytomedicine*, 16, 97-110.

Waldhauer, I. and Steinle, A. (2008). NK cells and cancer immunosurveillance. *Oncogene*, 27, 5932–5943.

Walker, N.F., Nadjm, B. and Whitty, C.J.M. (2014). Malaria. *Medicine*, 42 (2), 100-106

Wang, Y. (2007). The anti-oxidation and anti-microbial activities of tea polyphenols and its increased reagents. *J. Biol.*, 24, 54–56.

Wansi, J.D., Devkota, K.P., Tshikalange, E. and Kuete, V. (2013). Alkaloids from the Medicinal Plants of Africa. In: Kuete, V. (ed.), *Medicinal Plant Research in Africa: Pharmacology and Chemistry*, Elsevier, London, pp. 557–605.

Washington, I.M. and Van Hoosier, G. (2012). Clinical Biochemistry and Hematology. In: Suckow, M.A., Stevens, K.A. and Wilson, R.P. (eds.), The Laboratory Rabbit, Guinea Pig, Hamster, and Other Rodents, Academic Press, San Diego, pp. 57–116.

Wassmer, S.C. and Grau, G.E.R. (2017). Severe malaria: what's new on the pathogenesis front? *International journal for parasitology*, 47(2), 145-152.

Weatherburn, M.W. (1967). "Urea", In: Analytical Chemistry. 39 (8), 971-974.

Weemhoff, J.L., Woolbright, B.L., Jenkins, R.E., McGill, M.R., Sharpe, M.R., Olson, J.C., Antoine, D.J., Curry, S.C. and Jaeschke, H. (2017). Plasma biomarkers to study mechanisms of liver injury in patients with hypoxic hepatitis. *Liver International*, 37(3), 377-384.

Weinberg, J.B., Yeo, T.W., Mukemba, J.P., Florence, S.M., Volkheimer, A.D., Wang, H., Chen, Y., Rubach, M., Granger, D.L., Mwaikambo, E.D. and Anstey, N.M. (2014). Dimethylarginines: endogenous inhibitors of nitric oxide synthesis in children with falciparum malaria. *The Journal of infectious diseases*, 210(6), 913-922.

Wellems, T.E. (2004). Transporter of a malaria catastrophe. Nature medicine, 10(11), 1169-1171.

Wendling, D., Jeannin-Louys, L., Kremer, P., Fellmann, F., Toussirot, É. and Mornet, É. (2001). Adult hypophosphatasia. Current aspects. *Joint Bone Spine*, 68(2), 120-124.

Wheeler, M.D., Nakagami, M., Bradford, B.U., Uesugi, T., Mason, R.P., Connor, H.D., Dikalova, A., Kadiiska, M. and Thurman, R.G. (2001). Overexpression of manganese superoxide dismutase prevents alcohol-induced liver injury in the rat. *Journal of Biological Chemistry*, 276(39), 36664-36672.

White, N.J. (2011) The parasite clearance curve. *Malaria Journal*, 10(1), 278.

WHO. (2010). Global report on antimalarial drug efficacy and drug resistance: 2000-2010. Geneva: World Health Organization. pp. 10, 90.

WHO. (2011). Haemoglobin Concentrations for the Diagnosis of Anaemia and Assessment of Severity. Vitamin and Mineral Nutrition Information System. Geneva: World Health Organization.

WHO. (2016). World Malaria Report 2016. Geneva: World Health Organization.

Wickham, M.E., Culvenor, J.G. and Cowman, A.F. (2003). Selective inhibition of a two-step egress of malaria parasites from the host erythrocyte. *Journal of Biological Chemistry*, 278(39), 37658-37663.

Wiesner, J., Ortmann, R., Jomaa, H. and Schlitzer, M. (2003). New antimalarial drugs. *Angewandte Chemie International Edition*, 42(43), 5274-5293.

Williams, T.N., Mwangi, T.W., Wambua, S., Alexander, N.D., Kortox, M., Snow, R.W. and Marsh, K. (2005). Sickle cell trait and the risk of *Plasmodium falciparum* malaria and other childhood diseases. *The Journal of Infectious Diseases,* 192(1), 178–186.

Williamson, E.M. (2001). Synergy and other interactions in phytomedicines. *Phytomedicine,* 8, 401-409.

Woodrow, C.J. and Krishna, S. (2006). Antimalarial drugs: recent advances in molecular determinants of resistance and their clinical significance. *Cellular and Molecular Life Sciences*, 63(14), 1586-1596.

Woodrow, C.J., Haynes, R.K. and Krishna, S. (2005). Artemisinins. *Postgraduate medical journal,* 81(952), 71-78.

Woreta, T.A. and Alqahtani, S.A. (2014). Evaluation of abnormal liver tests. The *Medical Clinics of North America*, 98(1), 1-16.

Wright, P.J. and Plummer, D.T. (1974). The use of urinary enzyme measurements to detect renal damage caused by nephrotoxic compounds. *Biochemical Pharmacology,* 23(1), 65-73.

Wróblewski, F. and Ladue, J.S. (1955). Lactic Dehydrogenase Activity in Blood. *Proceedings of the Society for Experimental Biology and Medicine,* 90(1), 210-213.

Wu, B. and Dong, D. (2012). Human cytosolic glutathione transferases: structure, function, and drug discovery. *Trends in Pharmacological Sciences,* 33(12), 656-668.

Wu, B., Kulkarni, K., Basu, S., Zhang, S. and Hu, M. (2011). First-pass metabolism via UDP-glucuronosyltransferase: a barrier to oral bioavailability of phenolics. *Journal of pharmaceutical sciences,* 100(9), 3655-3681.

Wu, G., Fang, Y.Z., Yang, S., Lupton, J.R. and Turner, N.D. (2004). Glutathione metabolism and its implications for health. *The Journal of nutrition*, 134(3), 489-492.

Yamaguchi, M. (2012). Role of regucalcin in brain calcium signaling: involvement in aging. *Integr. Biol. (Camb.),* 4, 825–837.

Yamauchi, L. M., Coppi, A., Snounou, G. and Sinnis, P. (2007). Plasmodium sporozoites trickle out of the injection site. *Cellular microbiology*, *9*(5), 1215-1222.

Yang, C.S., Wang, X., Lu, G. and Picinich, S.C. (2009a). Cancer prevention by tea: animal studies, molecular mechanisms and human relevance. *Nature Reviews Cancer*, 9(6), 429-439.

Yang, Q.C., Wu, W.H., Han, F.M. and Chen, Y. (2009b). Identification of in-vivo and in-vitro metabolites of palmatine by liquid chromatography–tandem mass spectrometry. *Journal of Pharmacy and Pharmacology,* 61(5), 647-652.

Yang, Y., Zhang, Z., Li, S., Ye, X., Li, X. and He, K. (2014). Synergy effects of herb extracts: Pharmacokinetics and pharmacodynamic basis. *Fitoterapia*, 92, 133–147.

Yoel, C. (2007). Clinical symptoms and electrolytes description of children with malaria: an outpatient setting in Kabupaten Mandailing Natal. *MKN,* 40(1).

Yong Feng, W. (2006). Metabolism of green tea catechins: an overview. *Current drug metabolism*, 7(7), 755-809.

York, M.J. (2017). Clinical Pathology. In: Faqi, A.S. (Ed.), *A Comprehensive Guide to Toxicology in Nonclinical Drug Development*, 2nd edition, Academic Press, San Diego, pp. 325–374.

Yoshinaga, T. and Ohta, K. (1990). Spectrophotometric determination of chloride ion using mercury thiocyanate and iron alum. *Analytical sciences*, 6(1), 57-60.

Youn, J.H. and McDonough, A.A. (2009). Recent advances in understanding integrative control of potassium homeostasis. *Annu Rev Physiol.*, 71, 381–401.

Young, I.S. and Woodside, J.V. (2001). Antioxidants in health and disease. *Journal of clinical pathology*, 54(3), 176-186.

Yunos, N.A.M., Bellomo, R., Story, D. and Kellum, J. (2010). Bench-to-bedside review: chloride in critical illness. *Critical care*, 14(4), 226.

Zanini, G.M., Martins, Y.C., Carvalho, L.J.M., Cabrales, P. and Frangos, J.A. (2012). S-nitrosoglutathione prevents experimental cerebral malaria. *J Neuroimmune Pharmacol*, 7, 477-487.

Zargar, R., Raghuwanshi, P., Rastogi, A., Koul, A.L., Khajuria, P., Ganai, A.W. and Kour, S. (2016). Protective and ameliorative effect of sea buckthorn leaf extract supplementation on lead induced hemato-biochemical alterations in Wistar rats. *Veterinary World*, 9(9), 929-934.

Zelko, I.N., Mariani, T.J. and Folz, R.J. (2002). Superoxide dismutase multigene family: a comparison of the CuZn-SOD (SOD1), Mn-SOD (SOD2), and EC-

SOD (SOD3) gene structures, evolution, and expression. *Free Radical Biology and Medicine*, 33, 337–349.

Zhang, L., Li, J., Ma, F., Yao, S., Li, N., Wang, J., Wang, Y., Wang, X. and Yao, Q. (2012). Synthesis and cytotoxicity evaluation of 13-n berberine and palmatine analogues as anticancer agents. *Molecules*, 17, 11295–11302.

Zhang, Y., Ma, K.L., Ruan, X.Z. and Liu, B.C. (2016). Dysregulation of the low-density lipoprotein receptor pathway is involved in lipid disorder-mediated organ injury. *International journal of biological sciences*, 12(5), 569.

Zhornitsky, S., McKay, K.A., Metz, L.M., Teunissen, C.E. and Rangachari, M. (2016). Cholesterol and markers of cholesterol turnover in multiple sclerosis: relationship with disease outcomes. *Multiple sclerosis and related disorders*, 5, 53-65.

Zhu, L., Gunn, C. and Beckman, J.S. (1992). Bactericidal activity of peroxynitrite. *Archives of biochemistry and biophysics*, 298(2), 452-457.

Zofou, D., Tematio, E.L., Ntie-Kang, F., Tene, M., Ngemenya, M.N., Tane, P. and Titanji, V.P.K. (2013). New Antimalarial Hits from Dacryodes edulis (Burseraceae)-Part I: Isolation, *In vitro* Activity, *In silico* "drug-likeness" and Pharmacokinetic Profiles. PLoS ONE, 8(11), e79544-e79553.

Zylin´ska, L. and Soszyn´ski, M. (2000). Plasma membrane Ca^{2+}-ATPase in excitable and nonexcitable cells. *Acta Biochim Pol*, 47, 529–539.

APPENDICES

APPENDIX I: PREPARATION OF REAGENTS AND SOLUTIONS

PREPARATION OF REAGENTS FOR B-HAEMATIN INHIBITION ASSAY

1.68 mM Hematin

10.953 mg of bovine hemin (molecular weight 651.94 g/mol) were dissolved in 10 mL of NaOH (0.1 M). This preparation was used within 60 mins.

0.1 M NaOH

0.4 g of NaOH was dissolved in 100 mL of distilled water.

1 M HCl

8.3 mL of Conc. HCl (specific gravity = 1.18; molar mass = 36.5; % purity = 36) was slowly added to 91.7 mL of distilled water.

$$\text{Molarity of a liquid} = \frac{\text{Specific gravity in g/mL} \times 1000}{\text{Molar mass in g/mol}} \times \frac{\%\ \text{purity}}{100}$$

Dilution formula $C_1V_1 = C_2V_2$

12.9 M sodium acetate solution

63.14 g of sodium acetate trihydrate was dissolved in 47.28 mL of glacial acetic acid. This was warmed at 60^{o}C with vigorous stirring to yield a viscous solution with pH of 5.

PREPARATION OF REAGENTS FOR DPPH RADICAL SCAVENGING ACTIVITY

0.11 mM DPPH

0.04338 g of DPPH (2,2-diphenyl-1-picrylhydrazyl) was dissolved in 1 dm^3 ethanol (80%).

PREPARATION OF REAGENTS FOR HYDROXYL RADICAL SCAVENGING ACTIVITY

1.5 mM $FeSO_4$

0.0228 g of $FeSO_4$ was dissolved and made up to 100 mL.

6 mM Hydrogen peroxide

0.123 mL of H_2O_2 (specific gravity = 1.11 g/mL; molar mass = 34.01 g/mol; % purity = 30%) was added to 199.877 mL distilled water.

$$\text{Molarity of a liquid} = \frac{\text{Specific gravity in g/mL} \times 1000}{\text{Molar mass in g/mol}} \times \frac{\%\ \text{purity}}{100}$$

Dilution formula $C_1V_1 = C_2V_2$

20 mM Sodium salicylate

0.320 g Sodium salicylate was dissolved and made up to 100 mL.

PREPARATION OF REAGENTS FOR NITRIC OXIDE SCAVENGING ACTIVITY

10 mM sodium nitroprusside

0.262 g of sodium nitroprusside was dissolved in 0.1 M phosphate buffer and made up to 100 mL.

PREPARATION OF REAGENTS FOR PLASMA OXIDATION ASSAY

200 µM $CuCl_2$

0.02689 g of copper (II) chloride was dissolved in distilled water and made up to 1 dm^3.

0.1 M PBS (pH = 7.4)

8 g of NaCl, 0.2 g KCl, 1.44 g Na_2HPO_4 and 0.24 g KH_2PO_4 were dissolved in distilled water. The pH was adjusted to 7.4 and the solution was made up to 1 Litre.

50 µg/mL Vit C

0.0050 g of vitamin C was dissolved in distilled water and made up to100 mL.

PREPARATION OF REAGENTS FOR OXIDATIVE HAEMOLYSIS INHIBITION ASSAY

200 mM AAPH

0.5424 g of 2,2-Azobis(2-amidinopropane) dihydrochloride was dissolved in distilled water and made up to 10 mL.

0.1 M PBS (pH = 7.4)

8 g of NaCl, 0.2 g KCl, 1.44 g Na_2HPO_4 and 0.24 g KH_2PO_4 were dissolved in distilled water. The pH was adjusted to 7.4 and the solution was made up to 1 Litre.

REAGENTS FOR ESTIMATION OF LIPID PEROXIDATION

Tris-KCl buffer (0.15 M, pH 7.4)

Tris (2.36 g) and KCl (1.12 g) were dissolved in distilled water, the pH was adjusted to 7.4 and the volume made up to 100 mL.

Trichloroacetic acid, TCA (30 %)

TCA (15 g) was dissolved in distilled water and was made up to 50 mL.

Thiobarbituric acid, TBA (0.75 %)

TBA (0.375 g) was dissolved in 0.1 M HCl and was made up to 50 mL with same.

REAGENTS FOR DETERMINATION OF SUPEROXIDE DISMUTASE ACTIVITY

0.05 M carbonate buffer (pH 10.2)

$NaHCO_3$ and $Na_2CO_3.10H_2O$ (14.3 g) were dissolved in 900 ml of distilled water, the pH was then adjusted to 10.2 and then made up to 1000 ml.

0.3 mM epinephrine (adrenaline)

Epinephrine (0.0137 g) was dissolved in 200 ml of distilled water and made up to 250 ml. To be prepared fresh.

REAGENTS FOR DETERMINATION OF CATALASE ACTIVITY

800 µmolar H_2O_2

49.2 ml of H_2O_2 was made up to 1000 mL with distilled water.

$$\text{Molarity of a liquid} = \frac{\text{Specific gravity in g/L}}{\text{Molar mass in g/mol}} \times \frac{\text{\% purity}}{100}$$

$$\text{Molarity of a liquid} = \frac{\text{Specific gravity in g/mL} \times 1000}{\text{Molar mass in g/mol}} \times \frac{\text{\% purity}}{100}$$

0.1 M phosphate buffer (pH 7.4)

0.1 M $Na_2HPO_4.12H_2O$ was made by dissolving 7.1628 g in 200 mL of distilled water. 0.1 M $NaH_2PO_4.2H_2O$ was made by dissolving 1.5603 g in 100 ml 0f distilled water. These two solutions were combined and the pH was adjusted to 7.4 by drops of conc. NaOH or HCl as required.

REAGENTS FOR DETERMINATION OF GLUTATHIONE PEROXIDASE

GSH (2mM)

GSH (0.0616 g) was dissolved in 100 mL of distilled water.

Sodium azide (10 mM)

Sodium azide (10 mM) was dissolved in 30 mL of distilled water.

DTNB (0.004 %) –Ellman's reagent

DTNB (0.04 g) was dissolved in 100 mL of distilled water.

Disodium hydrogen phosphate (0.3 M)

Na2HPO4 (12.78 g) was dissolved in 300 mL of distilled water.

Tris-HCl buffer (0.1 M pH 7.4)

8912 g of Tris-HCl was dissolved in 100 mL of distilled water and the total volume was made up to 120 mL.

REAGENTS FOR DETERMINATION OF GLUTATHIONE REDUCTASE

15 mM EDTA

EDTA (0.4384 g) was dissolved in distilled water and the final volume made up to 100 mL.

0.66 mM GSSG

GSSG (0.0404 g) was dissolved in distilled water and final volume made up to 100 mL.

0.1 mM NADPH

NADPH (0.0037 g) was dissolved in 50 mL of phosphate buffer (0.1 M pH 7.4).

REAGENTS FOR DETERMINATION OF GLUTATHIONE-S-TRANSFERASE ACTIVITY

20 mM 1-chloro-2,4-dinitrobenzene (CDNB)

3.37 mg of 1-chloro-2, 4-dinitrobenzene (CDNB) was dissolved in 1 mL of ethanol.

0.1 M GSH

GSH (0.3073 g) was dissolved in 10 mL of 0.1 M phosphate buffer (6.5 pH).

0.1 M phosphate buffer (pH 6.5)

KH_2PO_4 (4.96 g) and KH_2PO_4 (9.73 g) were dissolved in distilled water. The pH was adjusted to 6.5 and the final volume was made up to 1000 mL with distilled water.

REAGENTS FOR ESTIMATION OF REDUCED GLUTATHIONE

0.1 M, pH 7.4 phosphate buffer

0.1 M $Na_2HPO_4.12H_2O$ was made by dissolving 7.1628 g in 200 mL of distilled water. 0.1 M $NaH_2PO_4.2H_2O$ was made by dissolving 1.5603 g in 100 ml 0f distilled water. These two solutions were combined and the pH was adjusted to 7.4 by drops of conc. NaOH or HCl as required.

Ellman's Reagent or [5', 5'-Dithiobis-(2-nitrobenzoate) DTNB]

DTNB (80 mg) was dissolved in 0.1 M phosphate buffer (pH 7.4) and made up to 200 mL.

4% Sulphosalicylic Acid (Precipitating Agent)

4g of sulphosalicylic acid was dissolved in distilled water and the volume was made up to 100 mL.

GSH for Standard Curve (working standard)

40 mg of GSH was dissolved in phosphate buffer (0.1 M, pH 7.4) and up to 100 mL with the buffer.

REAGENTS FOR ESTIMATION OF TOTAL PROTEIN

Biuret Reagent

1.5 g of Cupric sulphate ($CuSO_4.5H_2O$) and 6.0 g of Sodium potassium tartrate were dissolved in 500 mL of distilled water and transferred to a 1 litre flask. 1 g of potassium iodide (KI) and 300 mL of 10% NaOH solution were added. The resulting solution was made up to the 1 litre mark with distilled water.

5 mg/mL Bovine Serum Albumin (BSA) Standard

50 mg BSA was dissolved in little quantity of 0.5 N NaOH and made up to 10 mL with the same 0.5 N NaOH solution.

PREPARATION OF REAGENTS FOR ESTIMATION OF ATPASES ACTIVITIES

200 mM NaCl/40 mM KCl/60 mM Tris buffer (pH 7.4)

NaCl (2.922 g), 0.745 g of KCl and 1.8165 g of Tris were dissolved in 200 ml of distilled water in a beaker. The pH was adjusted to 7.4 using HCl and the solution was then made up to 250 ml with distilled water in a standard volumetric flask.

240 mM KCl/60 mM Tris buffer (pH 7.4)

KCl (4.473 g) and 1.8165g of Tris were dissolved in 200 ml of distilled water in a beaker. The pH was adjusted to 7.4 using HCl and the solution was made up to 250 ml with distilled water in a standard volumetric flask.

$CaCl_2.2H_2O$ (4 mM)

$CaCl_2.2H_2O$ (0.0294 g) was dissolved in 80 ml of distilled water and made up to 100 ml with distilled water.

Ouabain (1 mM)

Ouabain (0.0582 g) was dissolved in 8 ml of distilled water.

ATP solution (8 mM)

ATP (0.22 g) was dissolved in distilled water and the solution was diluted to 50ml in a standard flask.

EGTA solution (20 mM)

0.3804g of EGTA was dissolved in distilled water and made up to 50ml in a standard flask.

$MgCl_2.6H_2O$ solution (80 mM)

0.8132 g of $MgCl_2.6H_2O$ was dissolved in distilled water and made up to 50 ml.

Sodium Dodecyl Sulphate (SDS) solution (5%)

5 g of SDS was dissolved in distilled water and made up to 100 ml

Reagent A (Ammonium molybdate/Tetraoxosulphate (VI) acid)

2 g of ammonium molybdate was dissolved in 310 ml of distilled water, after which 9 ml of conc. H_2SO_4 was added and thoroughly stirred.

Reagent B (9% Ascorbic acid solution)

9 g of ascorbic acid was dissolved in distilled water and made up to 100 ml.

Reagent C

This was prepared by mixing reagent A and B in ratio 8:2 (v/v). This was prepared for immediate usage.

Sodium dihydrogen phosphate solution (1 mM).

0.015 g of $NaH_2PO_4.2H_2O$ was dissolved in distilled water and made up to 100ml

APPENDIX II

Amino acid codes as used in docking studies

Code	Amino acid
Ala	Alanine
Arg	Arginine
Asn	Asparagine
Asp	Aspartic Acid
Cys	Cysteine
Gln	Glutamine
Glu	Glutamic Acid
Gly	Glycine
His	Histidine
Ile	Isoleucine
Leu	Leucine
Lys	Lysine
Met	Methionine
Phe	Phenylalanine

Pro	Proline
Ser	Serine
Thr	Threonine
Trp	Tryptophan
Tyr	Tyrosine
Val	Valine

APPENDIX III

CALCULATIONS OF INOCULUM SIZE AND COMPOUND ADMINISTRATION

Plasmodium Inoculum Size Calculation and Method

Step i. Preparation of Citrate-Glucose Solution

3.8 g of sodium citrate and 0.5 g of glucose were weighed, dissolved and made up to 100 mL with distilled water. Kept refrigerated until required.

Step ii. Determination of the percentage parasitaemia from the donor mouse.

$$\% \text{ Parasitaemia} = \frac{\text{Number of infected RBC}}{\text{Total number of RBC}} \times 100$$

Step iii. The donor mouse-tail was sterilized using ethanol-soaked cotton wool. Aliqout, 1 mL, of cold citrate-glucose solution was measured into a sterile bottle, and another 1 mL was drawn into a 2 mL syringe. The volume in the syringe was used to collect drops of blood from the donor mouse (about 10 – 15 drops, depending on the number of mice to be inoculated) and transferred to the sterile bottle.

Step iv. Appropriate volume from the sterile bottle was introduced into the Haemocytometer counting chamber and viewed under ×10 magnification. Cells (red blood cells) in 5 different square boxes were counted and the sum of values was multiplied by 5 and 10,000 to give the number of RBC per mL.

Step v. The number of RBC per mL was multiplied by the % parasitaemia to get the value of infected RBC per mL. This was then converted to get number of

infected RBC per 0.2 mL (inoculation volume) and was appropriately diluted to the desired inoculum size, with cold citrate-glucose solution, using $C_1V_1 = C_2V_2$.

Step vi. The mice were intraperitoneally inoculated at 45° using a sterile needle, preferably at the second nipple in female mouse.

Example:

Number of counted RBC (from haemocytometer) = 705

Total number of RBC per mL = 705 × 5 × 10,000 = 35,250,000 RBC/mL

NOTE: Haemocytometer has 9 large cubes (squares) and each cube has length, breadth and depth of 1 mm, 1mm and 0.1mm respectively. Hence volume of each cube = 1 mm × 1 mm × 0.1 mm = 0.1 mm^3 = 0.0001 mL. Since 1,000 mm^3 = 1 mL, therefore whatever is counted in one large cube is multiplied by 10,000 to get the 1 mL equivalent. RBC is counted in the central cube which has 25 smaller cubes. Therefore, number of RBC counted in 5 of these smaller cubes is multiplied by 5 to get equivalent value for all 25 smaller cubes within the central cube, i.e. Number of RBC per mL = no of RBC counted in 5 smaller cubes × 5 × 10,000.

%Parasitaemia = 14.3%

$$\text{Total number of infected RBC/mL} = \frac{14.3}{100} \times 35{,}250{,}000 = 5{,}040{,}750 \text{ iRBC/mL}$$

$$\text{Therefore, } \frac{5{,}040{,}750 \text{ iRBC/mL}}{5} = 1{,}008{,}150 \text{ iRBC/0.2 mL}$$

If the required inoculum size is 1×10^5 infected RBC, then this is to be diluted i.e.

$$C_1V_1 = C_2V_2$$

$$1{,}008{,}150 \times 0.2 = 1 \times 10^5 \times V_2$$

V_2 = 2.016, therefore 2.016 – 0.2 = 1.8163 mL

0.2 : 1.8163 = 1 : 9.08 (dilution factor of 10).

The required dilution will be 1 mL of stock inoculum in 9.08 mL of citrate-glucose solution.

Calculations for drug administration

Preparation of 5% DMSO

0.5 mL of DMSO was diluted with 9.5 ml of distilled water.

Taking 50 mg/Kg b.wt. group as example

If the average weight of mice for the group = 21.4 g

Volume of extract to be administered per mouse = 0.2 mL

Number of mice per group = 5 (but 6 shall be considered to cater for possible spillage)

Therefore;

Since 50 mg/Kg body weight implies that 50 mg of compound is to be administered to a mouse of 1000 g body weight, therefore, a mouse of 21.4 g weight requires 1.07 mg of compound [i.e. (21.4 ÷ 1000) × 50].

This implies that 1.07 mg of compound is to be dissolved in 0.2 mL of solvent and be administered to a 21.4 g mouse. Therefore, for six mice, 6.42 mg compound is to be dissolved in 1.2 ml of solvent for a day's administration.

For weight variation within the group, the precise volume of compound solution to be administered to mouse of about 22.5 g will be 0.21 mL i.e. [(22.5 ÷ 21.4) × 0.2].

$$\frac{\text{Weight of mouse}}{\text{Average weight of mice in the group}} \times 0.2 \text{ mL}$$

APPENDIX IV

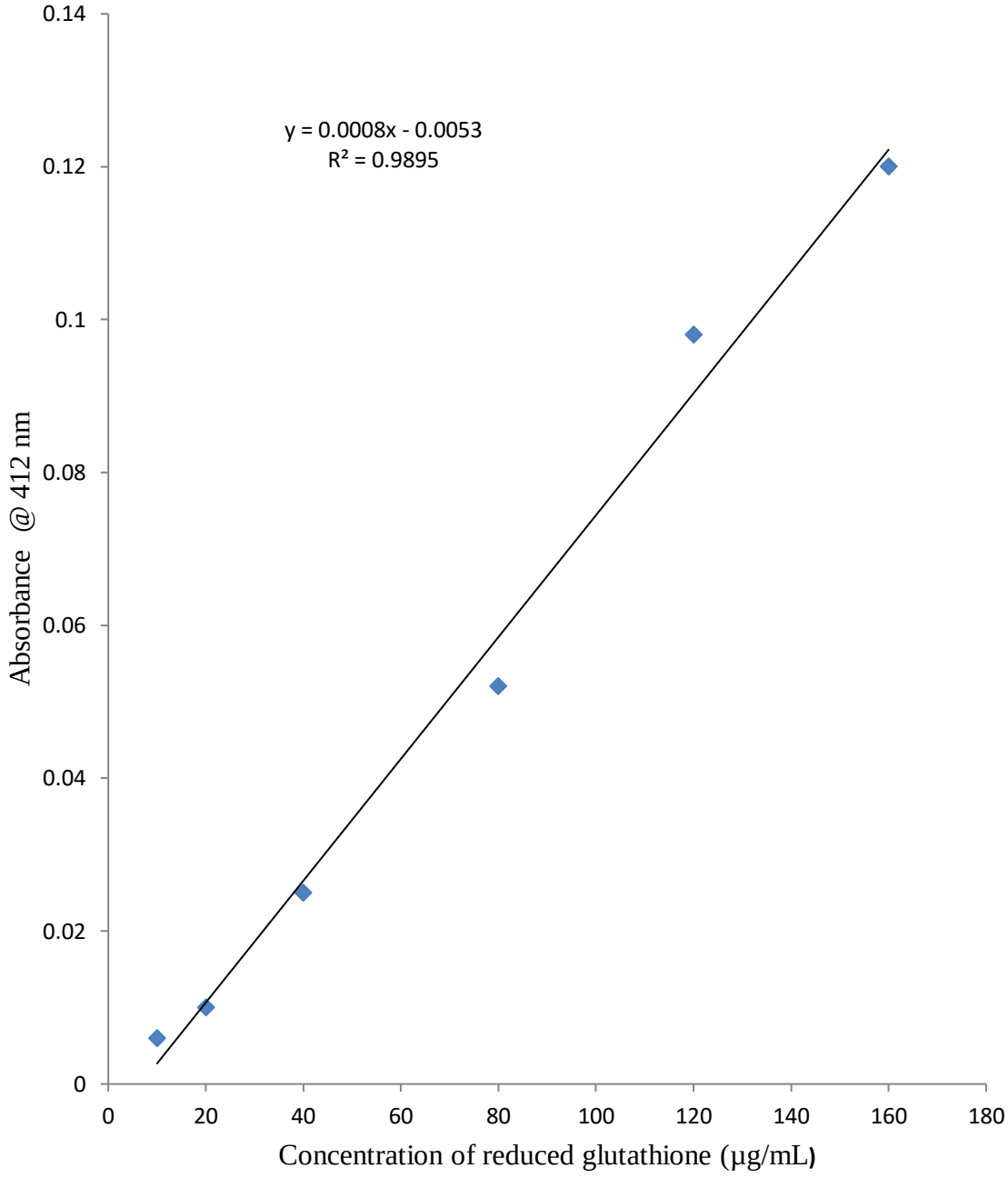

Calibration curve for GSH determination

APPENDIX V

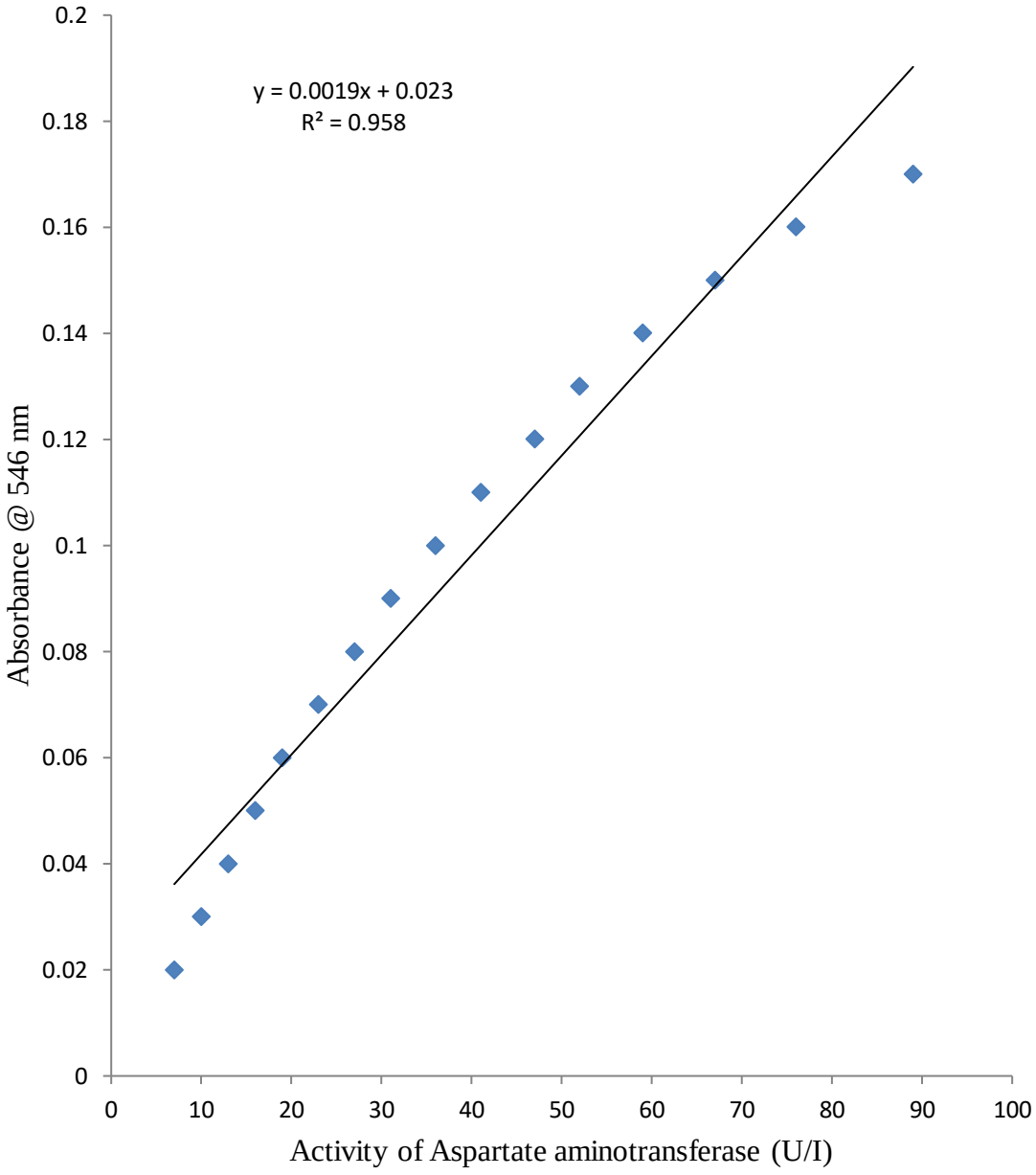

Calibration curve for determination of Aspartate aminotransferase activity

APPENDIX VI

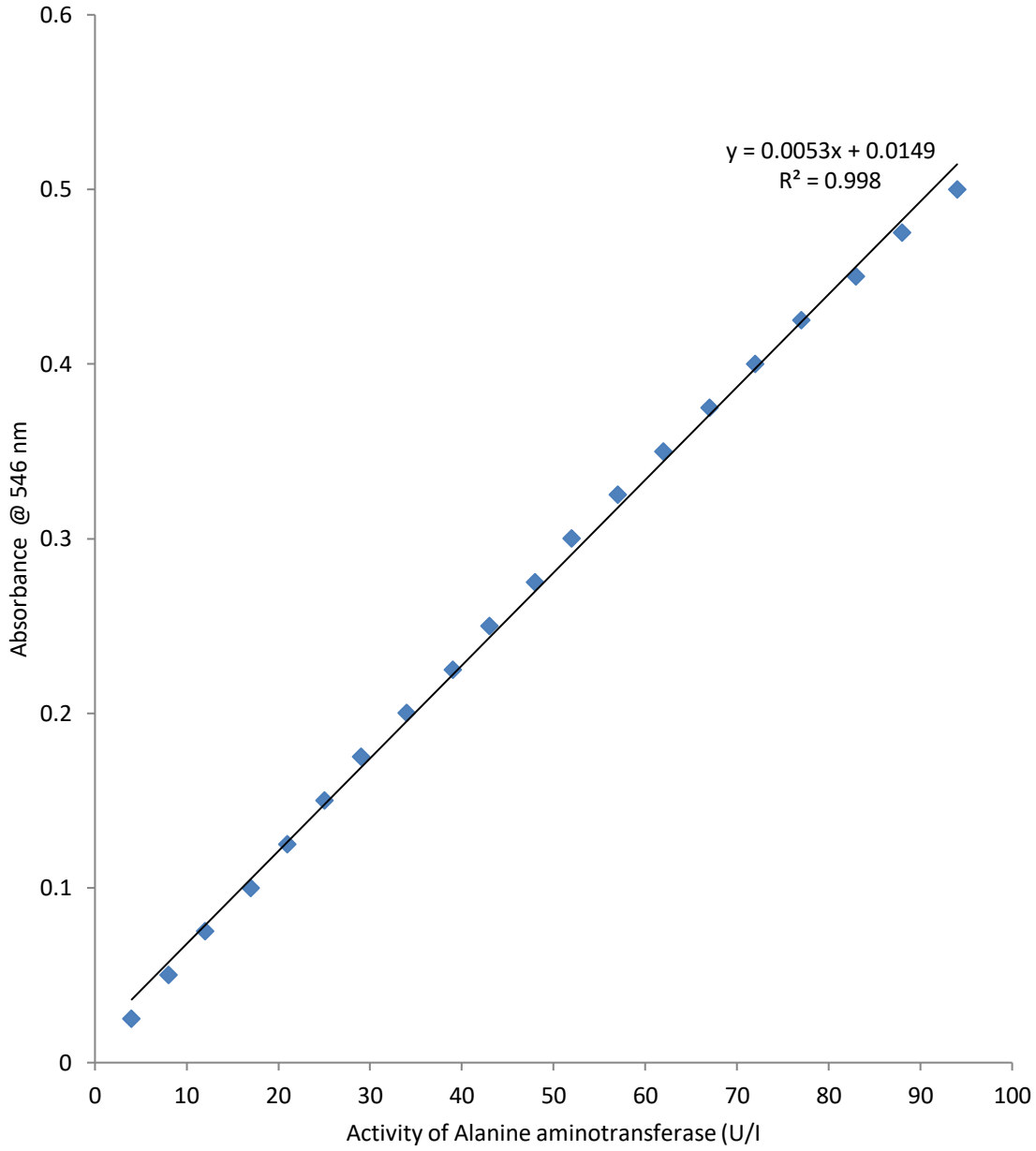

Calibration curve for determination of Alanine aminotransferase activity

APPENDIX VII

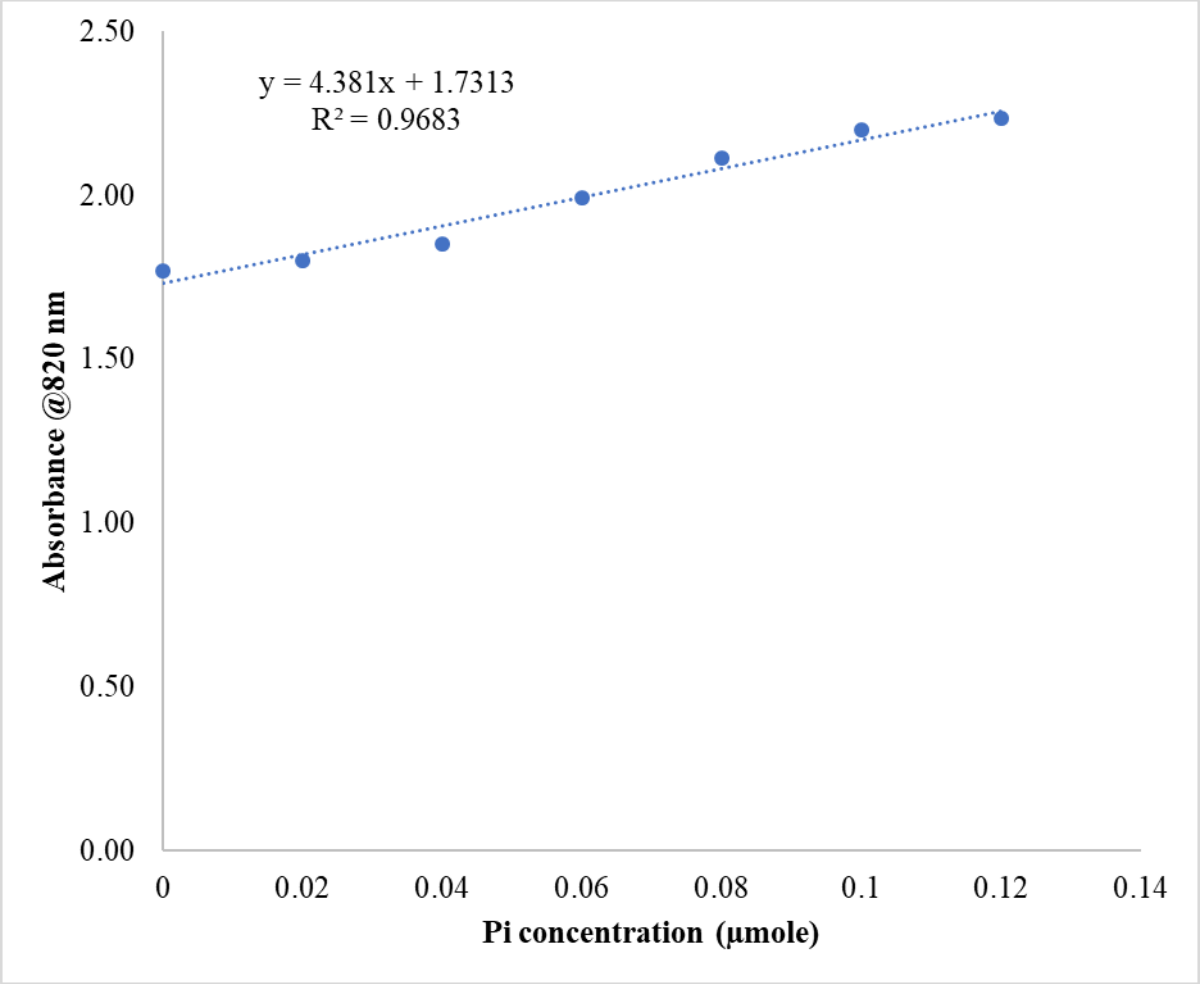

Calibration curve for inorganic phosphate

APPENDIX VIII

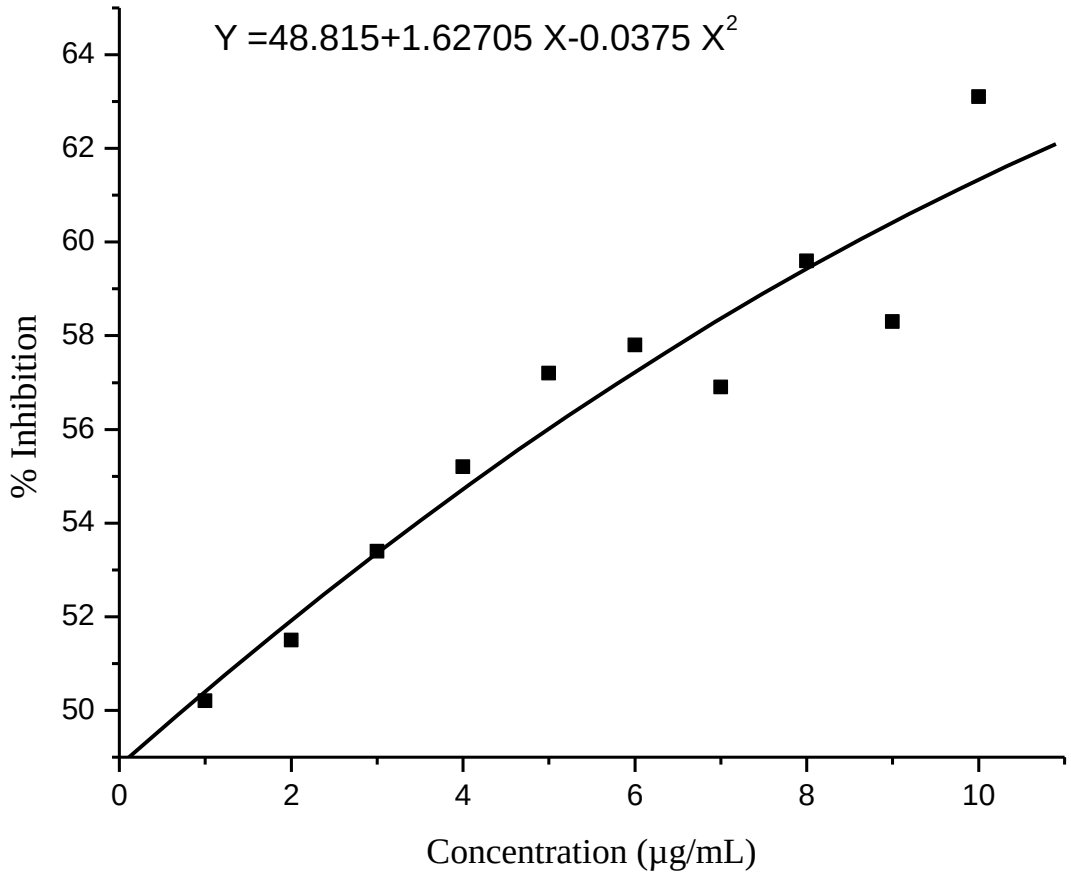

Percentage inhibition of β-hematin formation at various concentration of chloroquine

APPENDIX IX

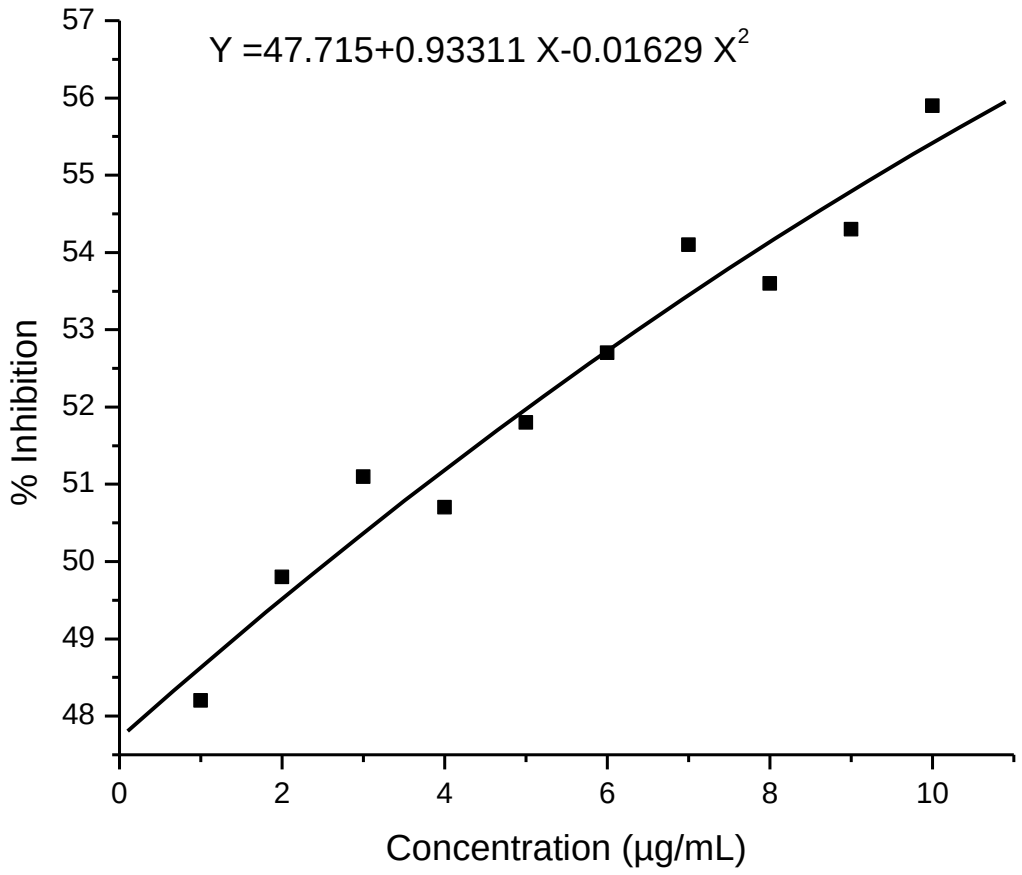

Percentage inhibition of β-hematin formation at various concentration of methyl gallate

APPENDIX X

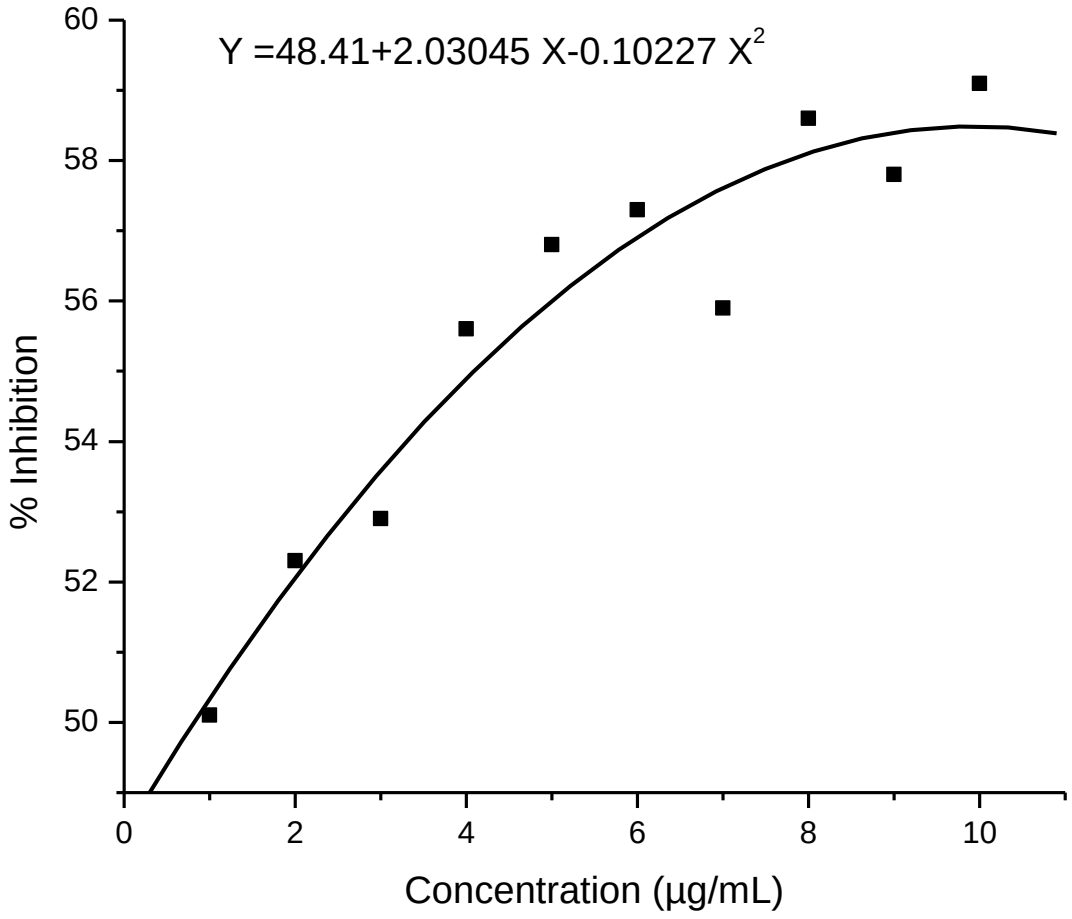

Percentage inhibition of β-hematin formation at various concentration of Palmatine

APPENDIX XI

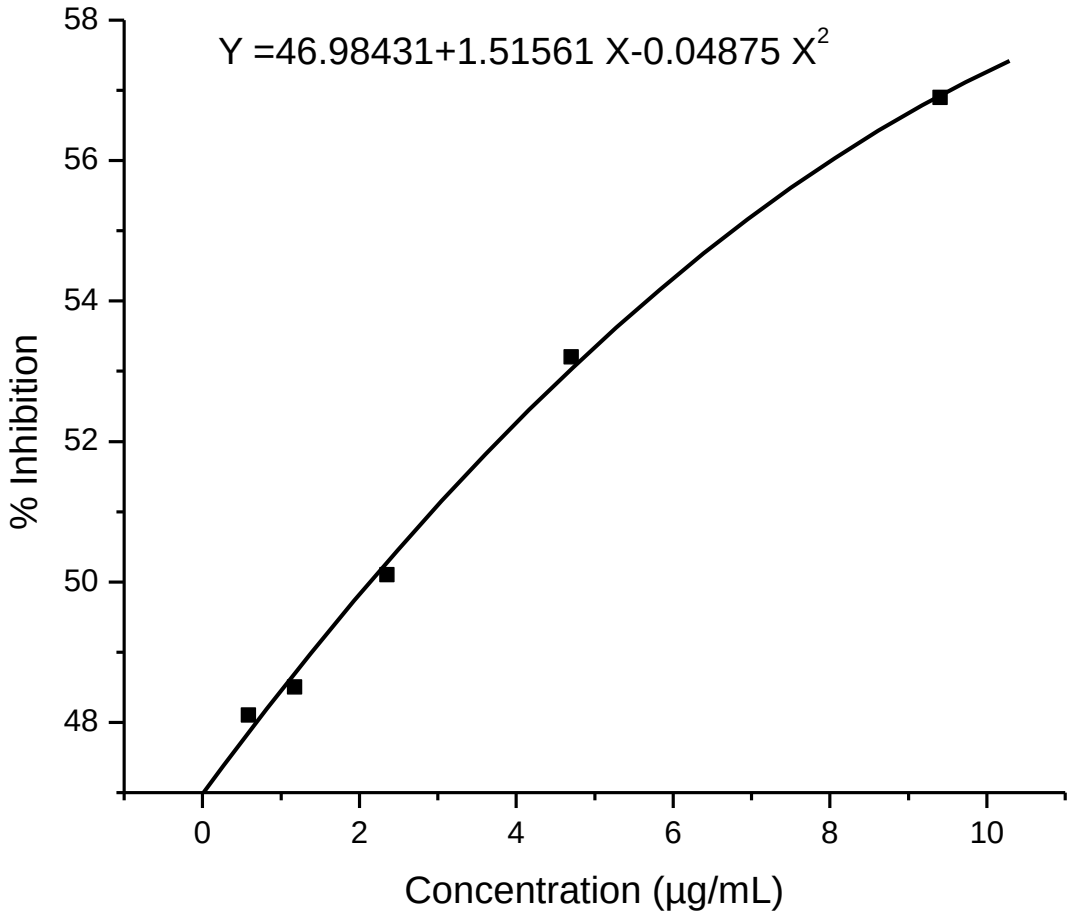

Percentage inhibition of β-hematin formation at various concentration of methyl gallate and Palmatine at ratio 1:4 combination

APPENDIX XII

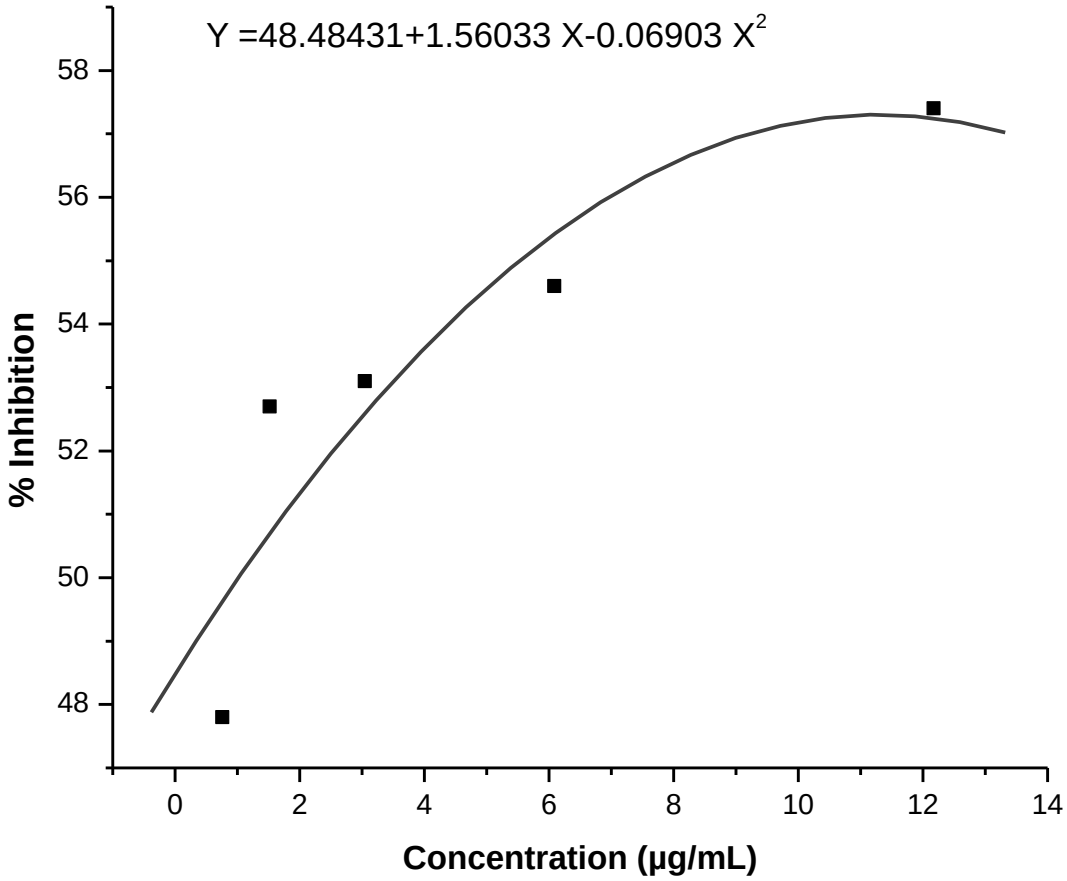

Percentage inhibition of β-hematin formation at various concentration of methyl gallate and Palmatine at ratio 2:3 combination

APPENDIX XIII

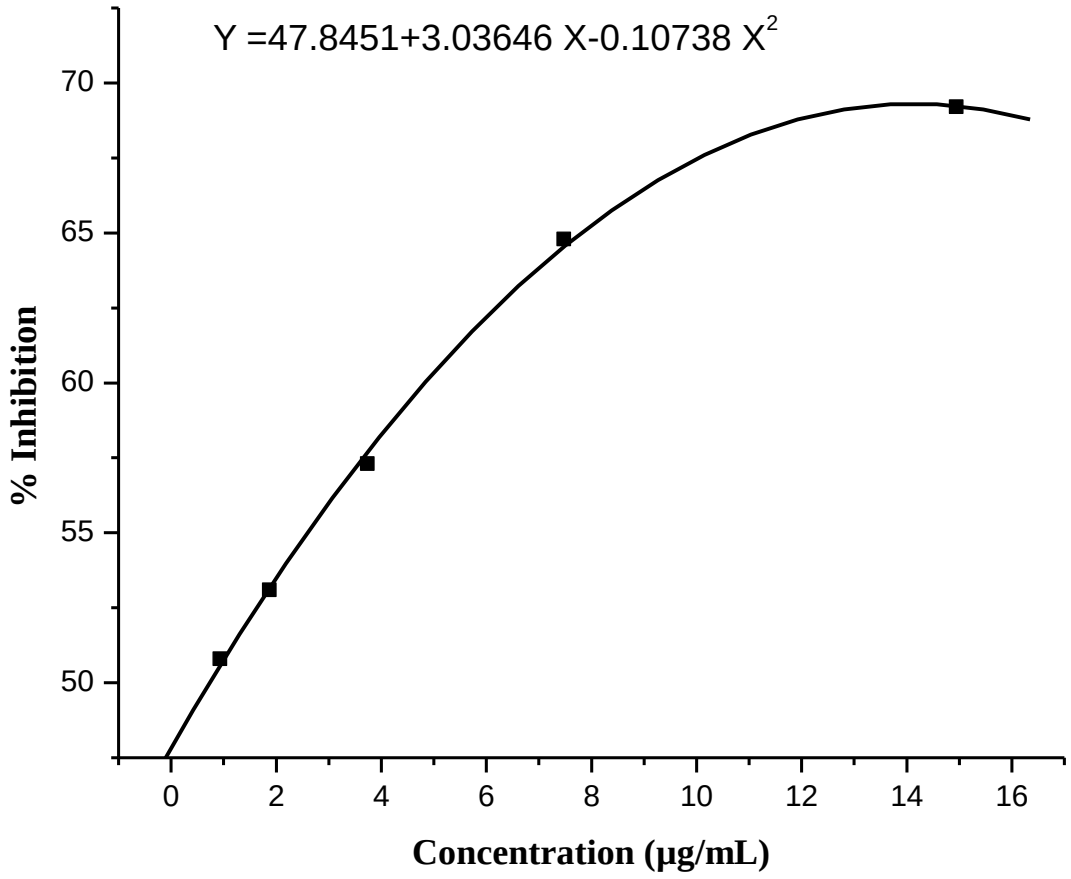

Percentage inhibition of β-hematin formation at various concentration of methyl gallate and Palmatine at ratio 3:2 combination

APPENDIX XIV

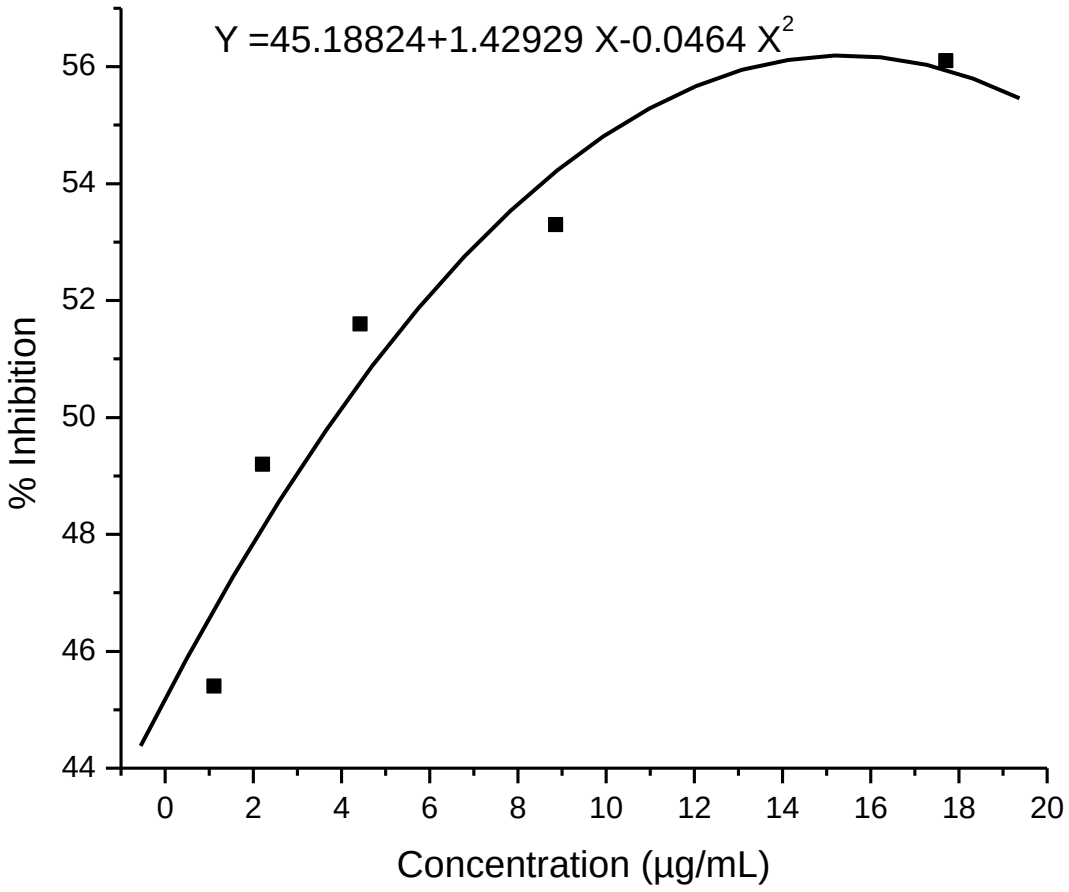

Percentage inhibition of β-hematin formation at various concentration of methyl gallate and Palmatine at ratio 4:1 combination